98-626

AIT CORPORATION

105-03695/

FINAL REPORT

MULTI-FUNCTION RADAR SIMULATION AND ECCM DATA ANALYSIS

SSC FILE NUMBER 05SV.W7714-3-9700
NOVEMBER 1993 TO JUNE 1995

DT-00892
AIT Corporation
Nepean, Ontario

Approvals	Title	Signature	Date
Prepared by: E. D. Brookes	Scientific Analyst	Dan Brookes	96/07/25
Reviewed by: MA [illegible]	VP R&D		96.07.25

Revision	A	B	C	D	E
Date	June 1995				

FINAL REPORT

MULTI-FUNCTION RADAR SIMULATION AND ECCM DATA ANALYSIS

Prepared by:

D. Brookes
A. Wilkinson

AIT Corporation
Nepean, Ontario
Canada
June, 1995

DT-00892
Revision A

Table of Contents

1.0 Introduction 1

1.1 Project Background 1

1.2 AIT Project Organization 3

1.3 Statement of Work 3

1.3.1 Main-beam and Side-lobe Canceller Data Analysis 3

1.3.2 MFR System Study 4

1.3.3 Radar Trial Support 4

2.0 Contract Management 5

2.1 Project Team Organization: 5

2.2 Project Control 5

3.0 Main Beam and Sidelobe Canceller Data Analysis 7

3.1 Task 1a) i) Simulation Studies of Anti-jamming Algorithms. 7

3.2 Task 1a) ii) Calibration and Formatting of Experimental Data 49

3.3 Task 1a)iii) Data Analysis and Testing the Effectiveness of the Main-beam and Side-lobe Canceller Software 56

3.4 Task 1b) i) Generation of I and Q Signals from IF Data. 59

3.5 Task 1b) ii) Calibration and Processing of the Aug.-Sept. 1994 Trials Data 62

3.6 Task 1b)iii) Sensitivity Analysis of Main-beam and Side-lobe Cancellation Methods using Aug.-Sept. 1994 Trials Data. 69

4.0 MFR System Study 112

4.1 Task 2a) i) Adding Side-lobe Canceller Array Configurations 112

4.2 Task 2a) ii) Adding Signals From up to 4 Noise Sources 112

4.3 Task 2a)iii) Modelling the Individual Array Elements . 113

4.4 Task 2a) iv) Formatting Simulator Output for Anti-Jamming Software 113

4.5 Task 2a) v) Simulation of Threat Scenarios and Performance Evaluation of Anti-jamming Algorithms 115
4.6 Task 2b) Performance Evaluation for Monopulse and RML Tracking 126

5.0 Radar Trials Support 136

ACKNOWLEDGEMENTS 137

APPENDIX A Statement of Work A1

APPENDIX B EARS Project Personnel B1

APPENDIX C Task Sheets C1

APPENDIX D List of Programs and Subroutines D1

APPENDIX E Brief Description of Sidelobe Cancelation Algorithm E1

APPENDIX F Area 5 Trials, July-Sept. 1995 . . . . F1

APPENDIX G Brief Description and Manual for GENXSLC . G1

1.0 Introduction

This report summarizes the work performed on the A.I.T. contract running from November 1993 to June 1995. The contract followed the statement of work outlined in Contract W7714-3-9700 (Appendix A) entitled "Multi-Function Radar Simulation and ECCM Data Analysis". This document will refer to work done primarily by AIT personnel: Mr. Dan Brookes and Ms. Anna Wilkinson. Some work, such as the collection of experimental data, was performed by other project personnel under separate contracts. Appendix B displays a list of the Experimental Array Radar System (EARS) Project personnel.

1.1 Project Background

The tracking of a target for a naval fire-control radar requires a continuous determination of the target range, height and azimuth. In low-angle situations the target height is difficult to determine due to propagation effects on the signal, multipath being the major source of problems. Figure 1.1 illustrates the multipath effect, where two rays (the direct and indirect) are reflected from the target back to the receiver via different paths. The combination of the target (direct) and image (indirect) signals, which are essentially coherent, results in a complex returned signal that often confuses conventional tracking radars. In addition to this basic physical problem, an enemy may try to further confuse the tracking radar by making use of frequency jamming techniques. The purpose of this contract was to assist the Surface Radar Section at the Defence Research Establishment Ottawa (DREO) with carrying out certain aspects of research on multi-function radar (MFR); the major emphasis being placed on Electronic Counter Counter Measures (ECCM) of MFR, including sidelobe and main-beam nulling of jamming signals. The studies were carried out using a combination of both simulated and real experimental data. The majority of the experimental data was acquired with the Experimental Array Radar System (EARS) located at the Area 5 test site located along the Ottawa river.

The EARS consisted of an inverted 'T' array configuration with a vertical eight element array for the main beam, centred just above a horizontal eight element array intended for use as the sidelobe canceller (SLC) array. A Rotman lens system was attached to the horizontal array to perform instantaneous RF beamforming; however, a switch was also installed in the SLC array to bypass the Rotman lens and allow conventional (eg. Fourier) beamforming to be done while analysing the data. This provided a means of testing the ability of the Rotman lens. A special feature of the new EARS was the inclusion of a data acquisition system for sampling signals from multiple range cells on a single scan. Each radar pulse was sampled with a 20 MHz sampling rate at the IF (4 MHz) for each of

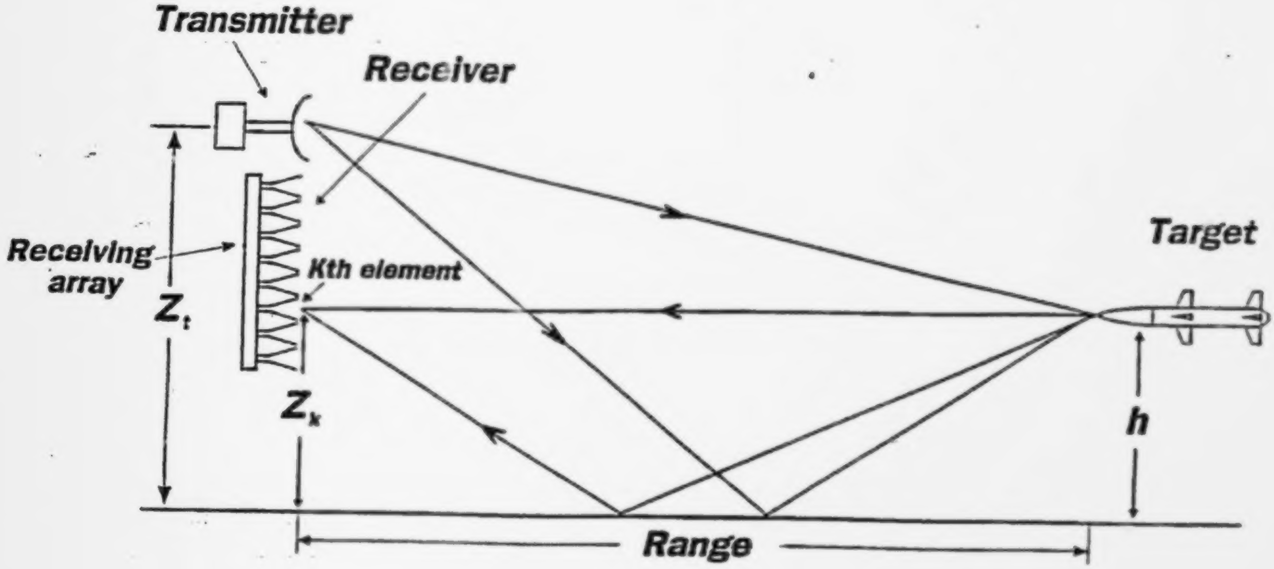
Transmitter
Receiver
Receiving array
Kth element
Z_t
Z_k
Target
h
Range

$$RC=\rho e^{-j\phi}$$

Figure 1.1 The low-angle tracking problem: RC is the reflection coefficient, ρ is the magnitude of RC and ϕ is the phase change on reflection.

the 16 channels of the combined horizontal and vertical arrays, and the pulse repetition rate was usually around 1000 Hz. Sampling at IF meant that In-phase (I) and Quadrature (Q) signals could be generated from this data by means of a Hilbert Transform, providing better results than would ordinarily be obtained by conventional electronic methods of quadrature sampling.

1.2 AIT Project Organization

TheHxanagement structure used in this contract was as outlined in the proposal for "Multi-Function Radar Simulation and ECCM Data Analysis- Part I- Technical and Management Proposal". This will be restated in Section 2 of this report.

1.3 Statement of Work

The statement of work was divided into 3 main tasks:

1) Main-Beam and Sidelobe Canceller Data Analysis
2) MFR System Study
3) Radar Trial Support

Except for 3), each of the main headings given above consisted of several additional sub tasks as will be shown in the report to follow.

1.3.1 Main-beam and Side-lobe Canceller Data Analysis

This task was divided into two major sections a) and b) which were further subdivided into three parts. Task 1a) consisted of: i) developing and implementing software to evaluate main-beam and side-lobe jammer cancellation algorithms supplied by the Scientific Authority using simulated data, ii) calibrating and formating the experimental array radar data for processing by the anti-jamming software developed in i), iii) evaluating the performance of the anti-jamming algorithms using the data processed in ii). Task 1b) consisted of: i)generating In-phase and Quadrature components from the intermediate frequency data (of the upgraded EARS) using standard algorithms, ii) calibrating and processing the experimental data for input into the anti-jamming software implemented in 1a), and iii) performing a sensitivity analysis on the algorithms using the EARS data and documenting the results.

1.3.2 MFR System Study

On a pervious contract a two-dimensonal phased array simulator was developed by Ms Wilkinson, in cooperation with the Scientific Authority, to evaluate azimuth and elevation phase-monopulse performance in the presence of multipath and ships motion. The simulator included the following features:

i) the antenna configuration.
ii) multipath simulation
iii)antenna beam manipulation to simulate beam steering with electronic stabilization, beamforming with Taylor and Bayliss aperture weighting for the sum and difference channels respectively, and array positioning due to ships motion.

The purpose of this task was to modify the above simulator to aid in the evaluation of the effect of multipath on jammer suppression. The modifications to the simulator were outlined in the Statement of Work and consisted of two parts, a) and b); a) was further subdivided into five sections. Task 2a) consisted of the following modifications to the simulator: i) adding side-lobe canceller (SLC) array configurations to the simulator with the specifications of the geometry and beamforming models supplied by the Scientific Authority, ii) adding signals from up to 4 wide-band noise sources, iii) modelling the individual array elements according to specifications given by the Scientific Authority, iv) modifying the format of the data output from the simulator to be of the form used by the anti-jamming algorithms developed in Task 1, v) simulating threat scenarios as set out by the Scientific Authority, and evaluating the performance of the anti-jamming algorithms developed in Task 1, with documented results. The purpose of Task 2b) was to evaluate the performance of the phased array antenna for azimuth and elevation monopulse (target) direction estimation, and refined maximum likelihood (RML) elevation estimation.

1.3.3 Radar Trial Support

The purpose of this task was to support radar trials at Area 5 and possibly other locations by aiding in the definition of experiments, assisting with data collection and system troubleshooting and helping to perform on-site analysis of logged data as required by the Scientific Authority.

2.0 Contract Management

Mr. Ed Riseborough of the DREO-Surface Radar Section was the Scientific Authority for duration of the contract. He was responsible for handling contracting matters (for DREO), specifying objectives, setting time-frames, stating the technical approach desired, and resetting priorities according to the changing circumstances of the research. A continual interaction was maintained between the Scientific Authority and contract personnel to determine progress and obtain results which would orient the direction of the research. A project Manager was supplied by AIT to ensure that the contracted commitments were met and a Project Leader was also supplied to provide the necessary technical leadership and supervision on site.

2.1 Project Team Organization:

The nature of the AIT Project Team is identified below and the AIT Systems Organization Chart during the period of the contract is shown in Figure 2.1.

Position Title	**Responsibilities**
Project Manager	Contract Management
Project Leader/ Scientific Analyst	Tasking and Scheduling Review of Documentation Technical coordination Data Analysis Scientific Reporting Trials Support
Senior Programmer	Assist Scientific Analyst

2.2 Project Control

A set of task sheets was prepared for the Scientific Analyst and the Senior Programmer. These were accepted by the Scientific Authority (see Appendix C). Monthly reports of activities were also produced (see Appendix F).

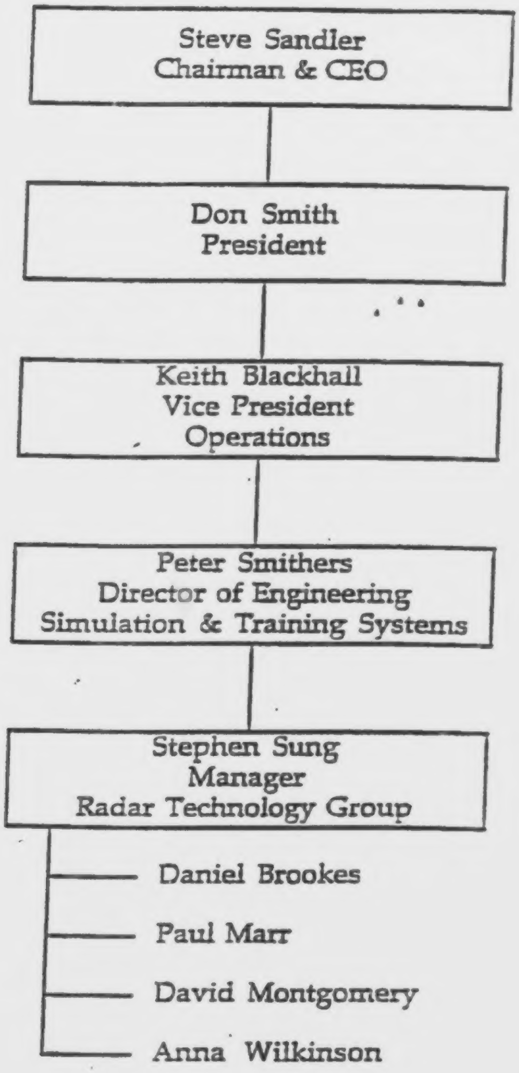
Steve Sandler
Chairman & CEO
Don Smith
President
Keith Blackhall
Vice President
Operations
Peter Smithers
Director of Engineering
Simulation & Training Systems
Stephen Sung
Manager
Radar Technology Group
Daniel Brookes
Paul Marr
David Montgomery
Anna Wilkinson

Figure 2.1 AIT Organization Chart Involving the Radar Technology Group

3.0 Main Beam and Sidelobe Canceller Data Analysis

3.1 Task 1a) i)-Simulation Studies of Anti-jamming Algorithms.

To carry out realistic simulations of the main-beam and side-lobe canceller algorithms, the data was generated by software using a realistic model of the Experimental Array Radar System (EARS) at Area 5. The software also included the option of assuming a more idealistic model employing omnidirectional elements for the receiver arrays. The most recent version of the main routine for the data generation software, called SIMGAUSJAM, contained the following options:

a) data generation with or without multipath with adjustable output signal to noise ratio
b) data generation using realistic or idealistic receiver elements
c) simulated narrow band cw (deterministic) jammer; ie jammer with constant amplitude
d) simulated narrow-band Gaussian noise jammer with adjustable signal to jammer power ratio.

As mentioned, the EARS consisted of two perpendicular arrays; the vertical, or main-beam, eight element array was centred just above a horizontal eight element array. The horizontal array was used as the sidelobe canceller (SLC) array. It included a Rotman lens for doing instantaneous RF beamforming as well as a switch for bypassing the lens and doing digital (Fourier) beamforming in postprocessing of the data. The Rotman lens was not included in any simulations but was replaced by digital beamforming.

The geometry of the EARS is shown in Figure 3.1.1. The main beam array consisted of eight horn-pair elements equally spaced over an aperture of 0.875 metres. Each half of a horn-pair was a pyramidal horn 6.25 cm in height by 4.0 cm in width and approximately 12.5 cm in length. The outputs of each half of a horn-pair were combined to give a single output. The horizontal array consisted of eight Narda 640 standard gain, pyramidal horns equally spaced over an aperture of 1.0 metre. Each Narda horn had dimensions of approximately 7.86 cm in height by 5.95 cm in width and a length of about 12.86 cm. Both the horizontal and vertical array were set up to receive microwave radiation with the E field horizontally polarized. The 1.4 meter high parabolic reflector shown in Figure 3.1 was used to compress the azimuthal beam pattern of the vertical array to about 4.5 degrees. According to the manufacturers (i.e. STC) specifications, the reflector was arranged to allow a 20 cm overlap at each end of the vertical array. It had an F/D ratio of 0.3, a focal length of 36 cm and an offset aperture of 60 cm.

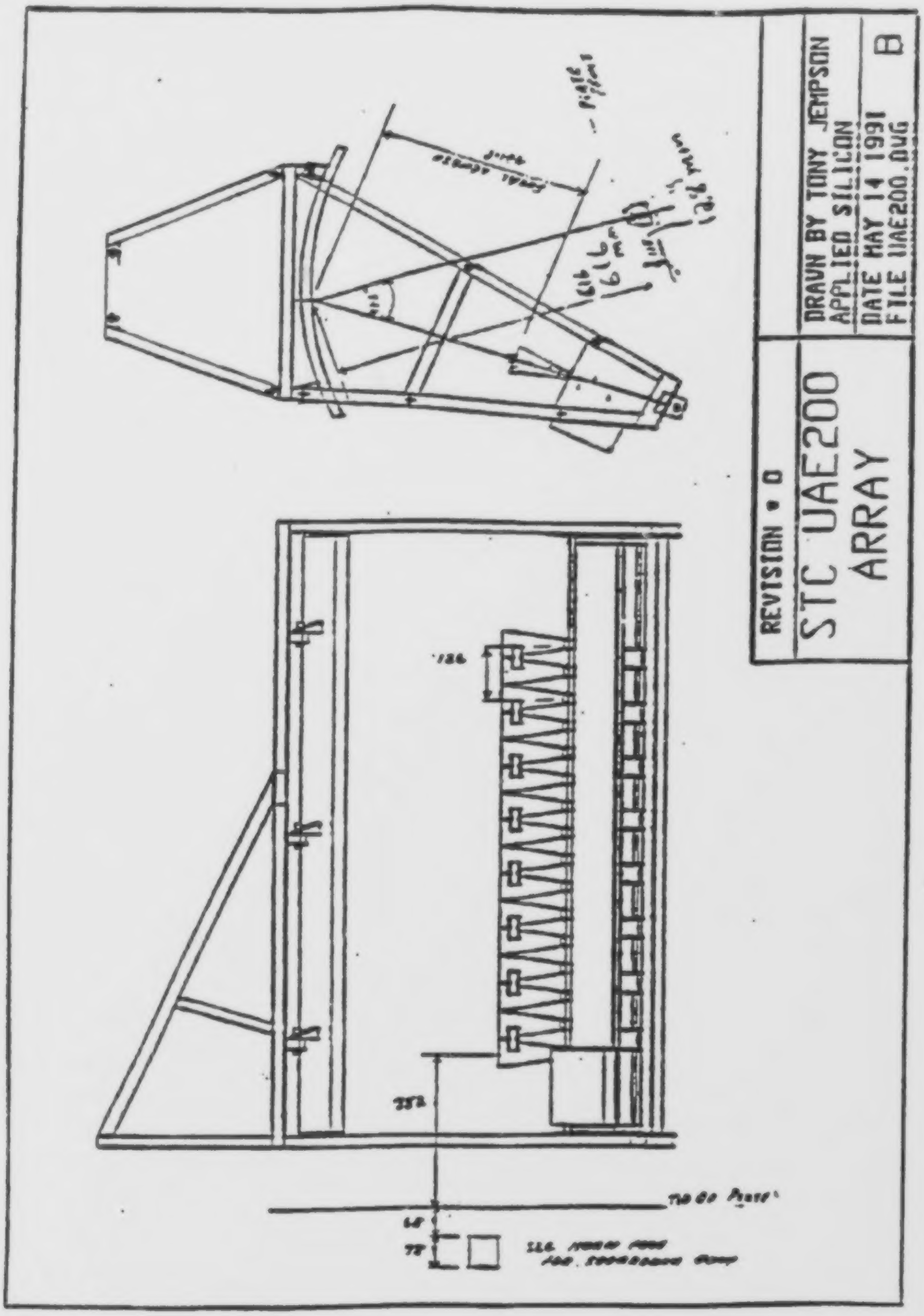
REVISION • 0
STC UAE200
ARRAY
DRAWN BY TONY JEMPSON
APPLIED SILICON
DATE MAY 14 1991
FILE UAE200.DWG
B

Figure 3.1.1 Scale drawing of the vertical main-beam array.

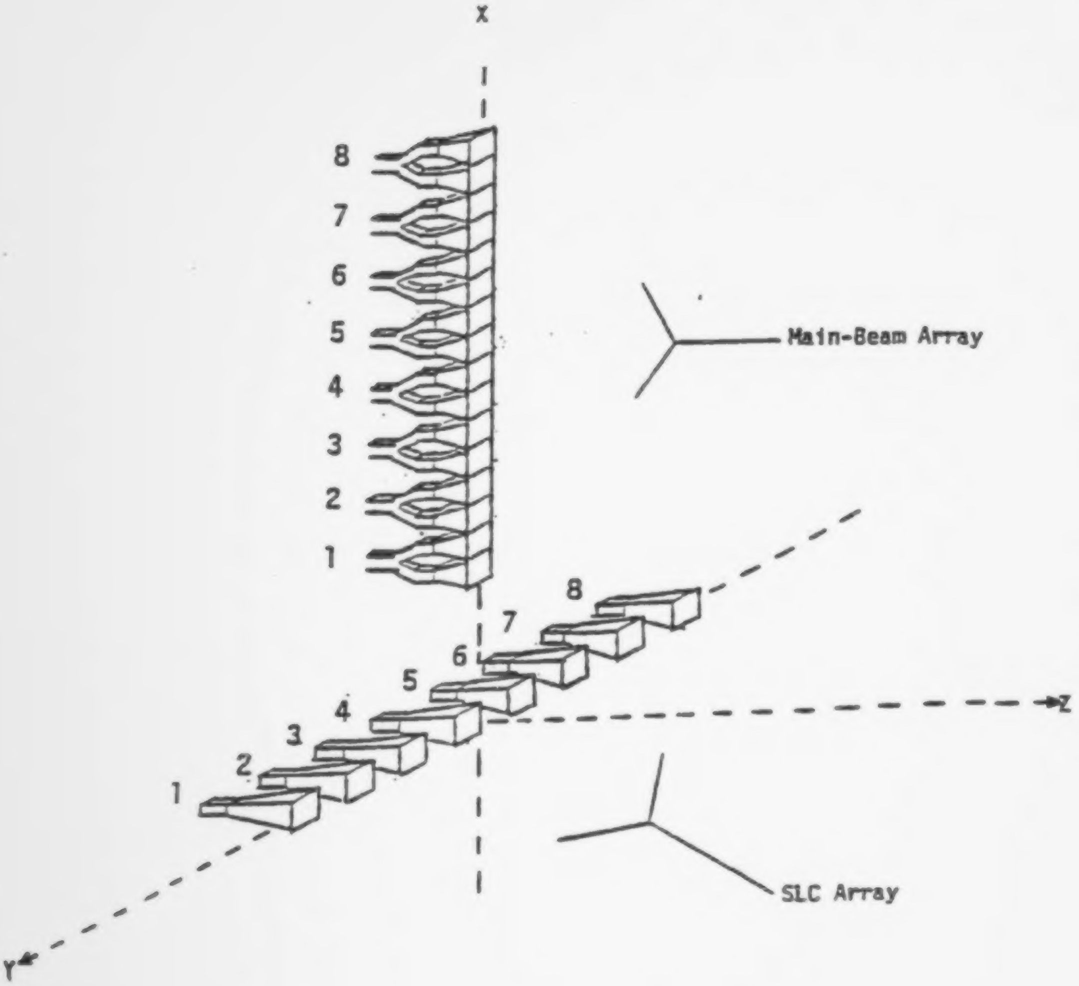
X
8
7
6
5
4
3
2
1
Main-Beam Array
8
7
6
5
4
3
2
1
Z
Y
SLC Array

Figure 3.1.2 Schematic diagram of the receiver system used in the simulations.

The feed column pointing angle was set to 45 degrees. The reflector itself was not included in the simuation software for the purposes of these studies and the resulting configuration is shown in Figure 3.1.2. More details of the antenna modelling can be found in the final report for the contract entitled "Multi-Function Radar Electronic Counter Counter Measure Studies" under SSC file no. 027ST.W7714-2-9607.

The subroutines used for modelling the more realistic data for the vertical and horizontal arrays were called BEAMPAT1 and BEAMPAT2 respectively. and the subroutine for simulating the signals received by an array with idealistic omnidirectional elements was named BEAMPAT0.

Since the source code for the first two subroutines was included in a previous report, it was not included in this one; however, a listing for BEAMPAT0 is included along with a listing of all the other software developed and used in this contract in a separate volume that was presented to the Scientific Authority. A list of the names of these programs and subroutines is included in Appendix D. The documentation of the software was presented in a separate volume because the amount of software developed under this contract was too large to be practically included in this report.

These subroutines were written in Fortran 77 and originally developed for a micro-VAX system, but were later imported for use in software developed for the SUN workstation. The SUN became the primary analysis platform after the array processor attached to the VAX 3800 became defective. The subroutine simulating the signals from the horizontal array was called by the main program in the following manner:

```
CALL BEAMPAT1(HRX,HTARG,RT,FREQ,SIGD,SIGI,THETA,SWH)
```

where

HRX = input height of the receiver element
HTARG= input height of the radiation source
RT = input horizontal distance between source and receiver
FREQ = input frequency of the radiation source in GHz
SIGI = complex output signal representing the beam pattern of the indirect (reflected) beam.
SIGD = complex output signal representing the beam pattern of the direct beam.
THETA = input azimuthal angle of radiation source off boresight
SWH = Significant Wave Height, a statistical measure of the surface roughness

Similarly, the subroutine for generating the received signal in the vertical array was called from the host routine as follows:

CALL BEAMPAT2(HRX,HTARG.RT.SIGD.SIGI,FREQ,THETA,I,SWH)

where I represents the index of the SLC receiver element, and the other eight parameters have the same meaning as in BEAMPAT1. Each of the above subroutines used FRESNEL and DREFCO for calculating the Fresnel functions, and estimating the surface reflection coefficient respectively. The reflection coefficient was calculated under the assumption of horizontal polarization.

The calling sequence and parameters for BEAMPAT0 were identical to that of BEAMPAT1, ie

CALL BEAMPAT0(HRX,HTARG,RT,FREQ,SIGD,SIGI,THETA,I,SWH)

The majority of the simulation studies were done to evaluate main-beam anti-jamming algorithms including Subspace Evaluation Without Eigenvectors (SEWE), Eigen Decomposition (ED), and Sampled Matrix Inversion (SMI).

The basis of the main-beam jammer cancellation techniques was to remove the jammer interference from the signal data using projection methods for adaptive beamforming. Each of the three methods listed involved the modification of the jammer plus noise covariance matrix (**R**) to generate the required projection matrix.

Ideally, a projection matrix (**P**) applied to a signal vector (**S**) containing the target (**T**) and jammer (**J**) signals will remove the jammer leaving only the target; ie

$$\mathbf{PS} = \mathbf{P(T+J)} = \mathbf{T}$$

With SMI the projection matrix is simply given by the (normalized) inverse of the jammer plus noise covariance matrix; ie $\mathbf{P} = \alpha\mathbf{R}^{-1}$. For an eight element linear array looking straight ahead, the normalization factor α is given by the formula:

$$\alpha = \sqrt{8}/| \mathbf{P}w |$$

where w^t=(1,1,1,1,1,1,1,1) is the array steering vector.

In the Eigendecompsition method, the projection matrix is constructed from the eigenvectors of the covariance matrix corresponding to the largest eigenvalues according to the formula:

$$\mathbf{P}=\mathbf{I}-\sum_{m=1}^{M}\mathbf{r}_m\mathbf{r}_m^H$$

where **I** is the identity matrix, $\mathbf{r}_m$ is the eigenvector of the m th largest eigenvalue, and M is the number of jammer signals to be removed. In the SEWE technique the eigenvectors are replaced by orthonormal basis vectors constructed from the rows (or columns) of the covariance matrix using Gram-Schmidt ortho-normalization.

The usefulness of the projection technique can be illustrated by using an example in which the noise is neglected and only one jammer is assumed, so that the covariance matrix is given by:

$$\mathbf{R} = \mathbf{J}\,\mathbf{J}^H$$

and the resulting orthornormal basis vector is just $\mathbf{J}/|\mathbf{J}|$. The resulting projection matrix applied to the target plus jammer signal gives:

$$\begin{aligned}\mathbf{PS} &= (\mathbf{I}-\frac{\mathbf{J}\mathbf{J}^H}{|\mathbf{J}|^2})(\mathbf{T}+\mathbf{J})\\ &= \mathbf{T}-(\frac{\mathbf{J}^H\mathbf{T}}{|\mathbf{J}|^2})\mathbf{J}\end{aligned}$$

If the jammer signal and the target signal vectors are sufficiently orthogonal then the above equation reduces to the desired result, i.e. **PS=T**

A MATLAB function called PMAKE.M was written to generate the required projection matrices from the jammer+noise covariance matrix, **R**. The inputs to the subroutine were simply the covariance matrix ,'cov1', and a parameter named 'ptype' for selecting the required projection method. The parameter ptype had only four possible values: ptype=0 would simply generate the identity matrix for **P**; ptype=1 would generate **P** using the SEWE technique; ptype=2 would generate **P** using the eigen decomposition method; ptype=3 would generate **P** using the SMI approach.

The procedure for carrying out the evaluation and comparison of the main-beam anti-jamming algorithms consisted of the following steps:

1) generate simulated data for N frequencies (N=1 to 4) using SIMGAUSJAM once for each frequency. This produced 2 data files for each frequency: one file of the vertical main-beam array data vectors and one file of slc array data vectors. The first 2560 data vectors of each file contain off-target data (ie jammer+noise signals) and the next 5120 sets of data correspond to the combined target+jammer+noise signals. The 5120 sets of data were broken up into 20 sets of 256 in which each setcorresponded to a different target height (constant range); the target height varied from 5m to 205m in 10m steps. To simulate a moving target, an artificial Doppler shift could be injected into the simulated signal. Each data vector was composed of 8 complex signals corresponding to the output of each receiver element of the main-beam array or slc array. For the present study only the main-beam data was used.

2) Analyse the data generated in 1) using the software package MULTIFRML. This software processed the data using the following steps:

a) read M off-target data vectors from each of the N data files.

b) use the results of a) to generate N jammer+noise covariance matrices.

c) generate N projection matrices (P_1 to P_N) from each of the N covariance matrices using one of 3 possible techniques: SEWE, ED or SMI.

d) apply the projection matrices to each data vector from the on-target data containing the (target+jammer+noise) signals for the corresponding frequency to remove the jammer.

e) In the case of a moving target, perform a 256 point time domain fast Fourier transform (FFT) using NFFT data points with zero filling (if NFFT was less than 256) on the resultant data vectors to separate the Doppler shifted target signal from other sources; or in the case of a stationary target do a simple average over NFFT points.

f) apply the modified data vectors to a target direction estimation algorithm such as the refined maximum likelihood (RML) method.

g) for each snapshot of NFFT data vectors plot the FFT power spectrum and indicate the Doppler frequency of the peak selected for RML processing, and show the baseline used to calculate the output peak to background (also referred to as the output signal to noise or signal to jammer+noise) ratios. The Doppler bin of the target signal for each frequency, along with the array output signal to background ratio for each frequency was saved to a data file called dbin*.dat and snr*.dat respectively (where *=1,2,3 or 4). A separate plot of the RML estimator vs height (with the height of the maximum estimator shown on the plot) was also created and the results saved in a file named htrmle.dat To save paper, 8 snapshots (2 plots each) of data were plotted on a single page. These plots were used to help spot any anomalies in the data. A typical example of such a series of plots is shown in Figure 3.1.3. This series of plots displays the results for 3 frequencies for the first 8 snapshots of datawhere each snapshot constists of 64 data vectors. In the FFT plots, the power spectra have been shifted 30 dB relative to each other, and the peak frequency pointer was removed to make it easier to distinguish the three sets of data.

3) Using MATLAB software, plot the estimated target height vs snapshot, the rml estimator vs snapshot and the array output signal to background level vs snapshot on separated graphs of the same page for comparison.

The above series of steps was carried out for a variety of scenarios considering the following parameters:

1) The effects of varying the output signal to noise ratio (SNR)

2) The effects of varying the output signal to jammer ratio (SJR)

3) The effects of varying the jammer height. Only two heights wereconsiderred: 2m and 50m. The 2 m height was intended as a simulation of the situation present during the September 8 1994 trials at Area 5.

4) The effect of increasing the number of frequencies to improve tracking.

5) Multipath vs free space (ie no multipath) assumptions

6) Comparison of results obtained with a narrow band deterministic jammer and a narrow-band Gaussian noise jammer.

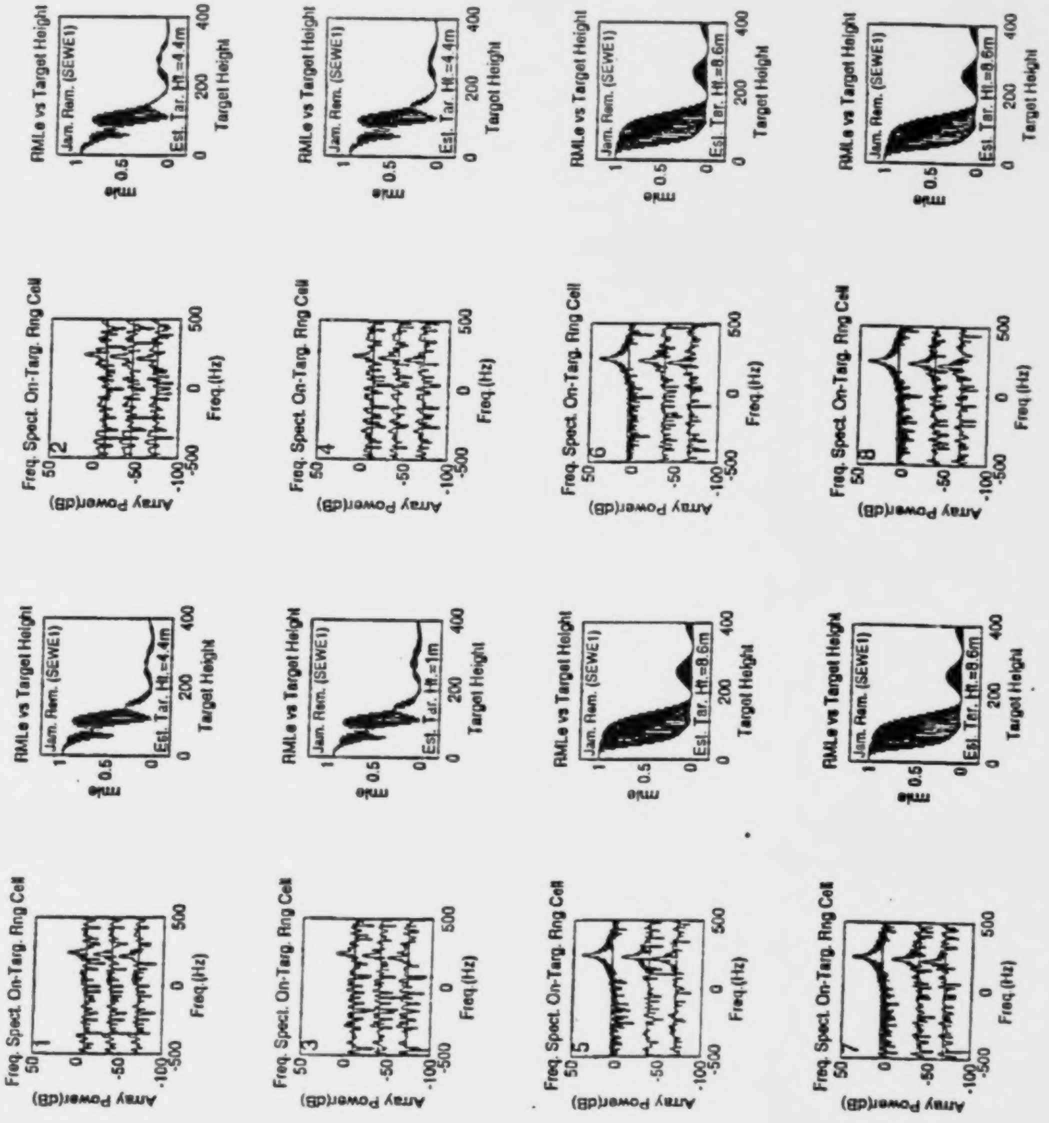
RMLe vs Target Height
Jam. Rem. (SEWE1)
Est. Tar. Ht.=4.4m
Est. Tar. Ht.=1m
Est. Tar. Ht.=8.6m
mile
1
0.5
0
Target Height
0
200
400
Freq. Spect. On-Targ. Rng Cell
1
2
3
4
5
6
7
8
Array Power(dB)
50
0
-50
-100
Freq.(Hz)
-500
0
500

Figure 3.1.3

Table 3.1.1

Jammer Type	Jammer Height (m)	Jammer Removed (y/n) (method)	Target Range (km)	Jammer Range (km)	Output SNR (dB)	Output SJR (dB)	Multi-path (y/n)	Freq. (GHz)	Elem. Type (d/o)	Fig. No.
Gauss. noise	2	n	4	2	10	30	n	8.17 9.17	d	3.1.4
Gauss. noise	2	y (SEWEI)	4	2	2	-30	y	8.17 9.17	d	3.1.5
Gauss. noise	2	n	4	2	20	30	n	8.17 9.17	d	3.1.6
Gauss. noise	2	n	4	2	2	-30	y	8.17 9.17	d	3.1.7
Gauss. noise	2	n	4	2	20	30	y	8.17 9.17	d	3.1.8
Gauss. noise	2	y (SEWEI)	4	2	2	-30	y	8.17 9.17	d	3.1.9
Gauss. noise	2	n	4	2	20	-30	y	8.17 9.17	d	3.1.10
Determ	2	y (SEWEI)	4	2	20	-30	y	8.17 9.17	d	3.1.11
Determ	2	n	4	2	20	-30	y	8.17 8.67 9.17	d	3.1.12
Determ	2	y (SEWEI)	4	2	20	-30	y	8.17 8.67 9.17	d	3.1.13
Determ	2	y (SEWEI)	4	2	20	-30	y	9.17 9.67 10.17	d	3.1.14
Determ	2	y (SEWEI)	4	2	20	-30	y	8.17 8.67 9.17 9.67	o	3.1.15
Determ	2	y (SEWEI)	4	2	20	-30	y	9.17 9.67 10.17	o	3.1.16

(continued)

Table 3.1.1 (cont'd)

Jammer Type	Jammer Height (m)	Jammer Removed (y/n) (method)	Target Range (km)	Jammer Range (km)	Output SNR (dB)	Output SJR (dB)	Multi-path (y/n)	Freq. (GHz)	Elem. Type (d/o)	Fig. No.
Determ	2	y (SEWE1)	4	2	20	-30	y	8.17 9.17 10.17	o	3.1.17
Determ	2	y (SEWE1)	4	2	20	-30	y	9.17 9.67 10.17	o	3.1.18
Determ	2	y (SEWE1)	4	2	20	-30	y	9.17 10.17	o	3.1.19
Determ	2	y (SEWE1)	4	2	20	-30	y	9.17	d	3.1.20
Determ	2	n	4	2	20	-30	y	9.17	d	3.1.21
Determ	2	y (SEWE1)	4	2	20	-30	y	9.17	d	3.1.22
Determ	2	n	4	2	30	-30	y	9.17	d	3.1.23
Determ	50	y (SEWE1)	4	2	30	-30	y	9.17	d	3.1.24
Determ	50	n	4	2	30	-30	y	9.17	o	3.1.25
Determ	50	n	4	2	30	-30	y	9.17	o	3.1.26
Determ	50	y (SEWE1)	4	2	30	-30	y	9.17	o	3.1.27

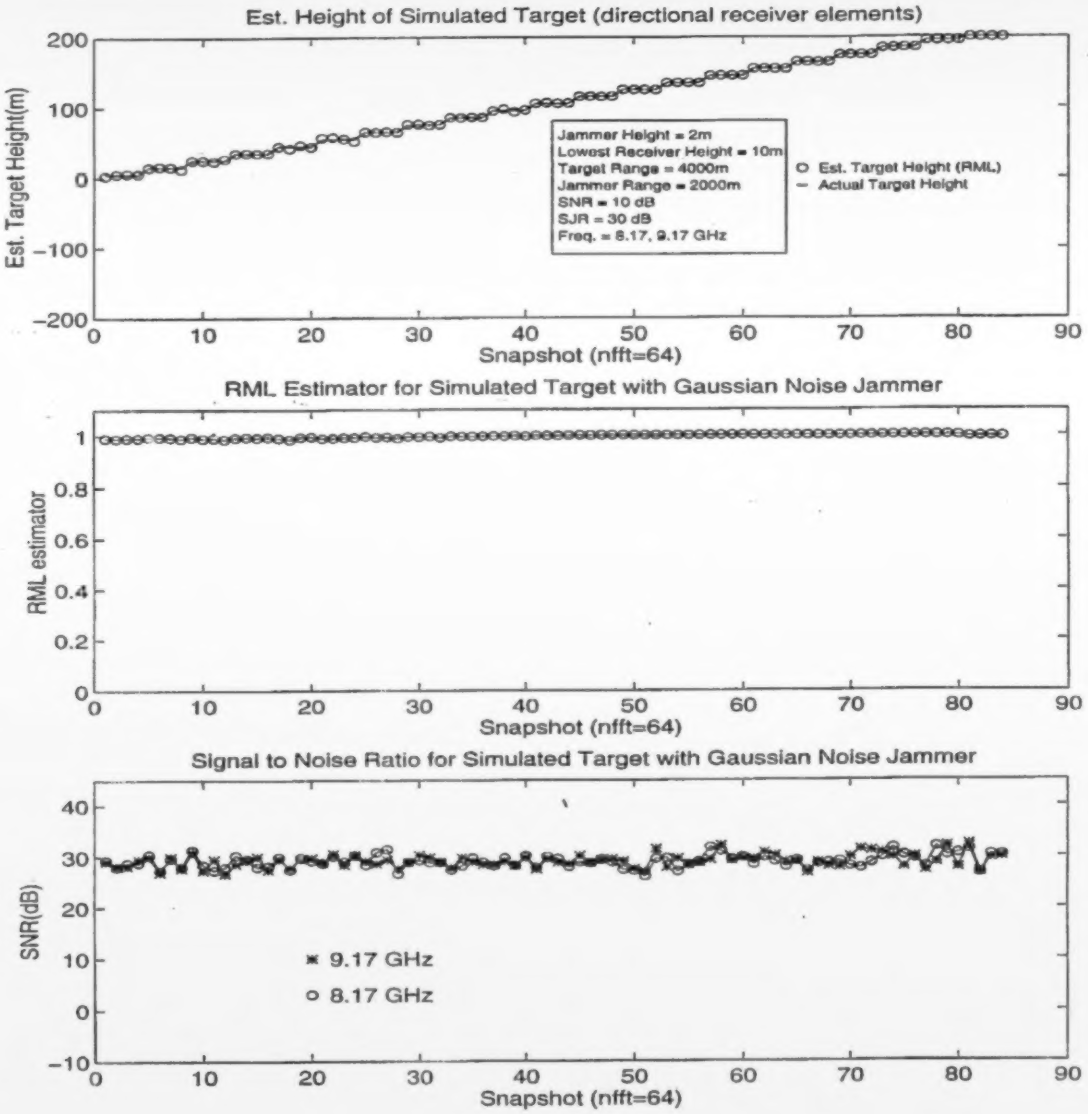
Est. Height of Simulated Target (directional receiver elements)
Est. Target Height(m)
200
100
0
−100
−200
Jammer Height = 2m
Lowest Receiver Height = 10m
Target Range = 4000m
Jammer Range = 2000m
SNR = 10 dB
SJR = 30 dB
Freq. = 8.17, 9.17 GHz
o Est. Target Height (RML)
− Actual Target Height
0
10
20
30
40
50
60
70
80
90
Snapshot (nfft=64)
RML Estimator for Simulated Target with Gaussian Noise Jammer
RML estimator
1
0.8
0.6
0.4
0.2
0
Snapshot (nfft=64)
Signal to Noise Ratio for Simulated Target with Gaussian Noise Jammer
SNR(dB)
40
30
20
10
0
−10
* 9.17 GHz
o 8.17 GHz
Snapshot (nfft=64)

Figure 3.1.4

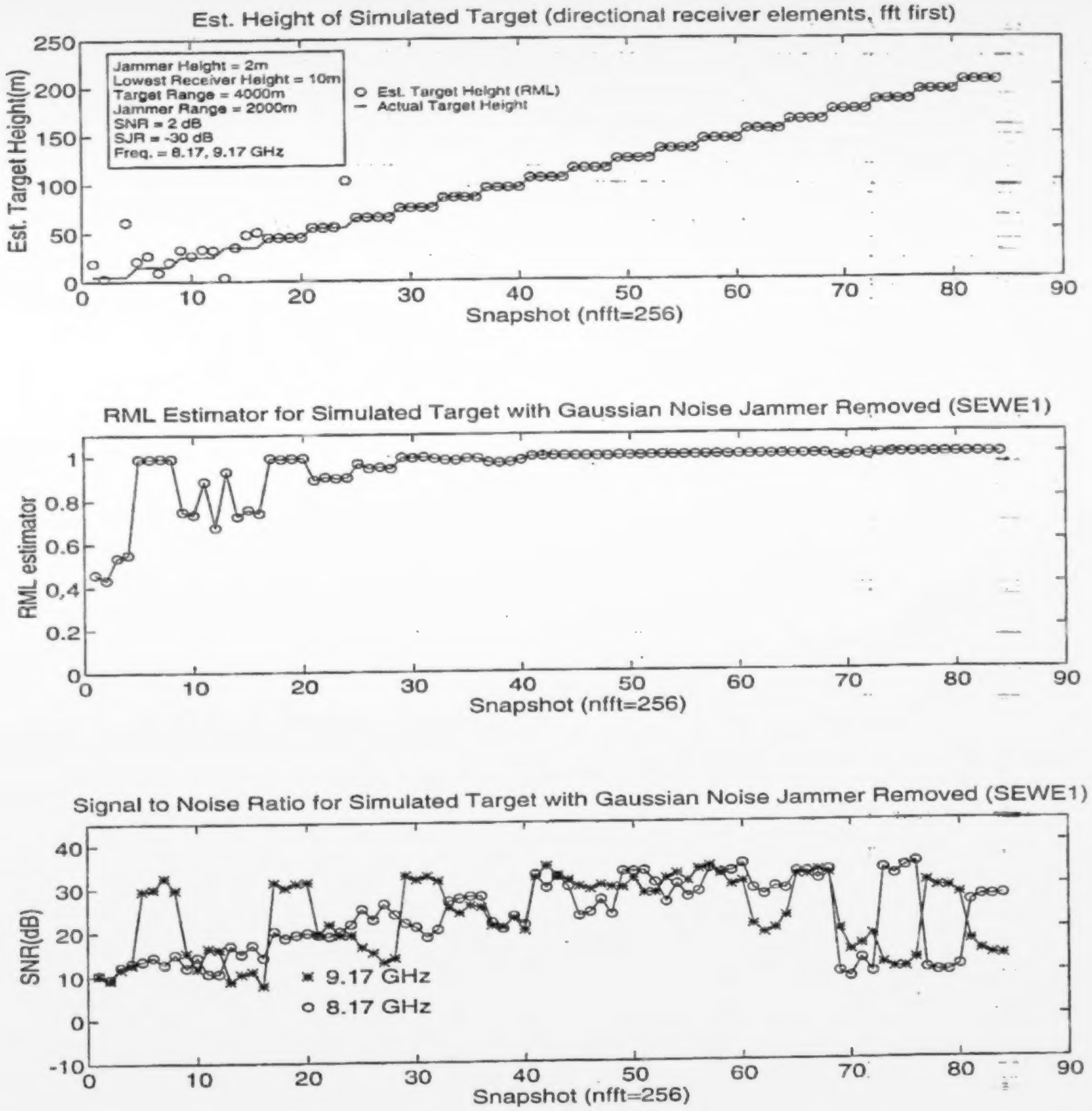
Est. Height of Simulated Target (directional receiver elements, fft first)
Jammer Height = 2m
Lowest Receiver Height = 10m
Target Range = 4000m
Jammer Range = 2000m
SNR = 2 dB
SJR = -30 dB
Freq. = 8.17, 9.17 GHz
o Est. Target Height (RML)
— Actual Target Height
Est. Target Height(m)
0
50
100
150
200
250
Snapshot (nfft=256)
0
10
20
30
40
50
60
70
80
90
RML Estimator for Simulated Target with Gaussian Noise Jammer Removed (SEWE1)
RML estimator
0
0.2
0.4
0.6
0.8
1
Snapshot (nfft=256)
0
10
20
30
40
50
60
70
80
90
Signal to Noise Ratio for Simulated Target with Gaussian Noise Jammer Removed (SEWE1)
SNR(dB)
-10
0
10
20
30
40
* 9.17 GHz
o 8.17 GHz
Snapshot (nfft=256)
0
10
20
30
40
50
60
70
80
90

Figure 3.1.5

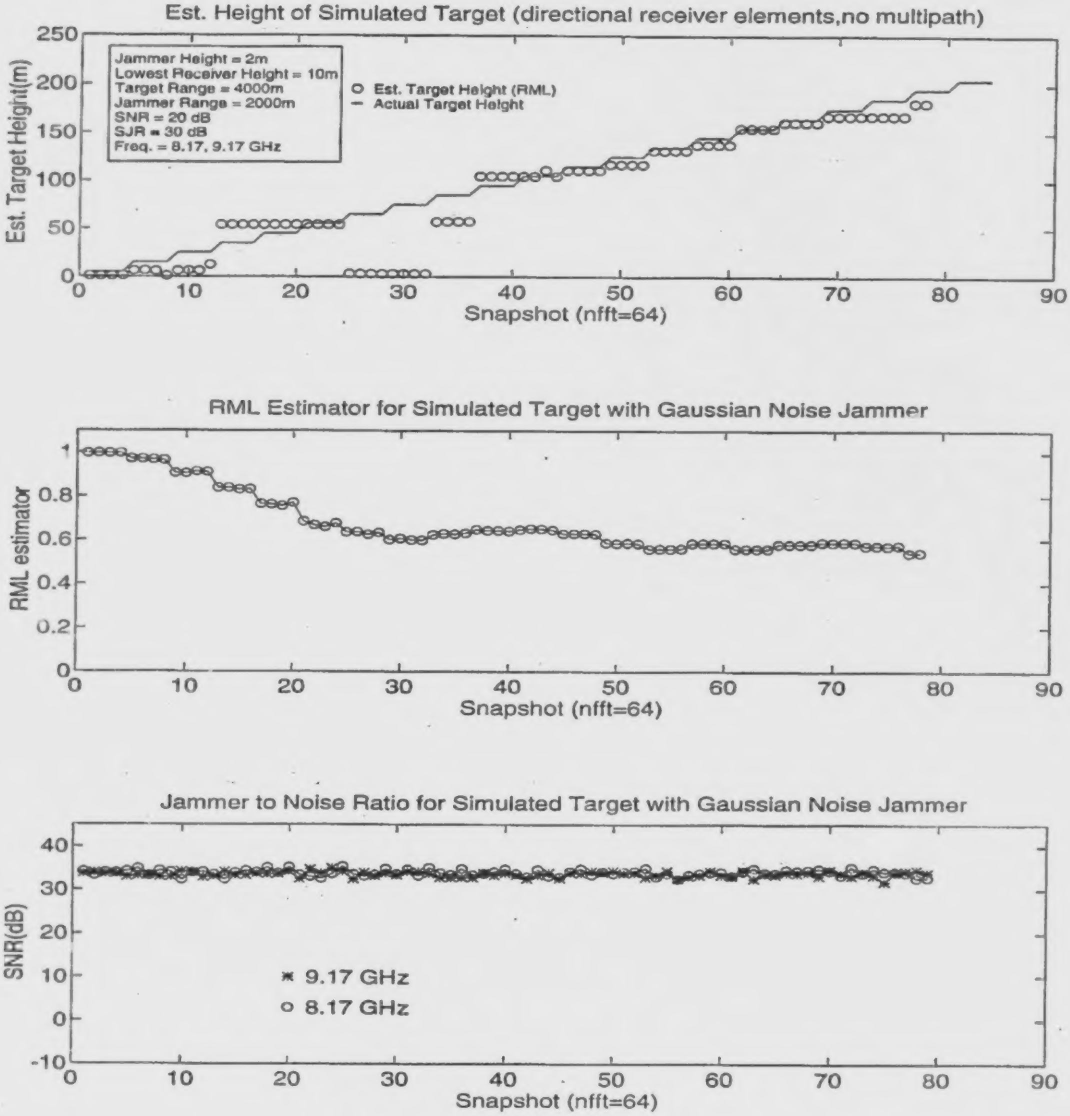
Est. Height of Simulated Target (directional receiver elements,no multipath)
Est. Target Height(m)
Jammer Height = 2m
Lowest Receiver Height = 10m
Target Range = 4000m
Jammer Range = 2000m
SNR = 20 dB
SJR = 30 dB
Freq. = 8.17, 9.17 GHz
o Est. Target Height (RML)
— Actual Target Height
250
200
150
100
50
0
0
10
20
30
40
50
60
70
80
90
Snapshot (nfft=64)
RML Estimator for Simulated Target with Gaussian Noise Jammer
RML estimator
1
0.8
0.6
0.4
0.2
0
0
10
20
30
40
50
60
70
80
90
Snapshot (nfft=64)
Jammer to Noise Ratio for Simulated Target with Gaussian Noise Jammer
SNR(dB)
40
30
20
10
0
-10
* 9.17 GHz
o 8.17 GHz
0
10
20
30
40
50
60
70
80
90
Snapshot (nfft=64)

Figure 3.1.6

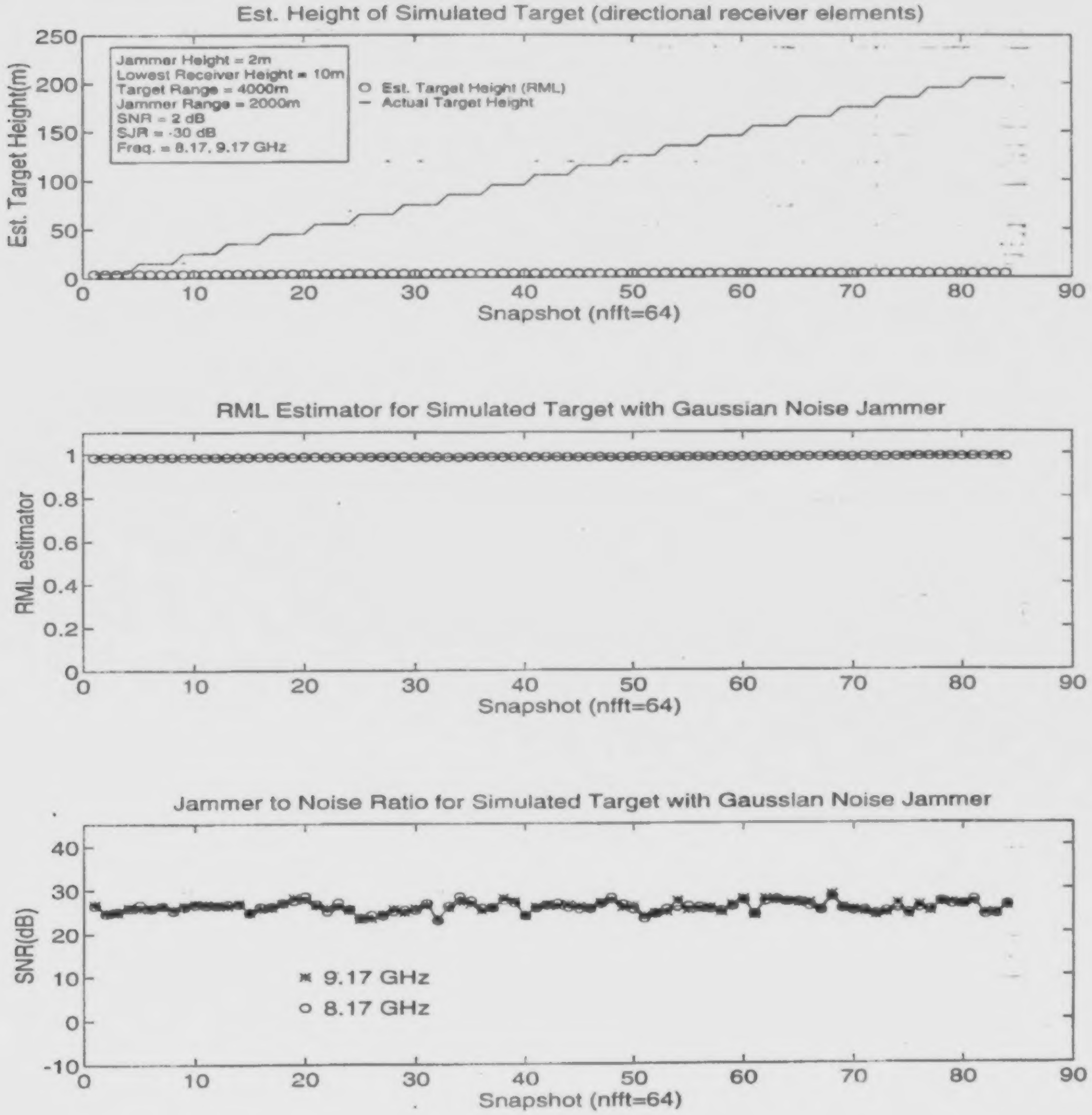
Est. Height of Simulated Target (directional receiver elements)
Jammer Height = 2m
Lowest Receiver Height = 10m
Target Range = 4000m
Jammer Range = 2000m
SNR = 2 dB
SJR = -30 dB
Freq. = 8.17, 9.17 GHz
○ Est. Target Height (RML)
— Actual Target Height
Est. Target Height(m)
250
200
150
100
50
0
0
10
20
30
40
50
60
70
80
90
Snapshot (nfft=64)
RML Estimator for Simulated Target with Gaussian Noise Jammer
RML estimator
1
0.8
0.6
0.4
0.2
0
0
10
20
30
40
50
60
70
80
90
Snapshot (nfft=64)
Jammer to Noise Ratio for Simulated Target with Gaussian Noise Jammer
SNR(dB)
40
30
20
10
0
-10
0
10
20
30
40
50
60
70
80
90
Snapshot (nfft=64)
✱ 9.17 GHz
○ 8.17 GHz

Figure 3.1.7

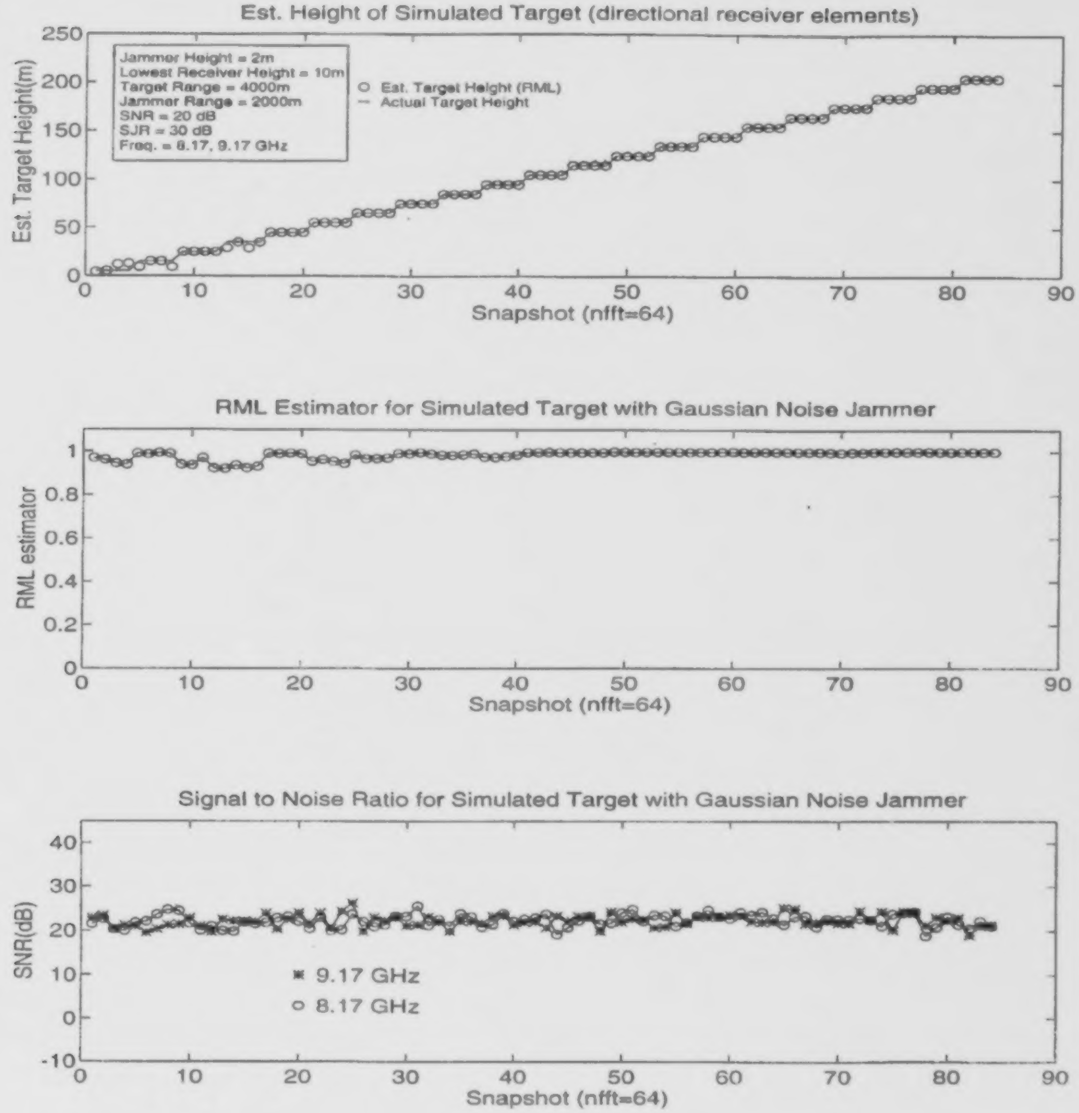
Est. Height of Simulated Target (directional receiver elements)
Jammer Height = 2m
Lowest Receiver Height = 10m
Target Range = 4000m
Jammer Range = 2000m
SNR = 20 dB
SJR = 30 dB
Freq. = 8.17, 9.17 GHz
○ Est. Target Height (RML)
– Actual Target Height
Est. Target Height(m)
250
200
150
100
50
0
0
10
20
30
40
50
60
70
80
90
Snapshot (nfft=64)
RML Estimator for Simulated Target with Gaussian Noise Jammer
RML estimator
1
0.8
0.6
0.4
0.2
0
0
10
20
30
40
50
60
70
80
90
Snapshot (nfft=64)
Signal to Noise Ratio for Simulated Target with Gaussian Noise Jammer
SNR(dB)
40
30
20
10
0
-10
* 9.17 GHz
○ 8.17 GHz
0
10
20
30
40
50
60
70
80
90
Snapshot (nfft=64)

Figure 3.1.8

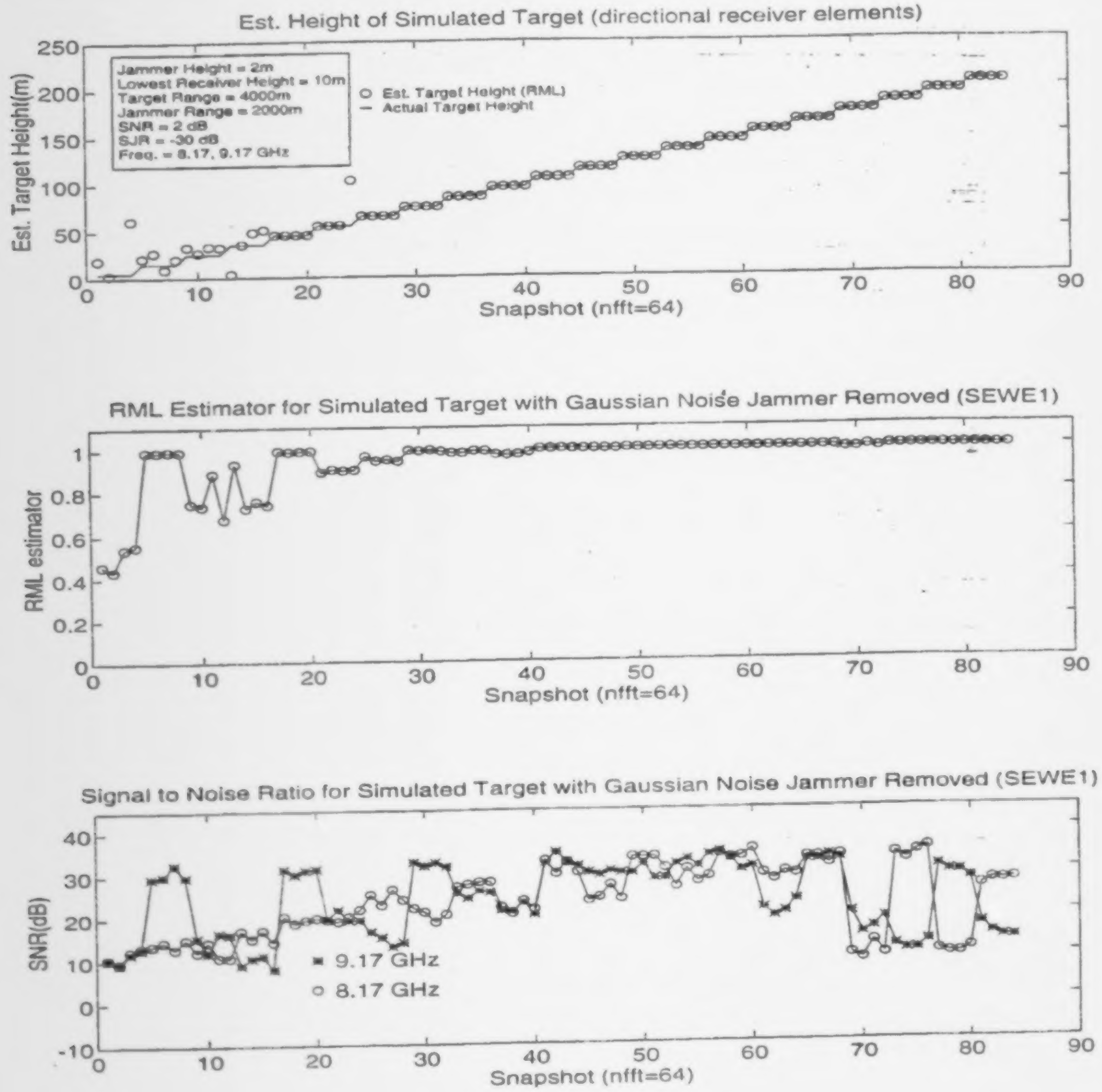
Est. Height of Simulated Target (directional receiver elements)

RML Estimator for Simulated Target with Gaussian Noise Jammer Removed (SEWE1)

Signal to Noise Ratio for Simulated Target with Gaussian Noise Jammer Removed (SEWE1)

Figure 3.1.9

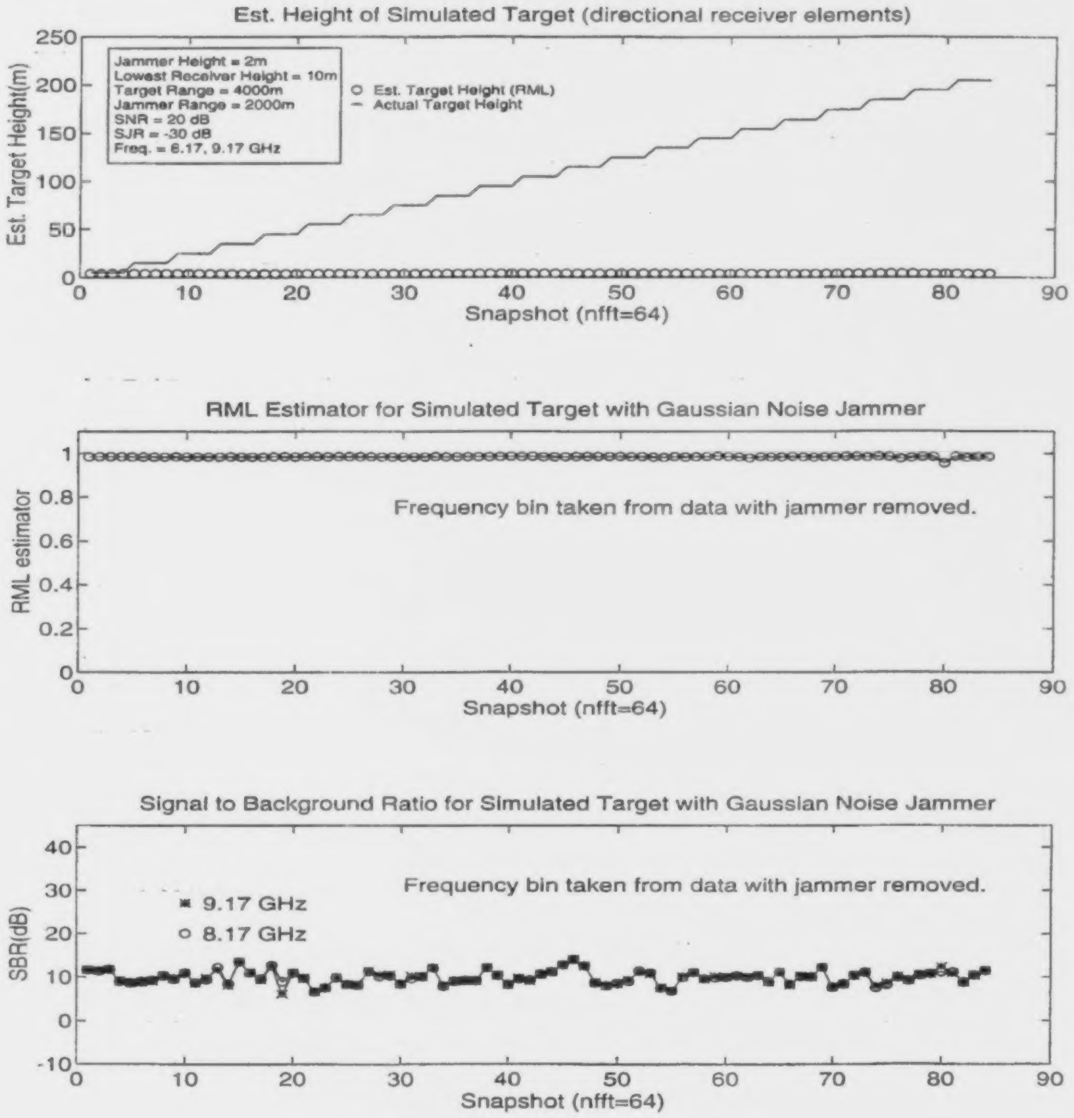
Est. Height of Simulated Target (directional receiver elements)
Jammer Height = 2m
Lowest Receiver Height = 10m
Target Range = 4000m
Jammer Range = 2000m
SNR = 20 dB
SJR = -30 dB
Freq. = 8.17, 9.17 GHz
○ Est. Target Height (RML)
— Actual Target Height
Est. Target Height(m)
0
50
100
150
200
250
0
10
20
30
40
50
60
70
80
90
Snapshot (nfft=64)
RML Estimator for Simulated Target with Gaussian Noise Jammer
Frequency bin taken from data with jammer removed.
RML estimator
0
0.2
0.4
0.6
0.8
1
Snapshot (nfft=64)
Signal to Background Ratio for Simulated Target with Gaussian Noise Jammer
Frequency bin taken from data with jammer removed.
✱ 9.17 GHz
○ 8.17 GHz
SBR(dB)
-10
0
10
20
30
40
Snapshot (nfft=64)

Figure 3.1.10

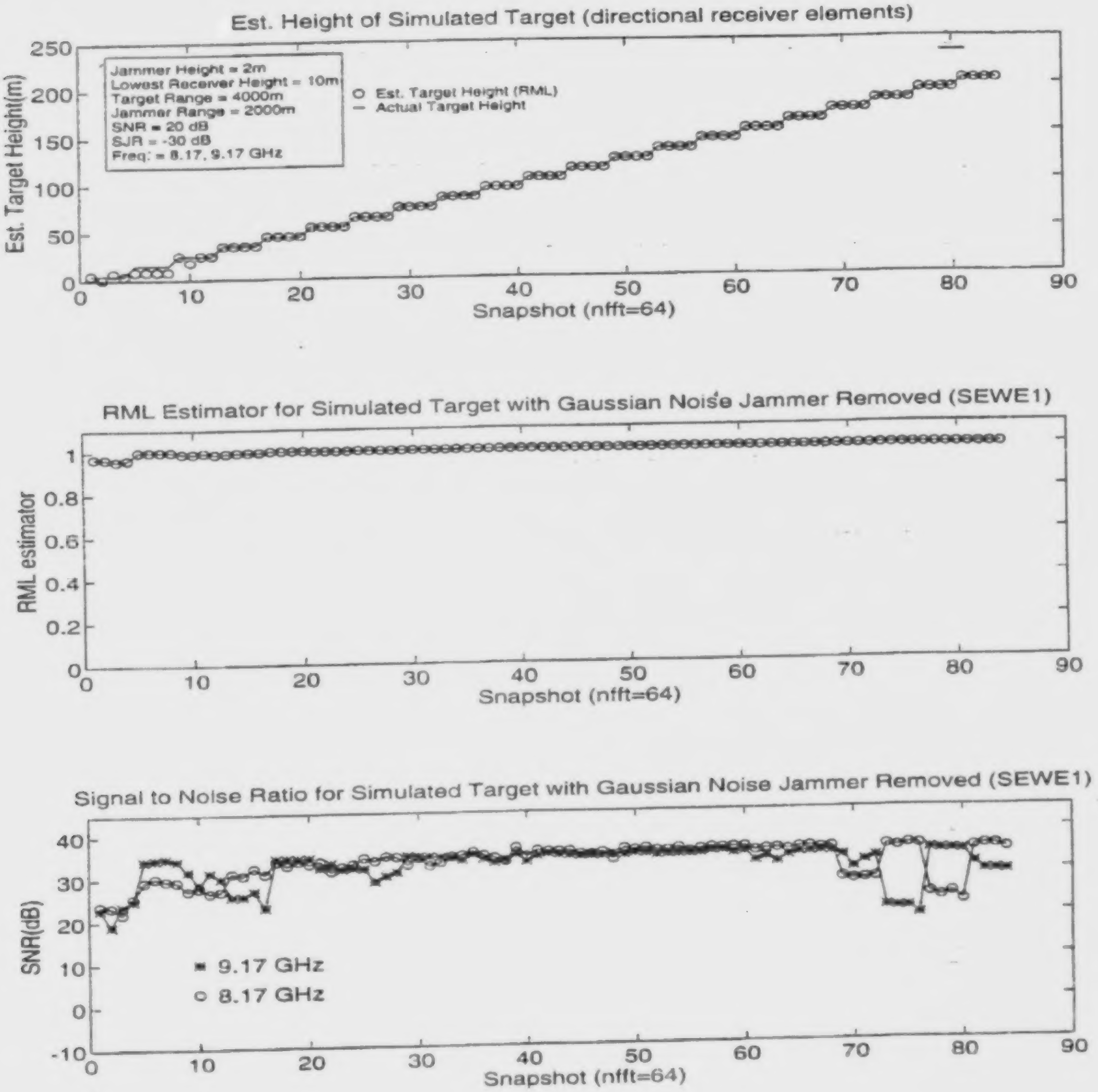
Est. Height of Simulated Target (directional receiver elements)
Jammer Height = 2m
Lowest Receiver Height = 10m
Target Range = 4000m
Jammer Range = 2000m
SNR = 20 dB
SJR = -30 dB
Freq: = 8.17, 9.17 GHz
○ Est. Target Height (RML)
— Actual Target Height
Est. Target Height(m)
0
50
100
150
200
250
0
10
20
30
40
50
60
70
80
90
Snapshot (nfft=64)
RML Estimator for Simulated Target with Gaussian Noise Jammer Removed (SEWE1)
RML estimator
0
0.2
0.4
0.6
0.8
1
0
10
20
30
40
50
60
70
80
90
Snapshot (nfft=64)
Signal to Noise Ratio for Simulated Target with Gaussian Noise Jammer Removed (SEWE1)
SNR(dB)
-10
0
10
20
30
40
* 9.17 GHz
○ 8.17 GHz
0
10
20
30
40
50
60
70
80
90
Snapshot (nfft=64)

Figure 3.1.11

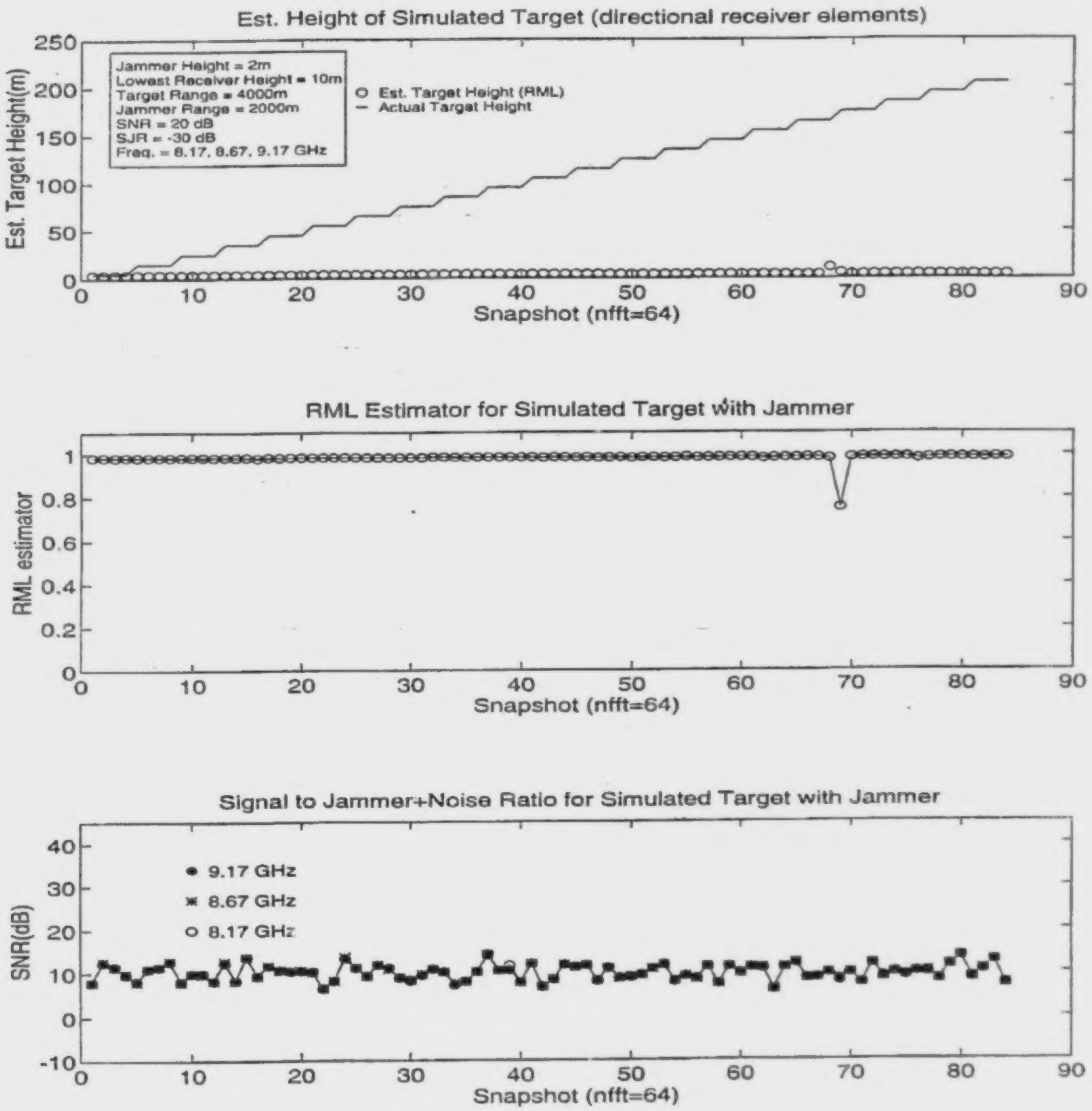
Est. Height of Simulated Target (directional receiver elements)
Jammer Height = 2m
Lowest Receiver Height = 10m
Target Range = 4000m
Jammer Range = 2000m
SNR = 20 dB
SJR = -30 dB
Freq. = 8.17, 8.67, 9.17 GHz
○ Est. Target Height (RML)
— Actual Target Height
Est. Target Height(m)
250
200
150
100
50
0
0
10
20
30
40
50
60
70
80
90
Snapshot (nfft=64)
RML Estimator for Simulated Target with Jammer
RML estimator
1
0.8
0.6
0.4
0.2
0
0
10
20
30
40
50
60
70
80
90
Snapshot (nfft=64)
Signal to Jammer+Noise Ratio for Simulated Target with Jammer
● 9.17 GHz
✱ 8.67 GHz
○ 8.17 GHz
SNR(dB)
40
30
20
10
0
-10
0
10
20
30
40
50
60
70
80
90
Snapshot (nfft=64)

Figure 3.1.12

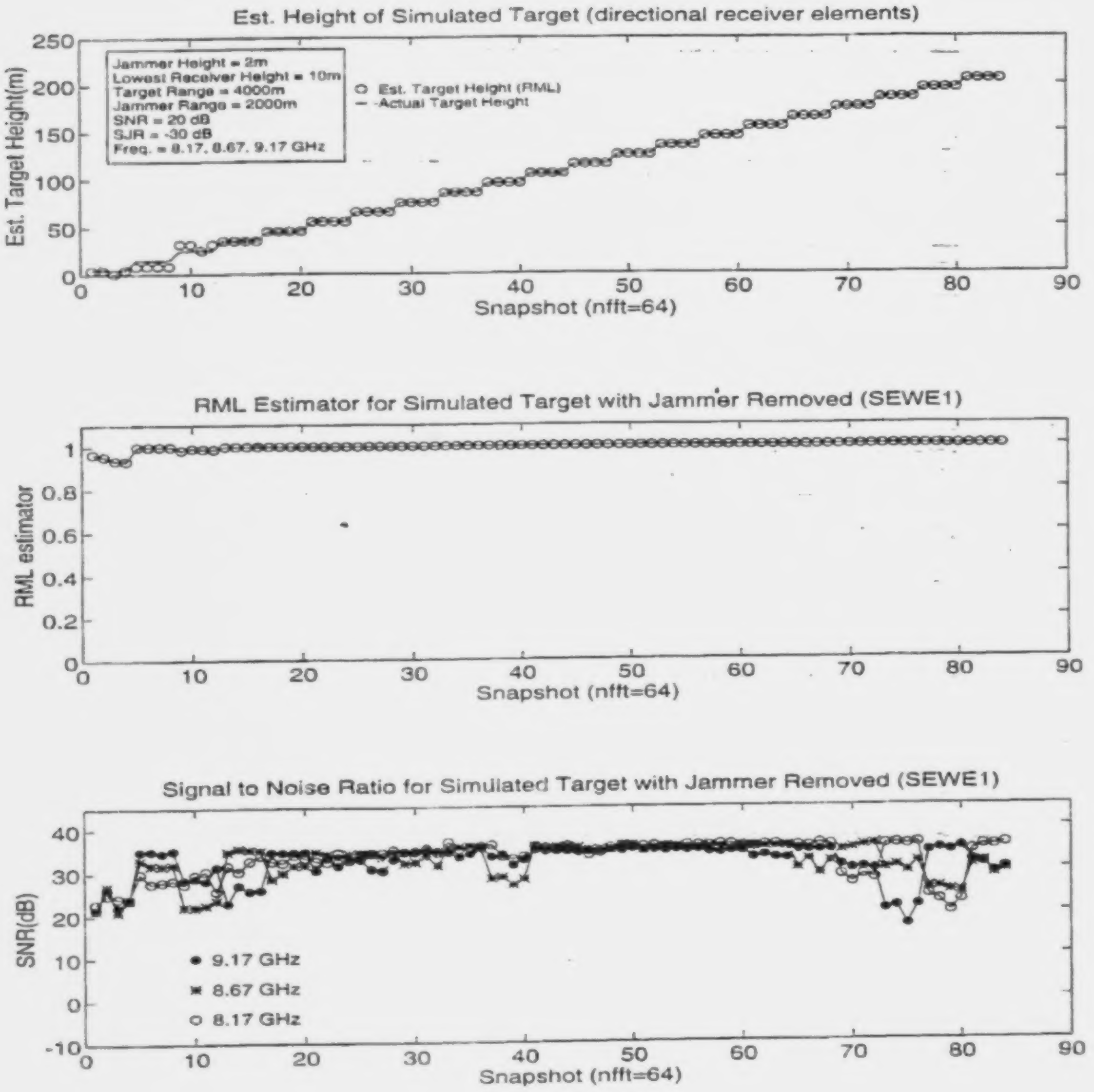
Est. Height of Simulated Target (directional receiver elements)
Jammer Height = 2m
Lowest Receiver Height = 10m
Target Range = 4000m
Jammer Range = 2000m
SNR = 20 dB
SJR = -30 dB
Freq. = 8.17, 8.67, 9.17 GHz
○ Est. Target Height (RML)
– -Actual Target Height
Est. Target Height(m)
250
200
150
100
50
0
0
10
20
30
40
50
60
70
80
90
Snapshot (nfft=64)
RML Estimator for Simulated Target with Jammer Removed (SEWE1)
RML estimator
1
0.8
0.6
0.4
0.2
0
Snapshot (nfft=64)
Signal to Noise Ratio for Simulated Target with Jammer Removed (SEWE1)
SNR(dB)
40
30
20
10
0
-10
● 9.17 GHz
✱ 8.67 GHz
○ 8.17 GHz
Snapshot (nfft=64)

Figure 3.1.13

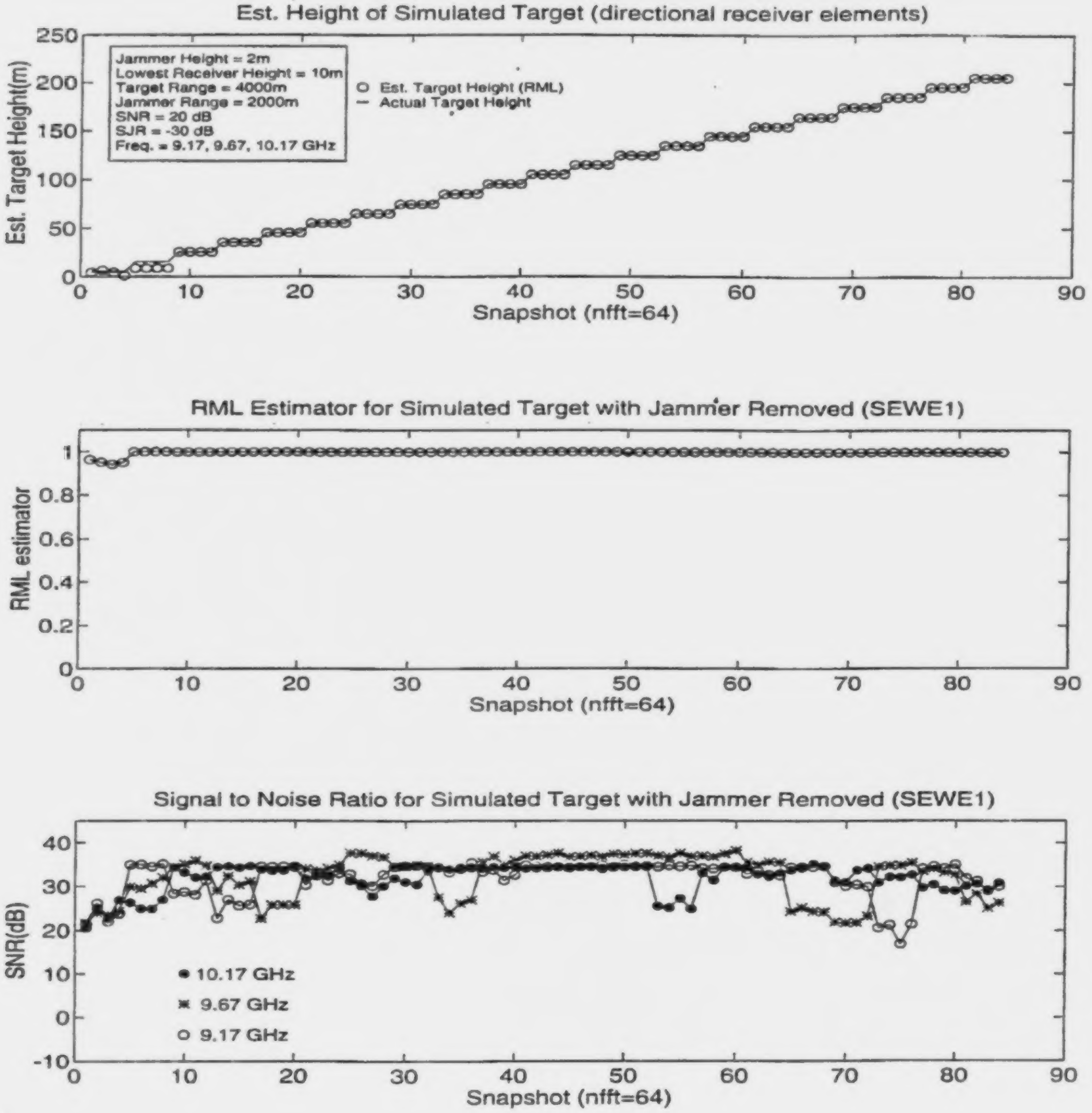
Est. Height of Simulated Target (directional receiver elements)
Jammer Height = 2m
Lowest Receiver Height = 10m
Target Range = 4000m
Jammer Range = 2000m
SNR = 20 dB
SJR = -30 dB
Freq. = 9.17, 9.67, 10.17 GHz
○ Est. Target Height (RML)
— Actual Target Height
Est. Target Height(m)
0
50
100
150
200
250
Snapshot (nfft=64)
0
10
20
30
40
50
60
70
80
90
RML Estimator for Simulated Target with Jammer Removed (SEWE1)
RML estimator
0
0.2
0.4
0.6
0.8
1
Snapshot (nfft=64)
0
10
20
30
40
50
60
70
80
90
Signal to Noise Ratio for Simulated Target with Jammer Removed (SEWE1)
SNR(dB)
-10
0
10
20
30
40
● 10.17 GHz
✱ 9.67 GHz
○ 9.17 GHz
Snapshot (nfft=64)
0
10
20
30
40
50
60
70
80
90

Figure 3.1.14

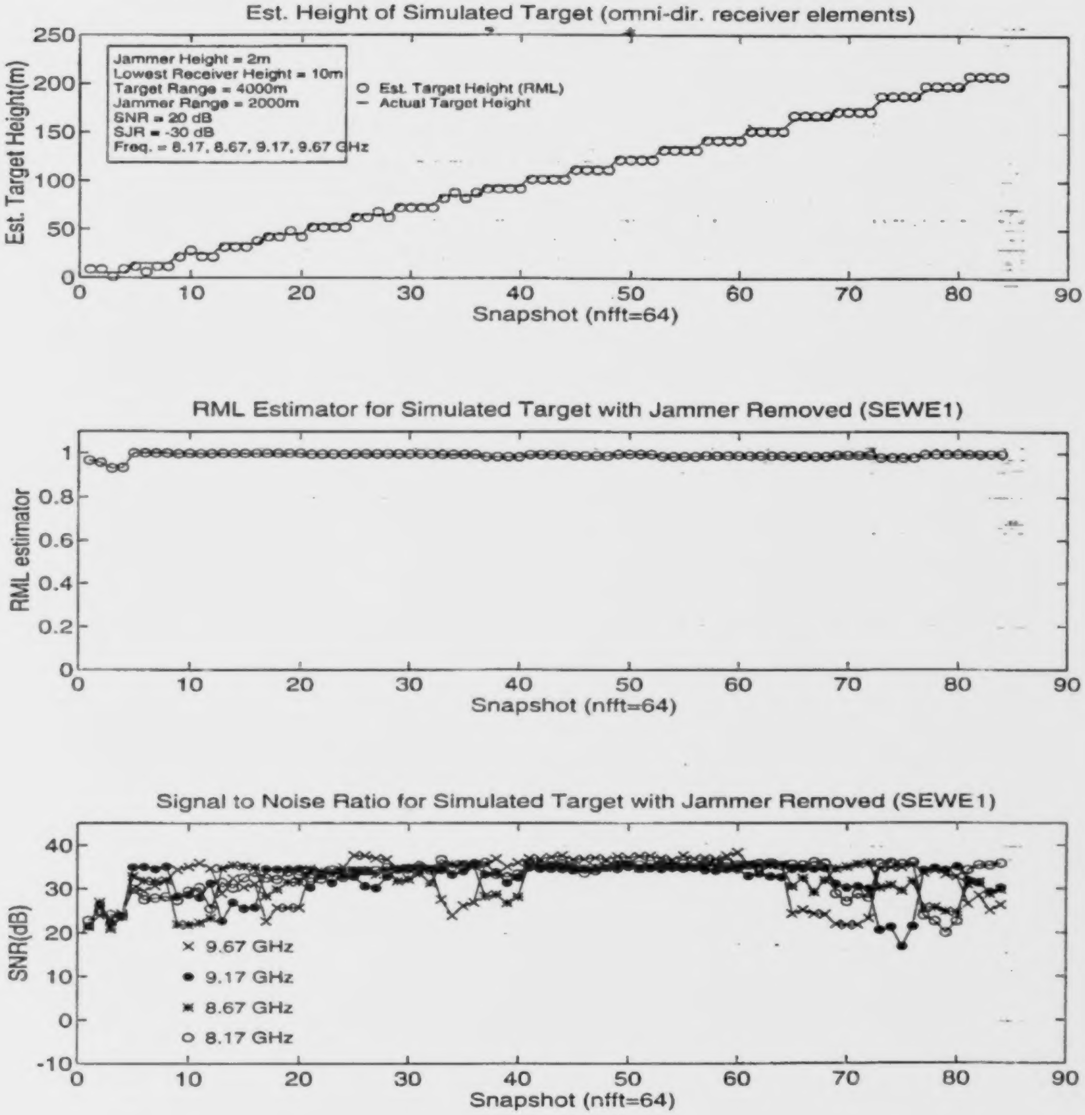
Est. Height of Simulated Target (omni-dir. receiver elements)
Jammer Height = 2m
Lowest Receiver Height = 10m
Target Range = 4000m
Jammer Range = 2000m
SNR = 20 dB
SJR = -30 dB
Freq. = 8.17, 8.67, 9.17, 9.67 GHz
○ Est. Target Height (RML)
— Actual Target Height
Est. Target Height(m)
250
200
150
100
50
0
0
10
20
30
40
50
60
70
80
90
Snapshot (nfft=64)
RML Estimator for Simulated Target with Jammer Removed (SEWE1)
RML estimator
1
0.8
0.6
0.4
0.2
0
Snapshot (nfft=64)
Signal to Noise Ratio for Simulated Target with Jammer Removed (SEWE1)
SNR(dB)
40
30
20
10
0
-10
× 9.67 GHz
● 9.17 GHz
✱ 8.67 GHz
○ 8.17 GHz
Snapshot (nfft=64)

Figure 3.1.15

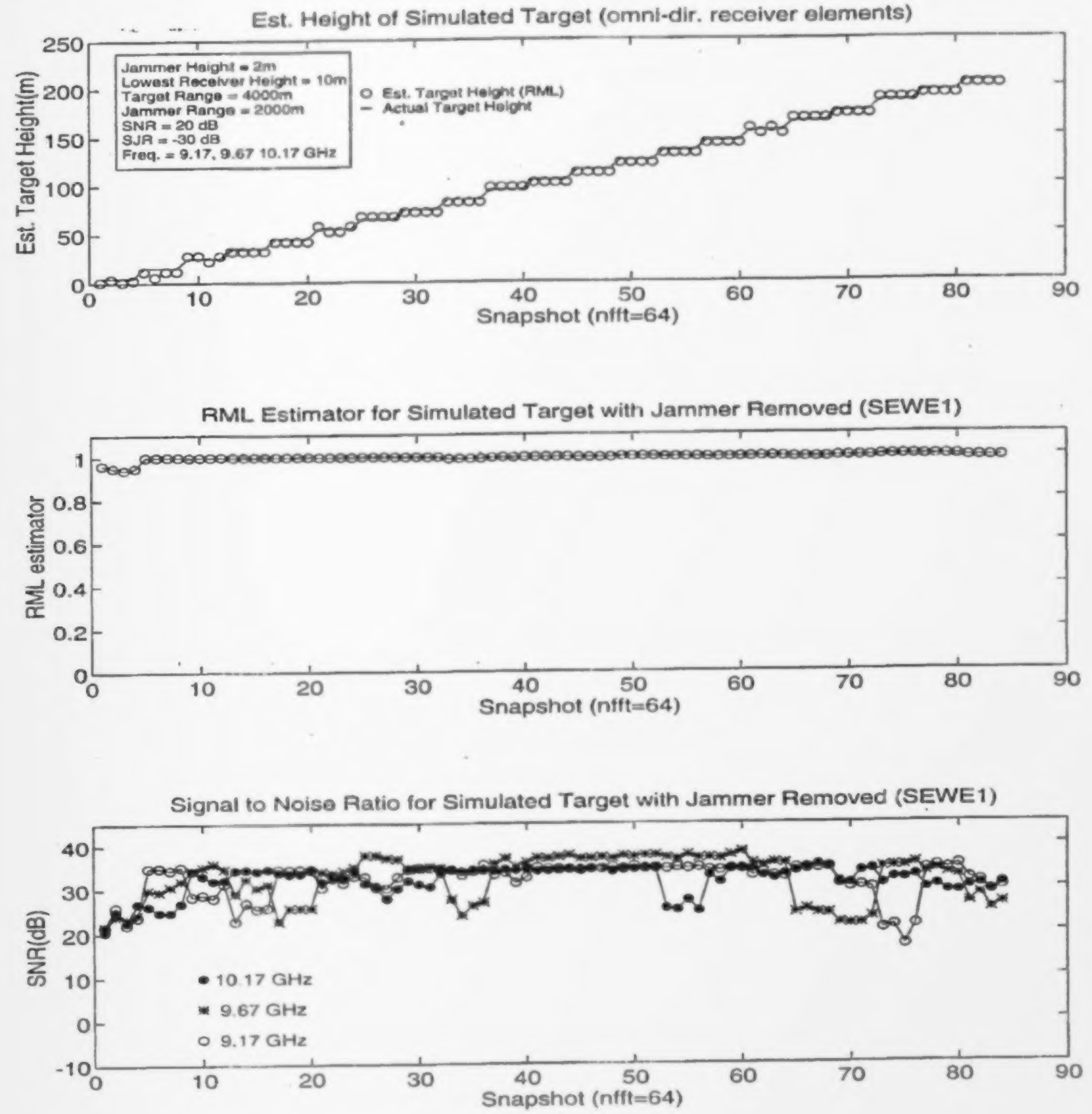
Est. Height of Simulated Target (omni-dir. receiver elements)
Jammer Height = 2m
Lowest Receiver Height = 10m
Target Range = 4000m
Jammer Range = 2000m
SNR = 20 dB
SJR = -30 dB
Freq. = 9.17, 9.67 10.17 GHz
○ Est. Target Height (RML)
— Actual Target Height
Est. Target Height(m)
0
50
100
150
200
250
0
10
20
30
40
50
60
70
80
90
Snapshot (nfft=64)
RML Estimator for Simulated Target with Jammer Removed (SEWE1)
RML estimator
0
0.2
0.4
0.6
0.8
1
0
10
20
30
40
50
60
70
80
90
Snapshot (nfft=64)
Signal to Noise Ratio for Simulated Target with Jammer Removed (SEWE1)
SNR(dB)
-10
0
10
20
30
40
● 10.17 GHz
✱ 9.67 GHz
○ 9.17 GHz
0
10
20
30
40
50
60
70
80
90
Snapshot (nfft=64)

Figure 3.1.16

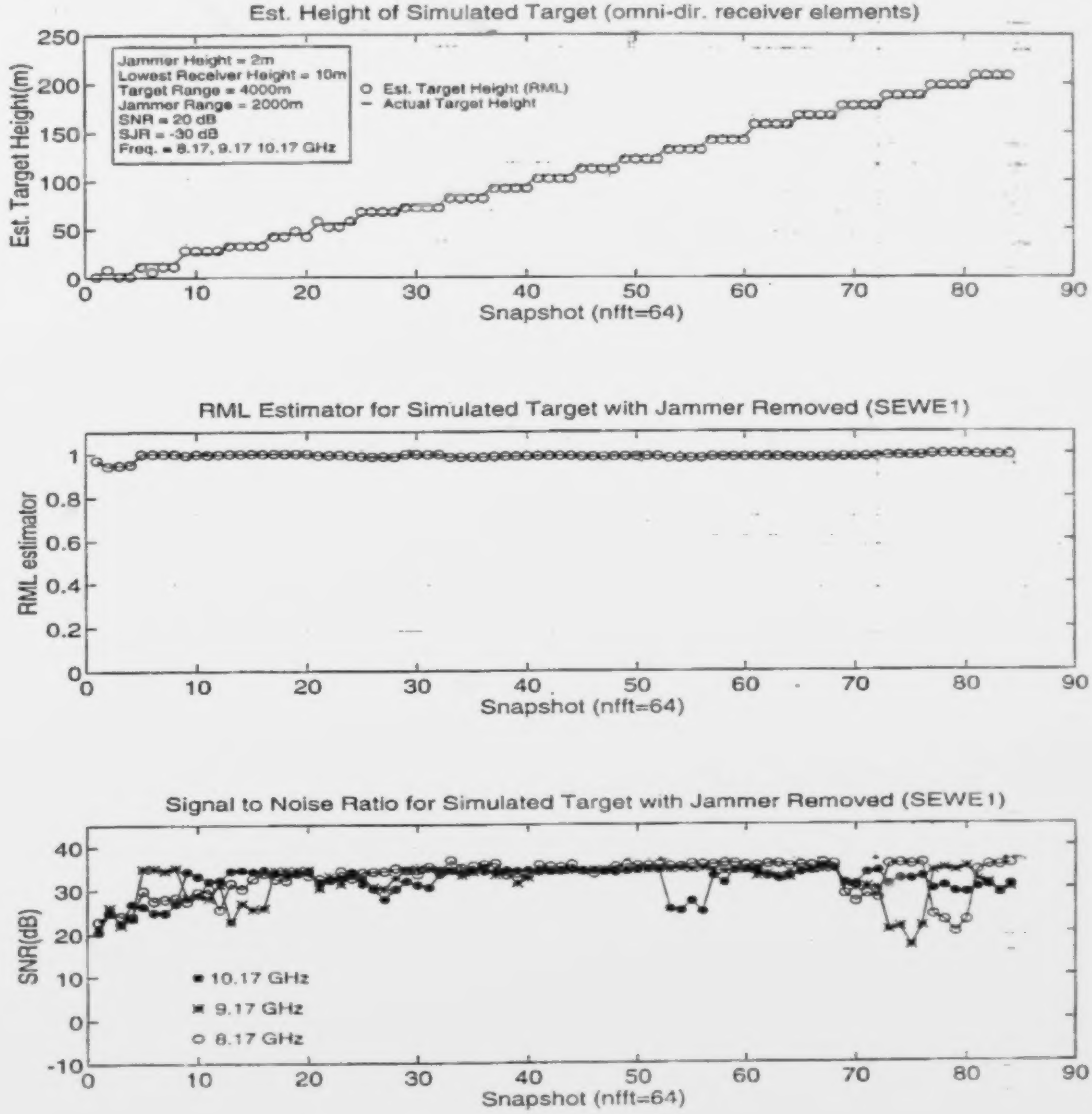

Est. Height of Simulated Target (omni-dir. receiver elements)

RML Estimator for Simulated Target with Jammer Removed (SEWE1)

Signal to Noise Ratio for Simulated Target with Jammer Removed (SEWE1)

Figure 3.1.17

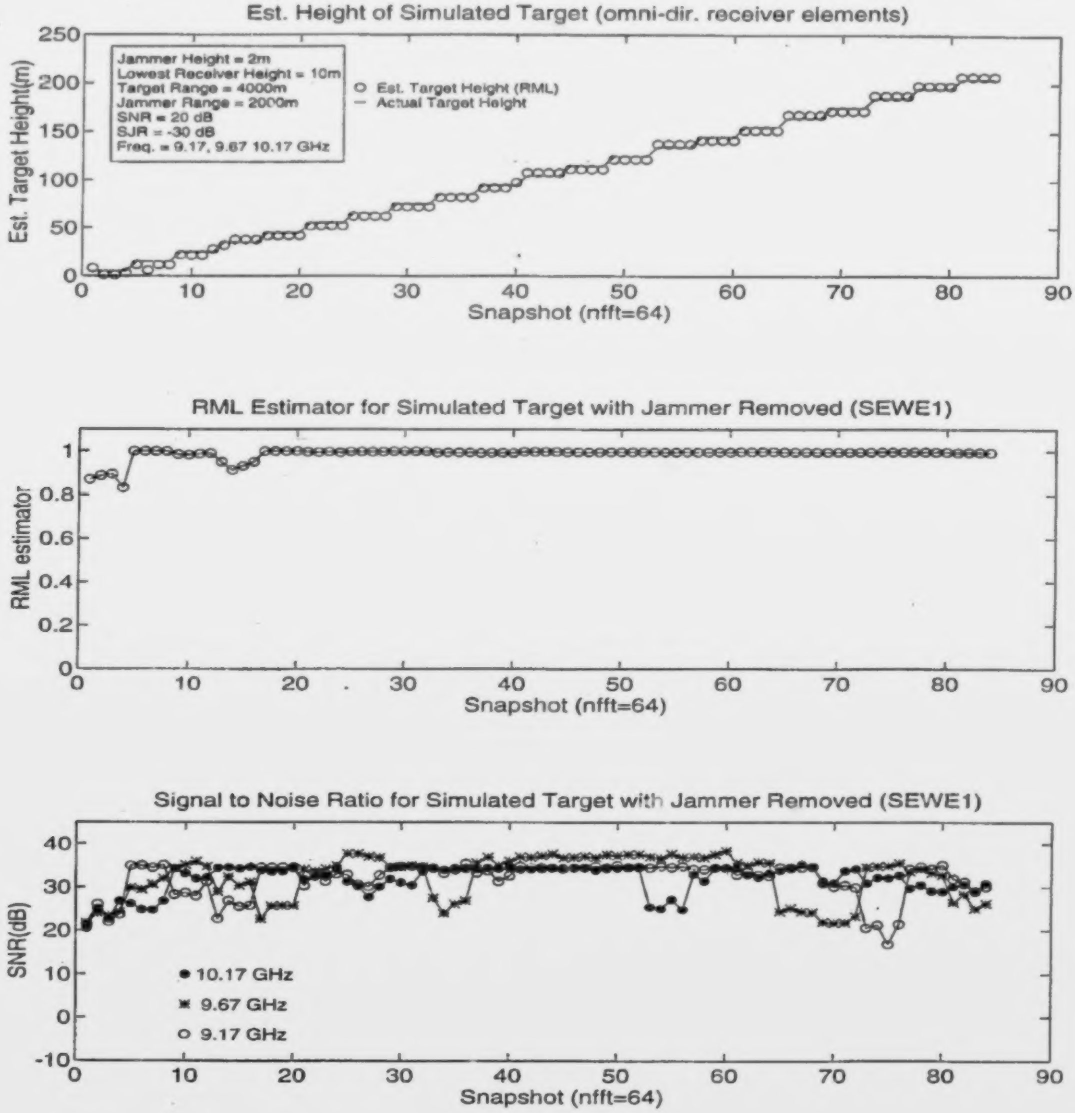
Est. Height of Simulated Target (omni-dir. receiver elements)
Jammer Height = 2m
Lowest Receiver Height = 10m
Target Range = 4000m
Jammer Range = 2000m
SNR = 20 dB
SJR = -30 dB
Freq. = 9.17, 9.67 10.17 GHz
○ Est. Target Height (RML)
— Actual Target Height
Est. Target Height(m)
250
200
150
100
50
0
0
10
20
30
40
50
60
70
80
90
Snapshot (nfft=64)
RML Estimator for Simulated Target with Jammer Removed (SEWE1)
RML estimator
1
0.8
0.6
0.4
0.2
0
0
10
20
30
40
50
60
70
80
90
Snapshot (nfft=64)
Signal to Noise Ratio for Simulated Target with Jammer Removed (SEWE1)
SNR(dB)
40
30
20
10
0
-10
● 10.17 GHz
✱ 9.67 GHz
○ 9.17 GHz
0
10
20
30
40
50
60
70
80
90
Snapshot (nfft=64)

Figure 3.1.18

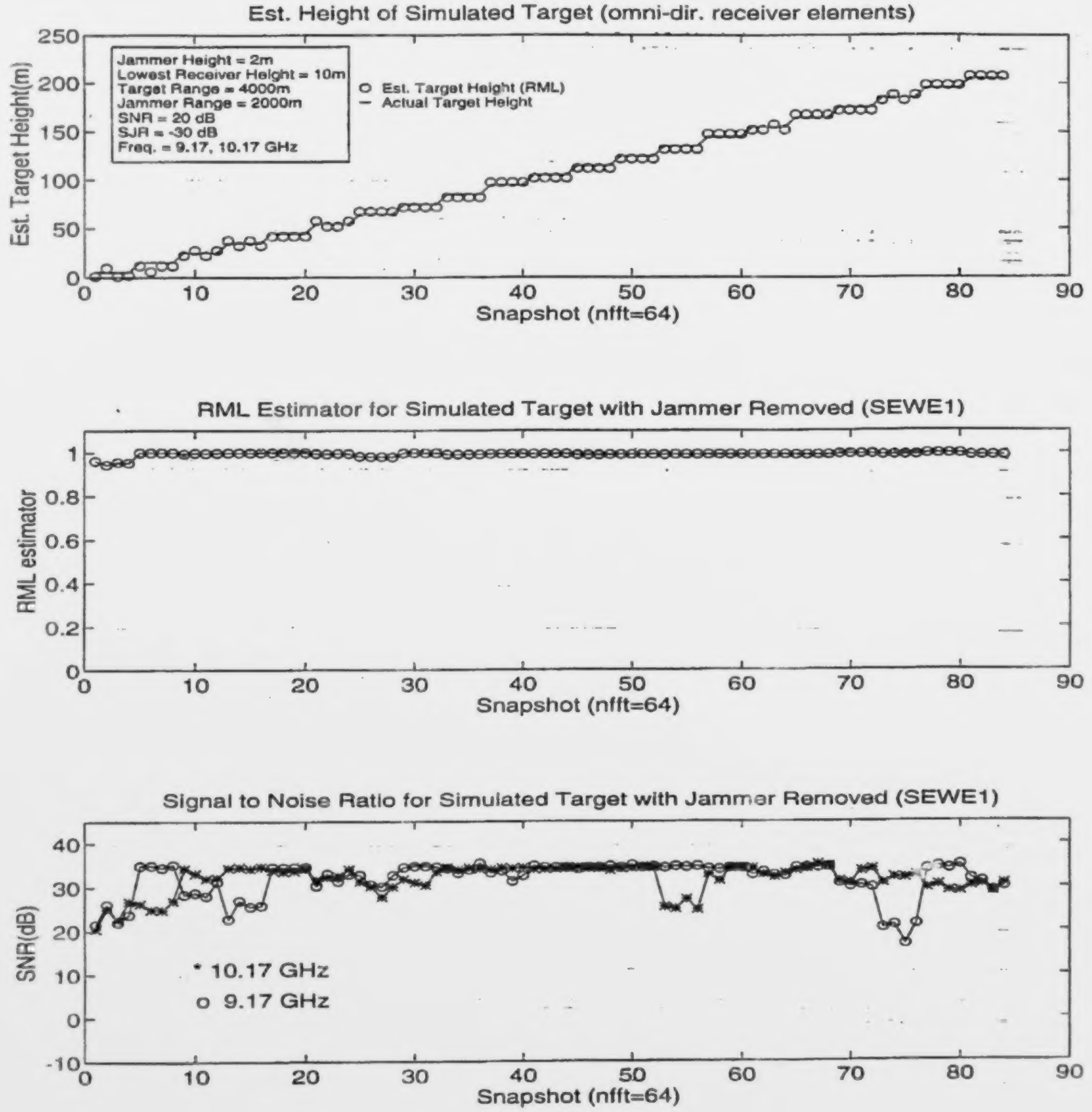
Est. Height of Simulated Target (omni-dir. receiver elements)
Jammer Height = 2m
Lowest Receiver Height = 10m
Target Range = 4000m
Jammer Range = 2000m
SNR = 20 dB
SJR = -30 dB
Freq. = 9.17, 10.17 GHz
o Est. Target Height (RML)
— Actual Target Height
Est. Target Height(m)
0
50
100
150
200
250
Snapshot (nfft=64)
0
10
20
30
40
50
60
70
80
90
RML Estimator for Simulated Target with Jammer Removed (SEWE1)
RML estimator
0
0.2
0.4
0.6
0.8
1
Snapshot (nfft=64)
Signal to Noise Ratio for Simulated Target with Jammer Removed (SEWE1)
SNR(dB)
-10
0
10
20
30
40
* 10.17 GHz
o 9.17 GHz
Snapshot (nfft=64)

Figure 3.1.19

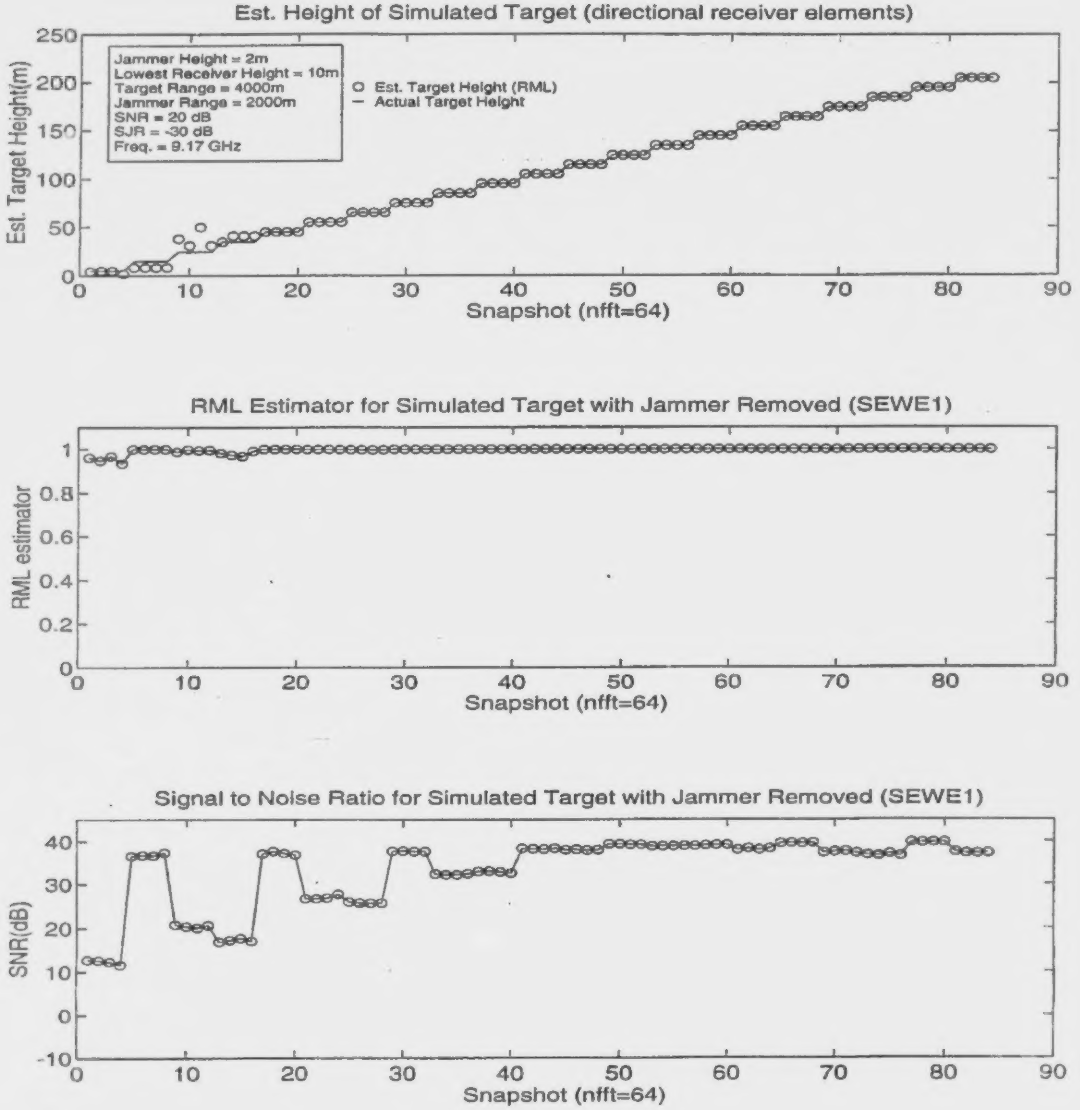

Est. Height of Simulated Target (directional receiver elements)

RML Estimator for Simulated Target with Jammer Removed (SEWE1)

Signal to Noise Ratio for Simulated Target with Jammer Removed (SEWE1)

Figure 3.1.20

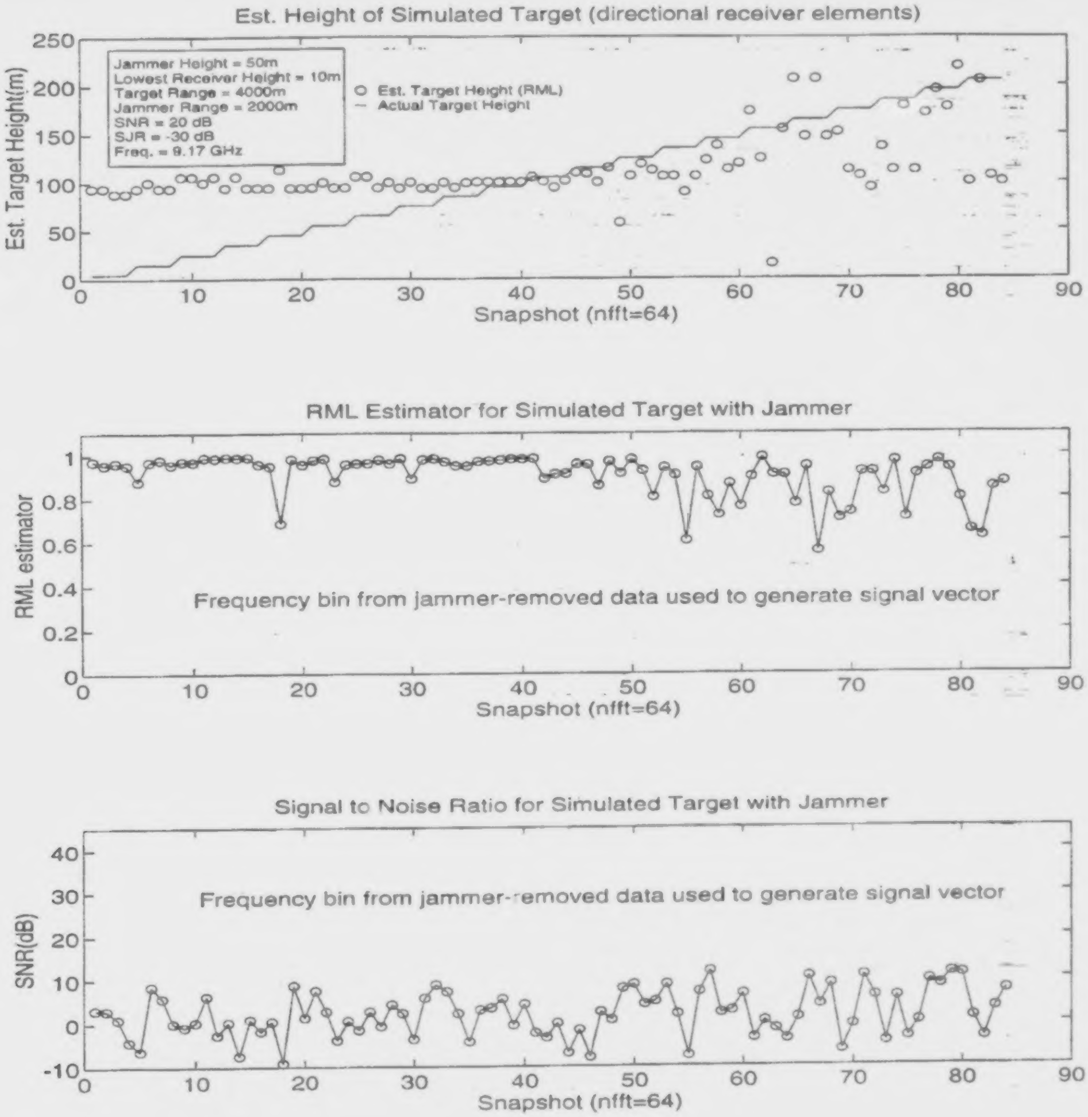
Est. Height of Simulated Target (directional receiver elements)
Jammer Height = 50m
Lowest Receiver Height = 10m
Target Range = 4000m
Jammer Range = 2000m
SNR = 20 dB
SJR = -30 dB
Freq. = 9.17 GHz
o Est. Target Height (RML)
— Actual Target Height
Est. Target Height(m)
0
50
100
150
200
250
Snapshot (nfft=64)
0
10
20
30
40
50
60
70
80
90
RML Estimator for Simulated Target with Jammer
RML estimator
0
0.2
0.4
0.6
0.8
1
Frequency bin from jammer-removed data used to generate signal vector
Snapshot (nfft=64)
Signal to Noise Ratio for Simulated Target with Jammer
SNR(dB)
-10
0
10
20
30
40
Frequency bin from jammer-removed data used to generate signal vector
Snapshot (nfft=64)

Figure 3.1.21

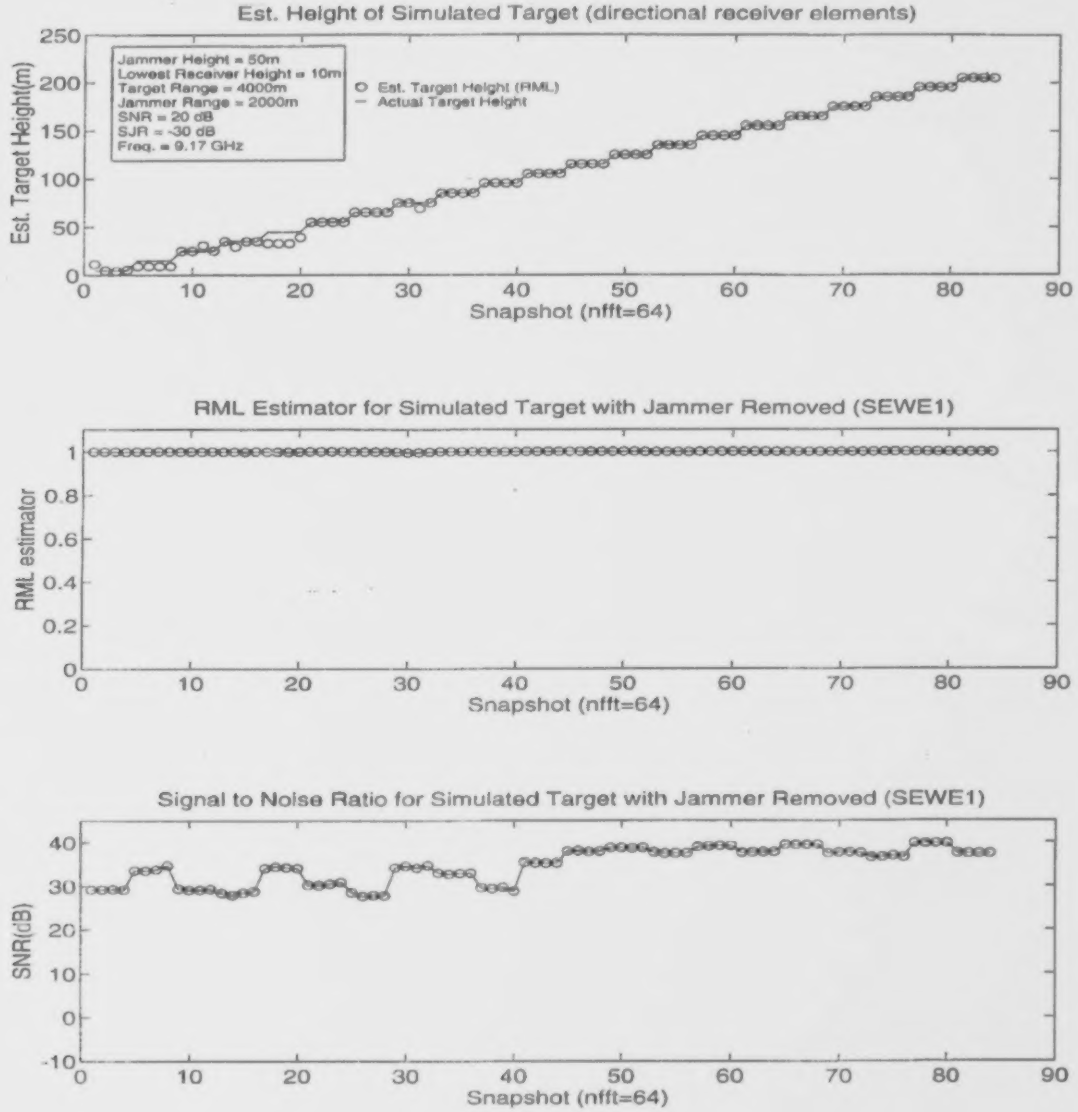
Est. Height of Simulated Target (directional receiver elements)
Jammer Height = 50m
Lowest Receiver Height = 10m
Target Range = 4000m
Jammer Range = 2000m
SNR = 20 dB
SJR = -30 dB
Freq. = 9.17 GHz
O Est. Target Height (RML)
— Actual Target Height
Est. Target Height(m)
250
200
150
100
50
0
0
10
20
30
40
50
60
70
80
90
Snapshot (nfft=64)
RML Estimator for Simulated Target with Jammer Removed (SEWE1)
RML estimator
1
0.8
0.6
0.4
0.2
0
0
10
20
30
40
50
60
70
80
90
Snapshot (nfft=64)
Signal to Noise Ratio for Simulated Target with Jammer Removed (SEWE1)
SNR(dB)
40
30
20
10
0
-10
0
10
20
30
40
50
60
70
80
90
Snapshot (nfft=64)

Figure 3.1.22

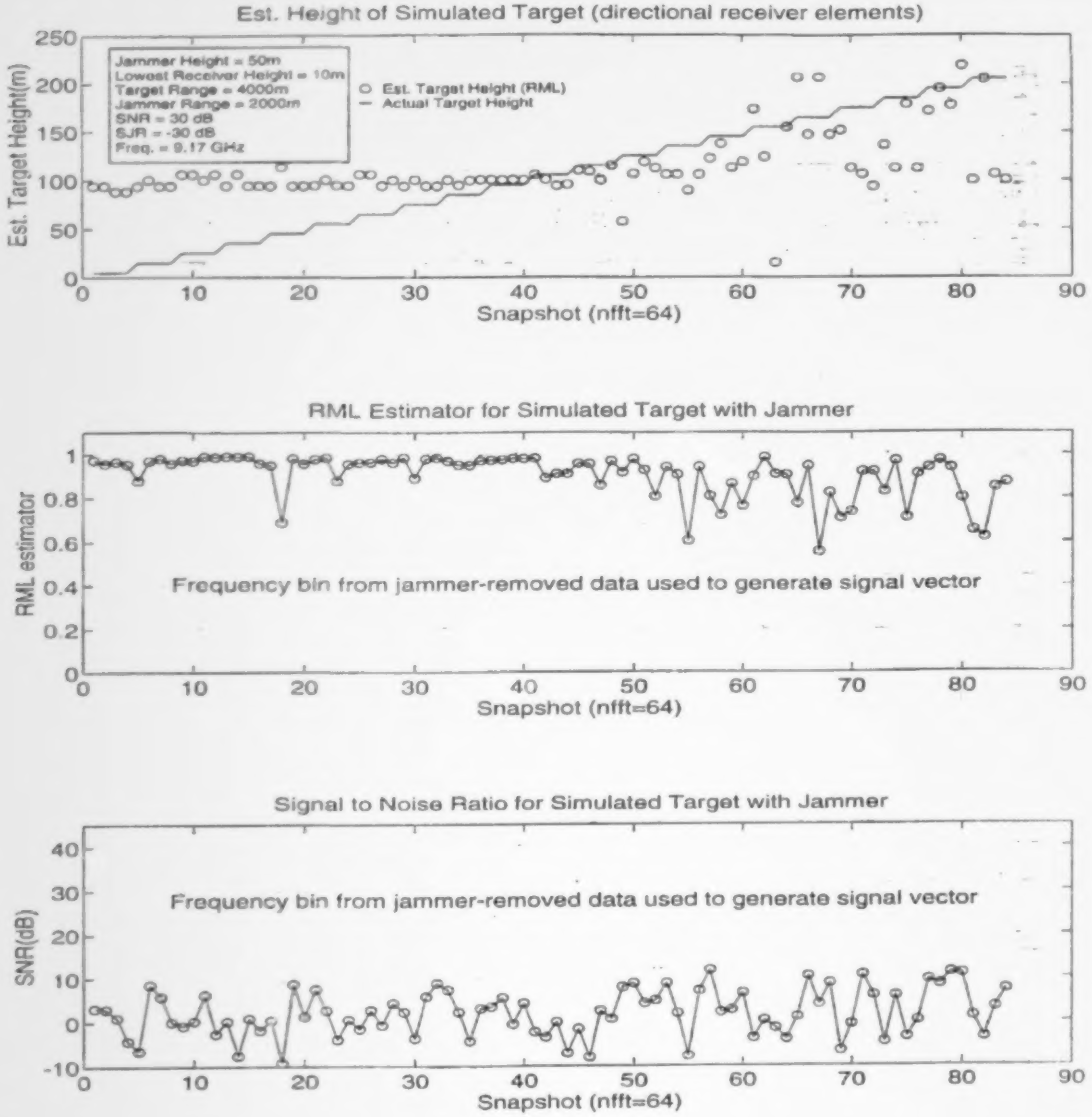
Est. Height of Simulated Target (directional receiver elements)
Jammer Height = 50m
Lowest Receiver Height = 10m
Target Range = 4000m
Jammer Range = 2000m
SNR = 30 dB
SJR = -30 dB
Freq. = 9.17 GHz
○ Est. Target Height (RML)
— Actual Target Height
Est. Target Height(m)
250
200
150
100
50
0
0
10
20
30
40
50
60
70
80
90
Snapshot (nfft=64)
RML Estimator for Simulated Target with Jammer
RML estimator
1
0.8
0.6
0.4
0.2
0
Frequency bin from jammer-removed data used to generate signal vector
Snapshot (nfft=64)
Signal to Noise Ratio for Simulated Target with Jammer
SNR(dB)
40
30
20
10
0
-10
Frequency bin from jammer-removed data used to generate signal vector
Snapshot (nfft=64)

Figure 3.1.23

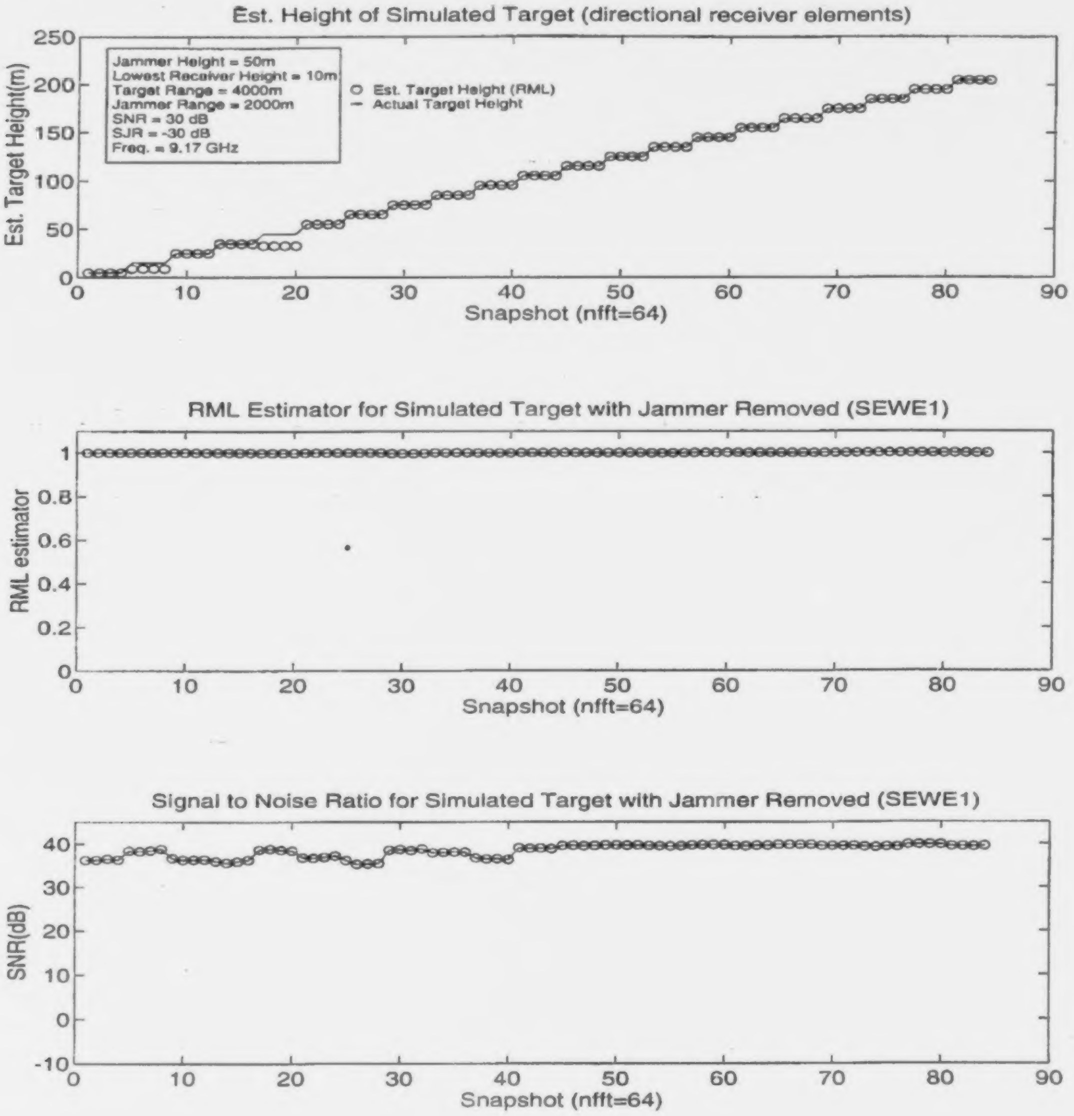
Est. Height of Simulated Target (directional receiver elements)

RML Estimator for Simulated Target with Jammer Removed (SEWE1)

Signal to Noise Ratio for Simulated Target with Jammer Removed (SEWE1)

Figure 3.1.24

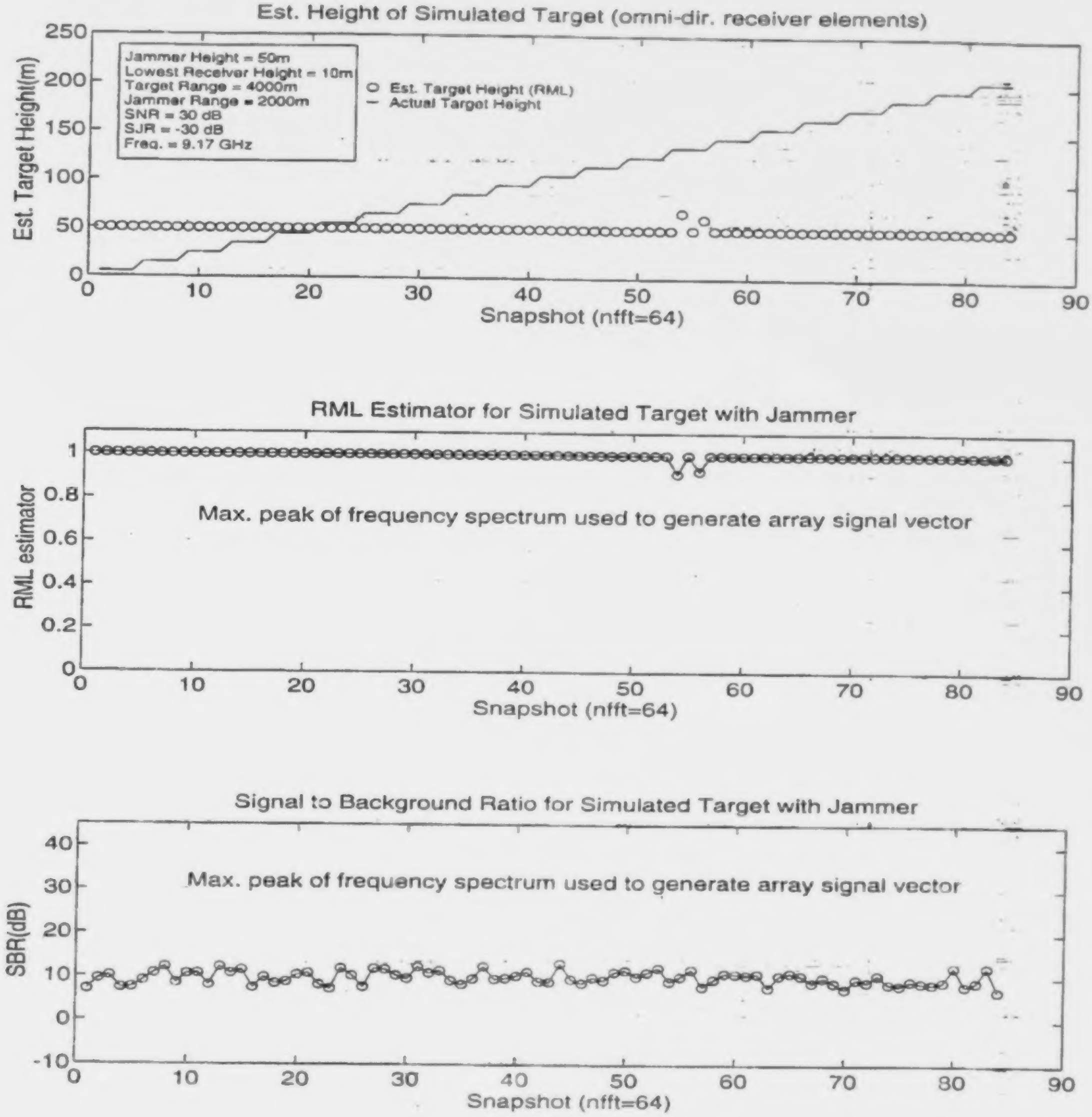
Est. Height of Simulated Target (omni-dir. receiver elements)
Jammer Height = 50m
Lowest Receiver Height = 10m
Target Range = 4000m
Jammer Range = 2000m
SNR = 30 dB
SJR = -30 dB
Freq. = 9.17 GHz
Est. Target Height (RML)
Actual Target Height
Est. Target Height(m)
250
200
150
100
50
0
0
10
20
30
40
50
60
70
80
90
Snapshot (nfft=64)
RML Estimator for Simulated Target with Jammer
Max. peak of frequency spectrum used to generate array signal vector
RML estimator
1
0.8
0.6
0.4
0.2
0
Snapshot (nfft=64)
Signal to Background Ratio for Simulated Target with Jammer
Max. peak of frequency spectrum used to generate array signal vector
SBR(dB)
40
30
20
10
0
-10
Snapshot (nfft=64)

Figure 3.1.25

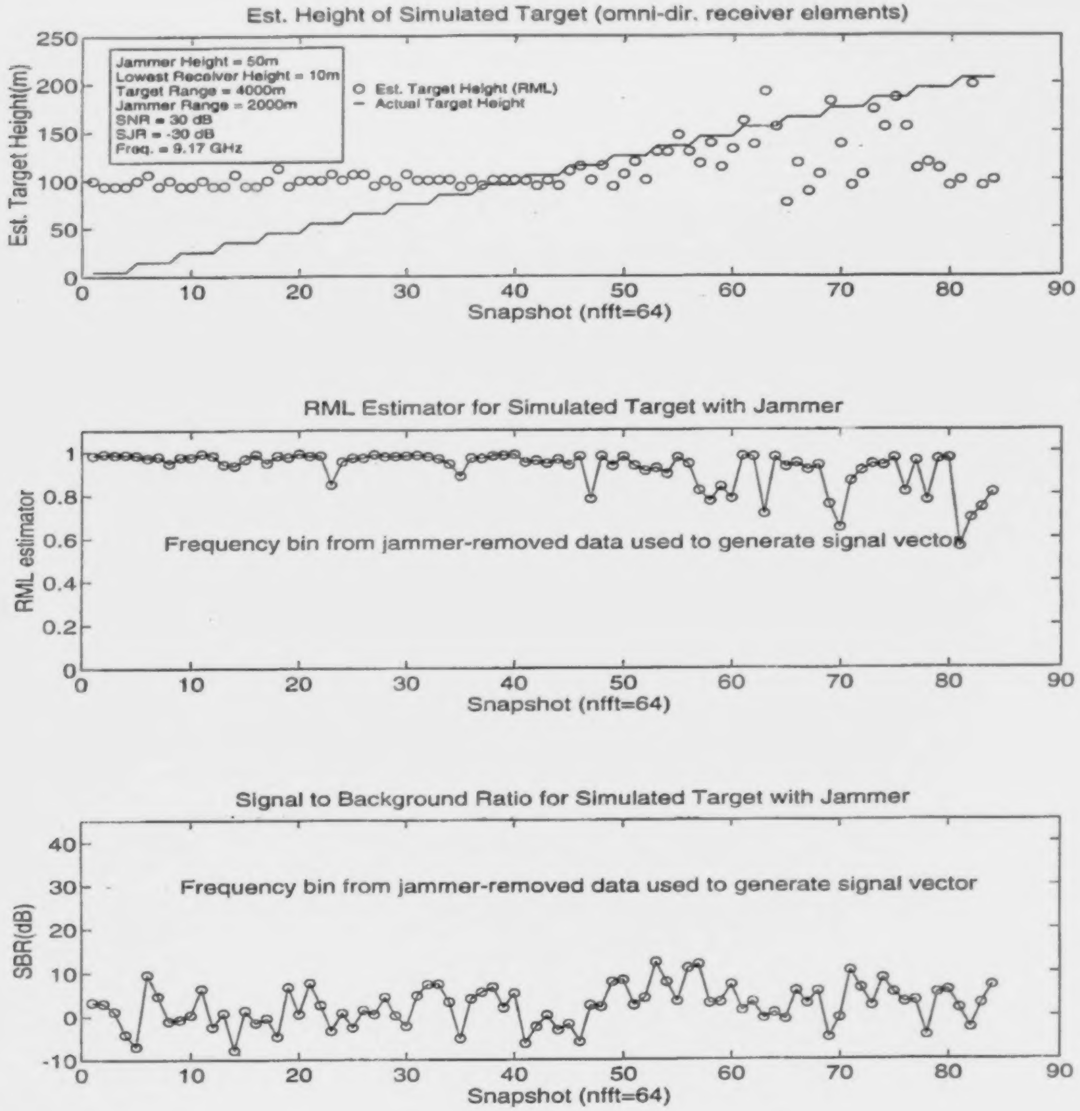
Est. Height of Simulated Target (omni-dir. receiver elements)
Jammer Height = 50m
Lowest Receiver Height = 10m
Target Range = 4000m
Jammer Range = 2000m
SNR = 30 dB
SJR = -30 dB
Freq. = 9.17 GHz
o Est. Target Height (RML)
— Actual Target Height
Est. Target Height(m)
0
50
100
150
200
250
Snapshot (nfft=64)
0
10
20
30
40
50
60
70
80
90
RML Estimator for Simulated Target with Jammer
Frequency bin from jammer-removed data used to generate signal vector
RML estimator
0
0.2
0.4
0.6
0.8
1
Snapshot (nfft=64)
0
10
20
30
40
50
60
70
80
90
Signal to Background Ratio for Simulated Target with Jammer
Frequency bin from jammer-removed data used to generate signal vector
SBR(dB)
-10
0
10
20
30
40
Snapshot (nfft=64)
0
10
20
30
40
50
60
70
80
90

Figure 3.1.26

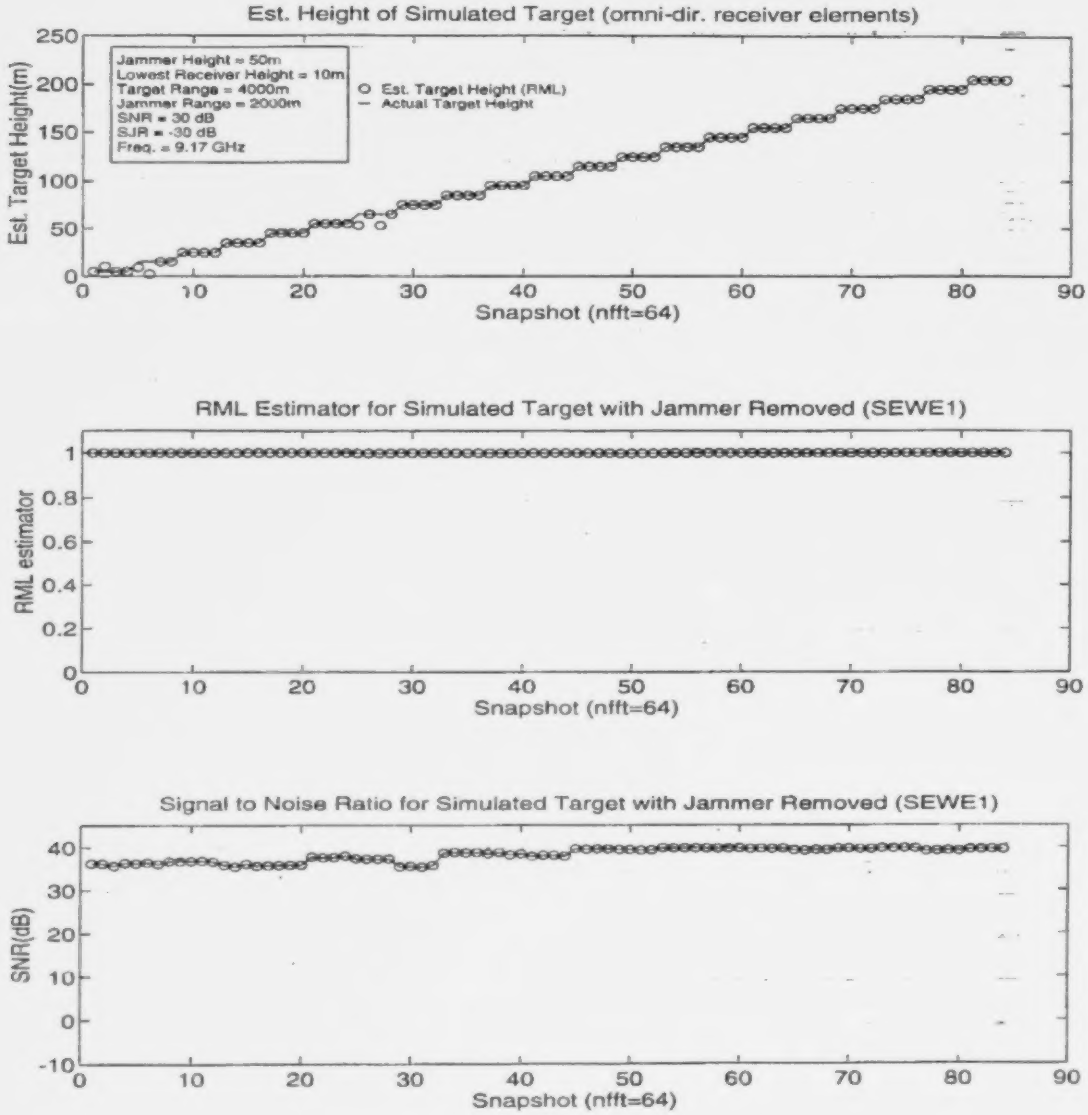
Est. Height of Simulated Target (omni-dir. receiver elements)
Jammer Height = 50m
Lowest Receiver Height = 10m
Target Range = 4000m
Jammer Range = 2000m
SNR = 30 dB
SJR = -30 dB
Freq. = 9.17 GHz
○ Est. Target Height (RML)
— Actual Target Height
Est. Target Height(m)
250
200
150
100
50
0
0
10
20
30
40
50
60
70
80
90
Snapshot (nfft=64)
RML Estimator for Simulated Target with Jammer Removed (SEWE1)
RML estimator
1
0.8
0.6
0.4
0.2
0
Snapshot (nfft=64)
Signal to Noise Ratio for Simulated Target with Jammer Removed (SEWE1)
SNR(dB)
40
30
20
10
0
-10
Snapshot (nfft=64)

Figure 3.1.27

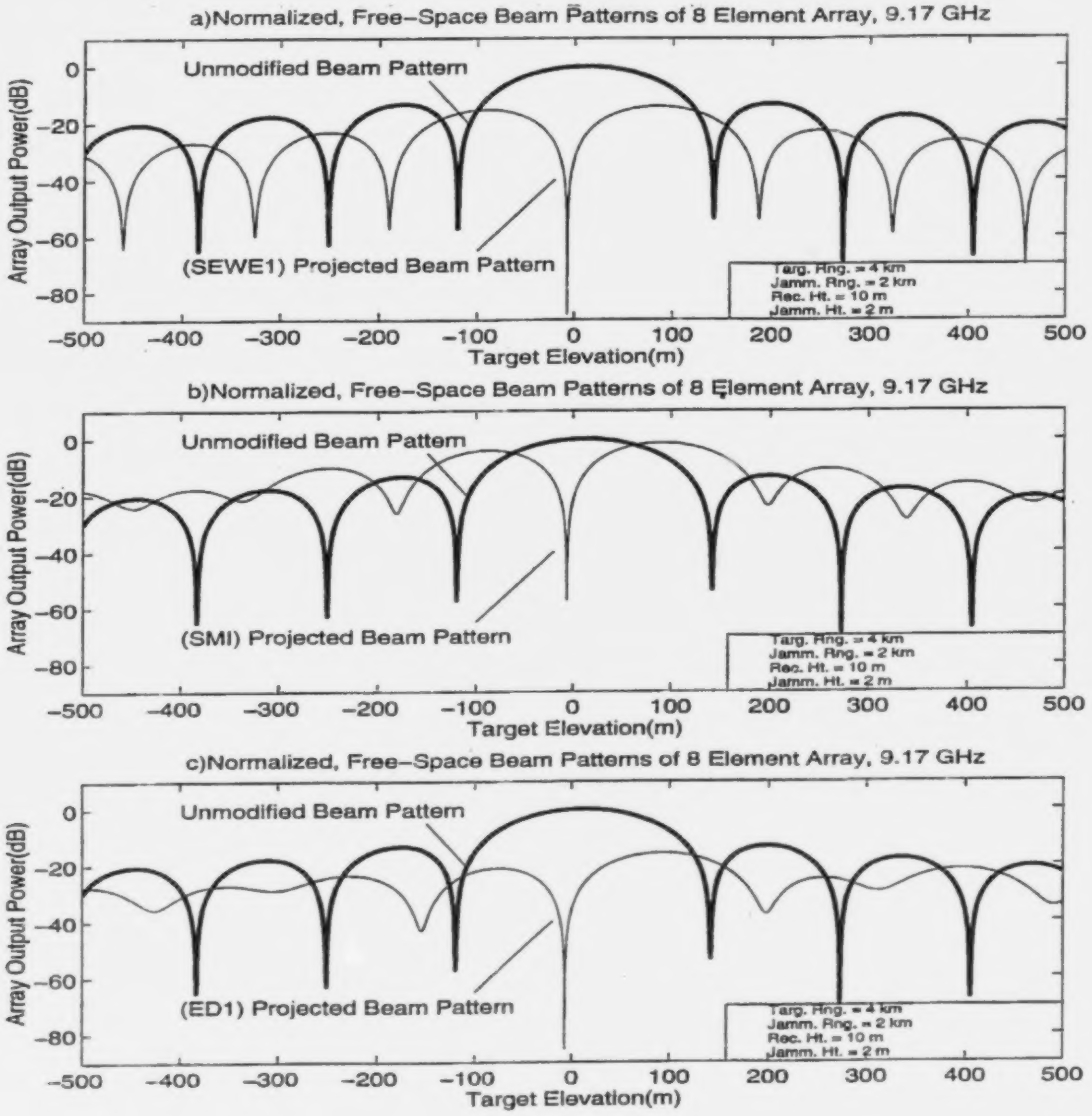

Figure 3.1.28 Free space antenna beam patterns before and after modification by projection matrix to remove 50m jammer at 2km. The results shown are for all three projection methods under study: a)SEWE, b)SMI and c)ED.

a)Normalized, Free-Space Beam Patterns of 8 Element Array, 9.17 GHz

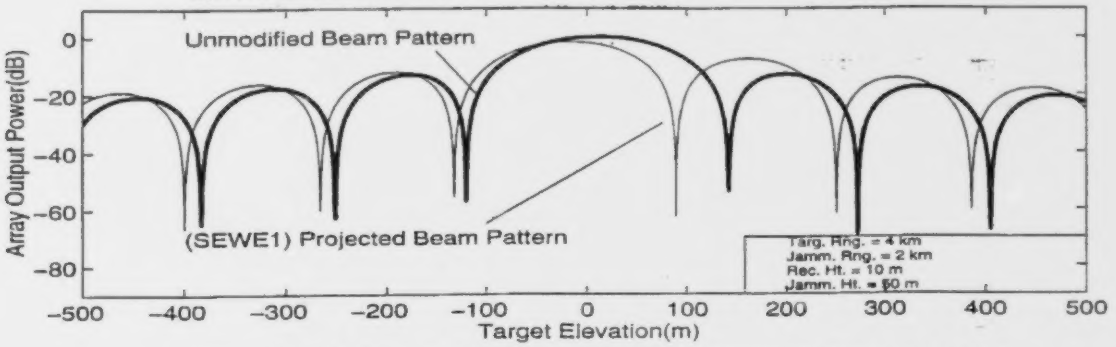

b)Normalized, Free-Space Beam Patterns of 8 Element Array, 9.17 GHz

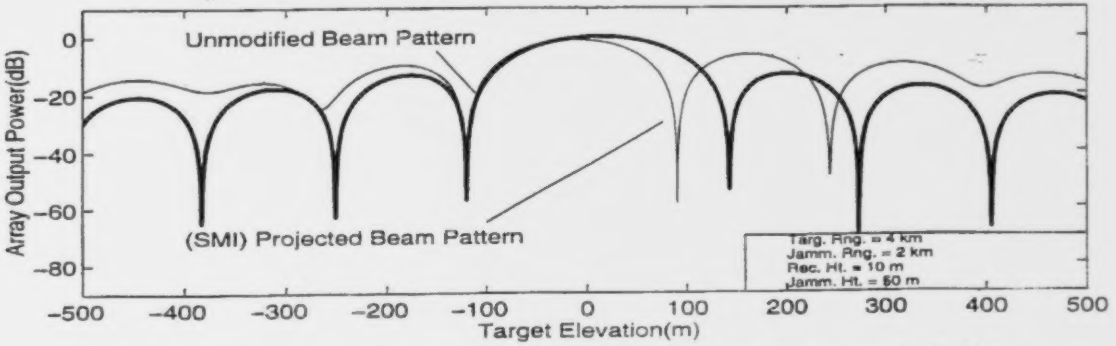

c)Normalized, Free-Space Beam Patterns of 8 Element Array, 9.17 GHz

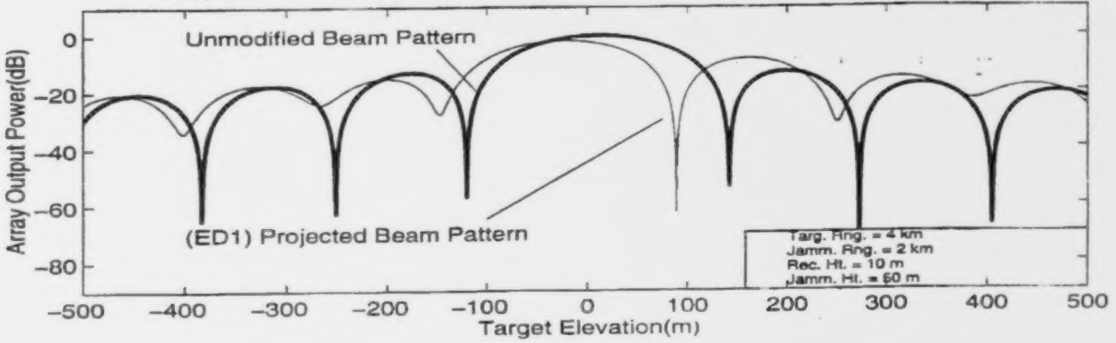

Figure 3.1.29 Free space antenna beam patterns before and after modification by projection matrix to remove 50m jammer at 2km. The results shown are for all three projection methods under study: a)SEWE, b)SMI and c)ED.

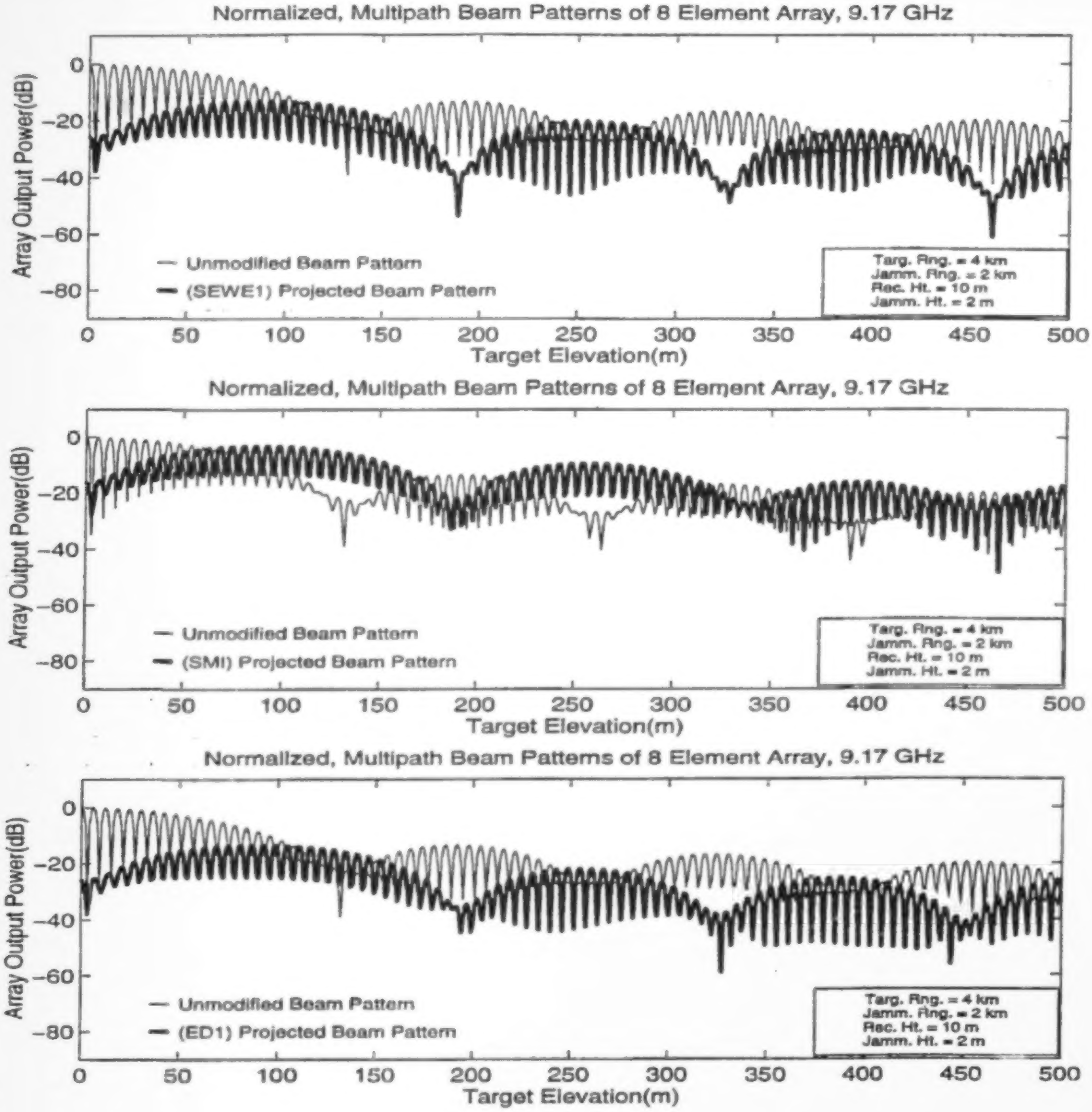

Figure 3.1.30 Multipath antenna beam patterns before and after modification by projection matrix to remove 2m jammer at 2km. The results shown are for all three projection methods under study: a)SEWE, b)SMI and c)ED.

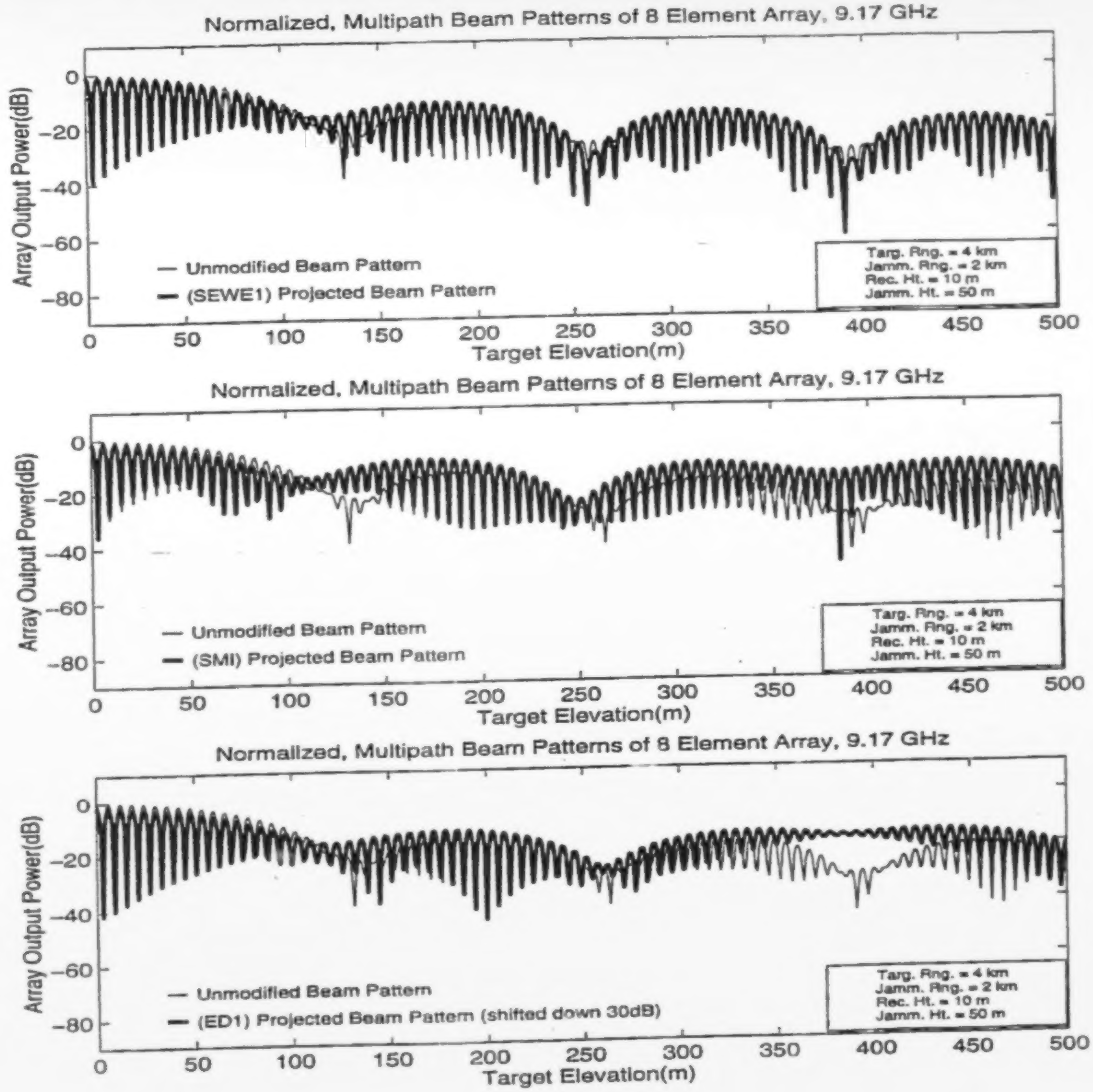

Figure 3.1.31 Multipath antenna beam patterns before and after modification by projection matrix to remove 50m jammer at 2km. The results shown are for all three projection methods under study: a)SEWE, b)SMI and c)ED. In this case the modified pattern and unmodified pattern overlap.

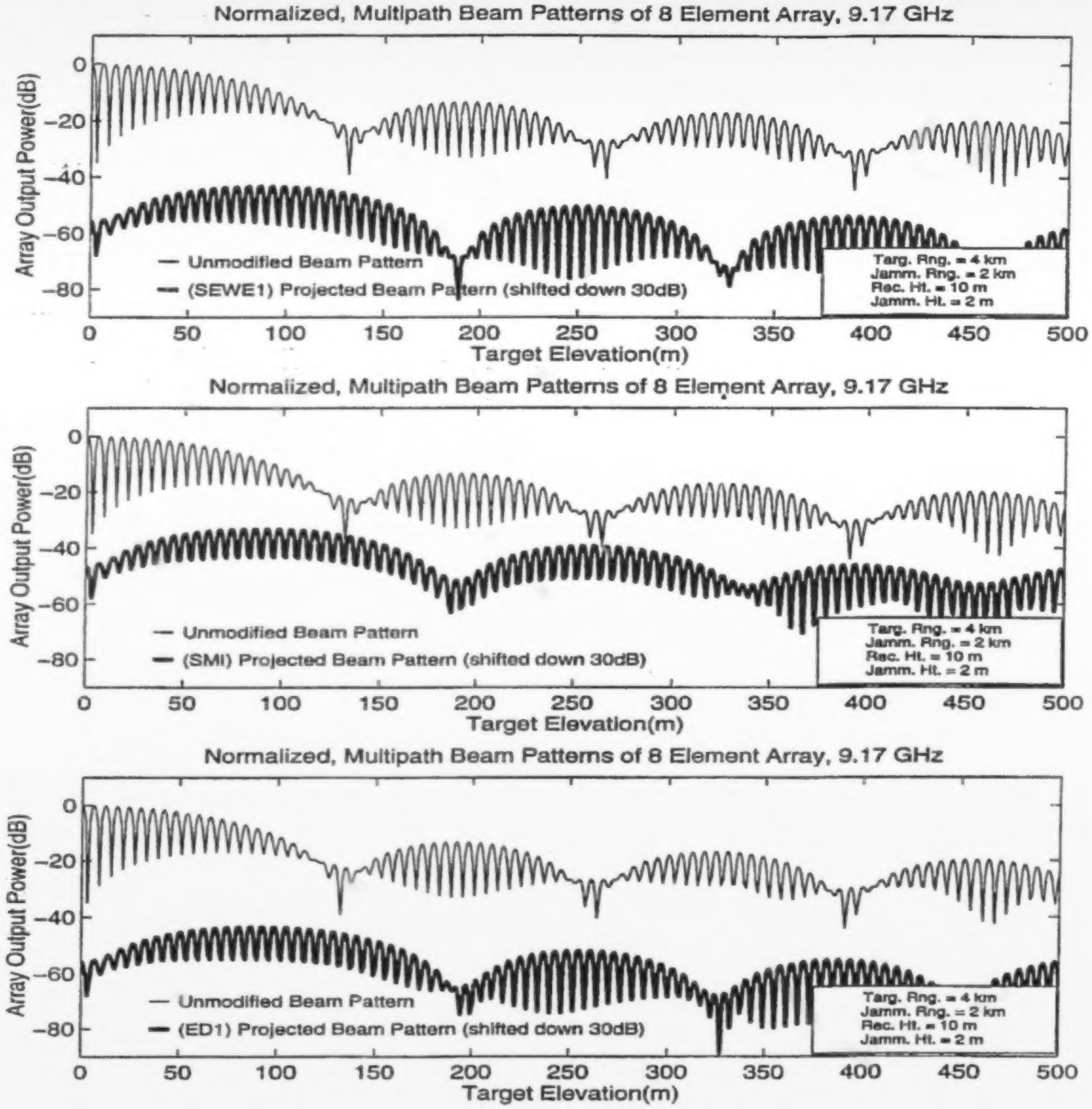

Figure 3.1.32 Multipath antenna beam patterns before and after modification by projection matrix to remove 2m jammer at 2km. These results are the same as shown in figure 3.3.3 but the modified beam pattern has been shifted down by 30 dB.

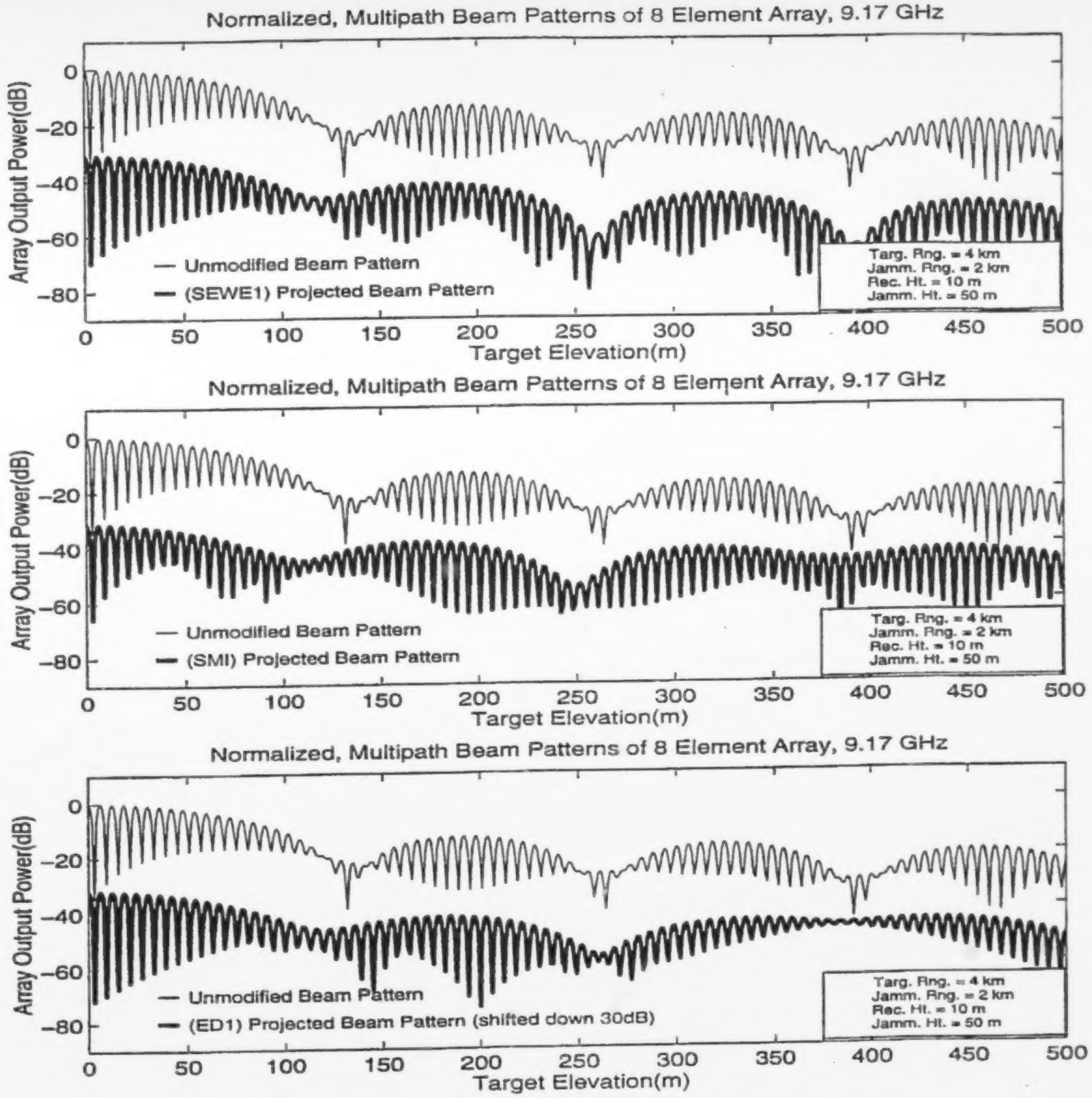

Figure 3.1.33 Multipath antenna beam patterns before and after modification by projection matrix to remove 50m jammer at 2km. These results are the same as shown in figure 3.3.4 but the modified beam pattern has been shifted down by 30 dB.

Table 3.1 displays a list of the various cases considered in the study and the corresponding figures. Only one jammer was considered in the analysis, hence the reason for the '1' following SEWE and ED in many of the figures.. It should be noted here that since the simulated multipath data was generated for different target heights, the target signal amplitude had to be changed for each height to maintain the same array output SNR. For a particular SNR input to SIMGAUSJAM the target amplitude A_t was calculated according to the formula:

$$A_t = \frac{10^{(SNR/20)}(4\sigma)}{\left|\sum_{n=1}^{8}[f_d(n)+f_i(n)]\right|}$$

where f_d and f_i represent the direct and reflected beams from the target arriving at the nth anttena element and $2\sigma^2$ was the noise power from each array element (ie σ^2 contribution from each of the I and Q channels). It should also be noted that the output SNR shown on the figures and in Table 3.1 for each of the cases considered was just the output SNR per data vector used as the input to the data generation software. Since the NFFT signal vectors were integrated in the FFT stage of the analysis software, and the FFT was normalized to the number of points in the FFT (ie 256), the actual output SNR should be approximately $10\log_{10}(256/NFFT)$ greater than shown. For most of the cases shown, NFFT=6, so the output SNR should be raised by approximately 6 dB.

Figure 3.1.31 shows a comparison of the free space (ie no multipath) antenna beam pattern before and after modification by the projection matrix from each of the three techniques for a jammer height of 2m. Similarly, Figure 3.1.32 shows the free space beam patterns for a 50 m jammer height. Figures 3.1.33 and 3.1.34 are the multipath equivalent of figures 3.1.31 and 3.1.32. Since the projected beam patterns in Figures 3.1.33 and 3.1.34 show considerable overlap of the unmodified pattern, they were shifted down by 30 dB and the results shown in Figures 3.1.35 and 3.1.36. It can be seen from these figures that the multipath beam patterns are much more complex than the free space versions and although the projected beam pattern for the 2m jammer exhibits a strong null near the same location as its free space counterpart, the same cannot be said for a 50 m jammer. In fact, the projected beam pattern for the 50 m jammer was very similar to the original unmodified beam pattern. The variation in the array output SNR is due to variations in the estimation of the background level of the FFT spectrum, and the effect of the jammer removal process.

3.2 Task 1a) ii) Calibration and Formatting of Experimental Data

During March and September of 1993, a series of main-beam and side-lobe jammer cancellation experiments were carried out. The data from these experiments had to be calibrated and formatted for use in evaluating the main-beam and side-lobe jammer cancellation algorithms that were implemented into software. A significant portion of the software required for calibration and formatting of the data was completed on a previous contract. However, some modifications had to be made to the software as more of the data files from those experiments were investigated during this contract. A program named SLCRD1 was written in Fortran 77 for use on both the VAX 3800 and the IBM PC to read the data files from data logger tapes and correctly format the data for use in the data analysis. The program was used to edit out bad sections of the data from certain files and store the results in 10 output files corresponding to: a) high frequency, on-target data from the main-beam array, b) high frequency, off-target data from the main-beam array, c) high frequency on-target data from the side-lobe canceller (SLC) array, d) high frequency, off-target data from the SLC array, e) four more similar files for low frequency (although only the high frequency was working during the experiments), f) a file indicating the on-target and off-target ranges for each data record of main-beam and SLC data, and g) a record of where the software encountered some problems with the data and may have tried to correct them. Despite the efforts of the SLCRD1 program to filter out things like voltage spikes in the data, some would still manage to pass through undetected and had to be spotted using other means of analysis, such as visual inspection of FFT spectra of the data. Whenever an anomaly was noted in the data that could not be corrected by a generalized software correction, the SLCRD1 program had to be modified to correct that particular error by 'hard coding' the fix into the software. This was often a tedious although necessary exercise.

During the data analysis it was determined that the signal from the helicopter could not be distiguished from the noise background for the main-beam data. However, since the helicopter signal could be seen in the data from the SLC array, it was decided that the SLC data would be used for evaluating the main-beam jammer cancellation software. Thus, the efforts to calibrate the data were confined to the SLC array data.

Examinations of the FFT power spectra seemed to imply that there was a strong I-Q phase and/or amplitude imbalance in each of the array elements that was difficult to compensate for. When either an amplitude or quadrature phase imbalance occurs, the effect is to produce a spectral image of the target in the FFT spectrum; the larger the imbalance, the larger the image becomes. Figure 3.2.1. displays a typical array output FFT power spectrum from run 8 of the March 4,

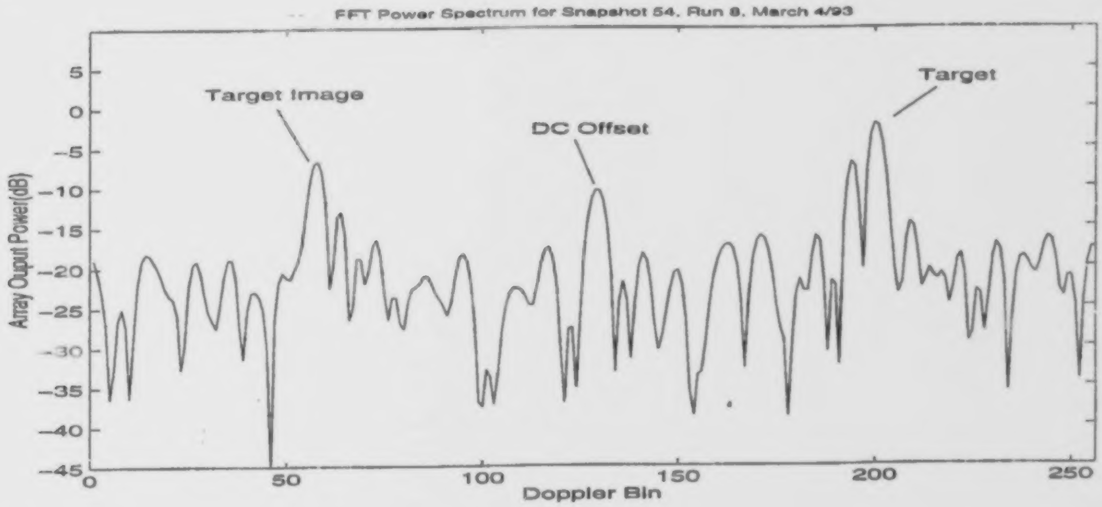

Figure 3.2.1 FFT power spectrum for array output from snapshot 54 of run 8, March 4, 1993 showing the 'target' signal and its spectral image as a function of the Doppler frequency bin.

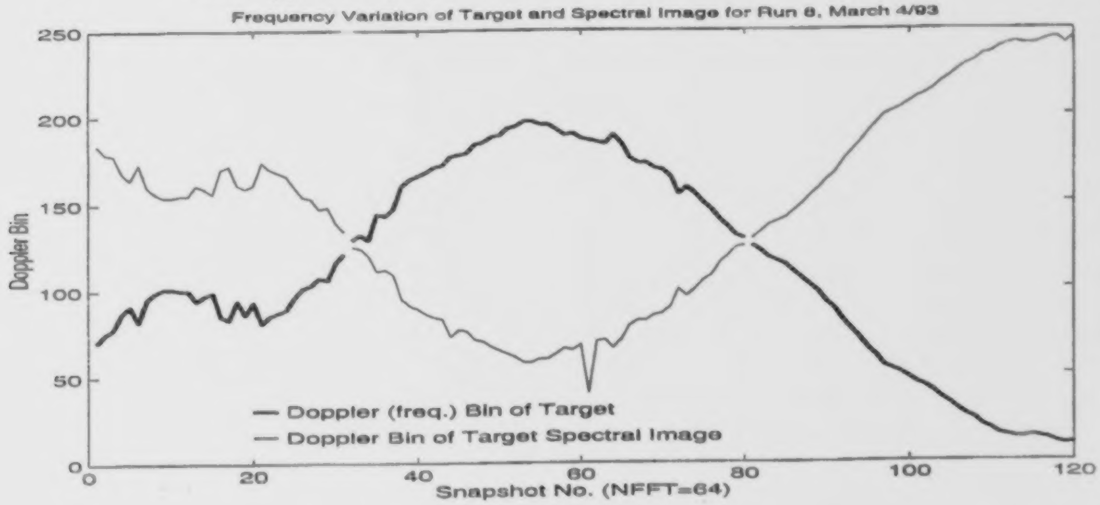

Figure 3.2.2 Tracking the frequency variation of the target and its spectral image for run 8. The data was obtained from 256 point FFT spectra using 64 data samples and zero filling.

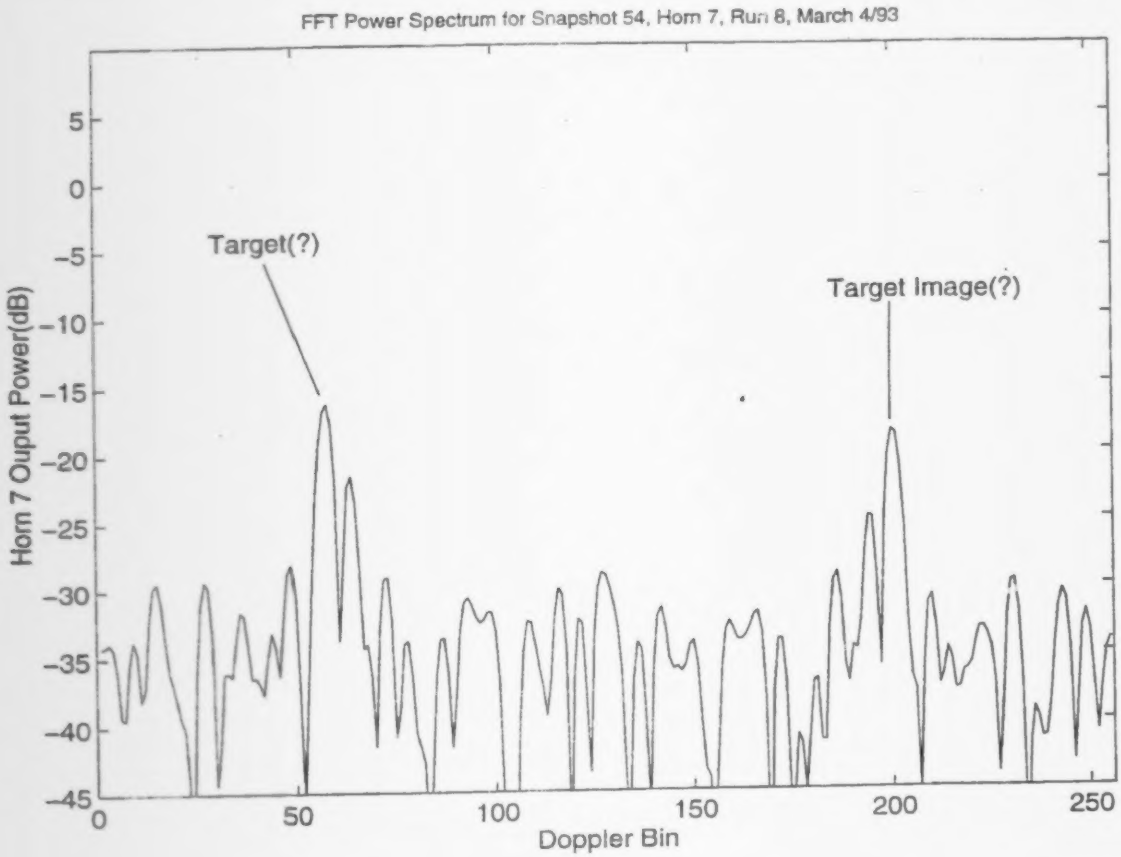

Figure 3.2.3 FFT power spectrum for horn 7, snapshot 54 of run 8, March 4, 1993. Here it can be seen that the 'target' and 'image' locations have reversed.

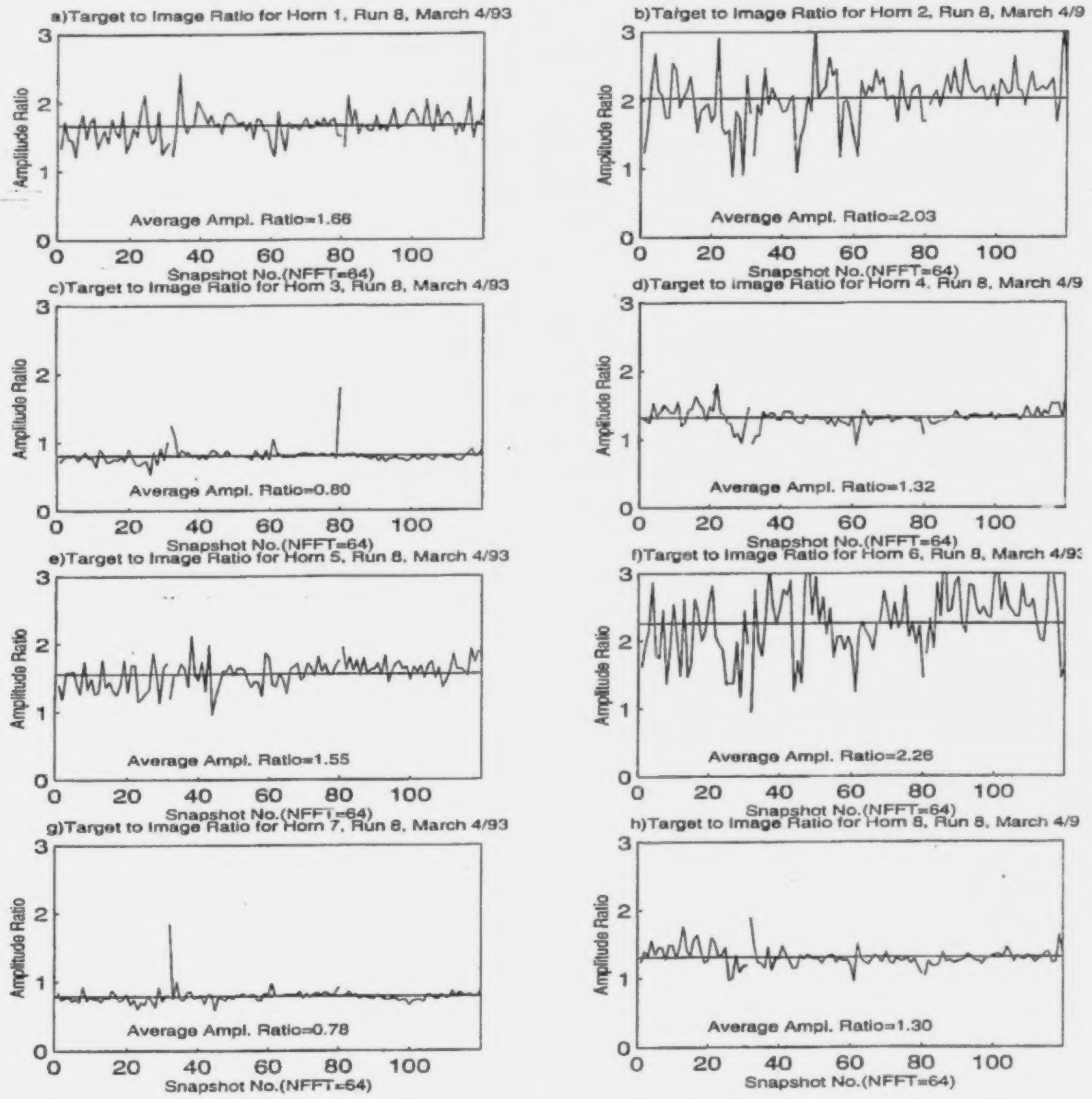

Figure 3.2.4 Plots of the target to image ratio for each receiver element of the vertical array for run 8, March 4, 1993.

1993 trials which appears to show such an effect. Although software has been written (see previous final report mentioned earlier) which can remedy some of the imbalances, when it was applied to this data there was ususally a significant image signal left which could not be removed. One factor which would partially account for this problem was the fact that the Doppler frequency of the target was continually changing, so that it would be very difficult to measure any constant quadrature phase imbalance. Figure 3.2.2 shows a plot of the variation in Doppler frequency (ie bin number) of the target and spectral image peaks as a function of time (ie snapshot) which points out the problem. This plot also shows without doubt that the two peaks are definitely correlated. The gaps at snapshot 32 and 81 were a result of the target and image converging with the DC offset peak at these locations, so that data from these points were not reliable. One piece of evidence that may invalidate the premise of amplitude and/or phase imbalance is the fact that one would expect that the target (larger peak in the spectrum) and the image (smaller) should be at the same location regardless of which array element the data was coming from. This was not the case as can be seen in Figure 3.2.3 showing data from horn 7, in which the larger peak is on the left, and the smaller is on the right, contrary to the other elements of the array except for horn 3. Figure 3.2.4 displays a series of plots giving the amplitude ratio of the target to image (target and image as defined in Figure 3.2.2) for each of the 8 elements over the course of the run. The results of this analysis may at some point be useful for calibrating the data.

Another possible explanation for the presence of two peaks in the frequency power spectra would be that the two peaks are due to the effects of the rotating blades of the helicopter; the peak on the right (+Doppler frequency) would be due to one blade approaching the radar and the peak on the left (-Doppler frequency) due to the receeding blade. There are several considerations which would argue against this idea, two of which are: 1) there were more than two blades on the main rotor of the helicopter, and 2) one would expect that the peaks should be virtually identical in amplitude.

One would also expect that if the two signals were due to the blades of the helicopter, then the target-radar geometry should have been virtually the same, hence the amplitude ratios between receiver elements should also have been the same for the approaching and receeding blades. These ratios are shown in Figure 3.2.5 and 3.2.6 for the 'target' and 'image' respectively. It can be seen that the two sets of plots are quite different.

As a result of the problems discussed above, the calibration of the March 1993 data was not very successful. These particular problems were not present in the data which was recorded during the September 1994 trials using the upgraded

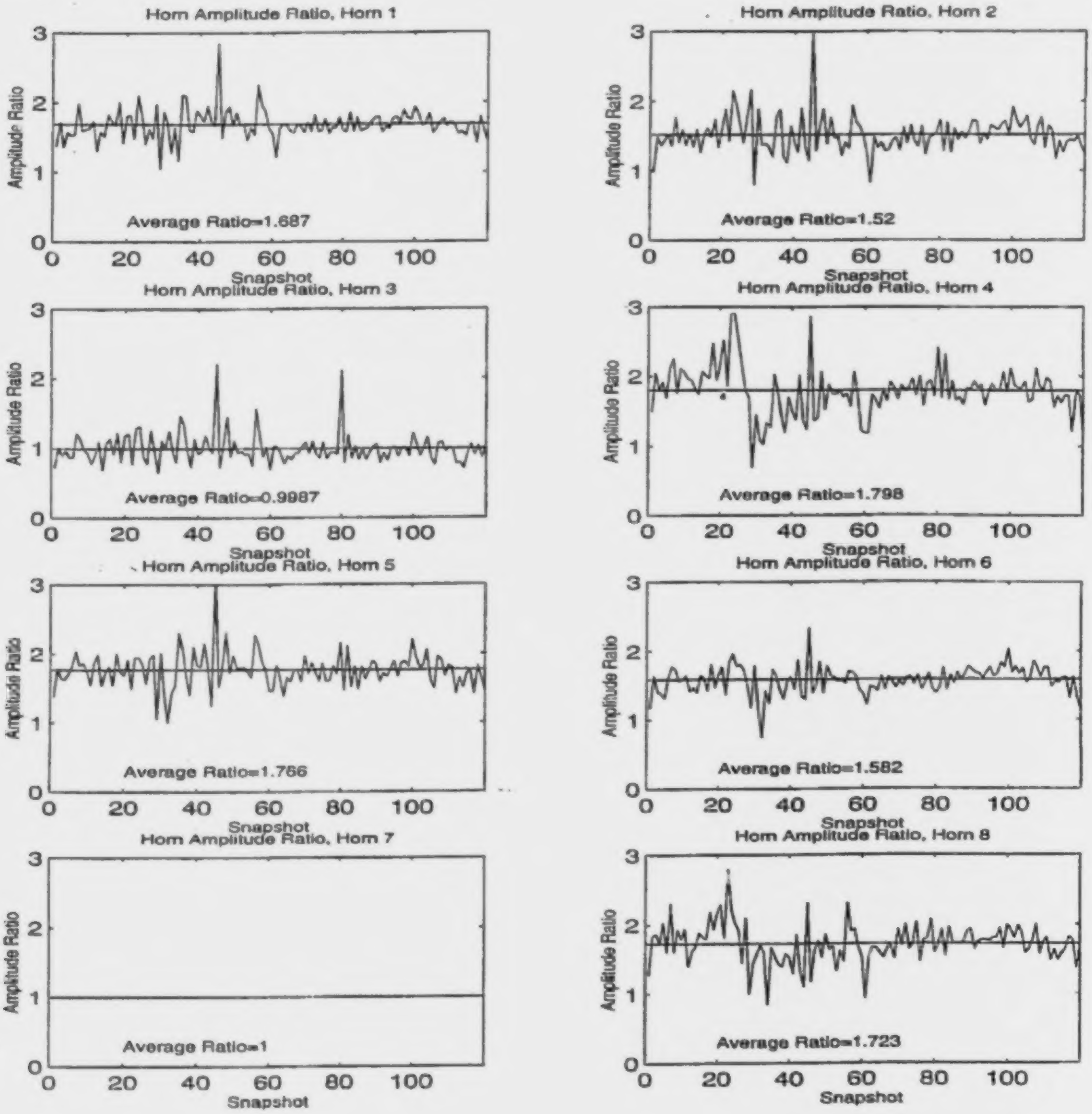

Figure 3.2.5 Plots of the received signal amplitude for each array element normalized to horn7. The results are taken from the 'Target' peak of the FFT.

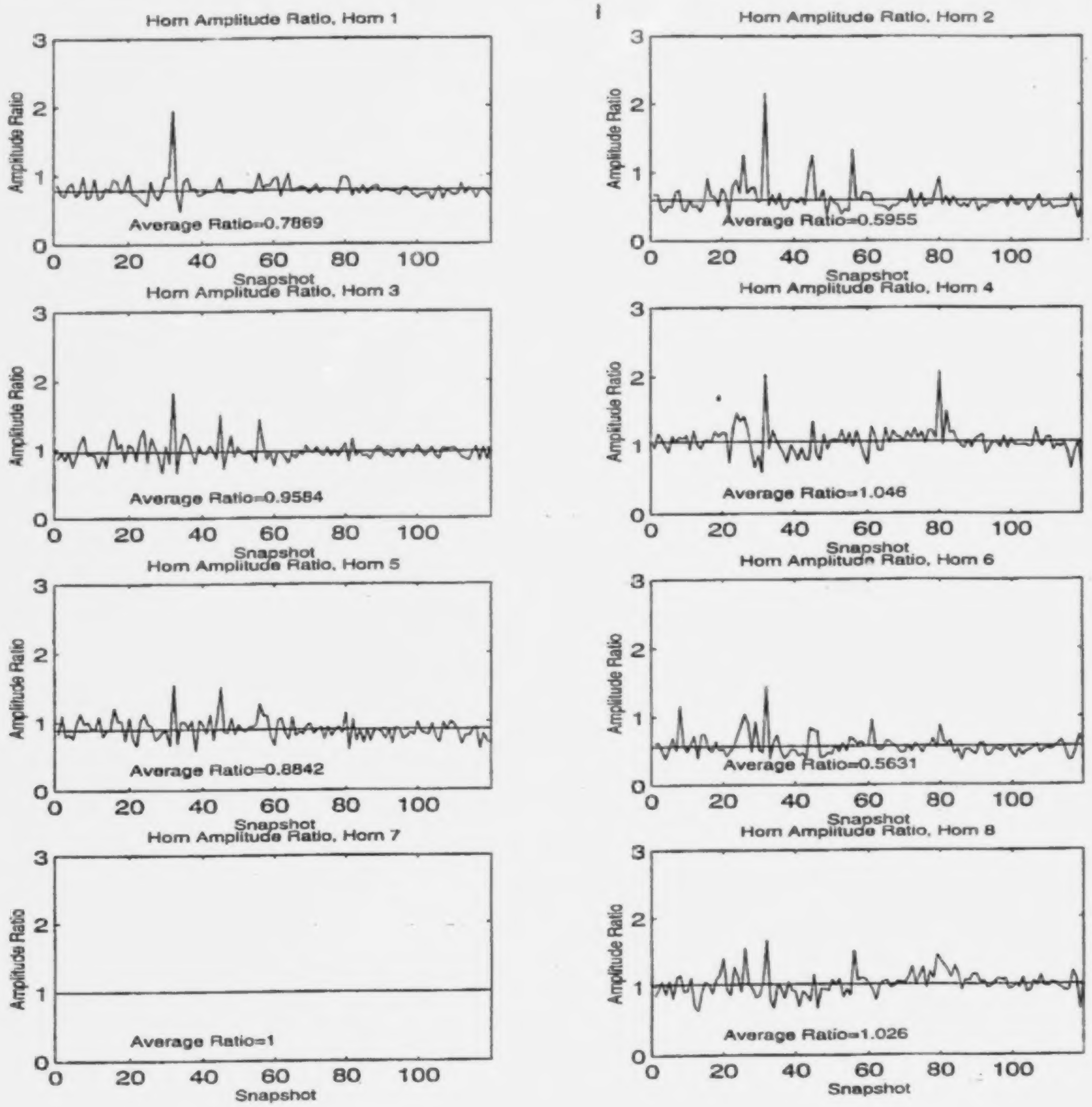

Figure 3.2.6 Plots of the received signal amplitude for each array element normalized to horn7. The results are taken from the spectral image peak of the FFT.

experimental array radar system (EARS), with the new data acquisition system that was capable of sampling real data at the radar systems intermediate frequency. The I and Q signals generated from this data using the Hilbert transform, by definition, did not suffer from the same amplitude and/or phase imbalances in each receiver and the DC offsets in this data turned out to be negligible in most cases. Further discussion on the calibration of the 1994 data will be postponed until section 3.5.

3.3 Task 1a)iii) Data Analysis and Testing the Effectiveness of the Main-beam and Side-lobe Canceller Software

Initial tests of the effectiveness of the main-beam and side-lobe canceller routines were carried out using data gathered during experimental trials at Area 5, in March and September of 1993. The March helicopter trials were mainly used for testing the main-beam jammer cancellation routines whereas, the September trials were primarily for testing the SLC routines with the Rotman lens attached to the SLC array. The Rotman lens attachment was supposed to provide instantaneous RF beamforming of the incoming radar signals. Its ability to carry out this task was proven in previous trials that were documented in the previous final report cited earlier.

As mentioned in the previous section (3.2), difficulties with the quality of the data, as well as calibration problems, made the analysis of the March data difficult. However it was useful in demonstrating that the main-beam jammer cancellation routines were capable of significantly improving the signal detection ability after jammer removal. Figure 3.3.1 shows the FFT power spectrum of a typical jammed helicopter (target) signal before and after jammer cancellation using the SEWE technique. Since the helicopter signal could not be observed in the main-beam array, the SLC array was used to obtain these results.

The data obtained from the Sept. 7/93 SLC trials with the Rotman lens was tested with the side-lobe cancellation software; however none of the data files from that day showed a very significant improvement after jammer cancellation. The following method was used to carry out the analysis:

a)first, when only the target signal was present (no jammer), the average signal strength from each of the 8 Rotman lens outputs was determined Presumably, the output with the largest signal, corrected for the response of each output channel, would correspond to the direction of the signal. This data was recorded for future reference. Knowing which output belonged to the target direction was supposed to help eliminate certain outputs as possible jammer beam directions. However, the results of this

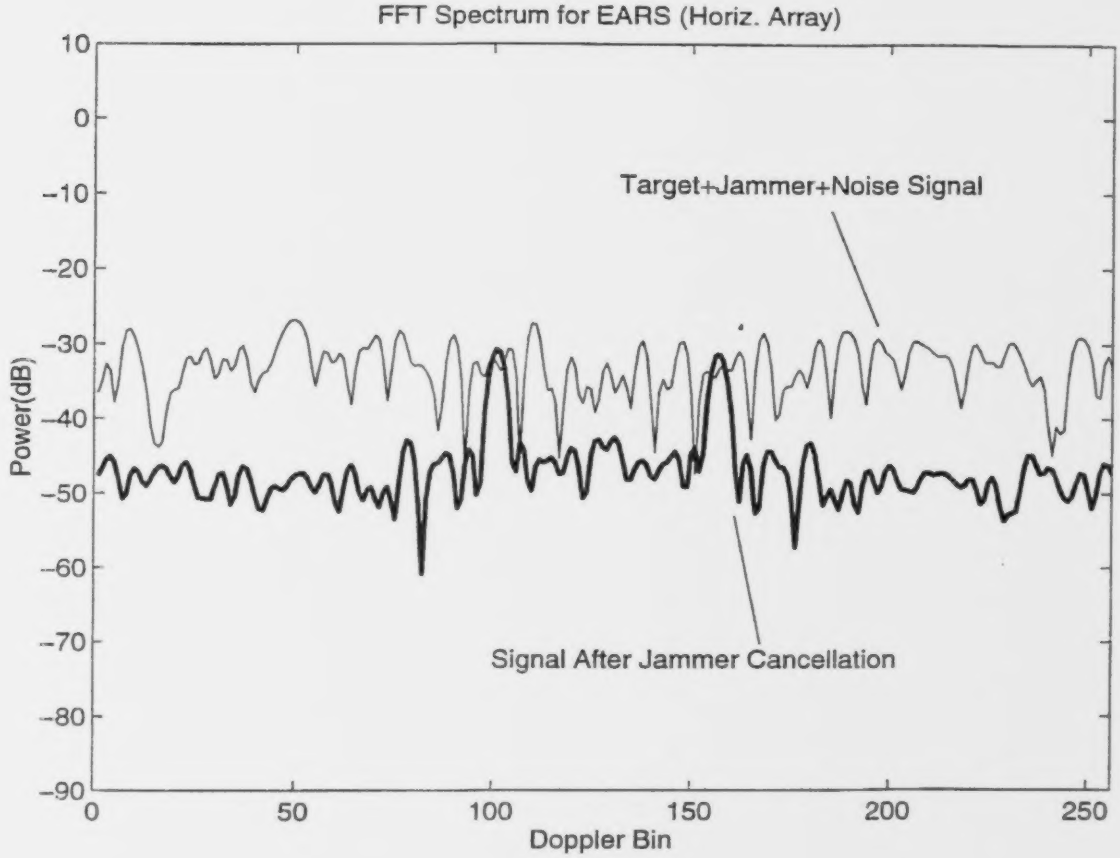

Figure 3.3.1 Typical FFT power spectrum from the March 1993 Helicopter runs using data from the side-lobe canceller array. The thin line shows the spectrum before jammer cancellation using SEWE and the thick line displays the results after cancellation.

part of the analysis were ambiguous.

b)next, because of the ambiguous results found in a), each one of the eight Rotman lens outputs was used as a possible jammer beam to carry out the jammer cancellation. The sidelobe cancellation algorithm was applied to each individual element of the main-beam array using a single output from the Rotman lens, then the results were summed to get the total 'cancelled' power from the main-beam array. These results were compared graphically with the total uncancelled power, for each Rotman lens beam output. There did not appear to be a significant difference in the cancelled power results between different Rotman lens ouputs. The plots that were created in the above analysis were shown to the Scientific Authority for inspection, and copies were kept for future reference.

Because of the negative results of this analysis, and because similar experiments carried out in Aug.-Sept. 1994 provided much better results (see section 3.6), the plots mentioned above were not included in this report.

3.4 Task 1 b) i) Generation of I and Q Signals from IF Data.

The following is a brief outline of the technique used for generating the I and Q signal components using the Hilbert transform. For a continuous function x(t)., the Hilbert transform y(t) is given by:

$$\begin{aligned} y(t) &= \frac{1}{\pi}\int_{-\infty}^{\infty}\frac{x(\tau)}{t-\tau}d\tau \\ &= x(t)*\frac{1}{\pi t} \end{aligned}$$

where * denotes the convolution operation. The convolution property of the Fourier transform was used to generate the Hilbert transform because of its conduciveness to digital computer calculations. Based on this property we have that:

$$\begin{aligned} \boldsymbol{Y}(f) &= \boldsymbol{X}(f)\cdot\boldsymbol{H}(f) \\ &= \left(\int_{-\infty}^{\infty}x(t)e^{-2\pi ft}dt\right)\cdot\left(\int_{-\infty}^{\infty}\frac{e^{-2\pi ft}}{\pi t}dt\right) \\ &= -j\cdot\boldsymbol{X}(f)\cdot sgn(f) \end{aligned}$$

where the signum function (*sgn*) is defined as:

$$\begin{aligned} sgn(f) &= \frac{|f|}{f} \\ &= \begin{bmatrix} 1 \ for \ f>0 \\ 0 \ for \ f=0 \\ -1 \ for \ f<0 \end{bmatrix} \end{aligned}$$

It follows that the Hilbert transform is simply the inverse Fourier transform of $\boldsymbol{Y}(f)$:

$$y(t) = \int_{-\infty}^{\infty}\boldsymbol{Y}(f)e^{2\pi ft}df$$

Since the data was sampled at discrete time intervals, the continuous functions and transforms given above were replaced by their discrete counterparts; ie the continuous Fourier transform was replaced by the Fast Fourier Transform (FFT), a fast computer algorithm for calculating the discrete Fourier transform (DFT). Some additional signal processing was done on the data to filter out the IF carrier. The full technique is discussed in the paper by D.W. Rice and R.H.Wu, "Quadrature Sampling with With Dynamic Range", IEEE Trans. AES, Vol. 18, No.4, Nov. 1992.

Some of the software developed for generating the I and Q signals from the IF data a is described briefly as follows:

MOODE1	(Main-beam array **O**n-target **O**ff-target **D**ata **E**xtractor ver. **1**) This program was used for preprocessing data from the EARS data logger tapes. It reads the data from a single radar pulse, performs a Hilbert transform and associated signal processing to generate I and Q signals for each vertical array receiver channel, extracts data from the pulse corresponding to a specified on-target and off-target location in the pulse, and finally stores the results in a file for later retrieval. This version of the software did the required signal processing by interfacing with MATLAB functions and subroutines such as **piq3avg**. Version 2 of this program, called **MOODE2**, bypassed MATLAB and did the required signal processing by calling the FORTRAN subroutines **HILBT** and **FFTPC**.
piq3avg.m	-a MATLAB function for doing the appropriate signal processing of the data (ie Hilbert transform, etc) to create the Quadrature signal component from the In-phase signal.
HILBT.FOR	-the FORTRAN subroutine equivalent of **piq3avg**. This subroutine replaced **piq3avg** to speed up some of the data processing routines. Since many of these routines were written in FORTRAN, they required a software interface between MATLAB and the host to access functions such as **piq3avg**, thus reducing processing efficiency. This subroutine called the fast Fourier transform subroutine **FFTPC**, written in FORTRAN, to calculate the Hilbert transform.

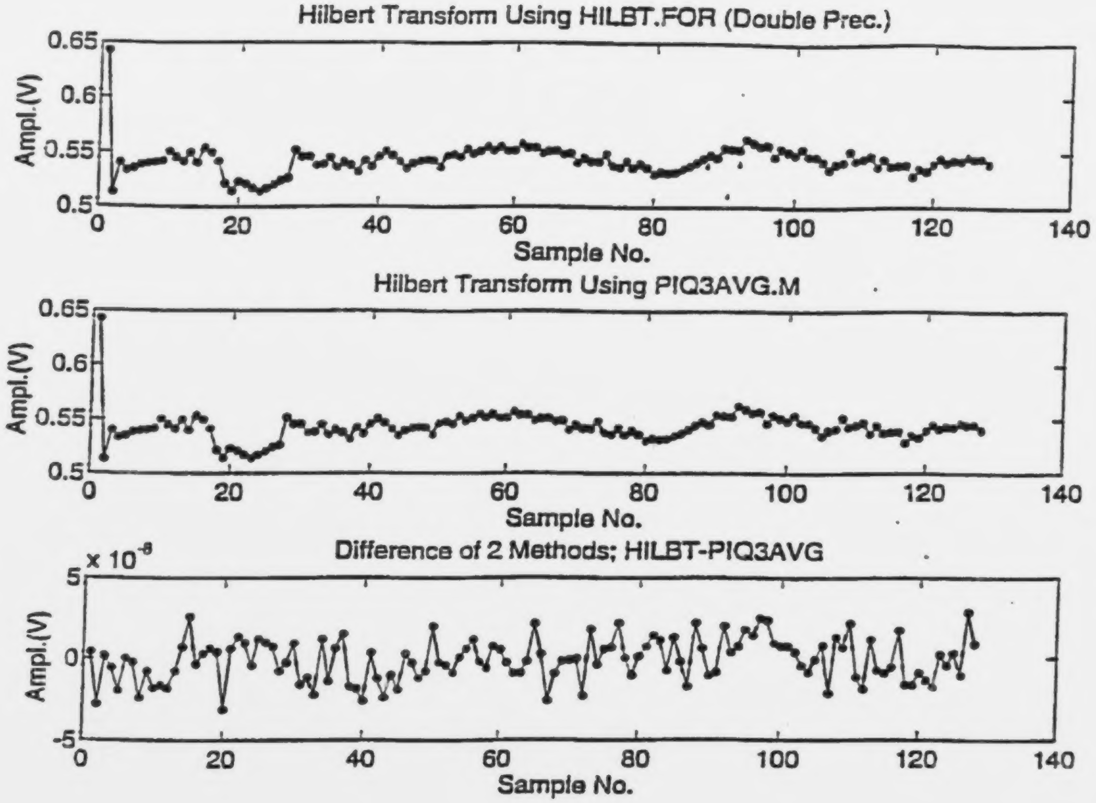

Figure 3.4.1 A comparison of the Fortran and MATLAB versions of the Hilbert transform software applied to one pulse of the Sept. 1994 trials. The results are virtually identical, with the bottom graph showing that the difference between the two results was less than 1 in 10^{7}.

3.5 Task 1b) ii) Calibration and Processing of the Aug.-Sept. 1994 Trials Data

As cited in section 3.2, the calibration of the Aug.-Sept. 1994 trials data from Area 5 presented fewer problems than the earlier trials in 1993. Using the upgraded EARS, with the new data acquisition system and sampling at the intermediate frequency, the I and Q signals generated via the Hilbert transform, by definition, could not suffer from the same amplitude and/or phase imbalances in each receiver. Also, in this data the DC offsets turned out to be negligible in most cases. However, there still remained the problem of calibrating the arrays for phase and amplitude mismatching between receiver elements.

Multipath can affect the far field signal from a target in unpredictable ways, hence it is very difficult to obtain a reliable estimate of the amplitude and phase offsets between the separate antenna elements. However, data that may be used for calibration purposes was generated from analysis of the data from Run 11 of the September 8 1995. Since the projection methods used for main-beam jammer cancellation (see Section 3.1) are somewhat nonlinear, it was useful to try removing the CW jammer from the received signal by modelling it, and directly subtracting the model. Ideally this would reduce the jammer peak in the FFT (power) spectra and leave only the return from the target; it could also be compared to the results of the projection methods to point out any undesirable artifacts of the projection techniques. This procedure turned out to be fairly successful, since it reduced the jammer signal strength by approximately 30 dB. The same procedure carried out on what was believed to be the target signal with similar results. Table 3.5.1 contains the frequency amplitude and phase information for each channel of the array that were used to model and subsequently remove the jammer for three sections of data: pulses 1-140 for the first section, pulses 141-200 for the second section and pulses 200-250 for the third section. The modelling by sections was required because the frequency of the jammer had a tendency to drift with time. It should also be noted here that the jammer data for Table 3.2.1 were taken from one sample point on the off-target range cell (after I and Q generation via Hilbert transform) for 250 consecutive pulses. Table 3.5.2 contains similar frequency, amplitude and phase data for the target, a helicopter hovering at about 60 m, range 3750 m. Only data for pulses 1-140 were considered for this part of the analysis. Figure 3.5.2 shows the FFT spectrum of the first 200 pulses sampled at the target range cell before, (a), and and after, (b), the jammer was removed by the modelling technique.

The parameters (ie amplitude, frequency, and phase offset) for modelling the jammer and target signals were obtained using a least mean squares (LMS)

Table 3.5.1
(Model Parameters for Jammer, Run 11 Sept.8/95)

	Section 1 Pulses 1-140			Section 2 Pulses 141-200			Section 3 Pulses 201-250		
Horn No.	A_o (volts)	ϕ_0 (deg)	Freq. (Hz)	A_o (volts)	ϕ_0 (deg)	Freq. (Hz)	A_o (volts)	ϕ_0 (deg)	Freq. (Hz)
1	0.520	-170	156.55	0.520	-108	155.38	0.520	-97	155.10
2	0.592	-144	"	0.592	-82	"	0.590	-72	"
3	0.649	-155	"	0.649	-93	"	0.649	-83	"
4	0.546	-93	"	0.546	-31	"	0.515	-23	"
5	0.545	-80	"	0.545	-18	"	0.515	-9	"
6	0.546	-67	"	0.546	-5	"	0.515	-355	"
7	0.538	-45	"	0.538	-343	"	0.500	-332	"
8	0.468	-24	"	0.468		"	0.450	-310	"

Table 3.5.2
(Model Parameters for Jammer+Target, Run 11 Sept 8/95)

Horn No.	Jammer Frequency (Hz)	A_0 (volts)	ϕ_0 (degrees)	Target Frequency (Hz)	A_1 (volts)	ϕ_1 (degrees)
1	156.55	0.520	-117	-41.3	0.065	-245
2	"	0.592	-90	"	0.040	-225
3	"	0.649	-100	"	0.025	-300
4	"	0.546	-40	"	0.050	-320
5	"	0.545	-27	"	0.075	-325
6	"	0.546	-14	"	0.095	-320
7	"	0.538	-352	"	0.095	-310
8	"	0.468	-331	"	0.080	-300

algorithm that was implemented using MATLAB software. A three dimensional search was performed to minimize the function **G** with respect to the three parameters A, f, and ϕ where **G** was given by:

$$G(A,f,\phi)=\sum_{m=1}^{M}(A\cdot\cos(2\pi f m\Delta t+\phi)-I(m))^2$$

and where A was the amplitude, f the frequency, m the (pulse) sample number, ϕ the phase offset, Δt the sample interval, and **I**(n) the actual in-phase signal after the Hilbert transformation. The initial estimate of f was obtained from the FFT power spectrum of the data, the initial estimate of the amplitude was obtained from the plot of the in-phase signal versus time, and the phase was obtained by searching through 360° in 1° steps. Some fine tuning of the parameters was accomplished by observation of the FFT spectrum after the subtraction of the modelled jammer signal.

Additional calibration information was obtained from the estimation of the beacon jammer and target directions using a spatial Fourier transform. Since the jammer was located at approximately 2m from the water surface at a range of 2 km, the radar beam directly from the jammer and the image due to reflection from the water surface could not be resolved. The peak in the spatial FFT spectrum showed a consistent value of 0.937° (for uncalibrated data). This can be seen in Figure 3.5.3 showing the results of the spatial FFT for run 5 of Sept. 8; similar results were observed from the other experiments. The data shown in Figure 3.5.3 was obtained without integration of the jammer signal. Figure 3.5.4 displays a series of 8 pairs of plots for each (integrated) snapshot of 256 array data vectors. The first plot of each pair shows the 256 point FFT frequency spectrum of the array output power and the estimated frequency of the jammer; the second plot show the results of the spatial FFT of the integrated data obtained from time sequence FFT. The number appearing above each peak in the spatial FFT indicates the jammer direction estimated from the peak.

For the given beacon-jammer geometry (receiver height of 10m, jammer height and range of 2m and 2km respectively) the beacon direction should have been approximately -0.229°. From these observations it became obvious that a tilt correction had to be incorporated into the data before any target tracking could be done using RML. This capability was incorporated into the MULTIFRML program used for analysing the data.

a) Frequency Spectrum of Target+Jammer+Noise Signal

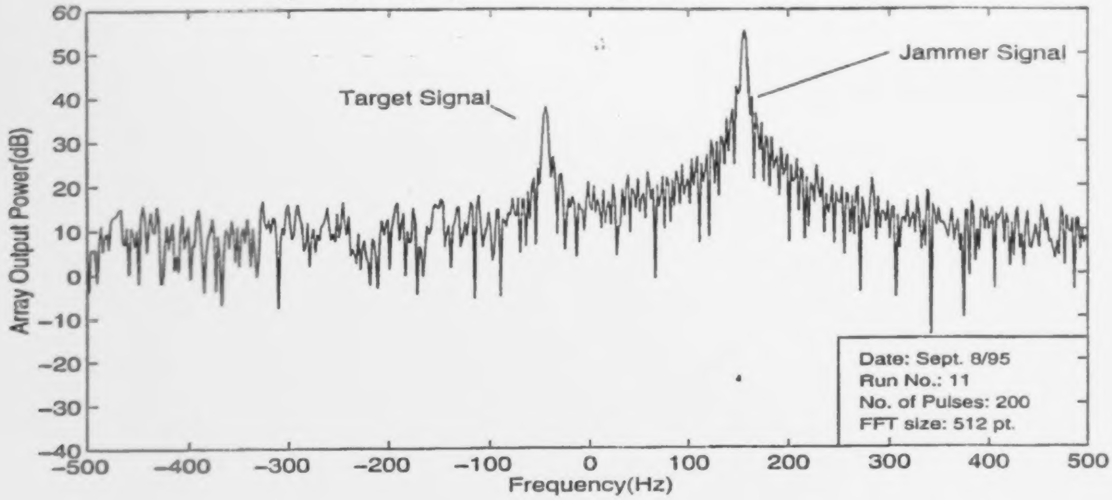

b) Frequency Spectrum with Reduced Jammer Signal

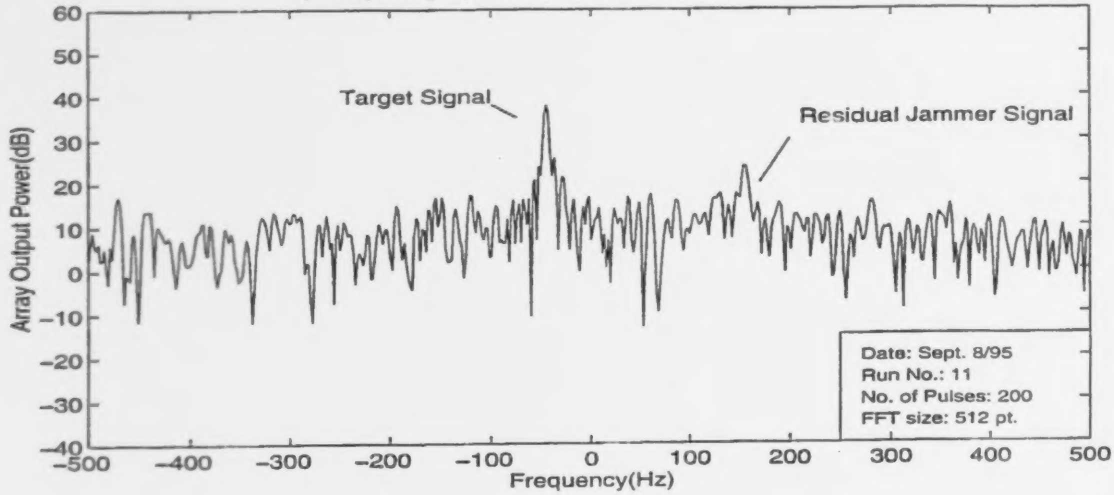

Figure 3.5.1 FFT power spectra of the received signal from Run 11, Sept.8/94 before, a), and after, b), the jammer removal using the modelled jammer signal.

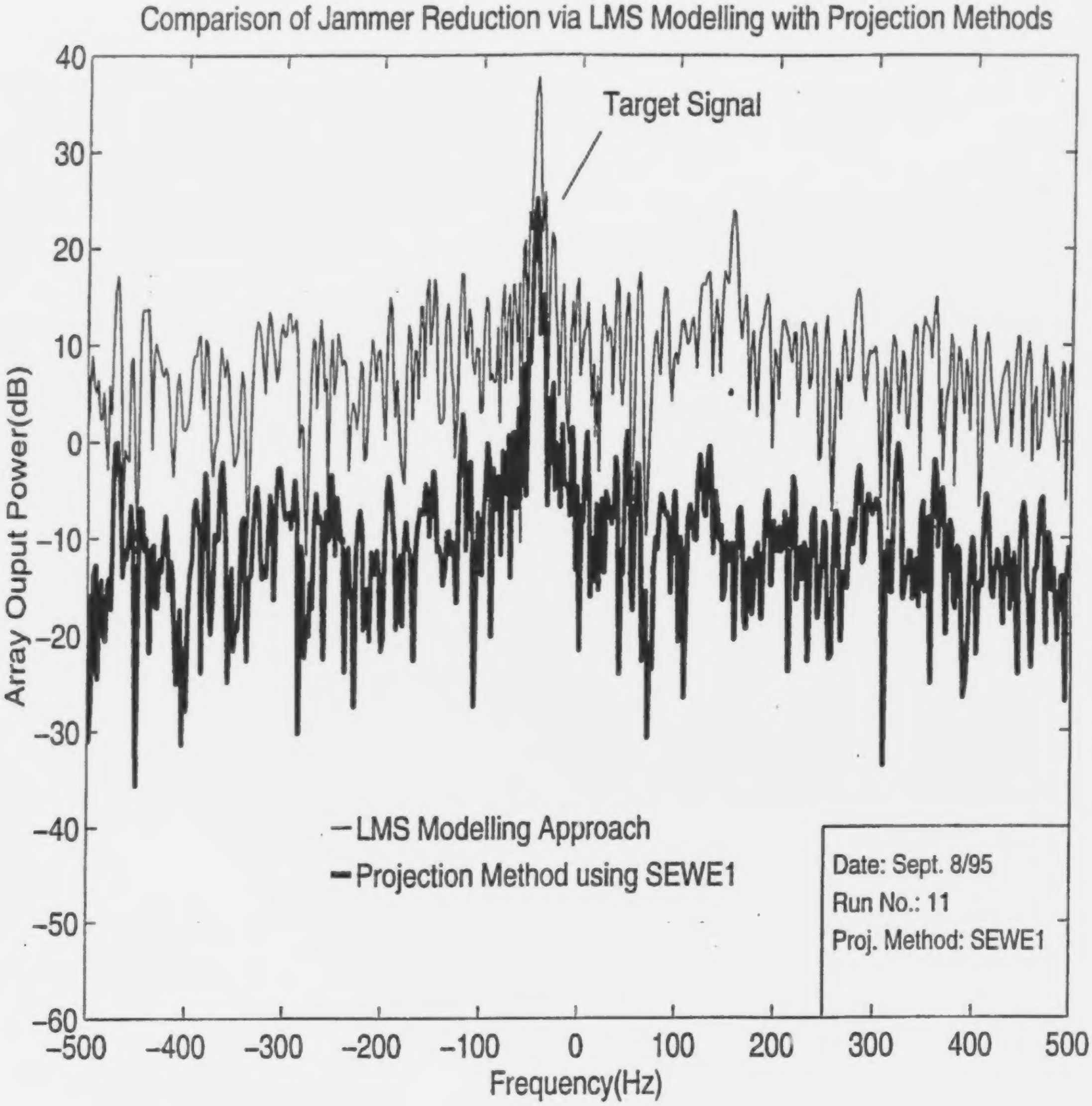

Figure 3.5.2 Comparison of the jammer removal using the LMS modelling and the SEWE projection technique. The projection method is superior in removing the jammer interference from the received signal.

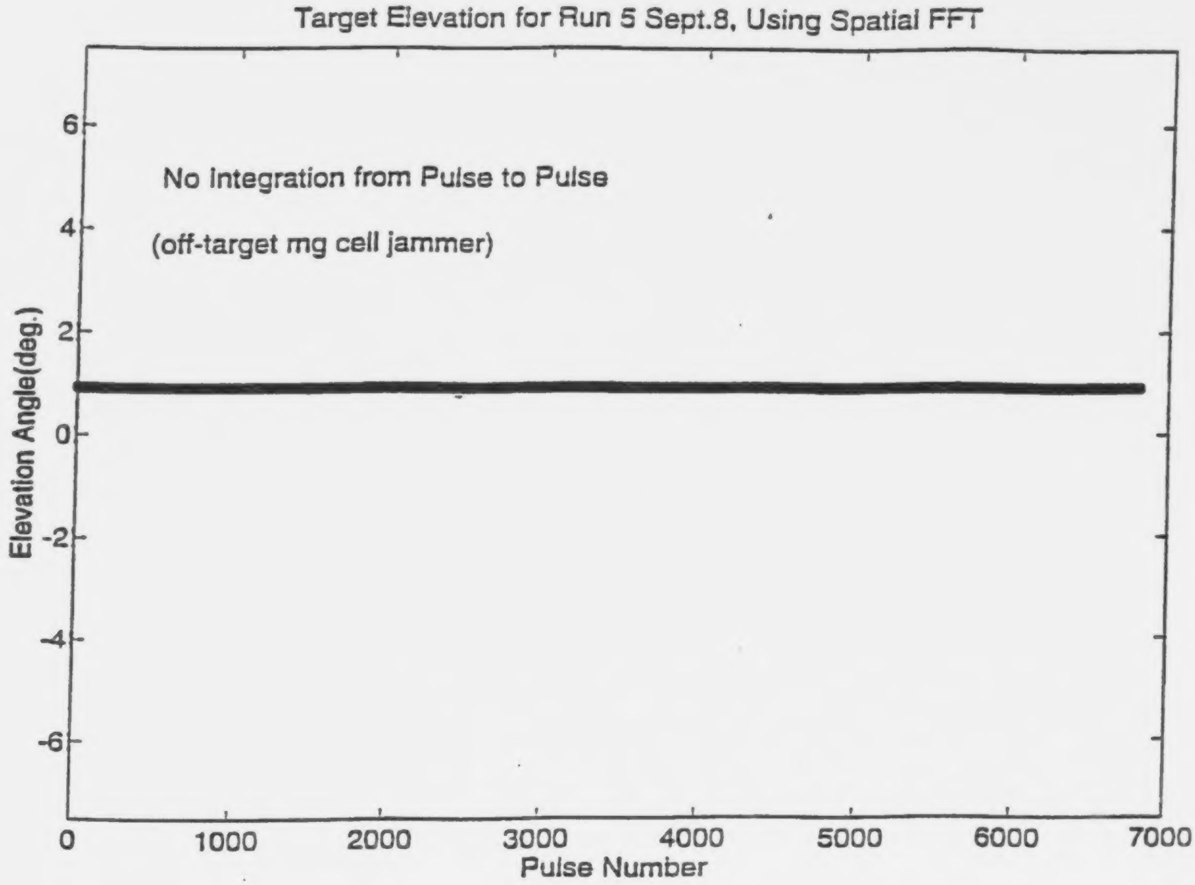
Target Elevation for Run 5 Sept.8, Using Spatial FFT
No Integration from Pulse to Pulse
(off-target rng cell jammer)
Elevation Angle(deg.)
6
4
2
0
-2
-4
-6
0
1000
2000
3000
4000
5000
6000
7000
Pulse Number

Figure 3.5.3

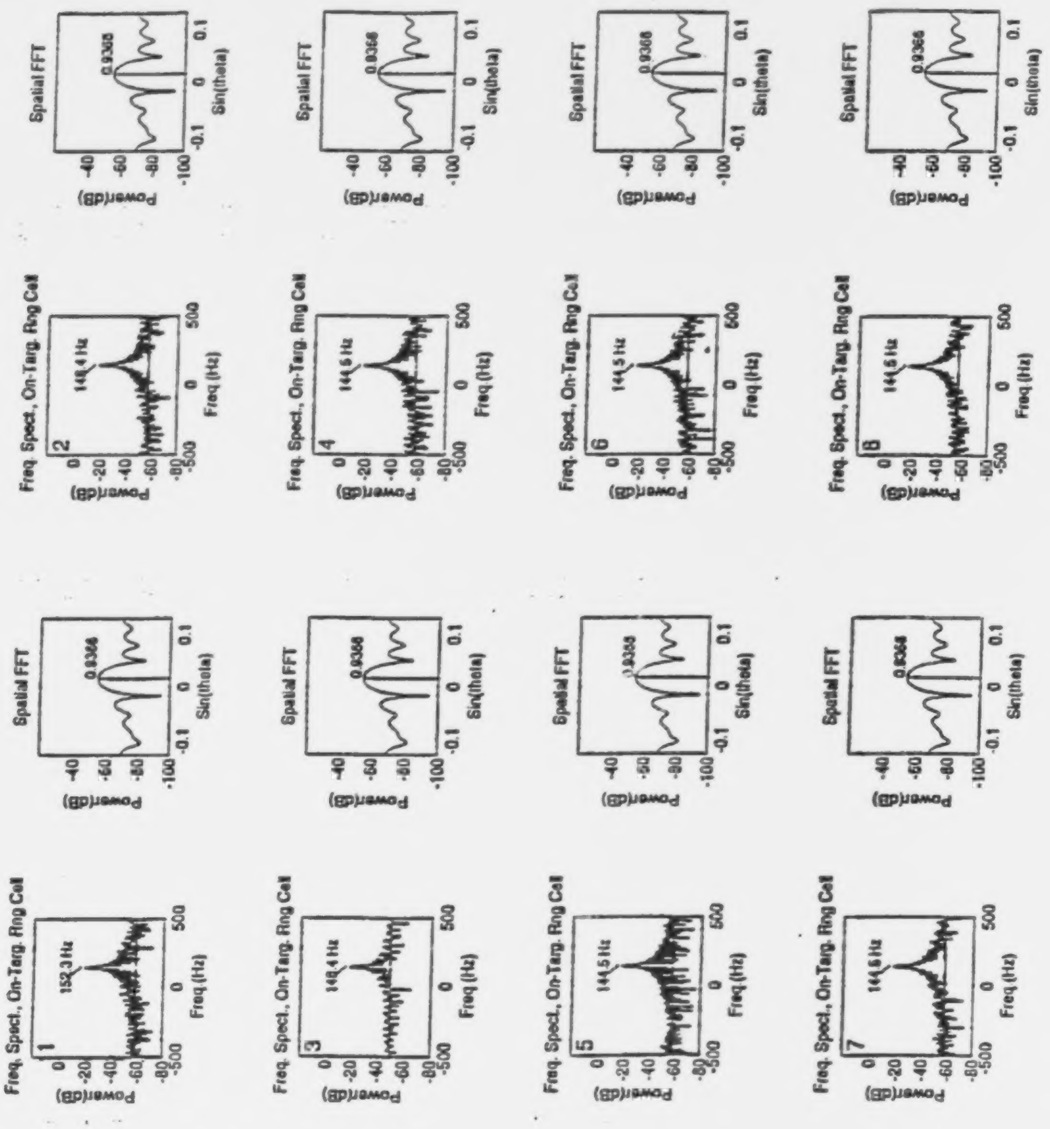
Freq. Spect., On-Targ. Rng Cell
Spatial FFT
Power(dB)
Freq (Hz)
Sin(theta)
1
2
3
4
5
6
7
8
152.3 Hz
0.9366
-500
0
500
-0.1
0.1

Figure 3.5.4

3.6 Task 1b) iii) Sensitivity Analysis of Main-beam and Side-lobe Cancellation Methods using Aug.-Sept. 1994 Trials Data.

The analysis of the 1994 trials data generally started by implementing the following steps:

1) read part of a data file from the data logger tape, eg. N pulses of data.
2) use a MATLAB program called **piq00avg.m** to gain a preliminary overview of the data (jammer off) and determine, among other things, the locations of targets and nulls within the return pulse. The null locations were later used to sample jammer+noise signals for the jammed data to generate the jammer+noise covariance matrix needed for the anti-jamming algorithms.
3) generate the covariance matrix and carry out the main-beam and/or SLC evaluation.

The program **piq00avg** (originally written by the Scientific Authority, then modified by AIT personnel) would read a specified number of pulses of radar return data, then generate 6 output plots. A typical example of such a series of plots is shown in Figure 3.6.1 for data obtained from the second receiver element from the bottom of the vertical array. Proceeding in a counter clockwise direction from the plot in the upper left corner, the 6 plots generated by **piq00avg** were as follows: a) a plot of phase vs range for each range sample in the pulse, b) Signal amplitude vs range after integration over N pulses, c) two plots of the raw signal data for two selected pulses d) a plot of the amplitude of the difference signal (between successive pulses) to help remove clutter and enhance the identification of moving targets (like MTI radar), and finally e) a plot of the Hilbert transform of the last of the N pulses in the train. A set of plots is shown in Figures 3.6.1 to 3.6.21 for the set of trials completed on Sept. 7, 1994. Each of the Figures display the results of integration of the data over 20 radar pulses. Similar plots were produced for the experiments completed on the other days and presented to the Scientific Authority.

The next step in the data analysis was to verify that the main-beam and side-lobe jammer cancellation algorithms could reduce the jammer interference and improve the target signal detection. This was done for both main-beam and side-lobe cancellation by applying the anti-jamming algorithm to each range cell of the return pulse of the jammed data and comparing the results with data free of the jammer interference.

MATLAB software was written to analyse the side-lobe canceller data from the September 1994 trials at Area 5, using the sampled matrix inversion (SMI) algorithm to do the jammer cancellation. A brief outline of the algorithm is presented in Appendix E. Two types of data were obtained from the SLC array and used to test the effectiveness of the SLC software: a) data obtained from the SLC array with the Rotman lens RF beamforming network in place, and b) data obtained from the SLC array with the Rotman lens removed, and digital (spatial Fourier) beamforming done in data processing. Some typical results of the analysis using digital beamforming are shown in Figures 3.6.22 to 3.6.25 for runs 5 and 6 of Sept. 14 using a boat and a raft with a corner reflector as targets. Figure 3.6.22 shows the data without any jammer interference. The radar return from the raft, located at a range of 2040m, is observed as the first peak in the plot, and the return from boat at 2400m is shown by the second peak. Figure 3.6.23 shows the data after the jammer has been turned on and the signal from the boat is nealy totally obscured. Figure 3.6.24 displays the results of SLC jammer cancellation on the two target returns using digital beamforming across the SLC array output. Clearly, the jammer cancellation technique worked very effectively. Figure 3.6.25 show the results of jammer cancellation using only one SLC array element to carry out the cancellation procedure. As might be expected, the results were not as good.

Figures 3.6.26 to 3.6.28 show some typical rusults (from runs 17 and 18 of Sept. 13) of the SLC jammer removal for data with the Rotman lens in place. Figure 3.6.26 displays the radar return signals from the boat at 2130m and the raft at 2400m with the jammer turned off. Figure 3.6.27 shows the data after the jammer had been turned on, and Figure 3.6.28 shows the results of the jammer removal with the Rotman lens data. These results indicate that the SLC procedure was quite efficient at reducing the jammer interference.

As with the SLC data analysis, MATLAB software (**remjam.m**) was created to evaluate the effectiveness of the main-beam jammer cancellation software to remove the interference and enhance the target signal detection. Figure 3.6.29 shows some typical results of analysis of the data from a run taken during Sept. 8/94, with jammer interference removed using SEWE1. Plots a) and b) show the full range window of a return pulse integrated over 40 pulses without and with MTI processing respectively. The MTI (Moving Target Indicator) processing was used to reduce the clutter effects, and enhance the signal for a moving target. Each plot also indicates the location of the target range cell observed in non-jammed data. Plots c) and d) show results after the jammer interference had been reduced. Very similar results (not shown) were obtained usning the eigendecomposition (ED1) and SMI methods of jammer cancellation.

Once it had been established that the jammer cancellation algorithms could substantially improve the target detection, it was necessary to determine whether the modified data was suitable for performing target direction estimation using algorithms such as RML. This stage of the analysis involved a study of the on-target and off-target data using Doppler processing. This stage of the analysis was used to perform a comparison of the three methods of jammer removal and to determine an optimal number of data vectors for creating the projection matrix. Figures 3.6.30 and 3.6.31 display the results for the three different projection methods, when the covariance (hence projection) matrix was calculated using 256 data vectors, and 16 data vectors respectively; the results in this case were virtually identical.

Finally, having confirmed the ability to reduce the jammer interference and improve the target detectability, it remained to be seen if the modified data was suitable for target direction estimation. This was done by trying to estimate the height of the helicopter in the series of runs carried out on Sept. 8/93, using the RML algorithm, and taking into account the array tilt mentioned in section 3.5. The results of the analysis are shown in figures 3.6.32 to 3.6.43.

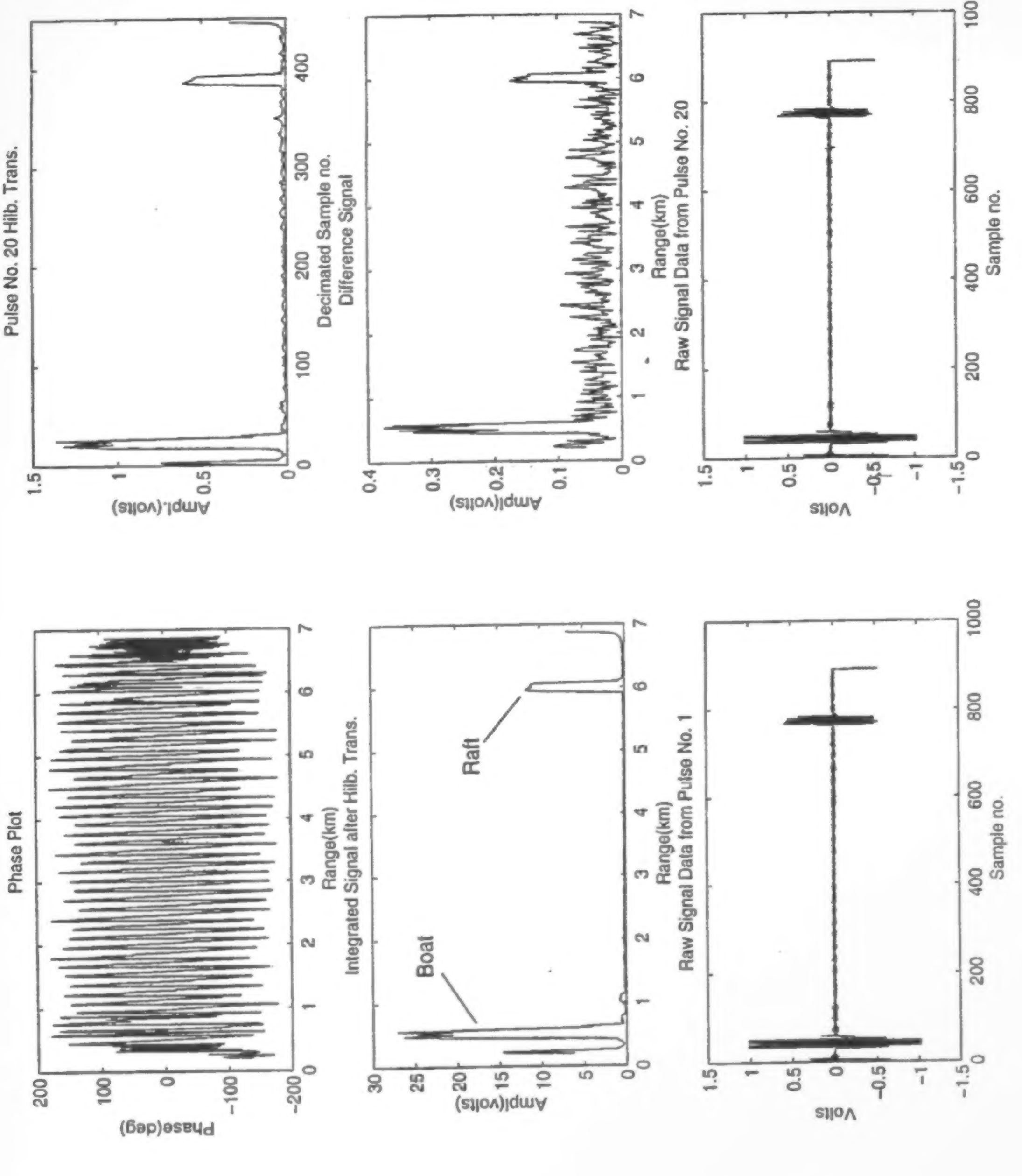

Figure 3.6.1 Plots from **piq00avg** for run 1 Sept. 7/94

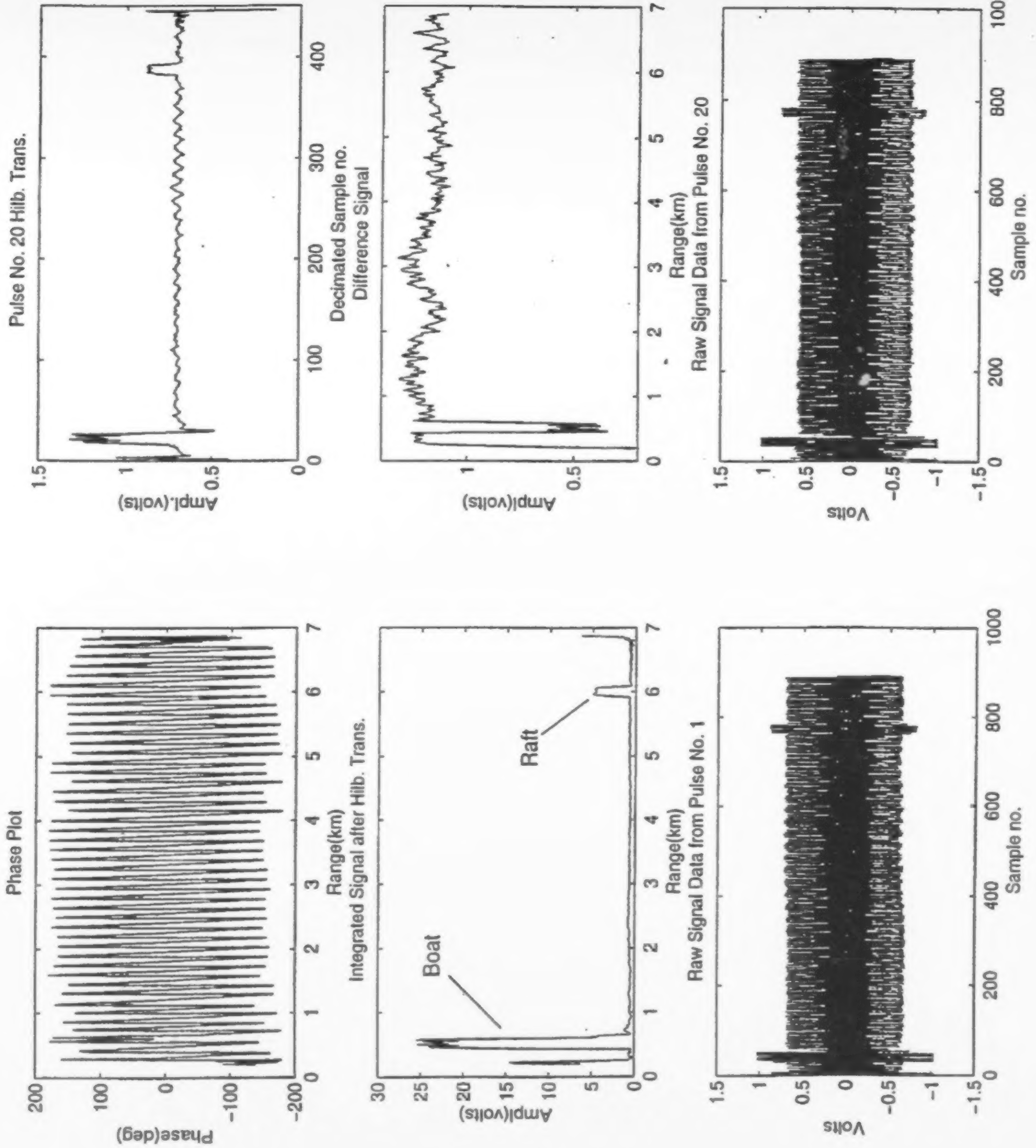

Figure 3.6.2 Plots from **piq00qvg** for run 2 Sept. 7/94

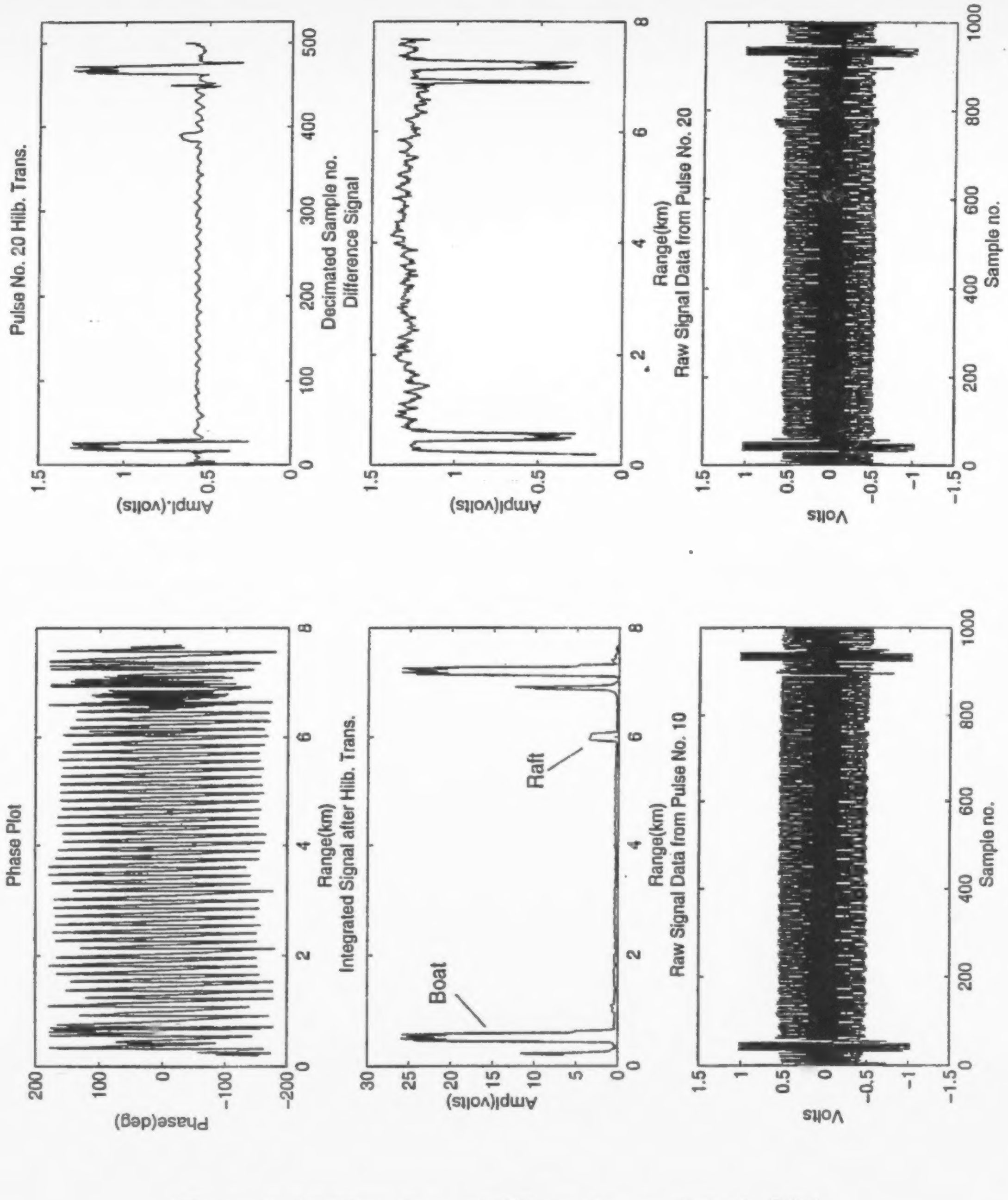

Figure 3.6.3 Plots from **piq00avg** for run 3 Sept. 7/94

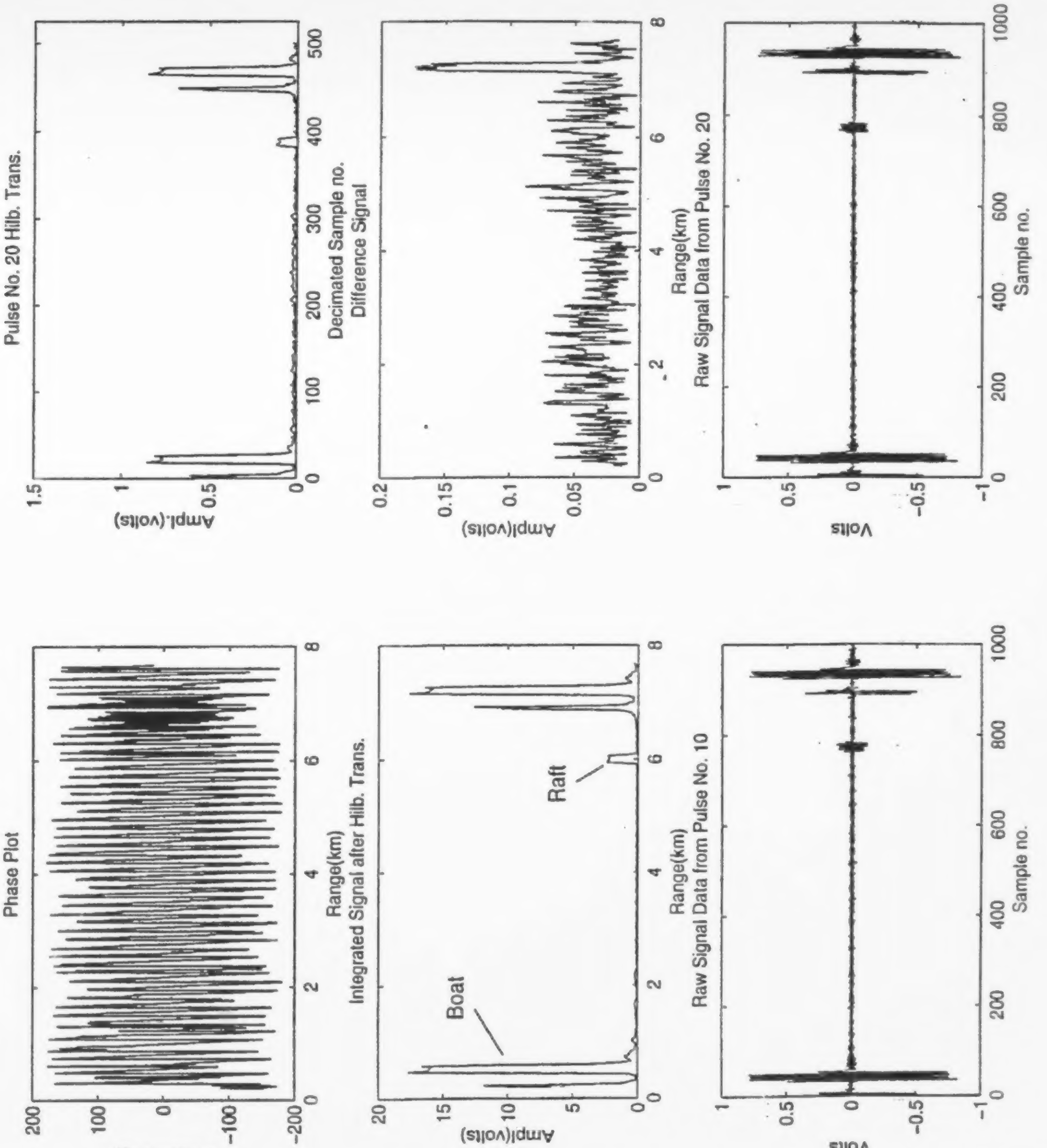

Figure 3.6.4 Plots from **piq00avg** for run 4 Sept. 7/94

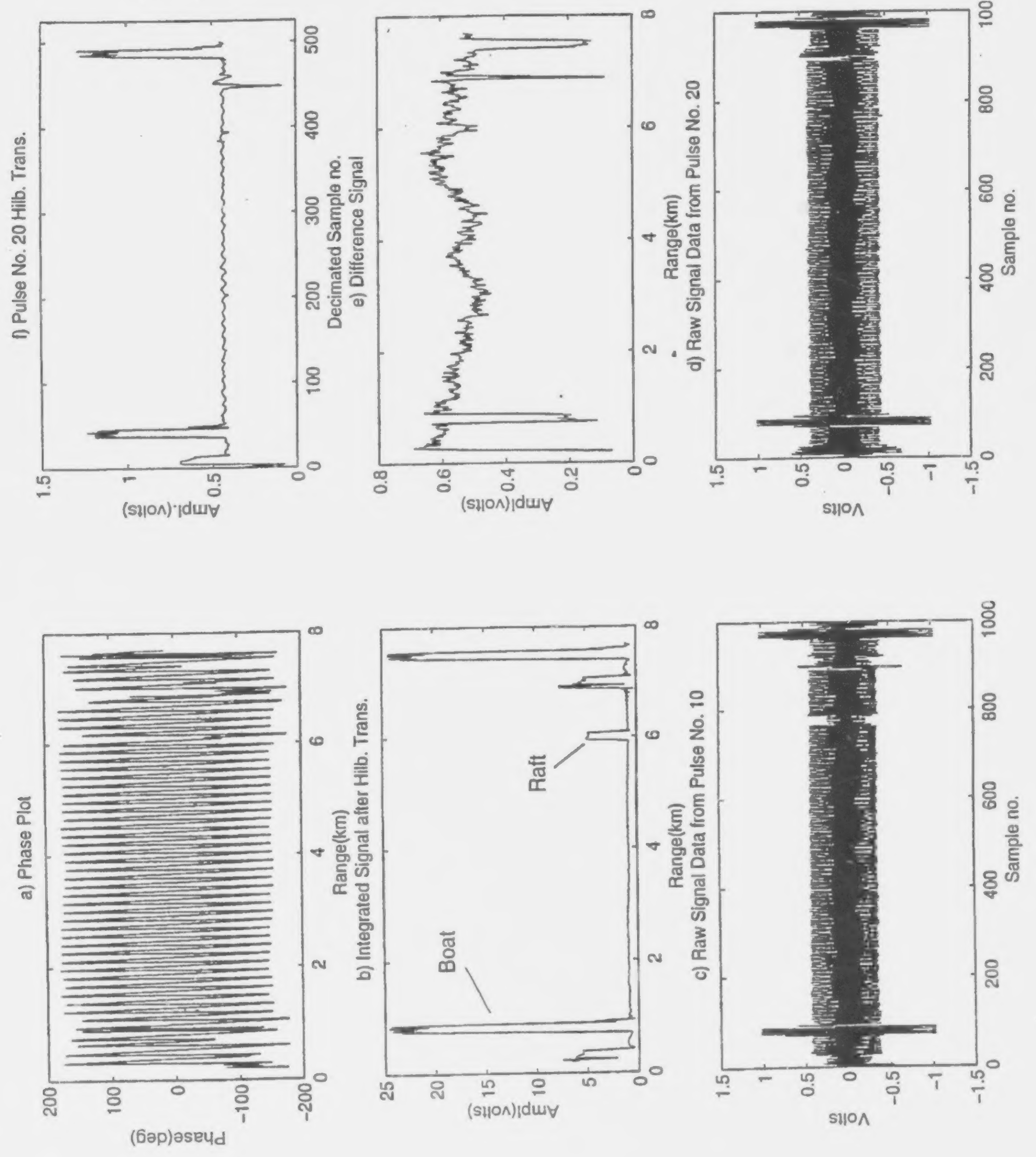

Figure 3.6.5 Plots from **piq00avg** for run 5 Sept. 7/94

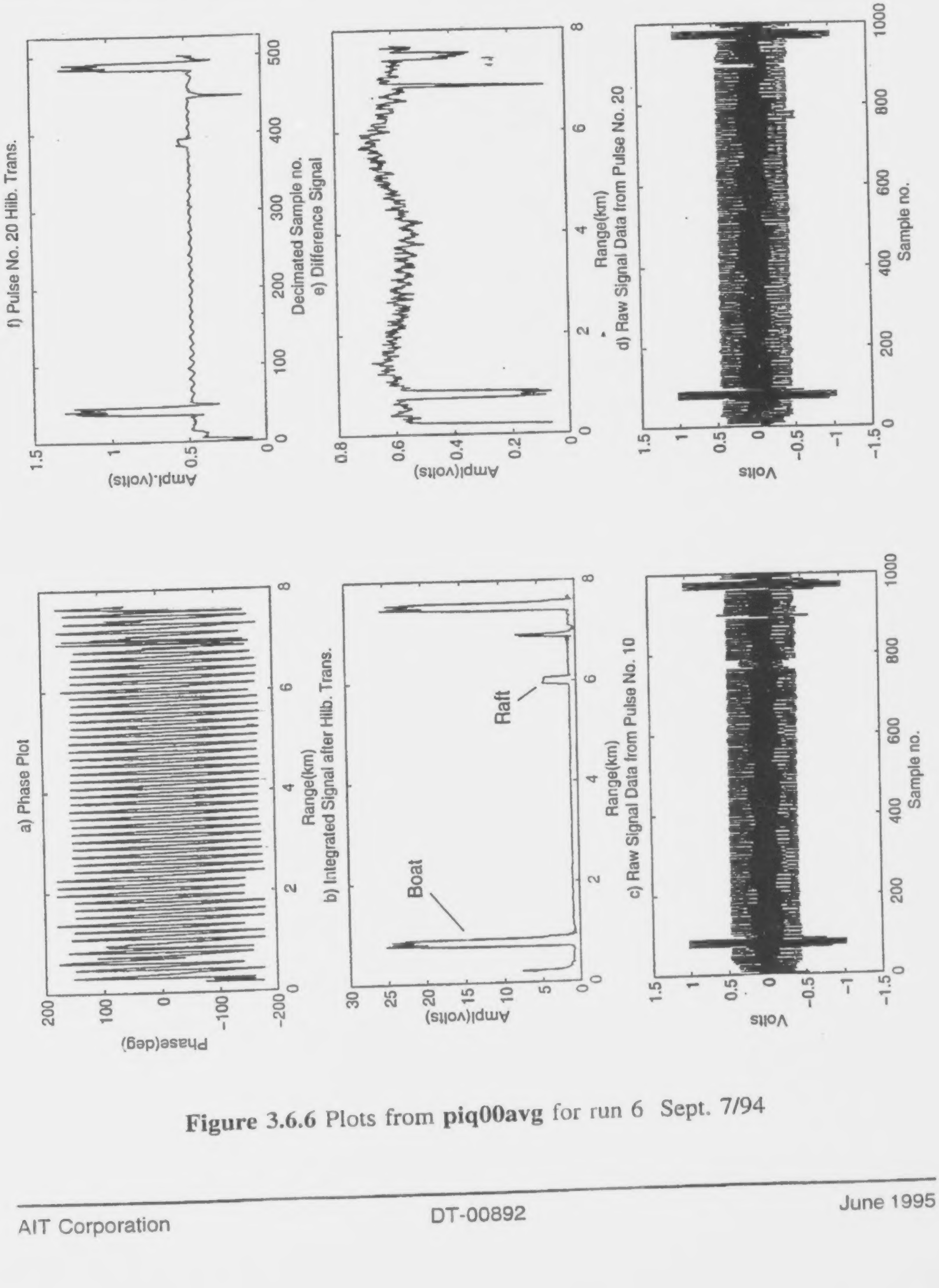

Figure 3.6.6 Plots from **piq00avg** for run 6 Sept. 7/94

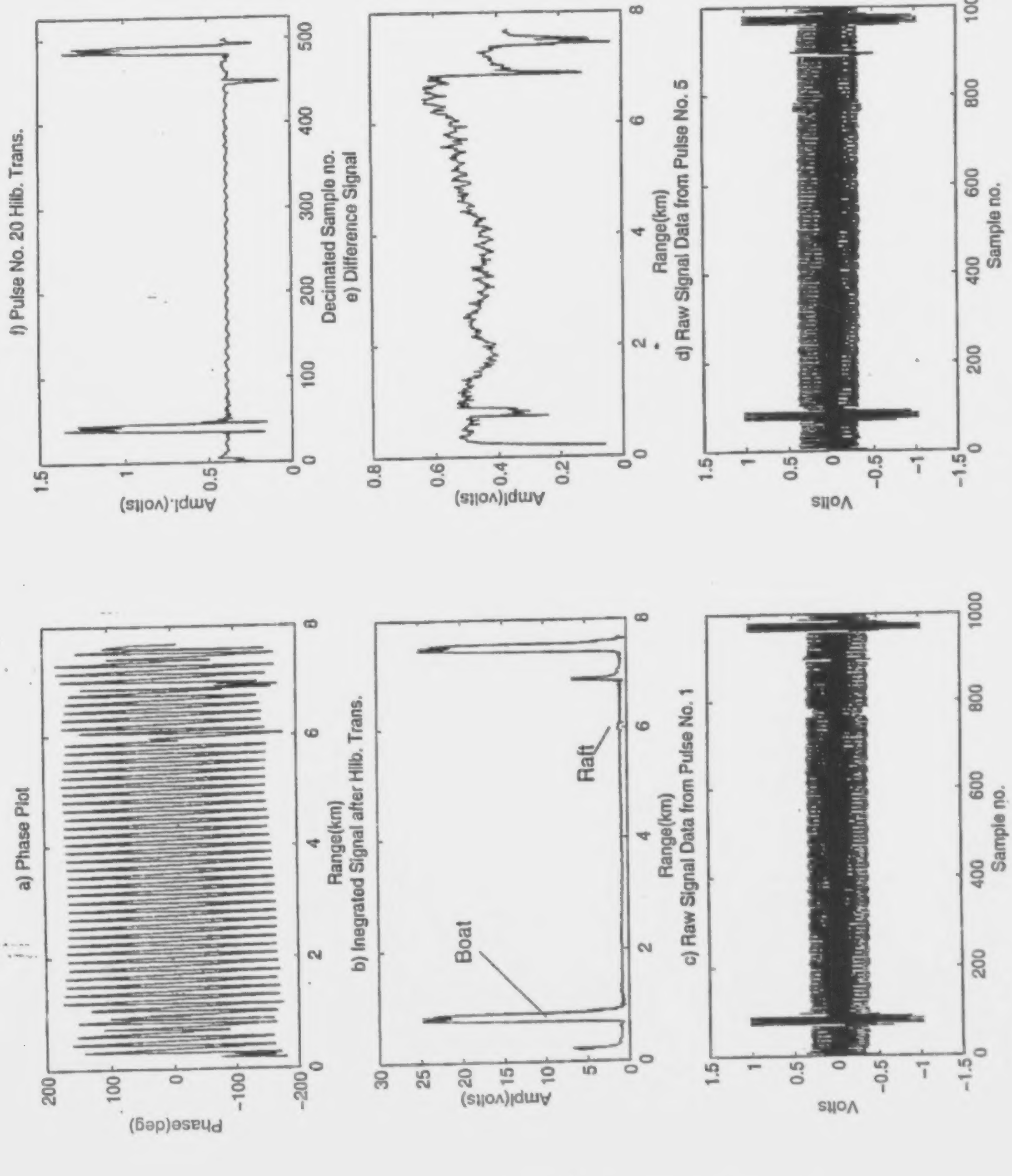

Figure 3.6.7 Plots from **piq00avg** for run 7 Sept. 7/94

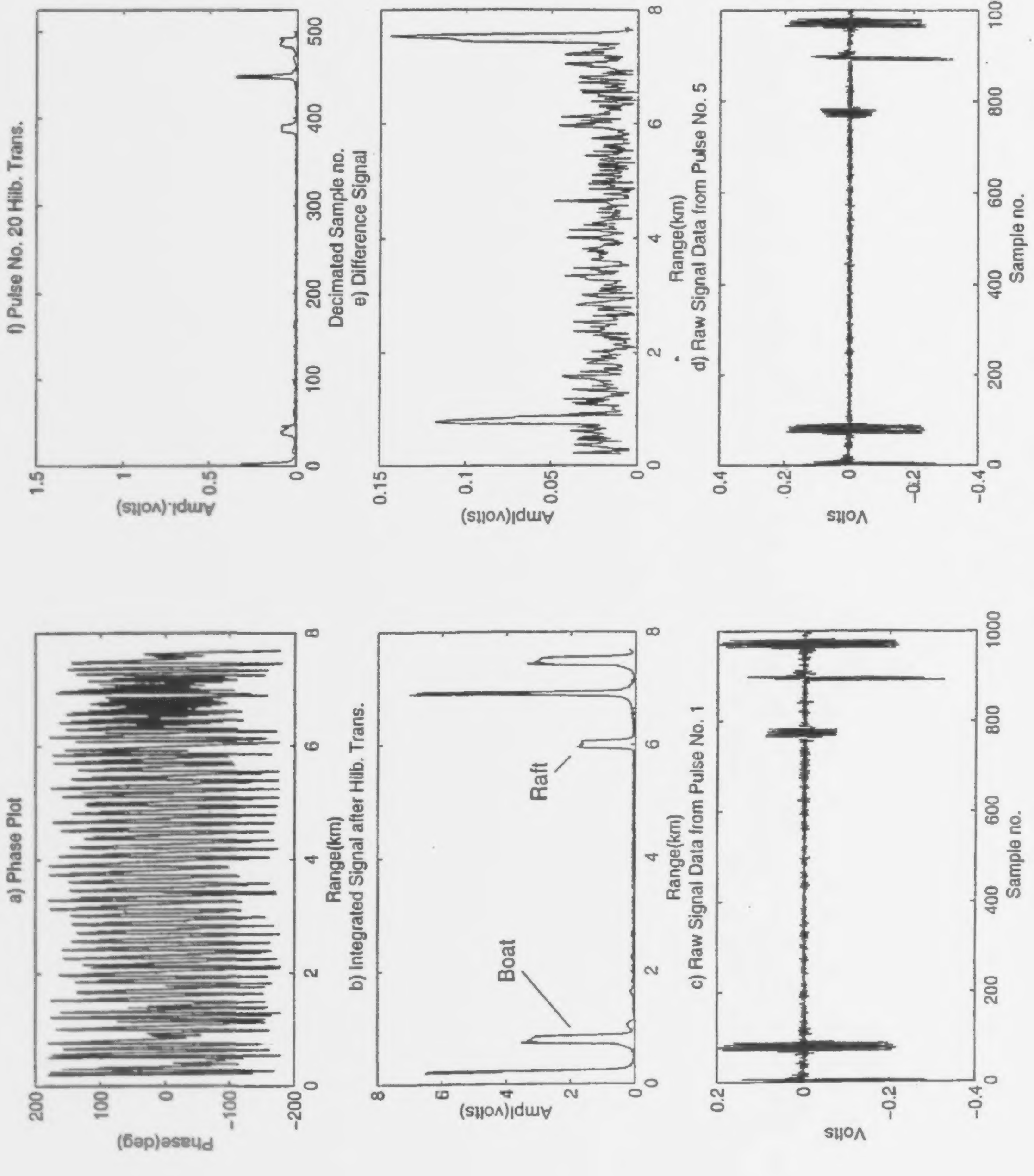

Figure 3.6.8 Plots from **piq00avg** for run 8 Sept. 7/94

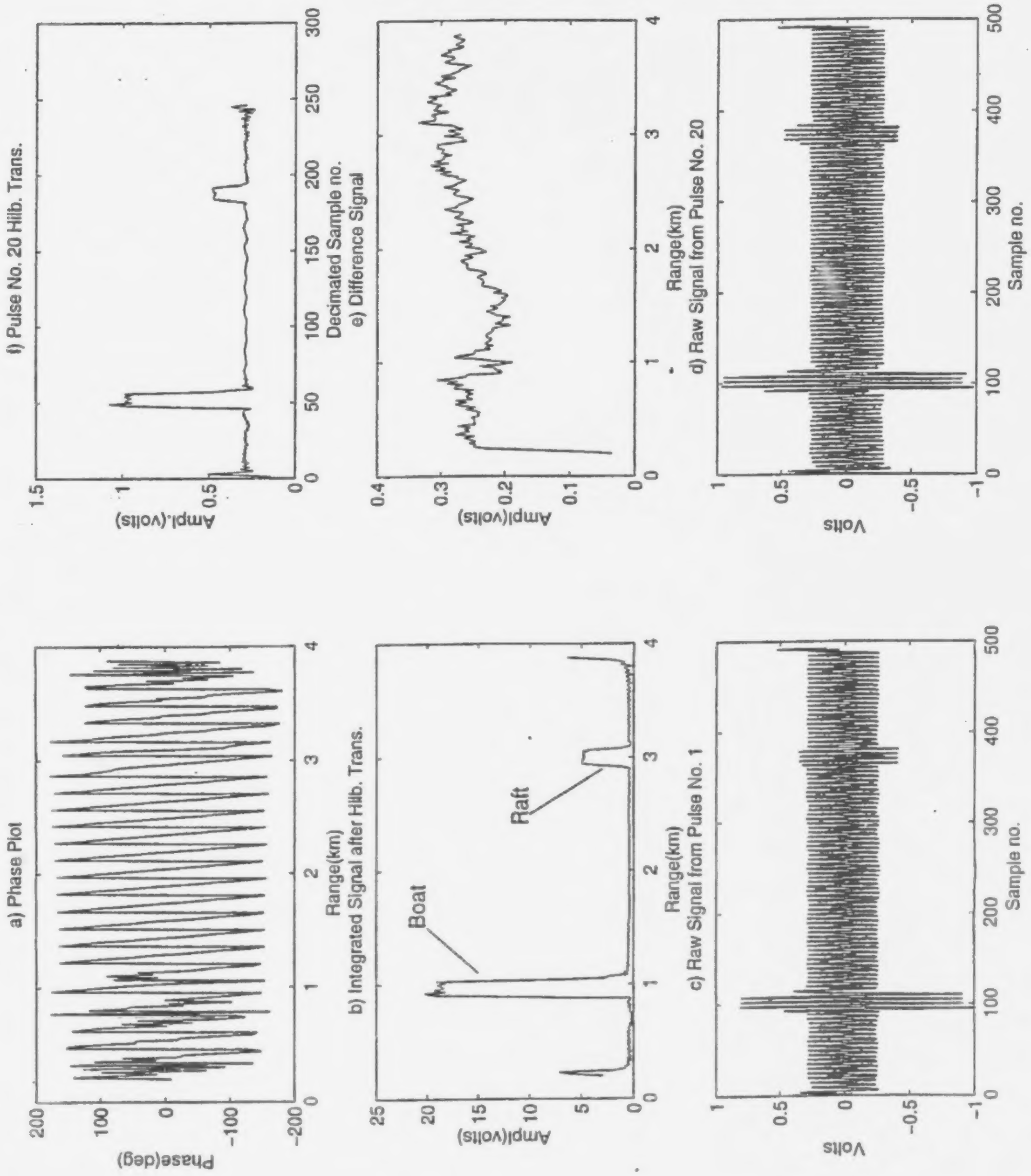

Figure 3.6.9 Plots from **piq00avg** for run 9 Sept. 7/94

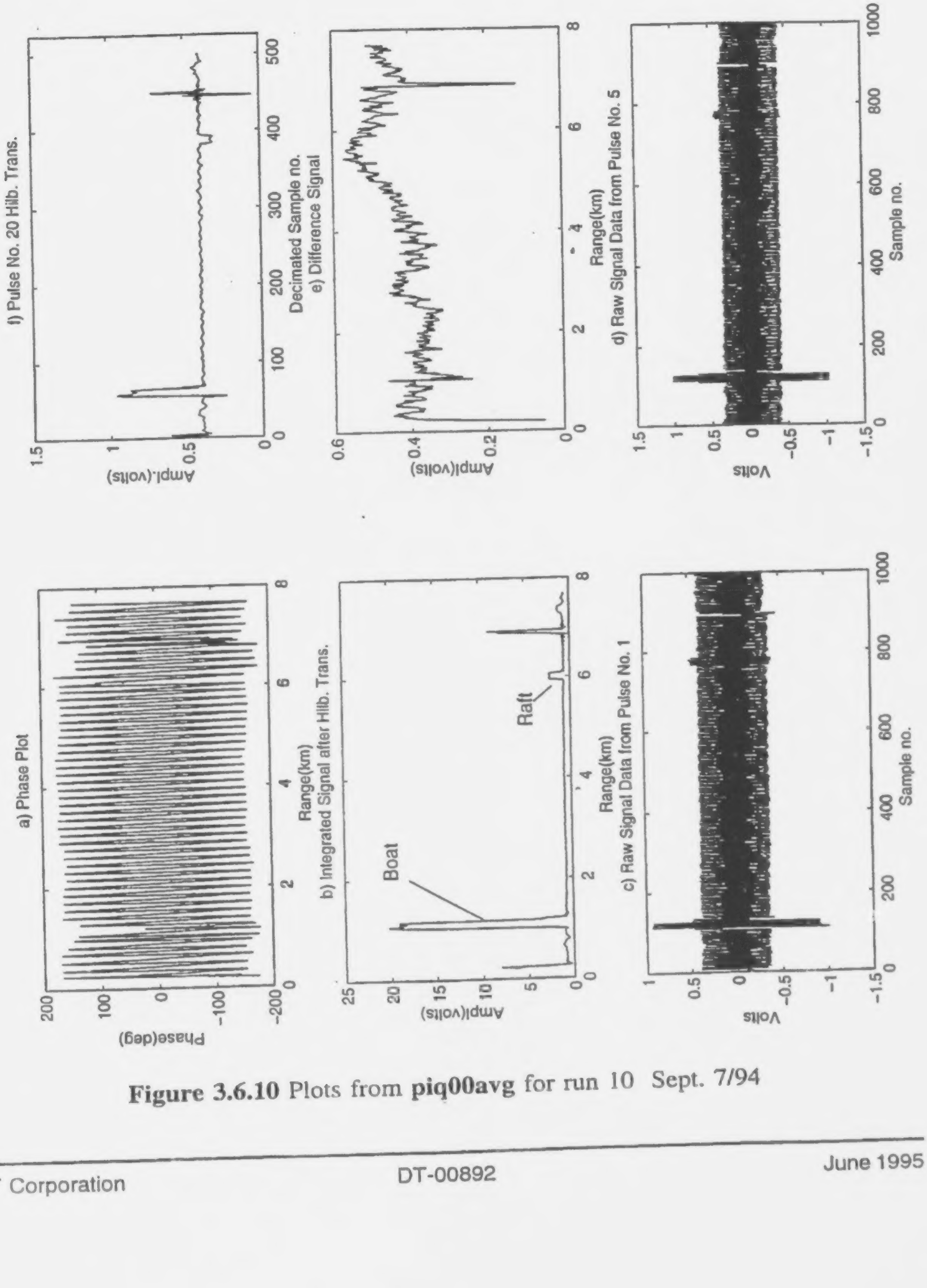

Figure 3.6.10 Plots from **piq00avg** for run 10 Sept. 7/94

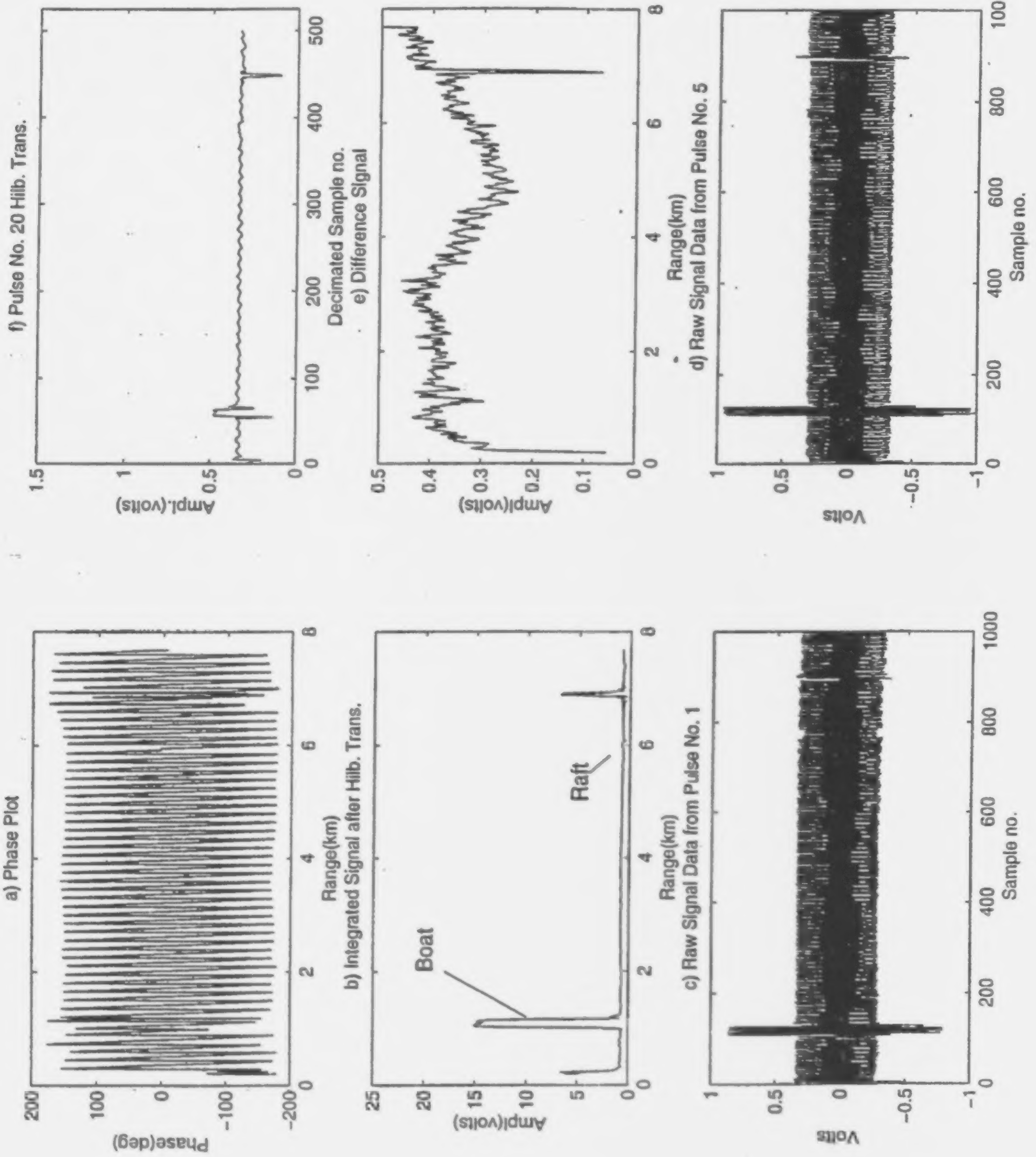

Figure 3.6.11 Plots from **piq00avg** for run 11 Sept. 7/94

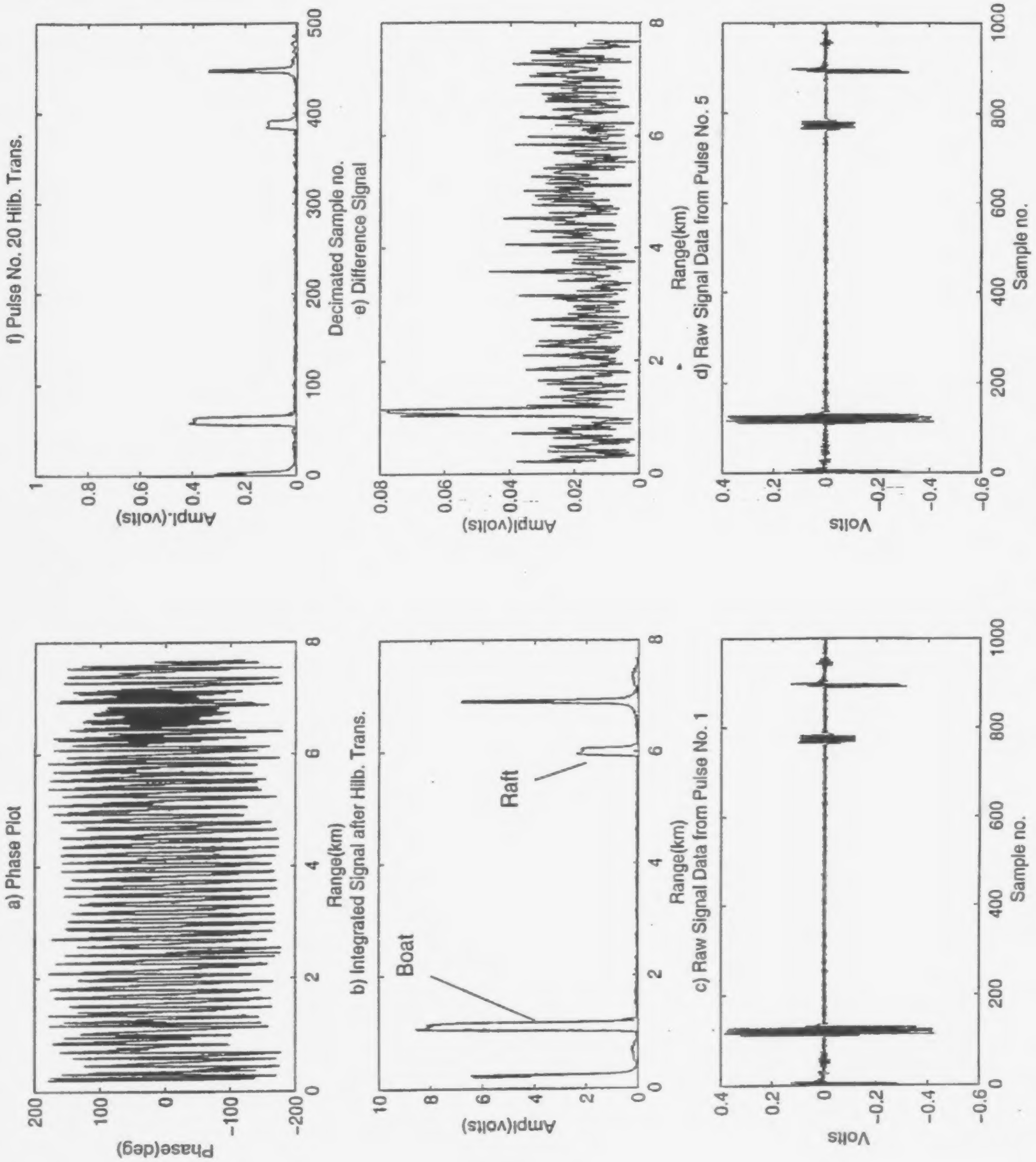

Figure 3.6.12 Plots from **piq00avg** for run 12 Sept. 7/94

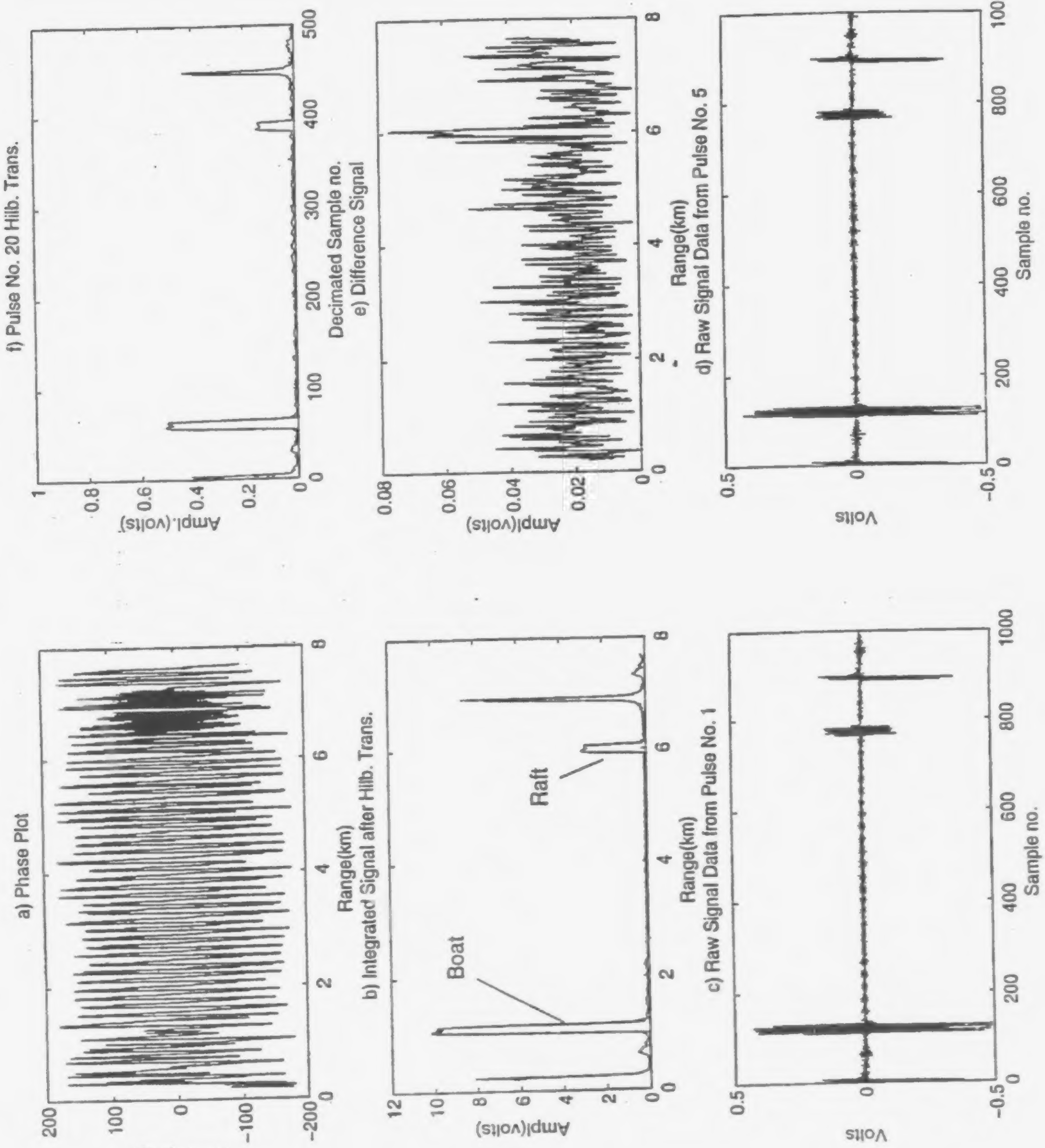

Figure 3.6.13 Plots from **piq00avg** for run 13 Sept. 7/94

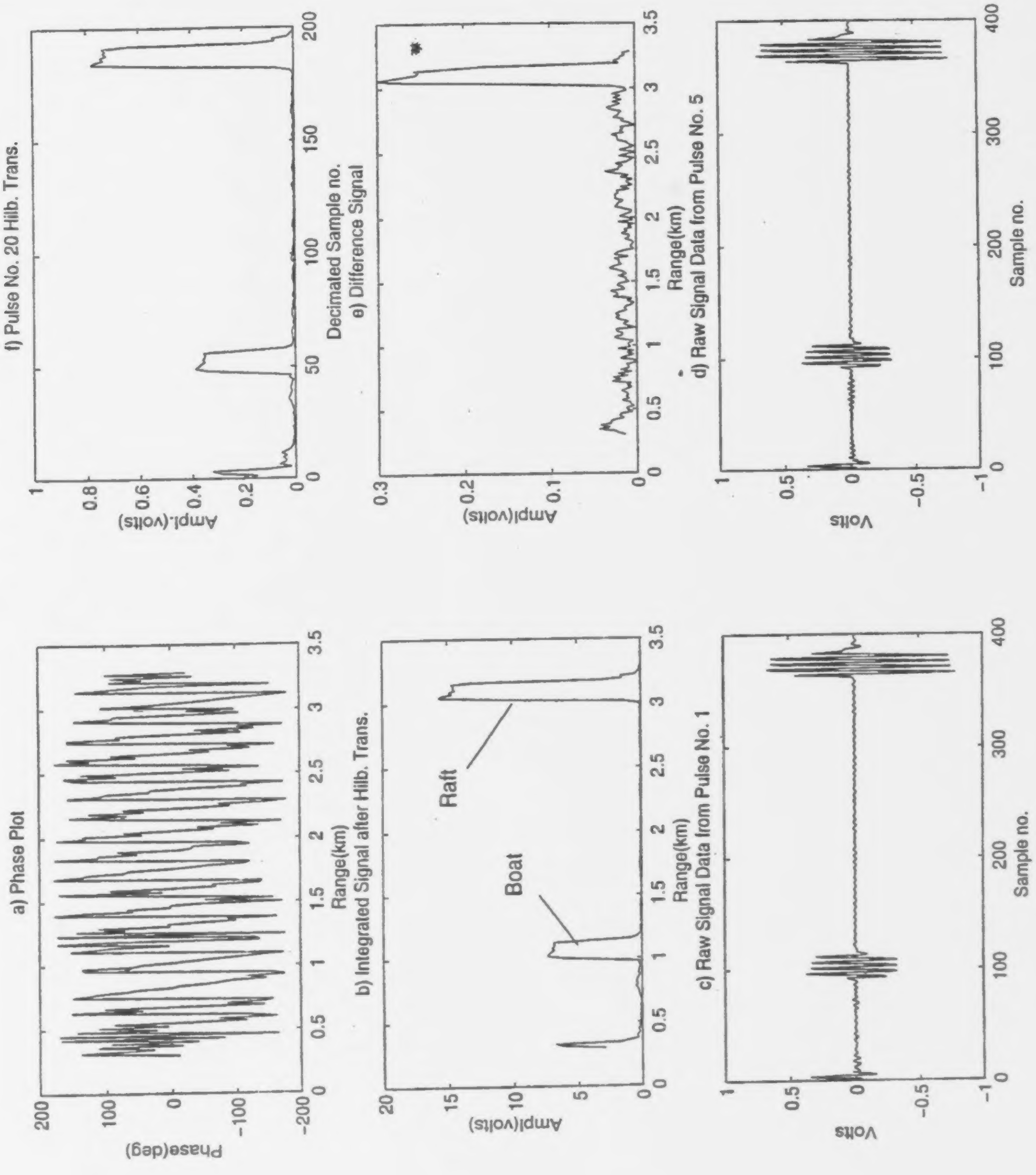

Figure 3.6.14 Plots from **piq00avg** for run 14 Sept. 7/94

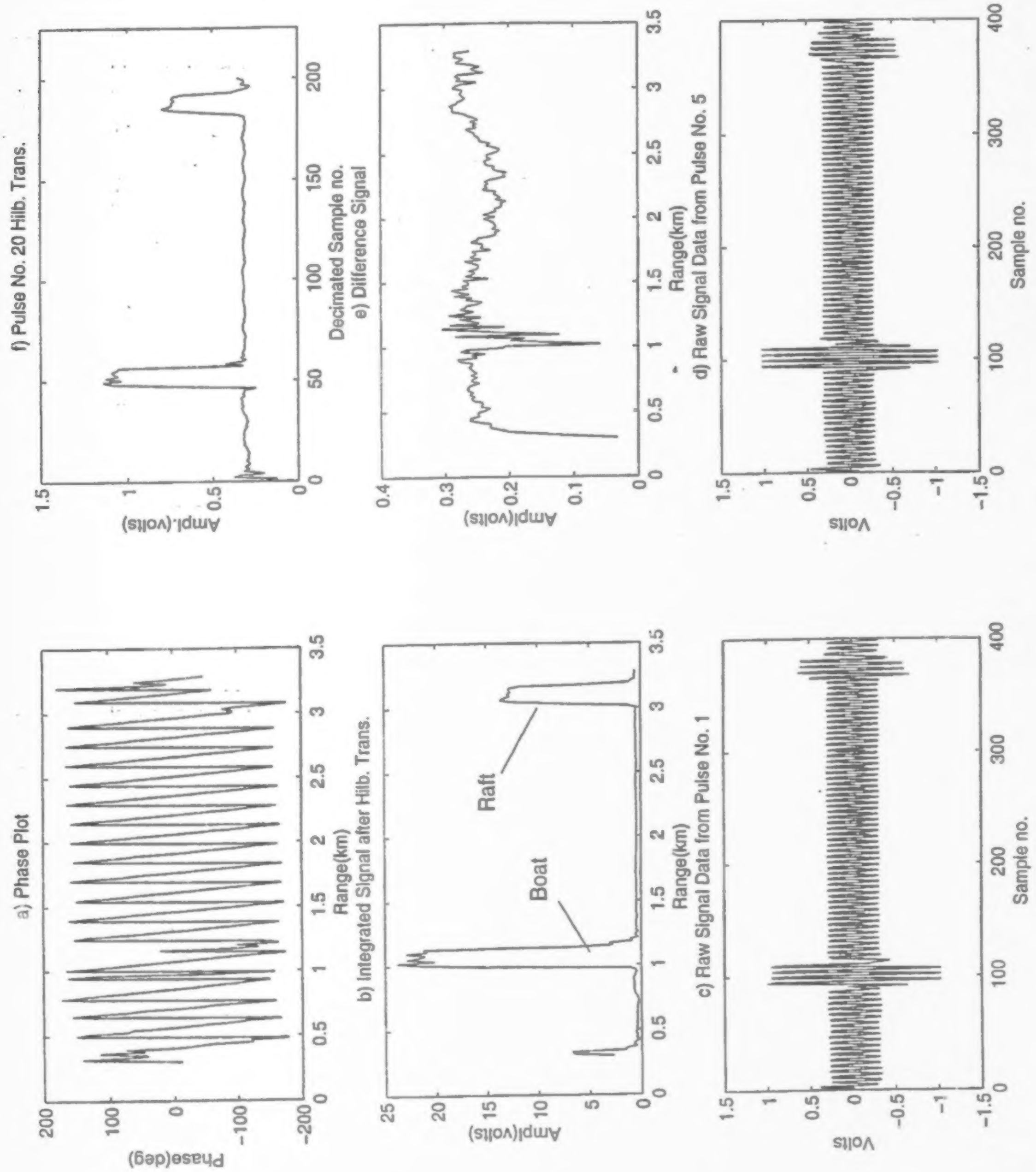

Figure 3.6.15 Plots from **piq00avg** for run 15 Sept. 7/94

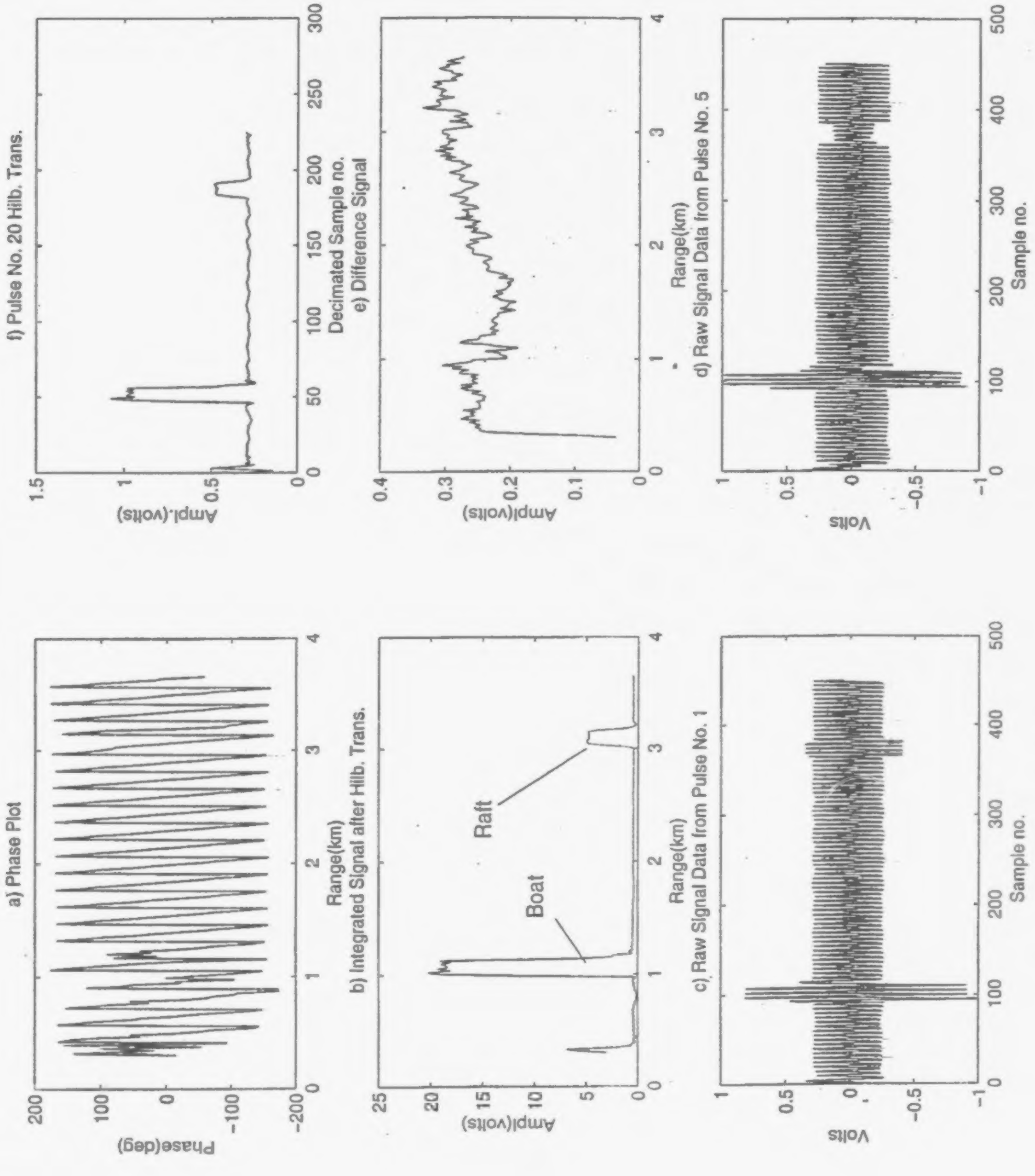

Figure 3.6.16 Plots from **piq00avg** for run 16 Sept. 7/94

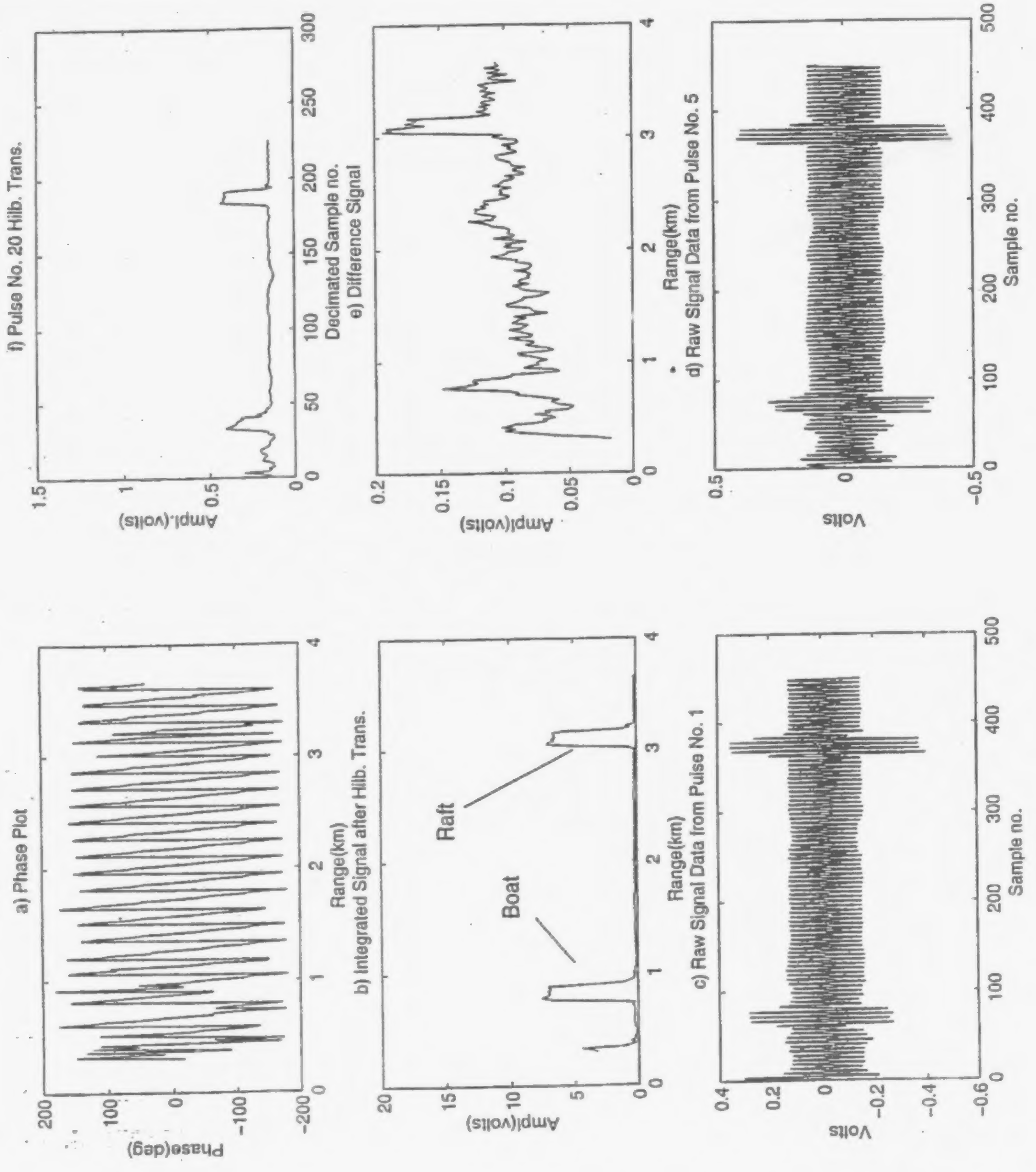

Figure 3.6.17 Plots from **piq00avg** for run 17 Sept. 7/94

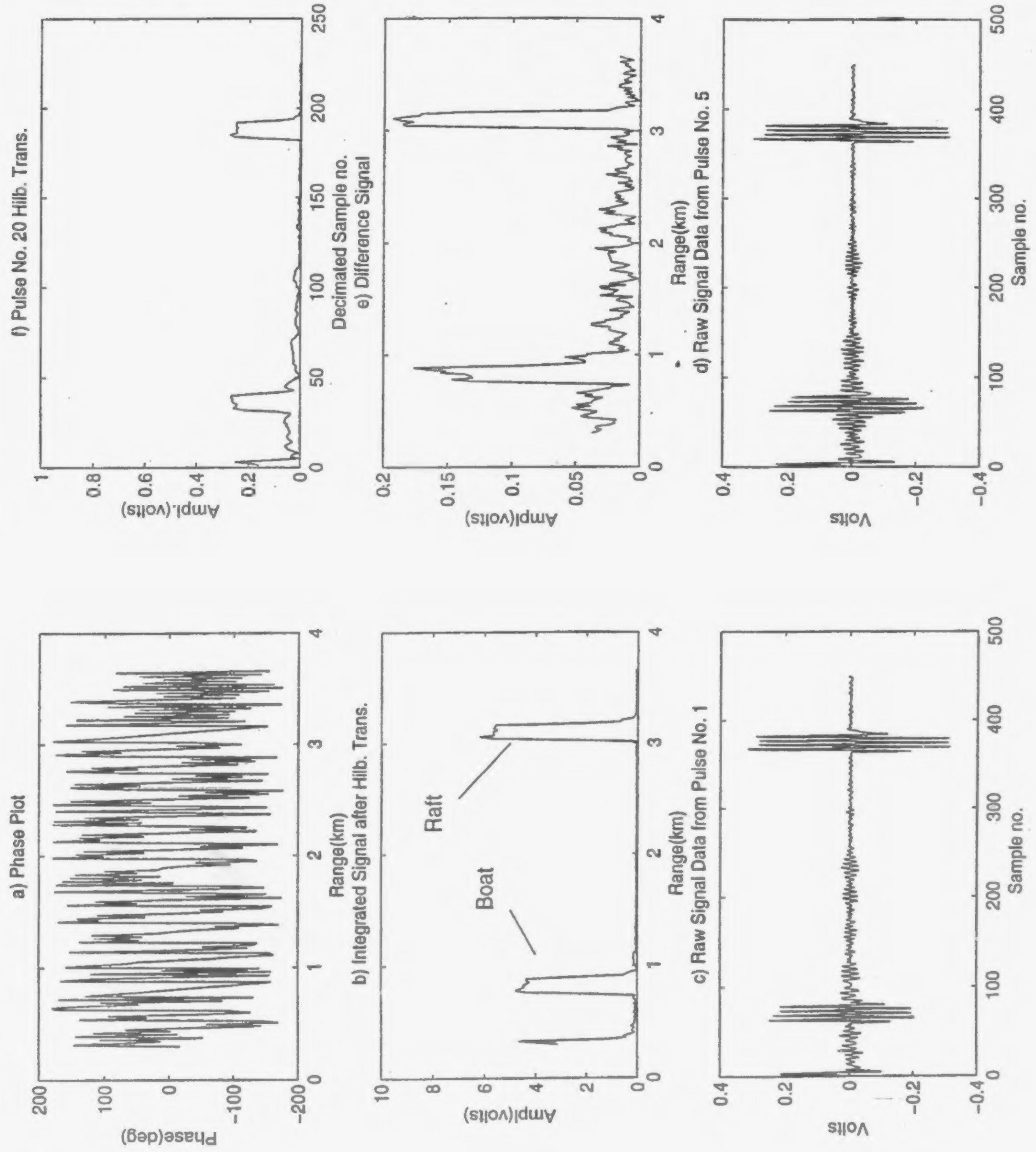

Figure 3.6.18 Plots from **piq00avg** for run 18 Sept. 7/94

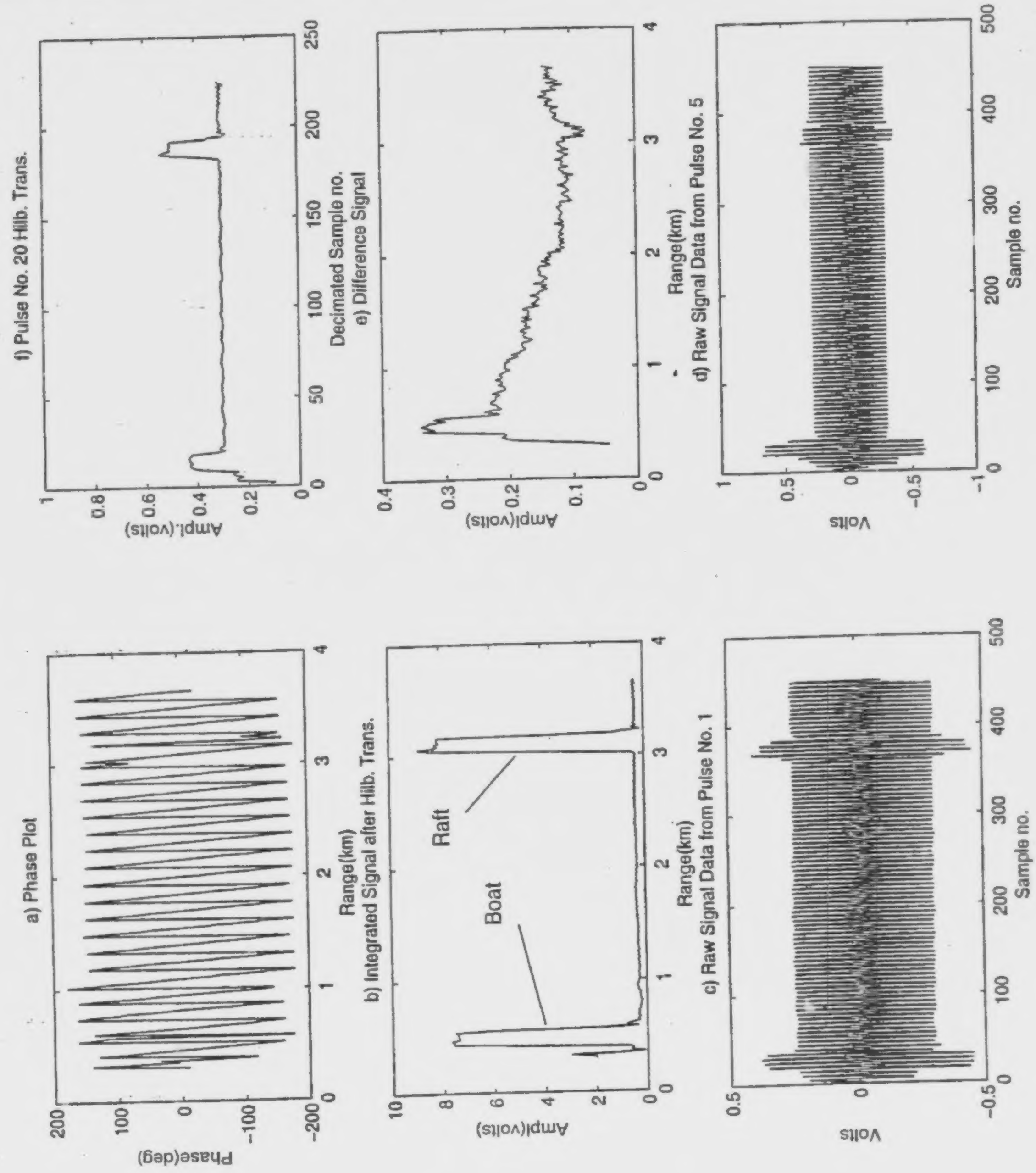

Figure 3.6.19 Plots from **piq00avg** for run 19 Sept. 7/94

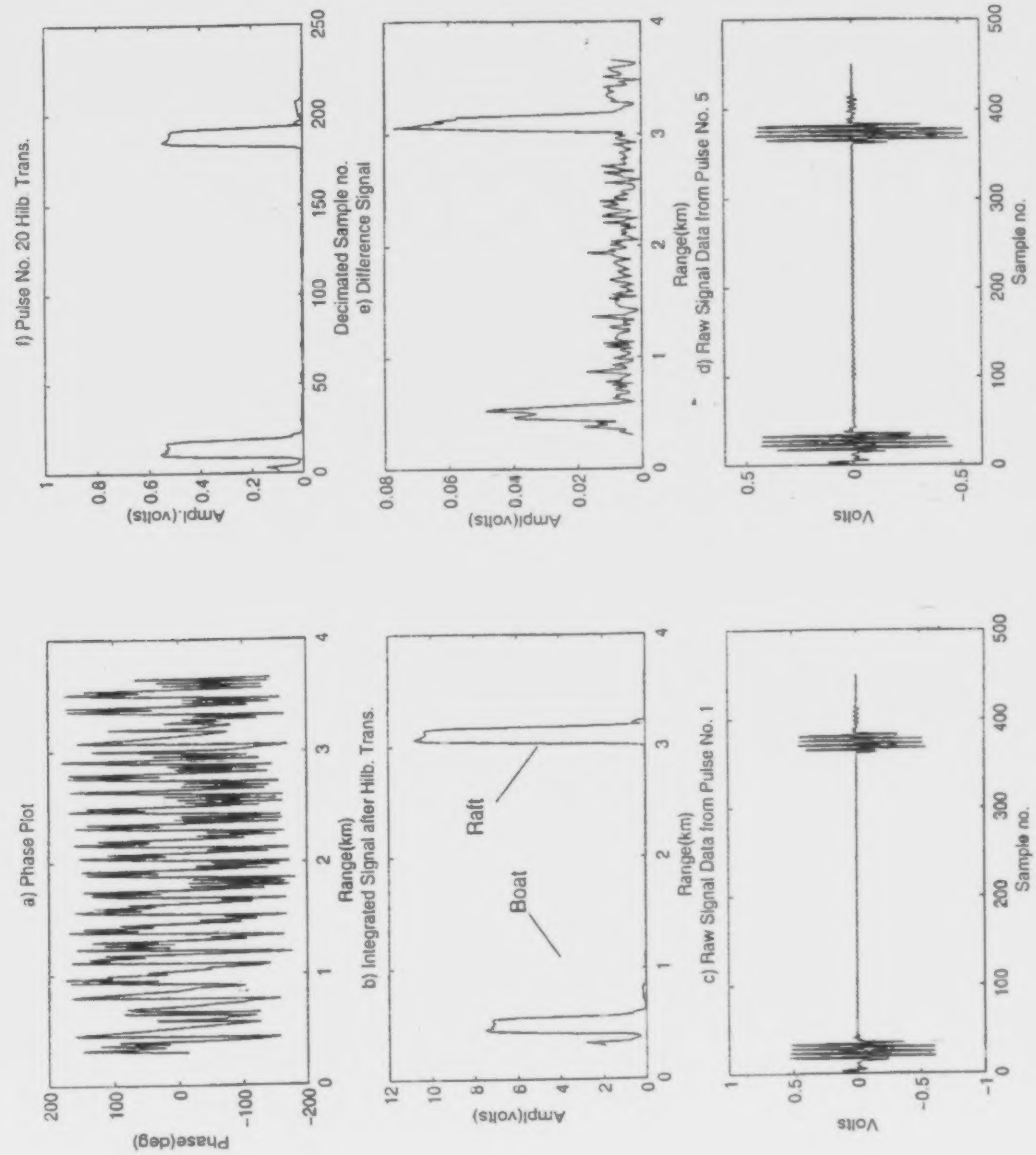

Figure 3.6.20 Plots from **piq00avg** for run 20 Sept. 7/94

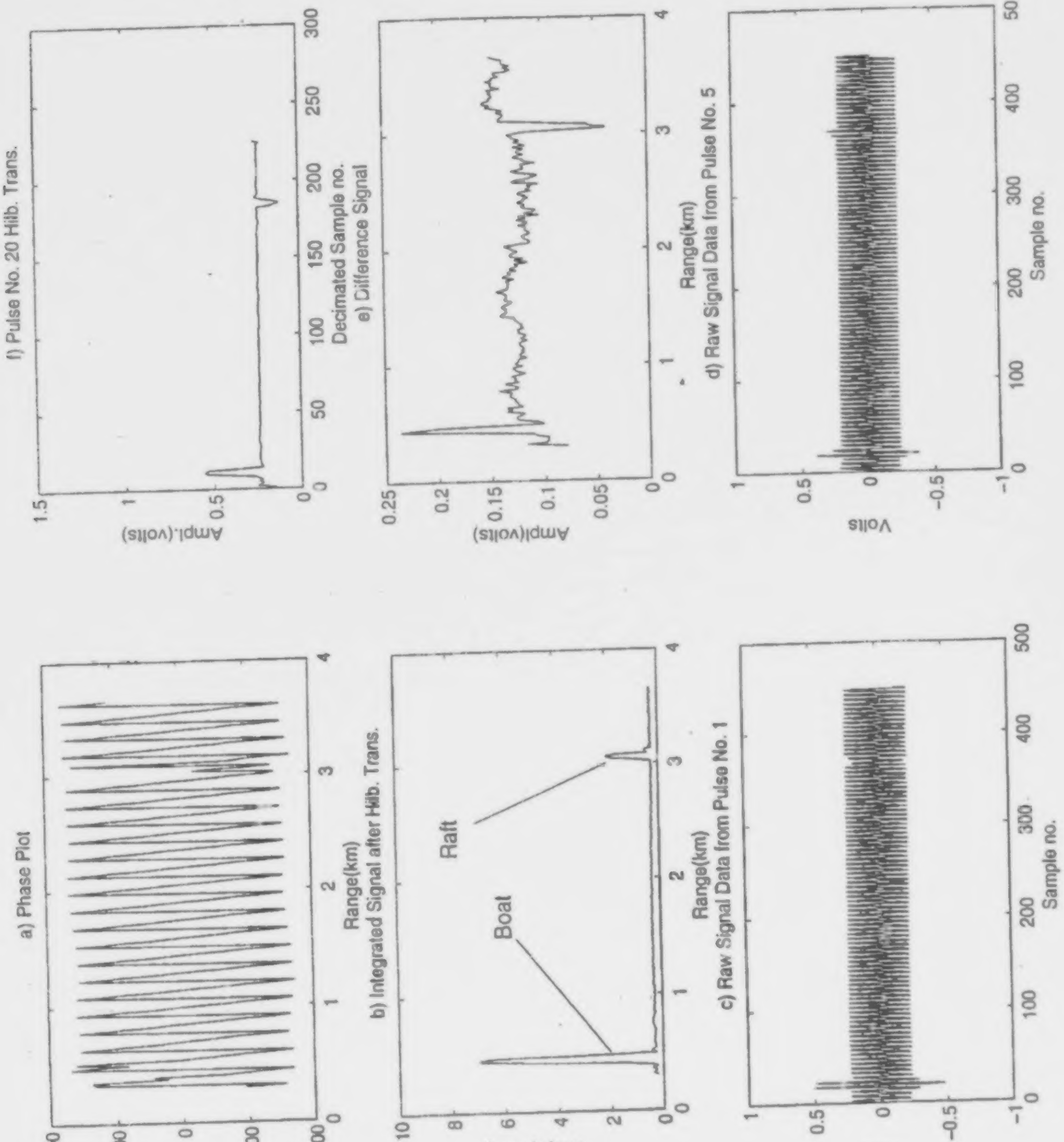

Figure 3.6.21 Plots from **piq00avg** for run 21 Sept. 7/94

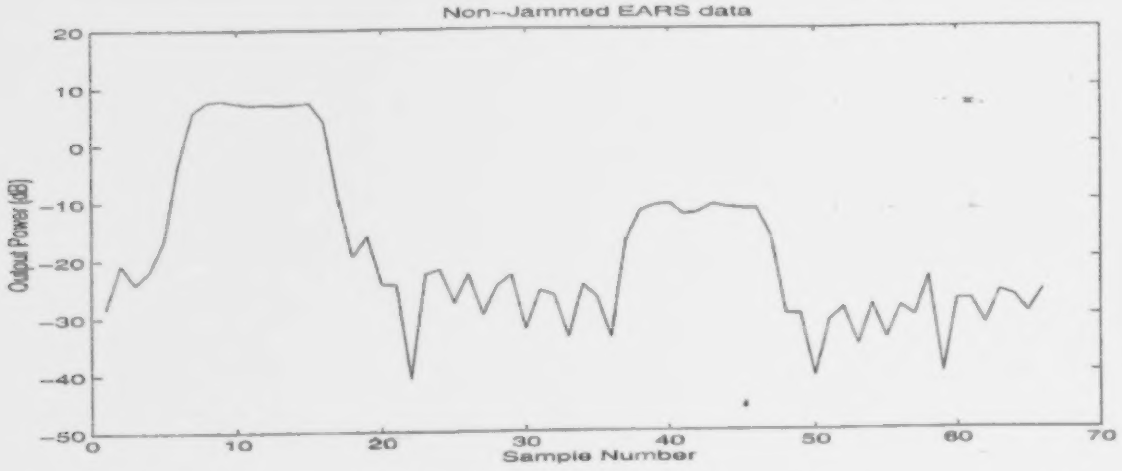

Figure 3.6.22 Non-jammed EARS data from the main array, Run 6, Sept. 14/95. The plot shows all the range cells for an integration of 10 radar pulses. The second peak at about sample no.40 was the target being jammed.

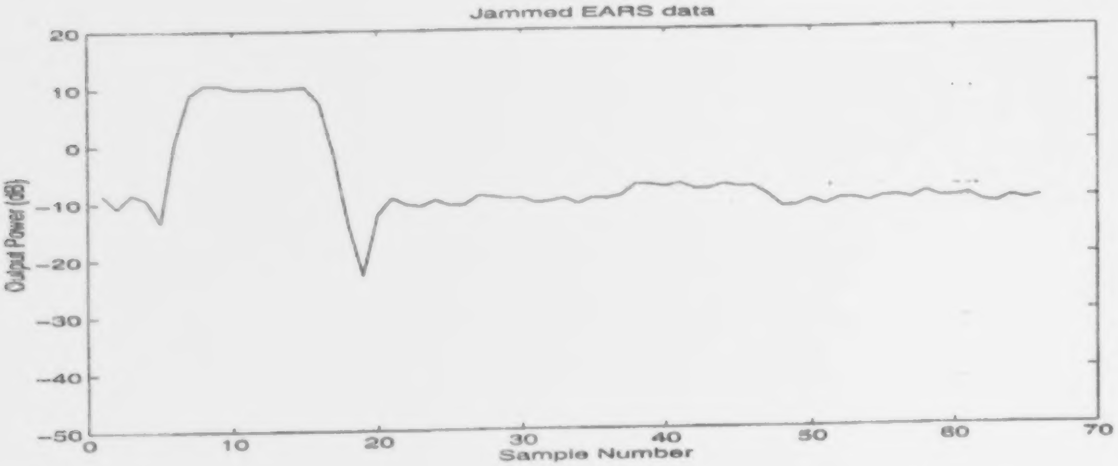

Figure 3.6.23 Jammed EARS data from the main array, Run 5, Sept. 14/95. The target peak of interest is just barely visible above the jammed bacground. This result is integrated over 10 radar pulses.

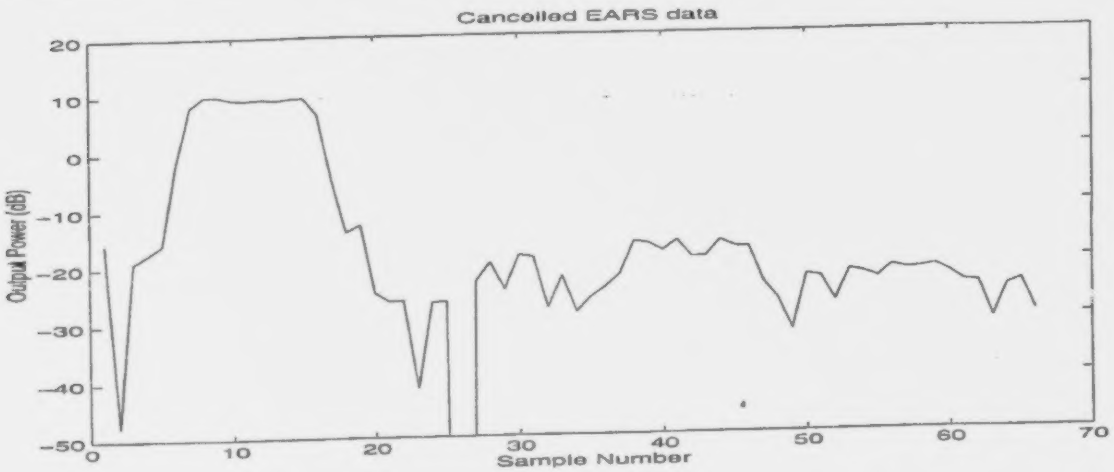

Figure 3.6.24 Jammed main array data with the jammer removed by the SMI method. The jammer signal from the SLC array was obtained using digital beamforming.

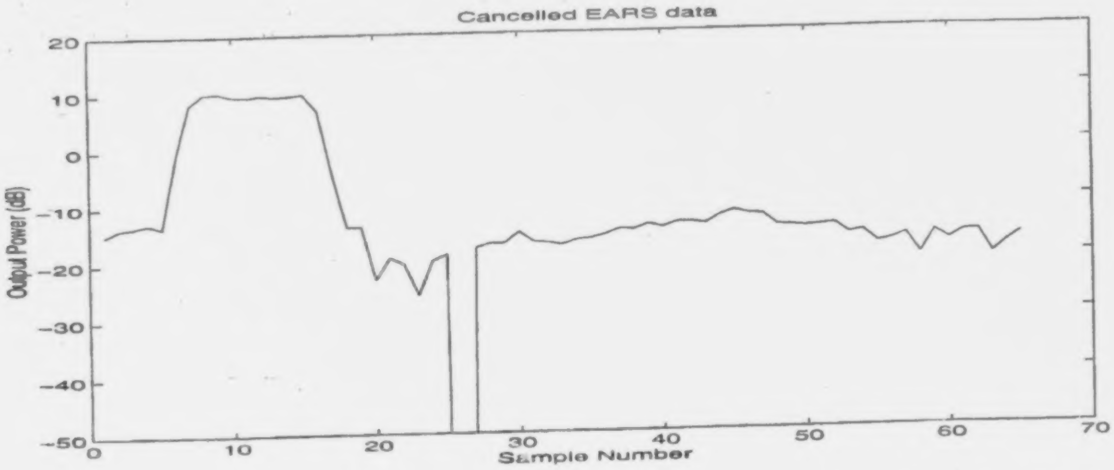

Figure 3.6.25 Jammed main array data with the jammer removed by the SMI method. The jammer signal for cancellation was obtained from a single receiver of the SLC array which had the largest amplitude response.

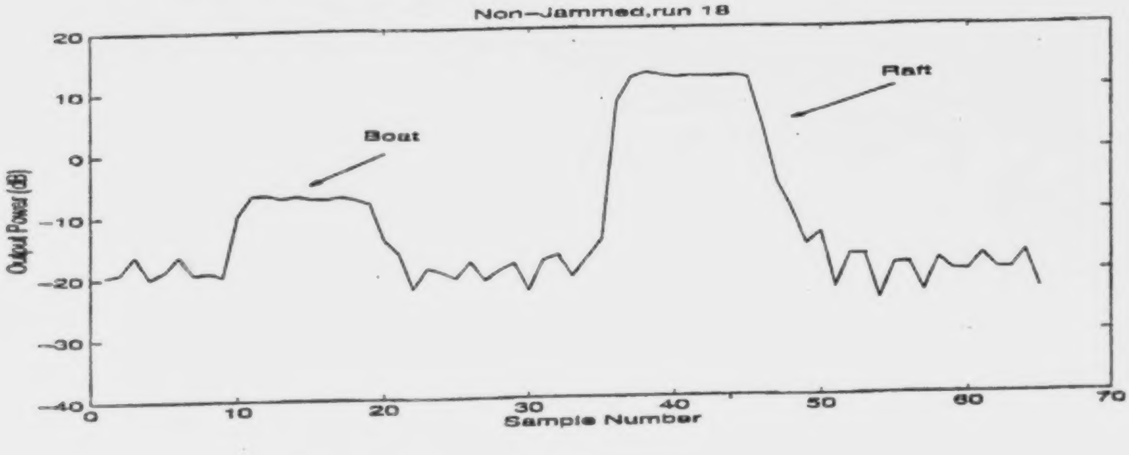

Figure 3.6.26 Non-jammed EARS data from the main array, Run 18, Sept. 13/94. The plot shows all the range cells for an integration of 10 radar pulses. As indicated, the first peak is due to the radar return from the boat, and the second corresponds to the return from the raft.

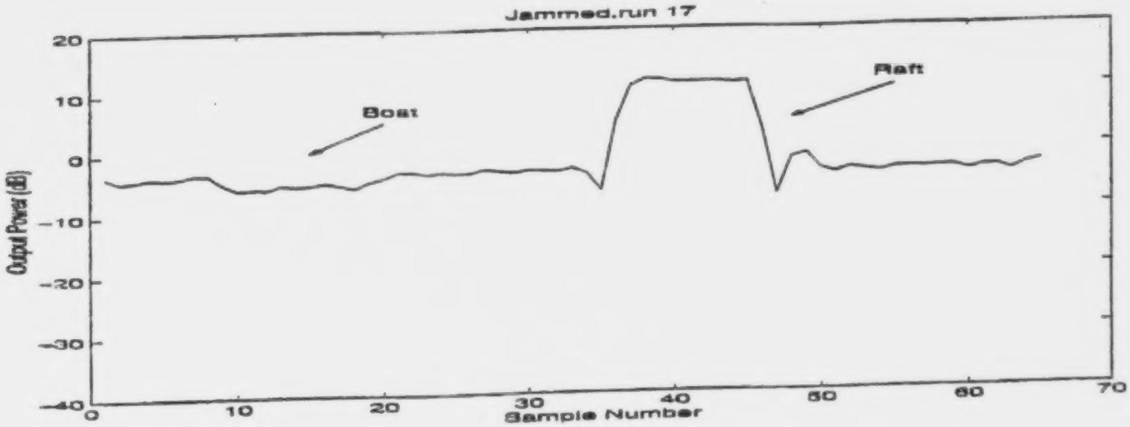

Figure 3.6.27 Jammed EARS data from the main array, Run 17, Sept., 13/94. The plot shows all the range cells for an integration of 10 radar pulses. It can be seen that the signal from the boat is almost obscured by the jammer.

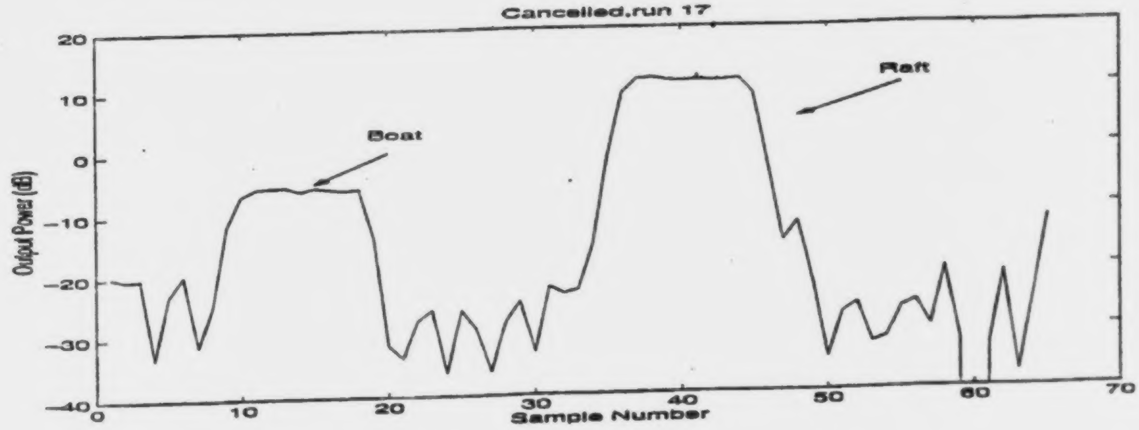

Figure 3.6.28 This plot show the results of (SMI) jammer cancellation on the same data as show in figure 3.3.6. In this case, the SLC data was obtained from the Rotman lens RF beamformed output with the largest response. The boat return was greatly enhanced using this procedure.

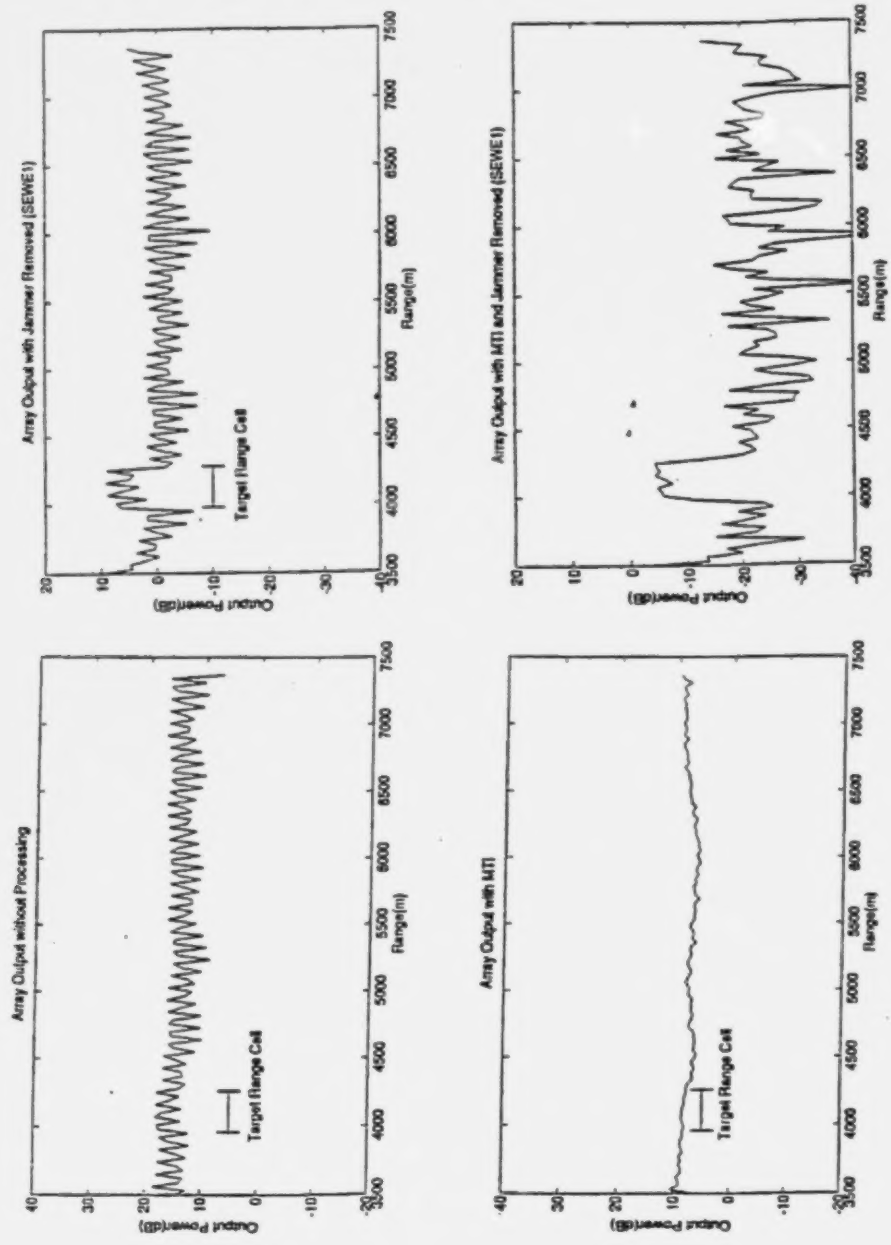

Figure 3.6.29 Detection enhancement by Main-beam jammer cancellation using SEWE1. a) and b) show the full return pulse averaged over 40 pulses and indicate the location of the target range cell observed in non-jammed data. c) and d) show the results after the jammer interference has been reduced.

a) Jammer Removal Using Projection Matrix Techniques

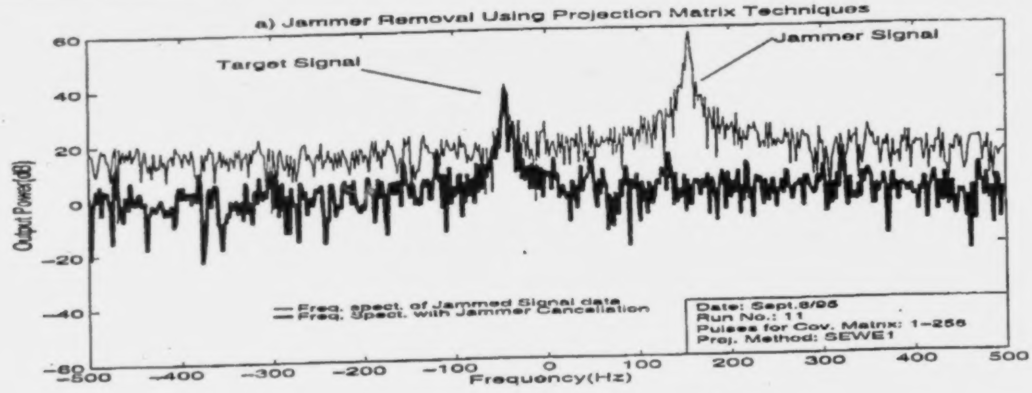

b)Jammer Removal Using Projection Matrix Techniques

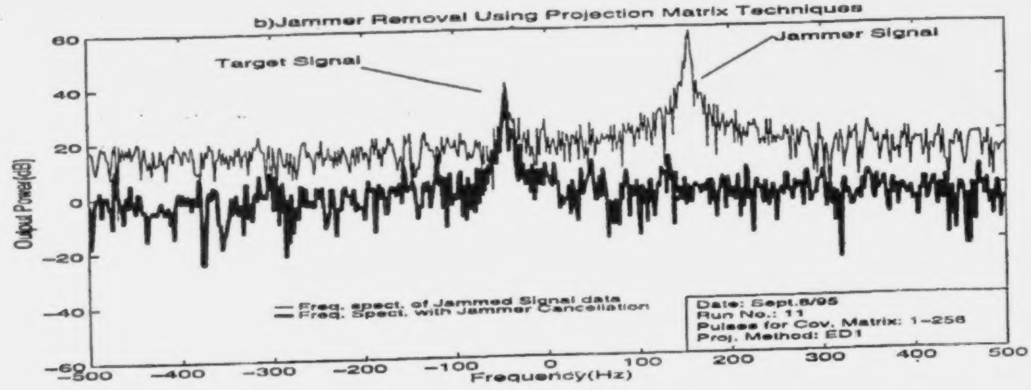

c) Jammer Removal Using Projection Matrix Techniques

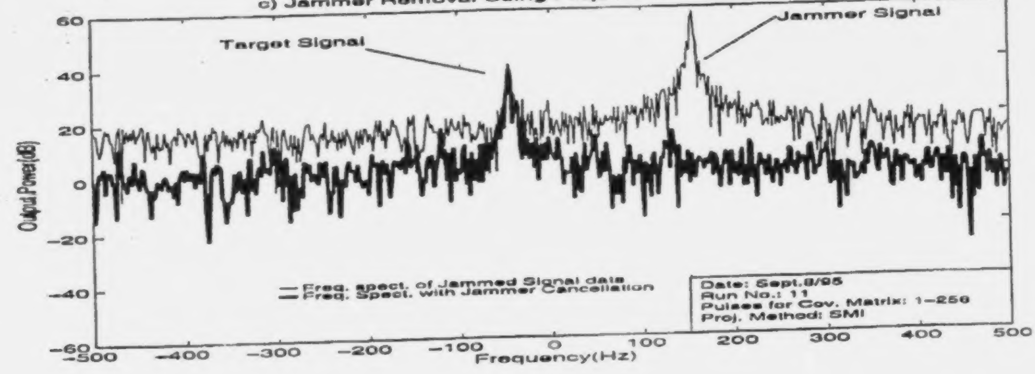

Figure 3.6.30 Comparison of FFT power spectra showing results for a)SEWE1, b)ED1 and c)SMI with 256 pulses used to create the covariance matrix.

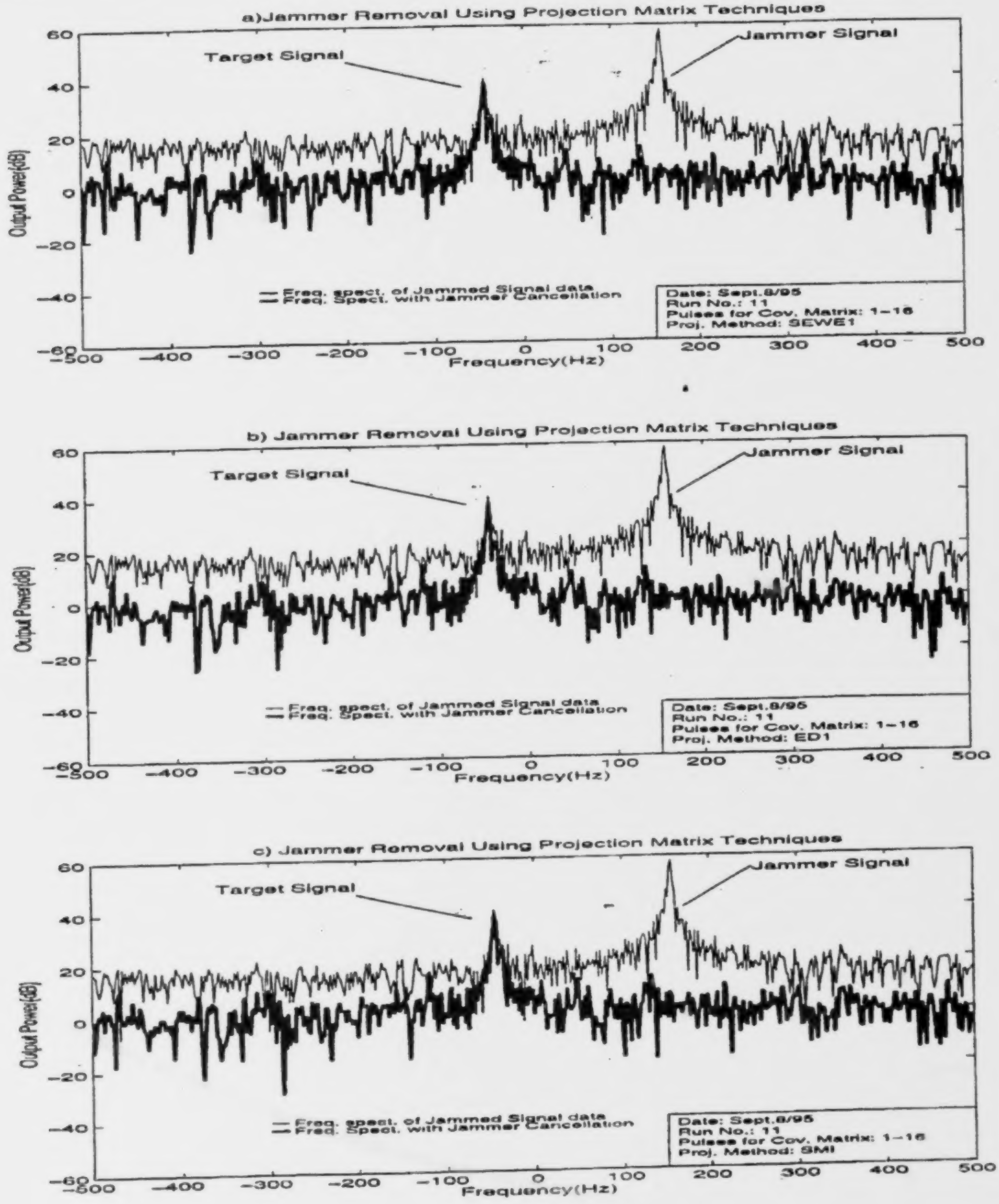

Figure 3.6.31 Comparison of FFT power spectra showing results for a)SEWE1, b)ED1 and c)SMI with 16 pulses used to create the covariance matrix.

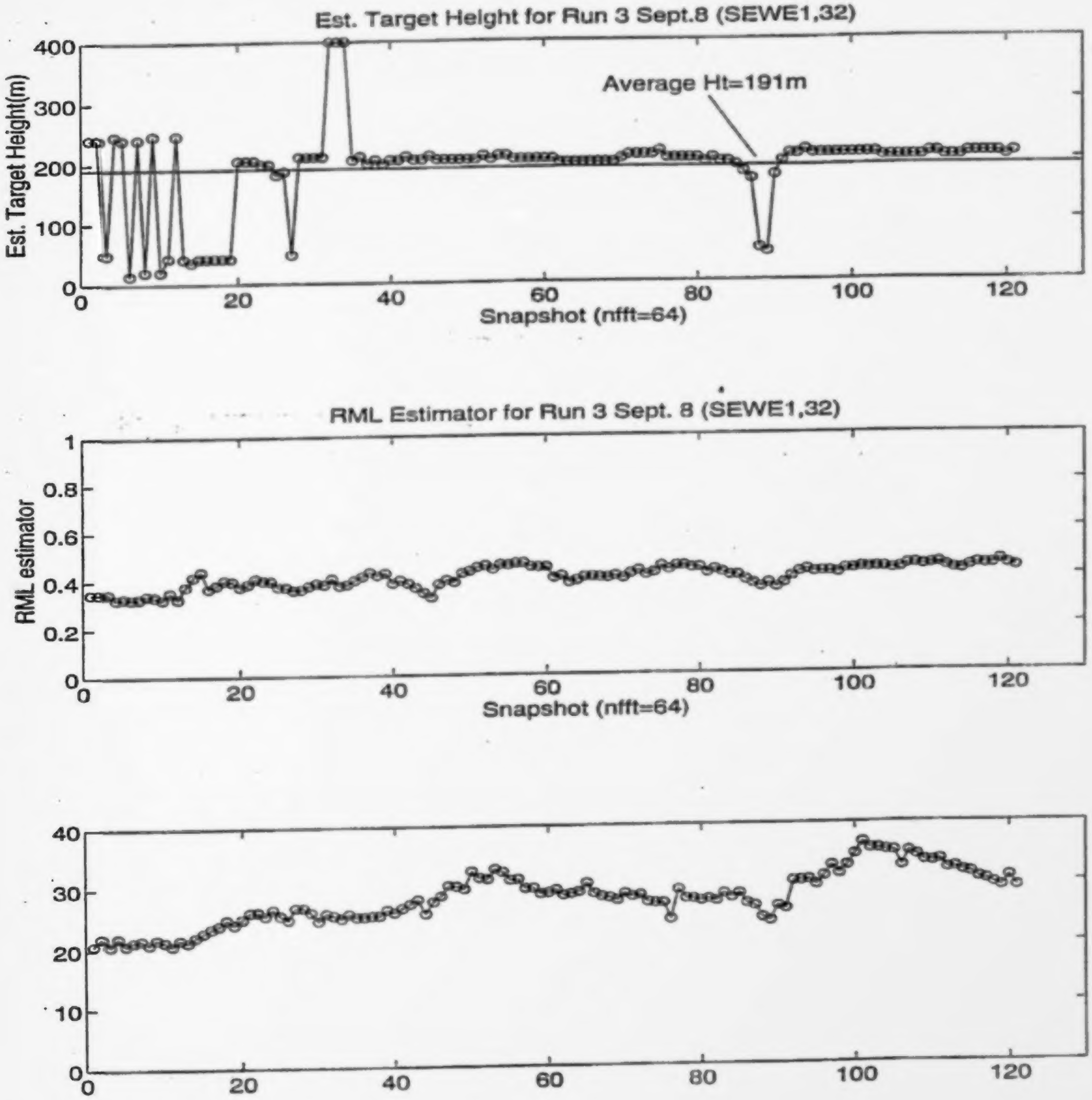
Est. Target Height for Run 3 Sept.8 (SEWE1,32)
Est. Target Height(m)
400
300
200
100
0
Average Ht=191m
0
20
40
60
80
100
120
Snapshot (nfft=64)
RML Estimator for Run 3 Sept. 8 (SEWE1,32)
RML estimator
1
0.8
0.6
0.4
0.2
0
0
20
40
60
80
100
120
Snapshot (nfft=64)
40
30
20
10
0
0
20
40
60
80
100
120

Figure 3.6.32

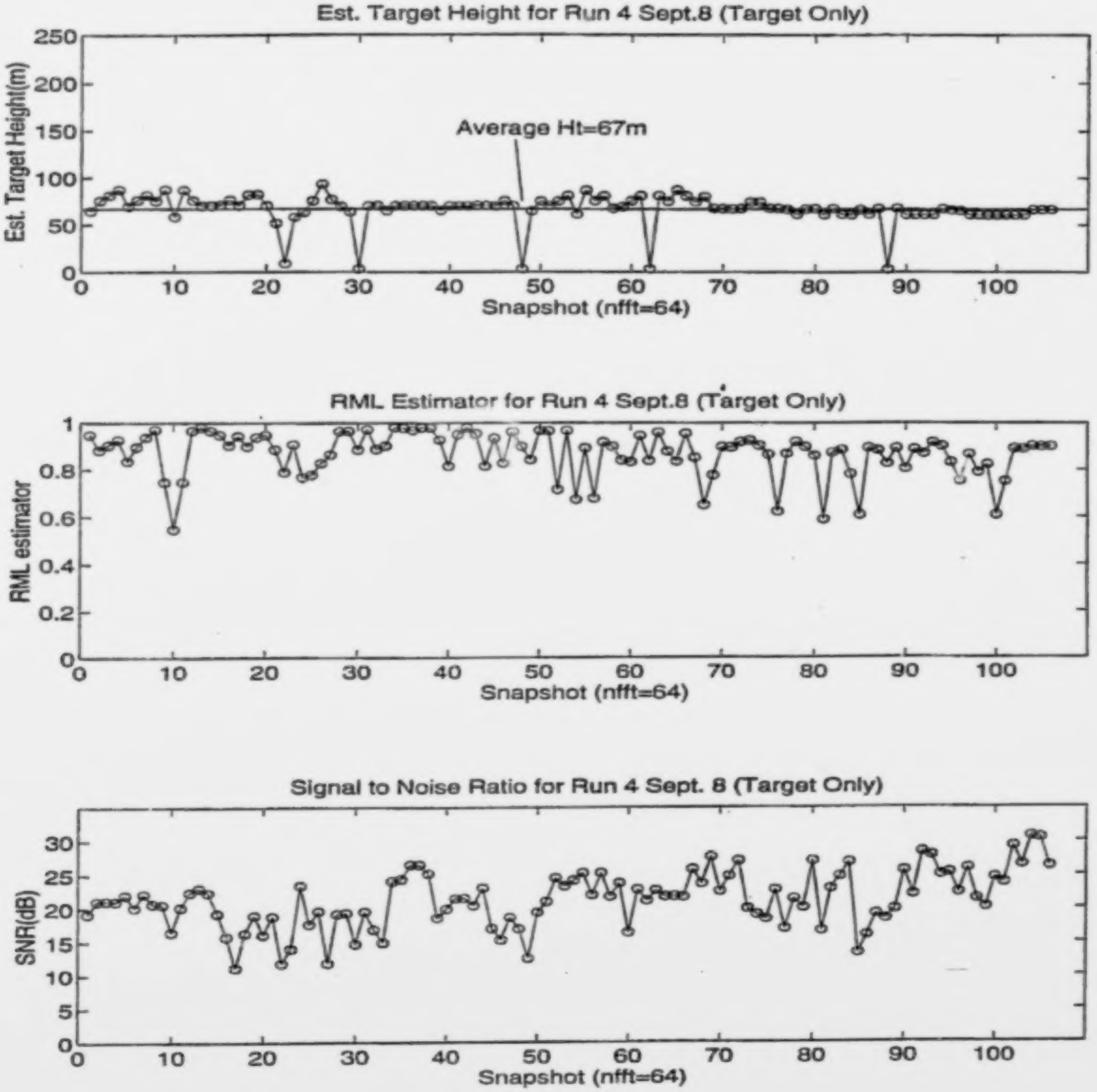
Est. Target Height for Run 4 Sept.8 (Target Only)
Est. Target Height(m)
250
200
150
100
50
0
Average Ht=67m
0
10
20
30
40
50
60
70
80
90
100
Snapshot (nfft=64)
RML Estimator for Run 4 Sept.8 (Target Only)
RML estimator
1
0.8
0.6
0.4
0.2
0
0
10
20
30
40
50
60
70
80
90
100
Snapshot (nfft=64)
Signal to Noise Ratio for Run 4 Sept. 8 (Target Only)
SNR(dB)
30
25
20
15
10
5
0
0
10
20
30
40
50
60
70
80
90
100
Snapshot (nfft=64)

Figure 3.6.33

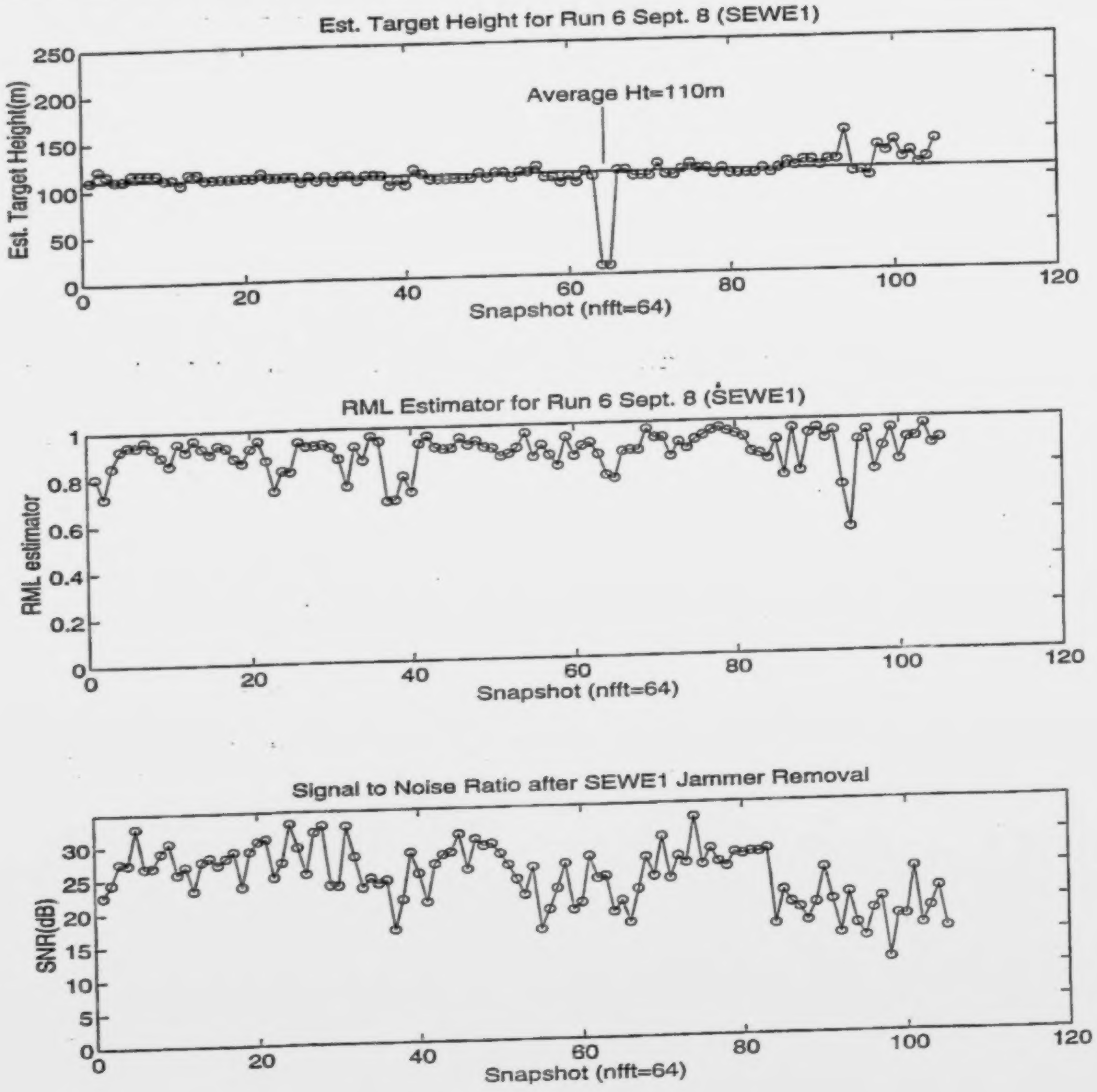

Est. Target Height for Run 6 Sept. 8 (SEWE1)

RML Estimator for Run 6 Sept. 8 (SEWE1)

Signal to Noise Ratio after SEWE1 Jammer Removal

Figure 3.6.34

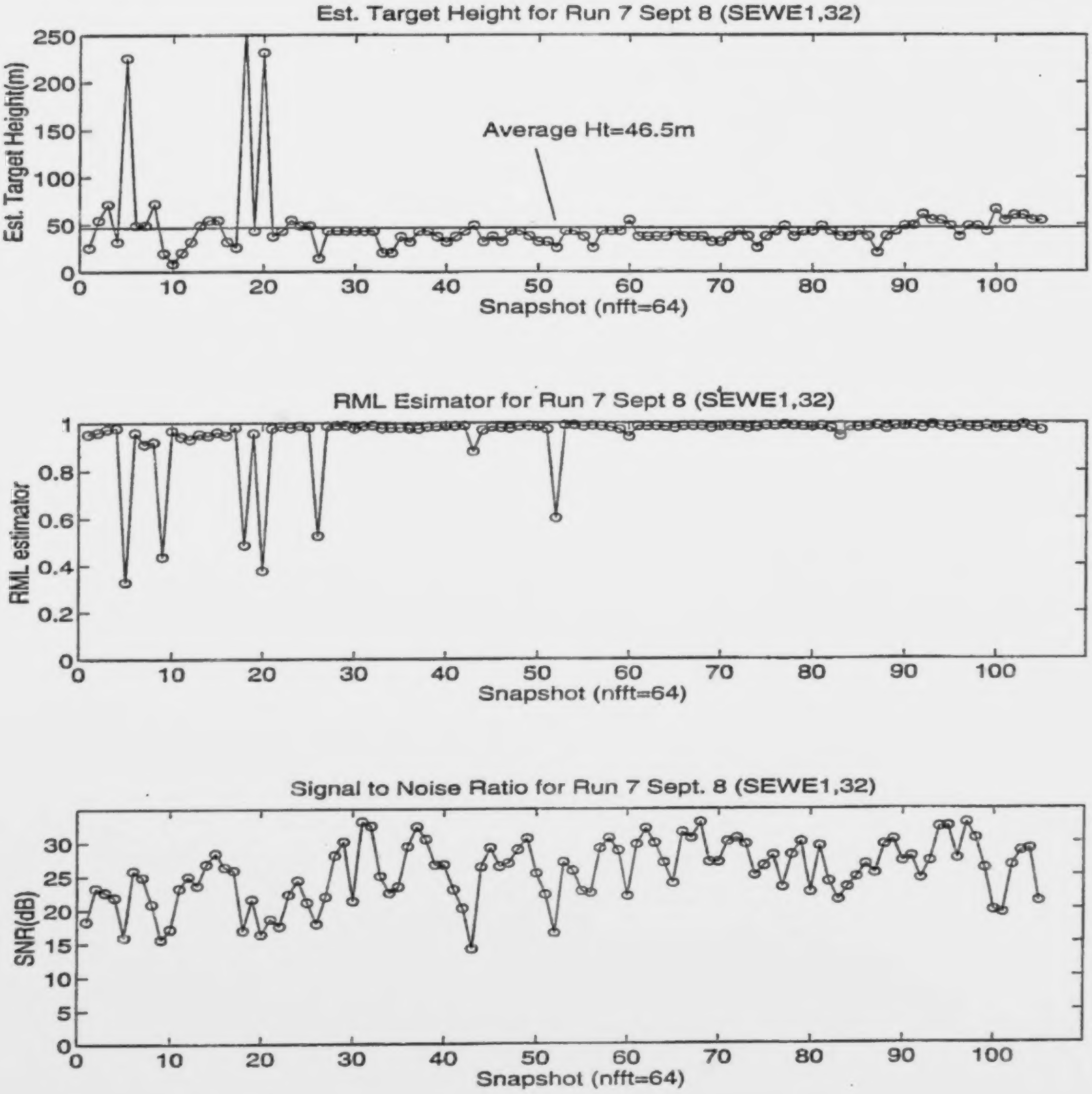

Est. Target Height for Run 7 Sept 8 (SEWE1,32)

RML Esimator for Run 7 Sept 8 (SEWE1,32)

Signal to Noise Ratio for Run 7 Sept. 8 (SEWE1,32)

Figure 3.6.35

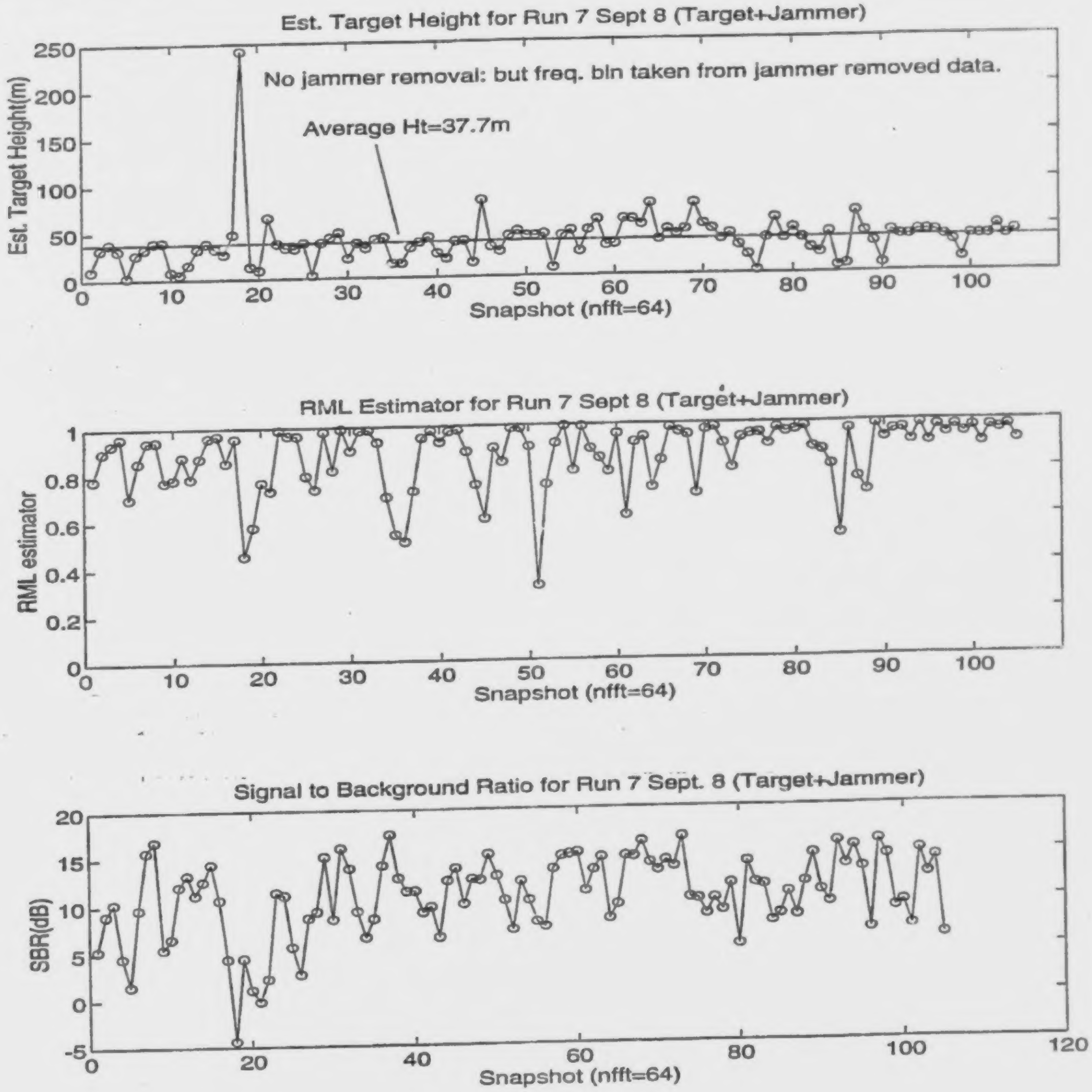
Est. Target Height for Run 7 Sept 8 (Target+Jammer)
No jammer removal: but freq. bin taken from jammer removed data.
Average Ht=37.7m
Est. Target Height(m)
250
200
150
100
50
0
0
10
20
30
40
50
60
70
80
90
100
Snapshot (nfft=64)
RML Estimator for Run 7 Sept 8 (Target+Jammer)
RML estimator
1
0.8
0.6
0.4
0.2
0
0
10
20
30
40
50
60
70
80
90
100
Snapshot (nfft=64)
Signal to Background Ratio for Run 7 Sept. 8 (Target+Jammer)
SBR(dB)
20
15
10
5
0
-5
0
20
40
60
80
100
120
Snapshot (nfft=64)

Figure 3.6.36

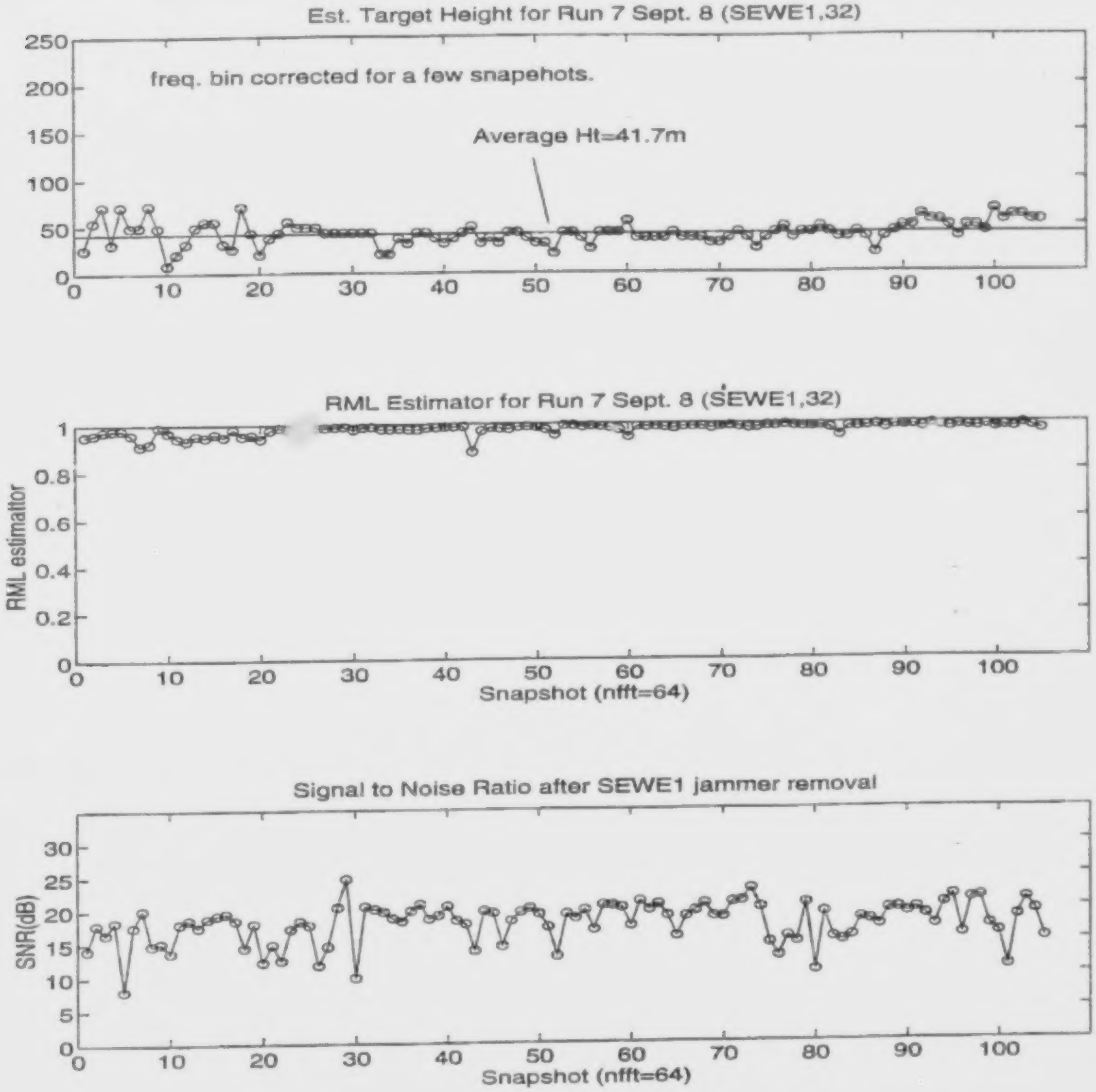
Est. Target Height for Run 7 Sept. 8 (SEWE1,32)
freq. bin corrected for a few snapehots.
Average Ht=41.7m
0
50
100
150
200
250
0
10
20
30
40
50
60
70
80
90
100
RML Estimator for Run 7 Sept. 8 (SEWE1,32)
RML estimattor
0
0.2
0.4
0.6
0.8
1
Snapshot (nfft=64)
Signal to Noise Ratio after SEWE1 jammer removal
SNR(dB)
0
5
10
15
20
25
30
Snapshot (nfft=64)

Figure 3.6.37

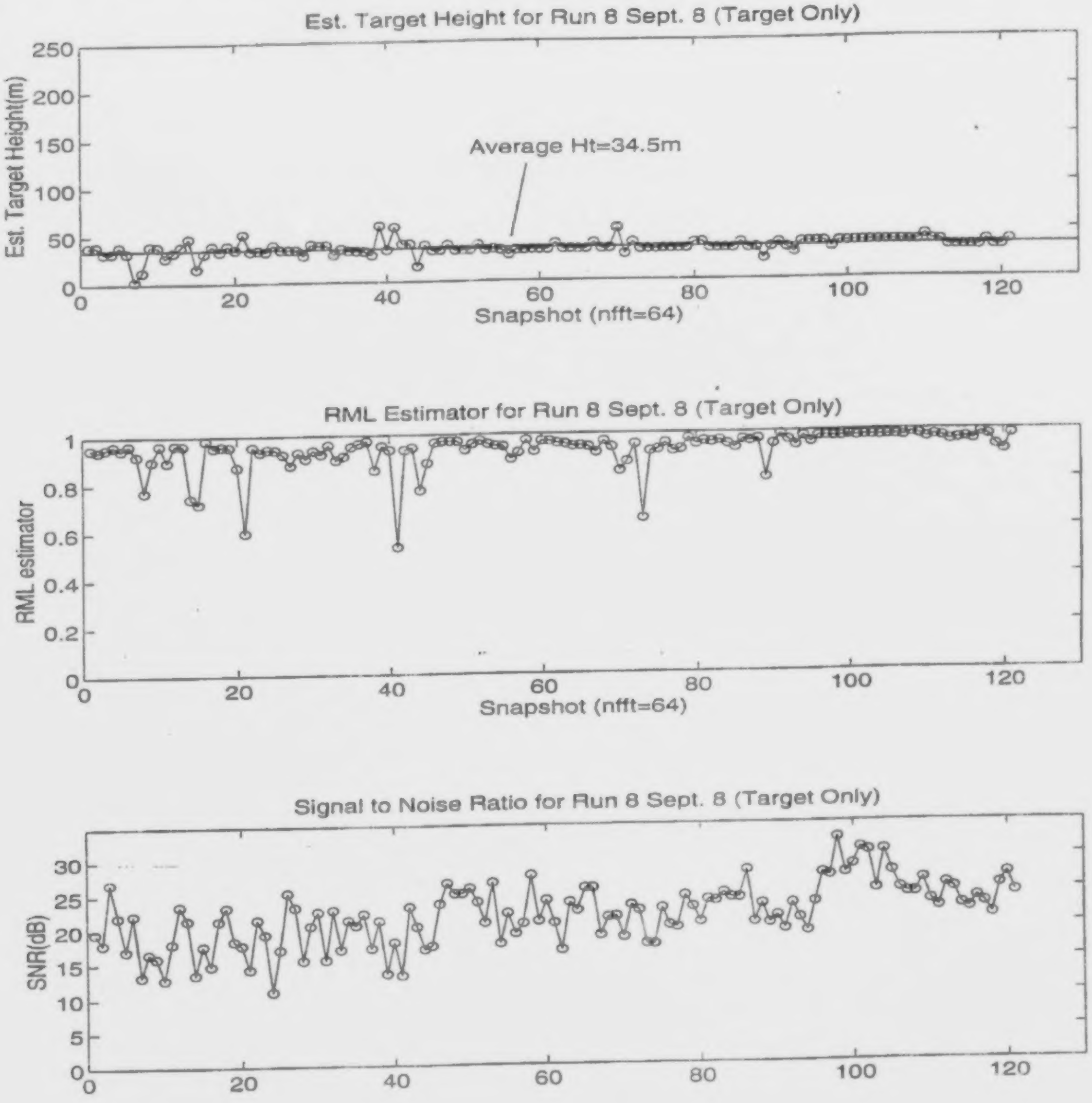
Est. Target Height for Run 8 Sept. 8 (Target Only)
Est. Target Height(m)
250
200
150
100
50
0
Average Ht=34.5m
0
20
40
60
80
100
120
Snapshot (nfft=64)
RML Estimator for Run 8 Sept. 8 (Target Only)
RML estimator
1
0.8
0.6
0.4
0.2
0
0
20
40
60
80
100
120
Snapshot (nfft=64)
Signal to Noise Ratio for Run 8 Sept. 8 (Target Only)
SNR(dB)
30
25
20
15
10
5
0
0
20
40
60
80
100
120

Figure 3.6.38

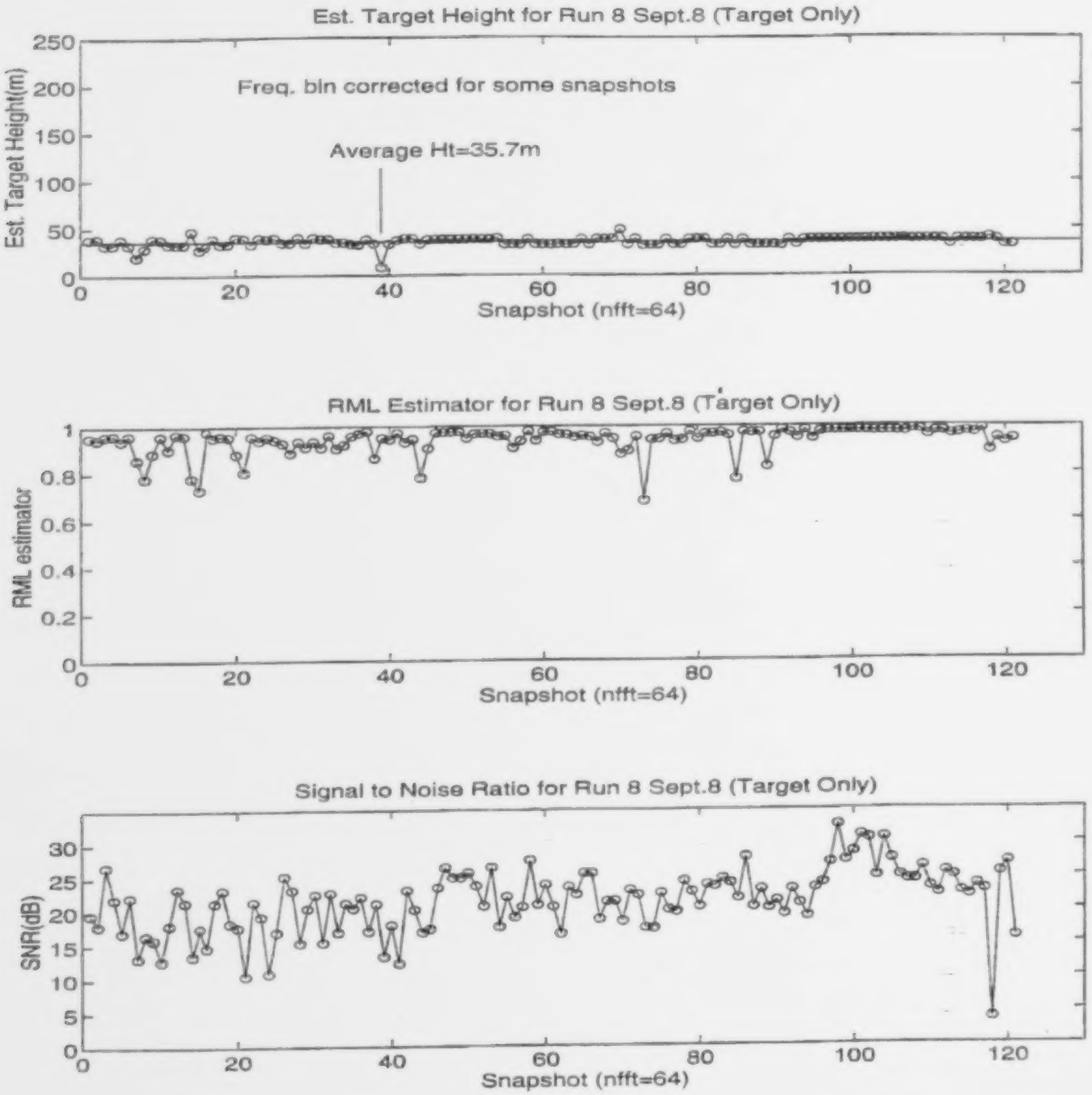
Est. Target Height for Run 8 Sept.8 (Target Only)
Freq. bin corrected for some snapshots
Average Ht=35.7m
Est. Target Height(m)
250
200
150
100
50
0
0
20
40
60
80
100
120
Snapshot (nfft=64)
RML Estimator for Run 8 Sept.8 (Target Only)
RML estimator
1
0.8
0.6
0.4
0.2
0
0
20
40
60
80
100
120
Snapshot (nfft=64)
Signal to Noise Ratio for Run 8 Sept.8 (Target Only)
SNR(dB)
30
25
20
15
10
5
0
0
20
40
60
80
100
120
Snapshot (nfft=64)

Figure 3.6.39

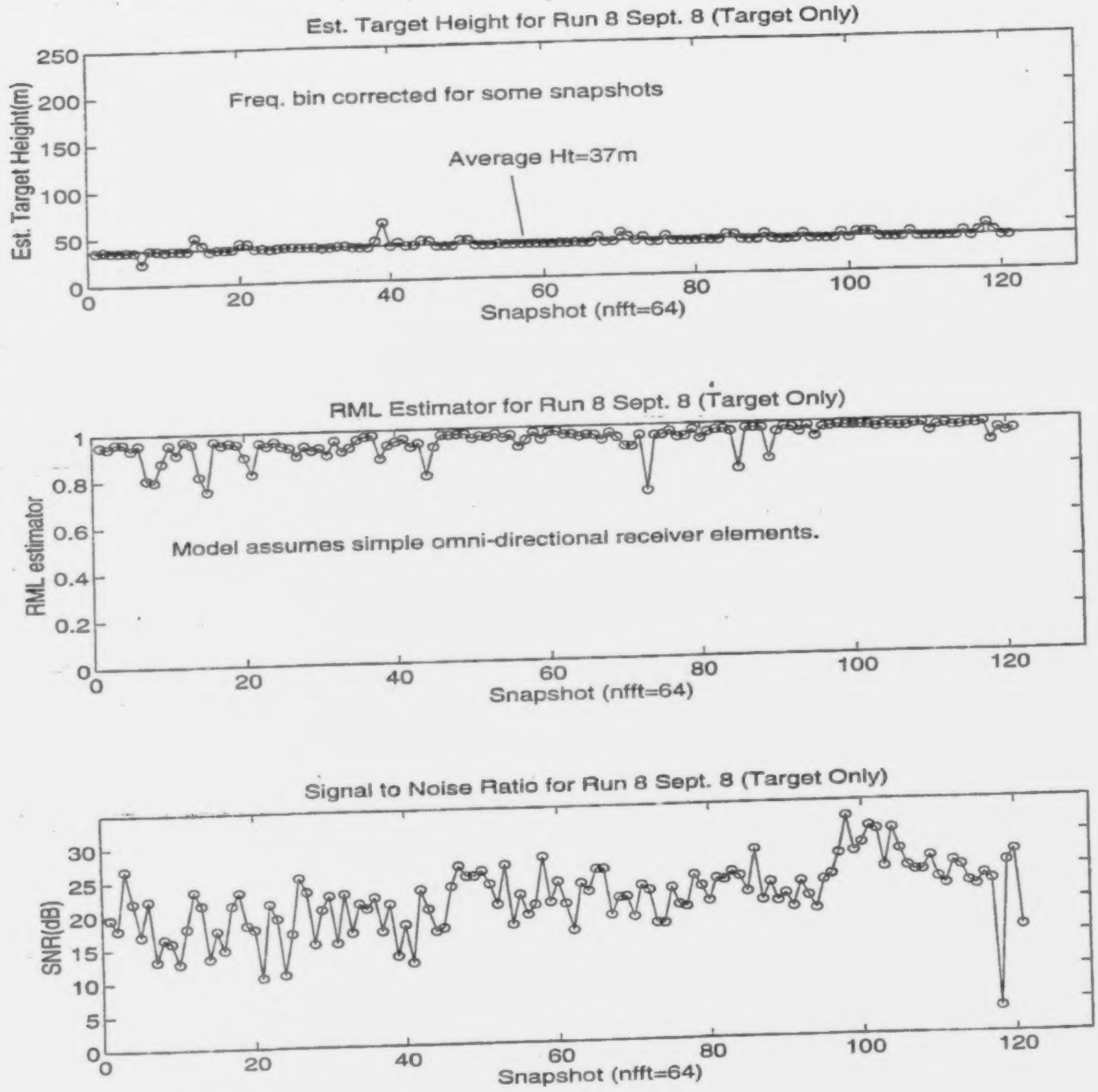
Est. Target Height for Run 8 Sept. 8 (Target Only)
Freq. bin corrected for some snapshots
Average Ht=37m
Est. Target Height(m)
0
50
100
150
200
250
0
20
40
60
80
100
120
Snapshot (nfft=64)
RML Estimator for Run 8 Sept. 8 (Target Only)
Model assumes simple omni-directional receiver elements.
RML estimator
0
0.2
0.4
0.6
0.8
1
0
20
40
60
80
100
120
Snapshot (nfft=64)
Signal to Noise Ratio for Run 8 Sept. 8 (Target Only)
SNR(dB)
0
5
10
15
20
25
30
0
20
40
60
80
100
120
Snapshot (nfft=64)

Figure 3.6.40

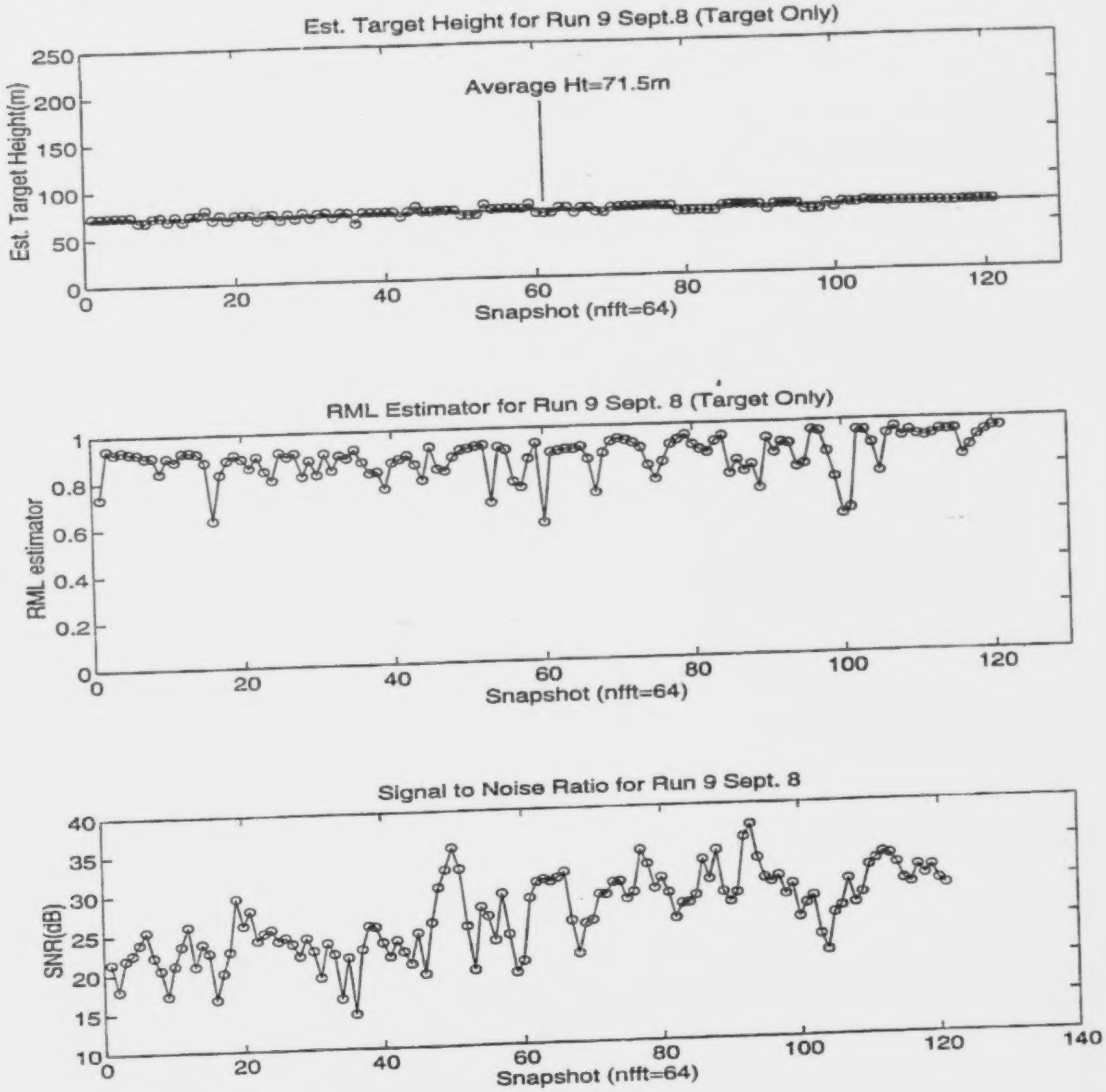
Est. Target Height for Run 9 Sept.8 (Target Only)
Average Ht=71.5m
Est. Target Height(m)
250
200
150
100
50
0
0
20
40
60
80
100
120
Snapshot (nfft=64)
RML Estimator for Run 9 Sept. 8 (Target Only)
RML estimator
1
0.8
0.6
0.4
0.2
0
0
20
40
60
80
100
120
Snapshot (nfft=64)
Signal to Noise Ratio for Run 9 Sept. 8
SNR(dB)
40
35
30
25
20
15
10
0
20
40
60
80
100
120
140
Snapshot (nfft=64)

Figure 3.6.41

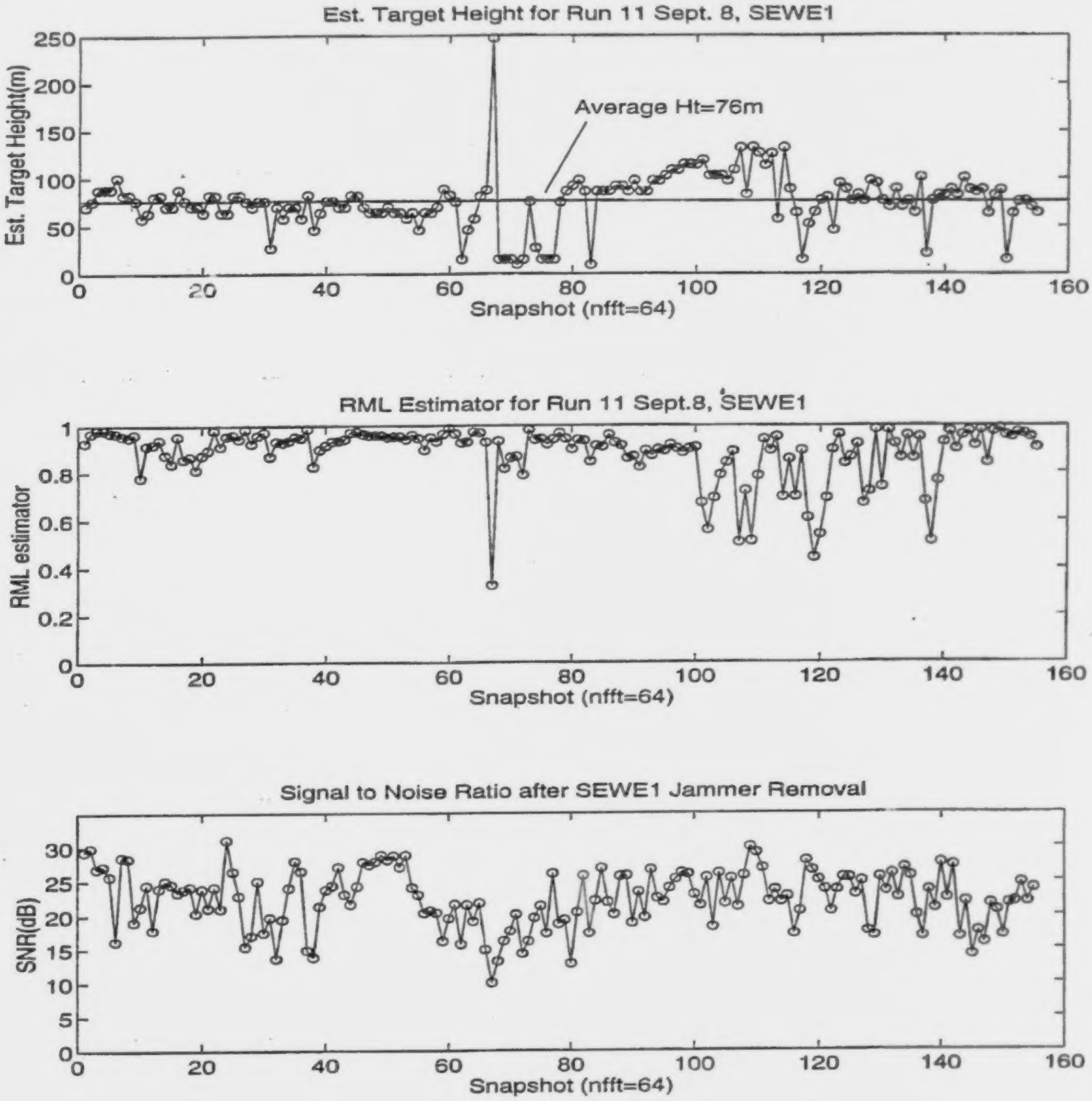

Est. Target Height for Run 11 Sept. 8, SEWE1

RML Estimator for Run 11 Sept.8, SEWE1

Signal to Noise Ratio after SEWE1 Jammer Removal

Figure 3.6.42

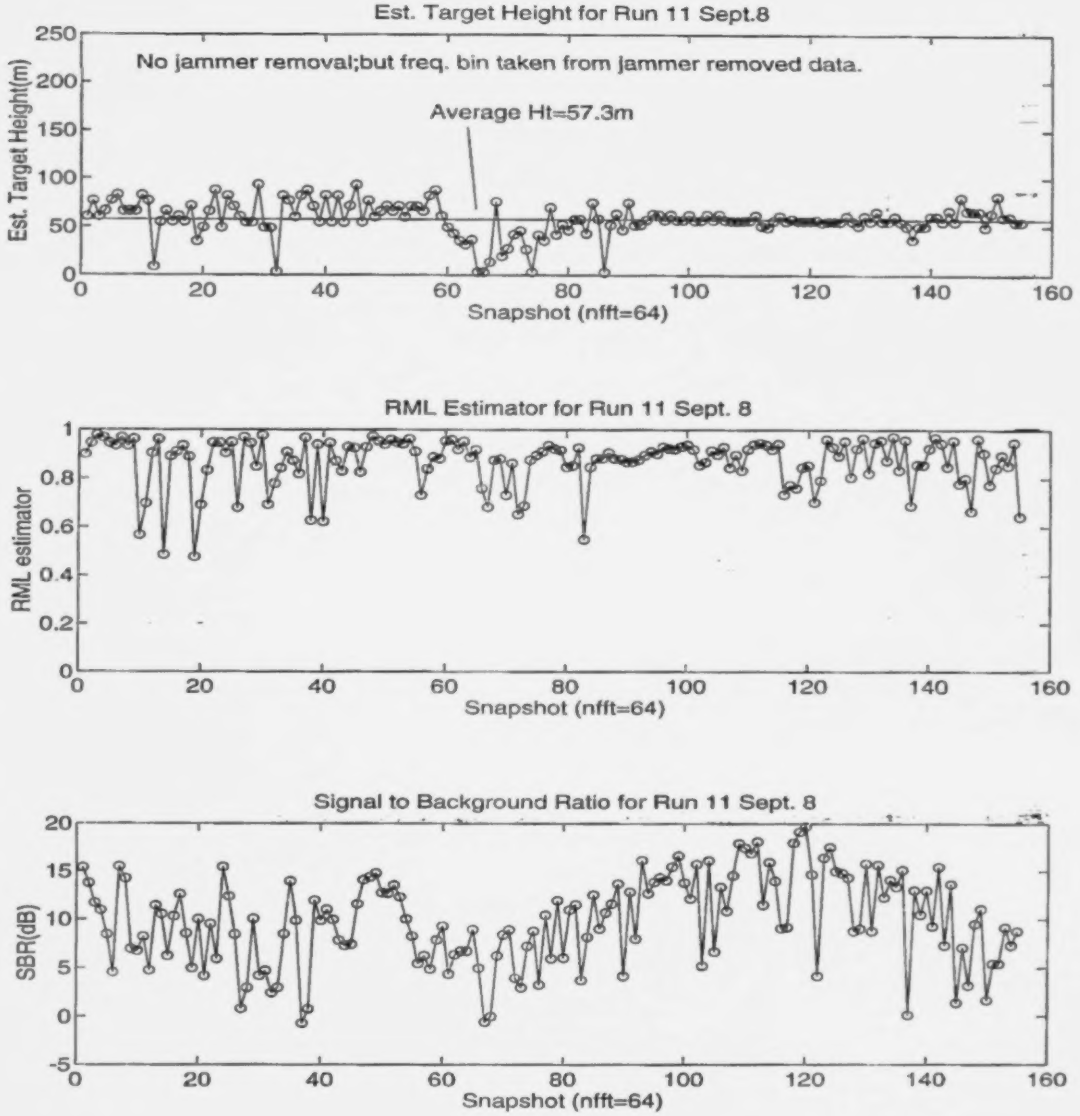
Est. Target Height for Run 11 Sept.8
No jammer removal;but freq. bin taken from jammer removed data.
Average Ht=57.3m
Est. Target Height(m)
250
200
150
100
50
0
0
20
40
60
80
100
120
140
160
Snapshot (nfft=64)
RML Estimator for Run 11 Sept. 8
RML estimator
1
0.8
0.6
0.4
0.2
0
0
20
40
60
80
100
120
140
160
Snapshot (nfft=64)
Signal to Background Ratio for Run 11 Sept. 8
SBR(dB)
20
15
10
5
0
-5
0
20
40
60
80
100
120
140
160
Snapshot (nfft=64)

Figure 3.6.43

4.0 APAR System Study

The various sections of Task 2 were directed toward evaluating a possible multi-function phased array radar system (APAR) under various propagation conditions and jamming situations. The most recent version of the simulator at the time of this document was named GENXSLC. A brief description of how to run this software package is provided in Appendix G.

4.1 Task 2a) i)- Adding Side-lobe Canceller Array Configurations

The simulation software was modified so that up to four side-lobe canceller arrays could be included in the simulations. The software was set up so that the SLC's used the same phase steering and curved earth software as used for generating the target and jammer signal data. The SLC's were set up in a separate menu which included the following parameters:

a) number of SLC's
b) SLC height
c) SLC angle off-boresight
d) SLC range

4.2 Task 2a) ii)-Adding Signals From up to 4 Noise Sources

Originally this task called for the inclusion of up to 4 wide-band noise sources but was later scaled down to simply 4 narrow-ban jammers. The jammer signals were generated using the same software used by the target signal simulator to calculate phase steering and curved earth effects. The jammers were set up in a separate menu which included the following parameters:

a) number of jammers
b) jammer heights
c) jammer angle off-boresight
d) jammer range
e) jammer to noise ratio

Gaussian noise was added to the jammer signals at each element according to the specifications of e) above. With the inclusion of the jammer signals the simulation software was able to generate data sampled from both on-target and off-target range cells. The simulated off-target data was generated by using just the jammer inputs to the software and the on-target data was obtained by adding the target signal inputs to the jammer inputs to produce the total target+jammer+noise signal.

4.3 Task 2a) iii)-Modelling the Individual Array Elements

Modelling of the individual array elements was kept to a very basic level such as simply specifying the signal to noise ratios per element and the the frequencies of operation. The receiver elements were assumed to have ideal omni-directional characteristics.

4.4 Task 2a) iv)-Formatting Simulator Output for Anti-Jamming Software

The side-lobe cancelation software written for use on the SUN workstation (SLCSUN) required the input of data sampled at the on-target and off-target range cells for doing side-lobe jammer cancellation using the sampled matrix inversion (SMI) technique. The off-target data was to consist of jammer+noise signals for both the main and slc arrays whereas the on-target data was to consist of target+jammer+noise signals for both types of array. For comparison purposes, the simulator also produced data corresponding to the same target-receiver geometry but without a jammer present. Thus the latest version of the simulator (named GENXSLC) would produce a total of 5 different output files for each simulation run corresponding to on-target (jammed) data for both slc and main arrays, off-target (jammed) data for both types of array and non jammed on-target data for the main array. Also three additional files were produced to hold signal to noise information, target direction information and jammer direction data. When operating the software to generate simulated data, the output file name would be entered by the user without a file type extension, then the software would generate several files with the same name but different extensions depending on the types of data it held. The following is a list of the different file types (ie extensions) produced by the simulator followed by a brief description.

file.dat -	main array target signal data with no jammer present. Each record consisted of the following information: target range, the main array difference signals for elevation monopulse, the main array difference signals for azimuthal monopulse, the sum signal for the main array,the target height, and the target angle off-boresight.
file.oft -	main array jammer+noise signal data simulating sampling of the radar signal outside the target range cell. Each record consisted of the following information: target range, main array difference signals for elevation monopulse, main array difference signals for azimuthal monopulse, main array sum signal, target angle off-boresight.

file.ont - main array target+jammer+noise data simulating sampling of the radar signal from the range cell of the target. Each record consisted of the following information: target range, main array difference signals for elevation monopulse, main array difference signals for azimuthal monopulse, main array sum signal, target angle off-boresight.

file.ofs - slc array data simulating the sampling of jammer+noise signals from the off-target range cell. Each record consisted of the following information: target range, sum signals for each of four possible slc arrays.

file.ons - slc array data simulating the sampling of target+jammer+noise data from the on-target range cell. Each record consisted of the following information: target range, sum signals for each of four possible slc arrays.

file.snr - main array data for output signal to noise ratio. Each record consisted of the following information: target range, output SNR for the left side of the array, output SNR for the the right side of the array, total output SNR for the entire main array.

file.tdi - Each record in this file consists of the following: target range, antenna height, target height, curved earth coefficient, target angle off-boresight.

file.jdi - similar to '.tdi' files except that this file contains the information pertaining to each of the jammers used in the simulation

4.5 Task 2a) v)- Simulation of Threat Scenarios and Performance Evaluation of Anti-jamming Algorithms

To carry out the performance evaluation of the anti-jamming algorithms, data was generated, using the GENXSLC simulator, to simulate a target incoming from 25 to 3 km with side-lobe jammer interference, for different signal to noise ratio, signal to jammer ratio and multiple jammer scenarios. This data was then processed by the SLCSUN software to remove the jammer, after which the data was processed by elevation and azimuthal monopulse tracking routines to estimate the target direction. Some typical results of these analyses are shown in figures 4.5.1 to 4.5.4. Figure 4.5.1 and 4.5.2 show the results of elevation monopulse for jammed data with the jammer cancelled (using SMI) and for data without a jammer initially present. It can be seen that the two results are virtually identical proving that the jammer cancellation routine works quite well for this case. The spikes in the data represent the effects of multipath on the target direction estimation. Figure 4.5.3 and 4.5.4 show the results of azimuthal monopulse direction estimates for jammed and non jammed data respectively. Again it can be seen that the jammer was removed quite effectively.

In conjunction with the mfr studies related to threat scenarios, an evaluation of various jammer types was carried out for the Scientific Authority. The results of the analysis were presented to the Scientific Authority in form of graphs, tables postscript files.

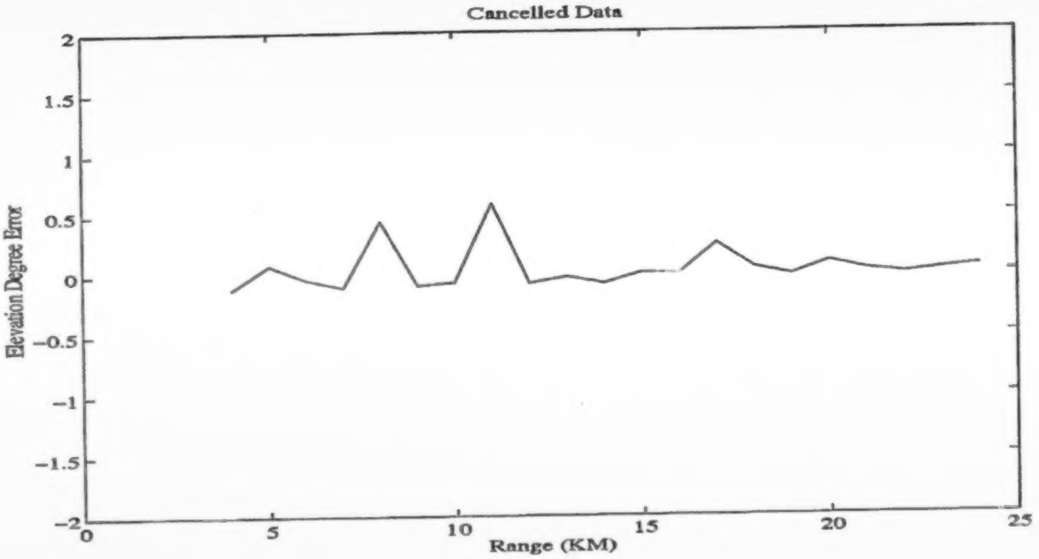

Figure 4.5.1 Elevation Amplitude Monopulse target direction estimation from data with jammer cancellation.

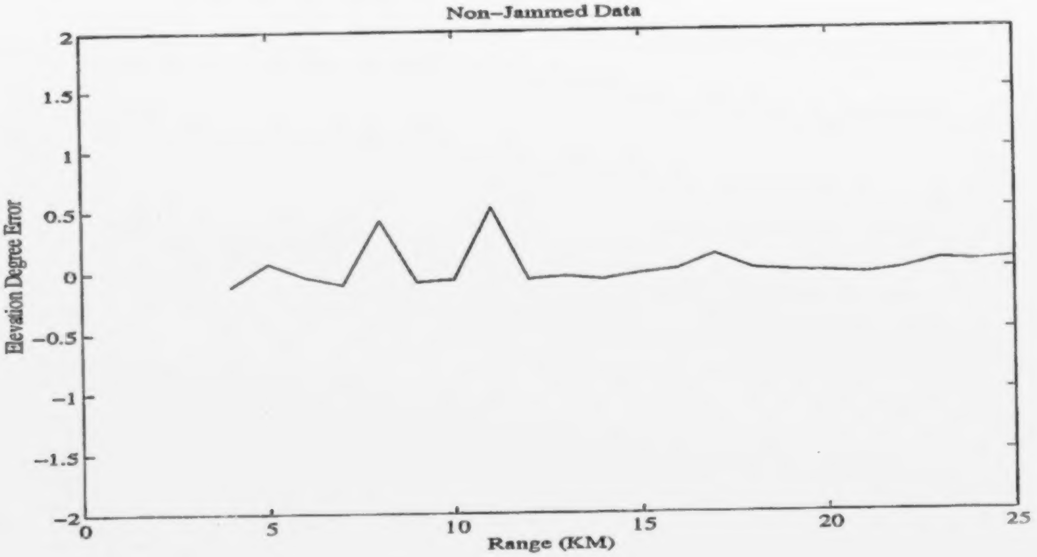

Figure 4.5.2 Elevation Amplitude Monopulse target direction estimation for a non-jammed target signal.

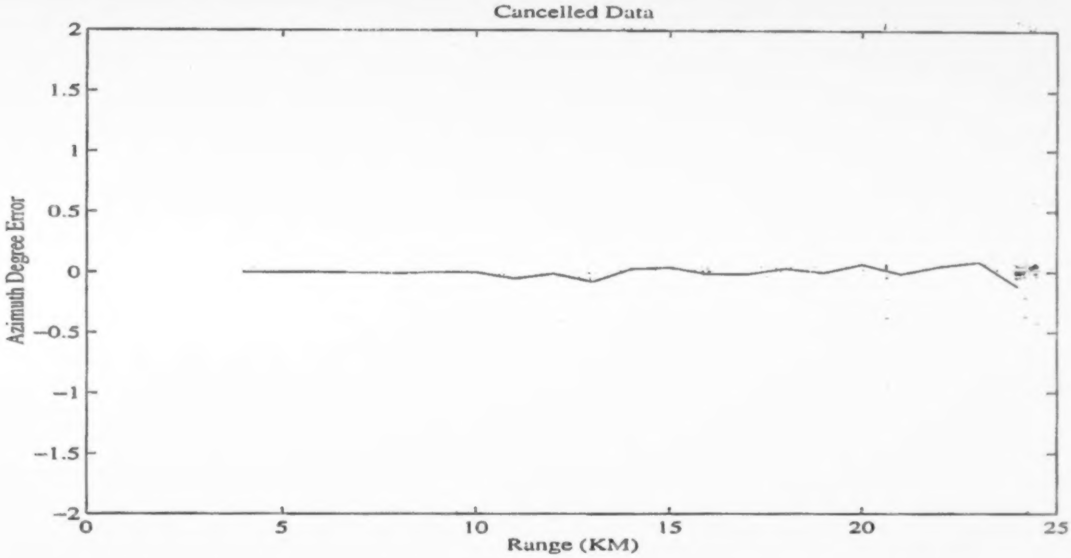

Figure 4.5.3 Azimuth Amplitude Monopulse target direction estimation from data with jammer cancellation.

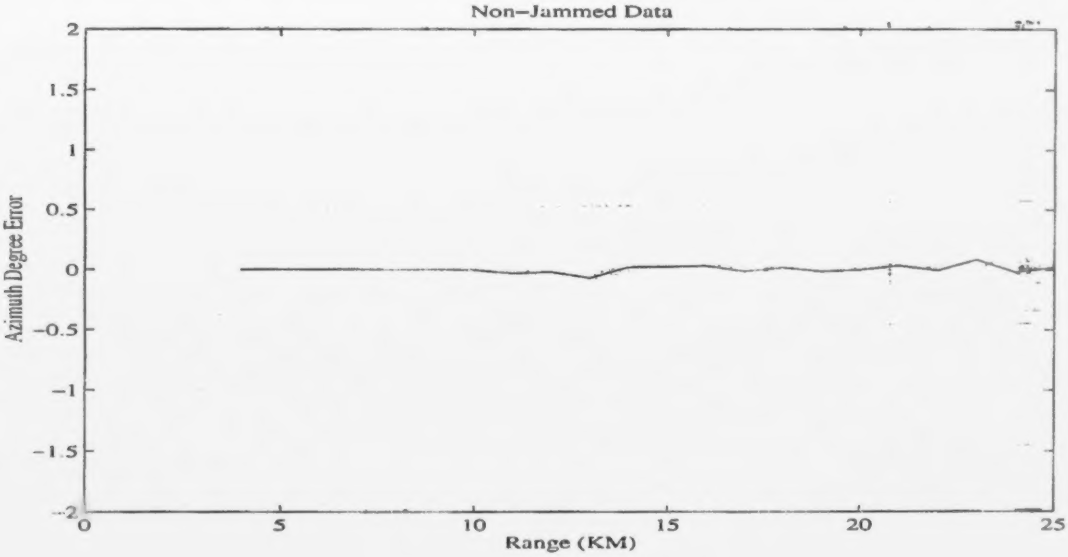

Figure 4.5.4 Azimuth Amplitude Monopulse target direction estimation for a non-jammed target signal.

4.6 Task 2b) Performance Evaluation for Monopulse and RML Tracking

Both amplitude and phase monopulse tracking in the elevation and azimuth directions were performed on data from the mfr simulator for a variety of possible scenarios including:

i) different array tilts
ii) different input signal to noise ratios
iii) different target heights
iv) different sets of frequencies
v) different weighting schemes for reducing the monopulse direction estimation errors when multiple frequencies were used.

The results of these different scenarios were plotted and presented to the Scientific Authority for evaluation. The details of these analyses that can be revealed in this report is limited; however, without revealing any of the crucial data, some typical results are shown in figures 4.6.1 to 4.6.9. Figure 4.6.1 is a comparison of amplitude and phase monopulse in the elevation and azimuth directions, for a single frequency, and an incoming target at 20m altitude. Plots a) and c) in the figure are for phase monopulse in the azimuth and elevation directions respectively, and plots b) and d) are the corresponding versions for amplitude monopulse. It can be seen from this set of plots that the amplitude and phase monopulse results are virtually identical. For this reason, all other simulations were done using only amplitude monopulse.

Figures 4.6.2 to 4.6.4 show the results of amplitude monopulse in the elevation direction for target heights of 5, 10 and 20 m, using sets of 3, 5 and 9 frequencies, a specified receiver tilt and input signal to noise ratio, and different methods of averaging the multiple frequency results. Plots a) b) and c) of Figure 4.6.2 show the results of simple averaging on the target direction estimation errors from amplitude monopulse in the elevation direction using 3 frequencies, for target heights of 5, 10 and 20m respectively. Plots d) e) and f) of the same figure show the results of a special weighted average developed by the Scientific Authority, for the same sets of data as in the previous three plots. It can be seen that there is a significant improvement in the target direction estimation using the weighted averaging technique. Similar results are shown in Figures 4.6.3 and 4.6.4 for 5 frequencies and 9 frequencies respectively. As one might expect the results are improved as the number of frequencies is increased.

Figures 4.6.5 to 4.6.7 show the corresponding results for the case of amplitude monopulse in the azimuthal direction.

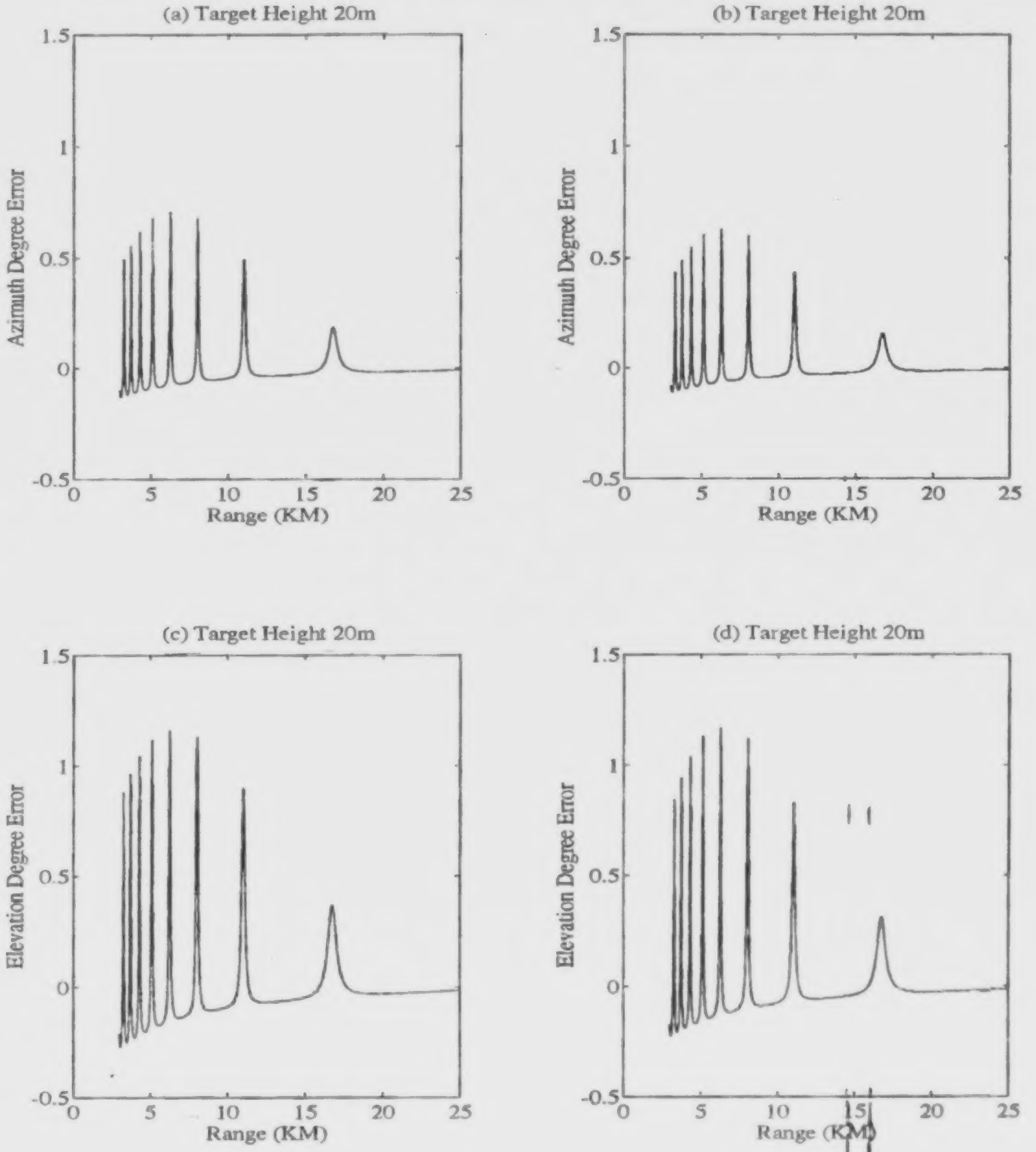

Figure 4.6.1 Comparison of amplitude (a,c) and phase (b,d) monopulse direction estimation in the elevation and azimuth directions.

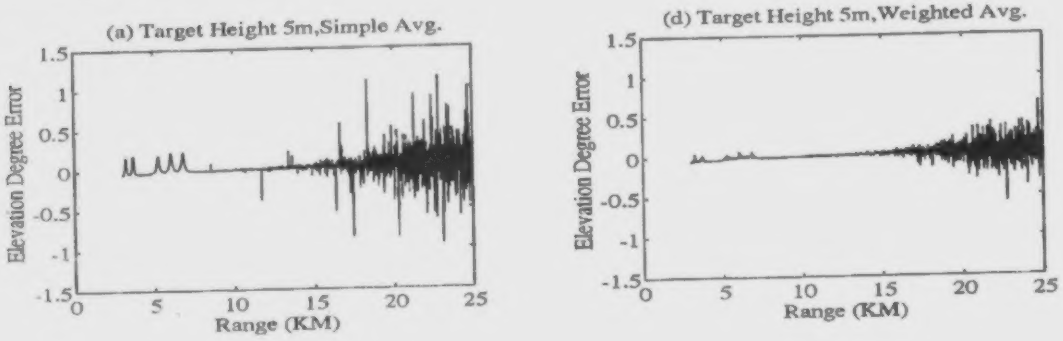

(a) Target Height 5m,Simple Avg.

(d) Target Height 5m,Weighted Avg.

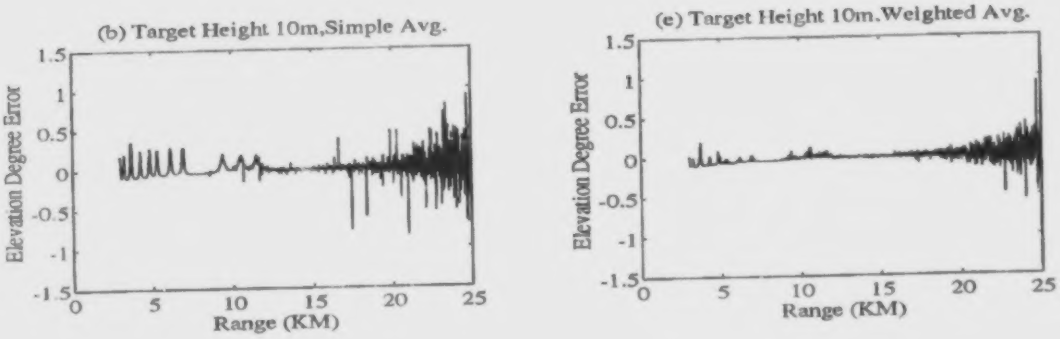

(b) Target Height 10m,Simple Avg.

(e) Target Height 10m,Weighted Avg.

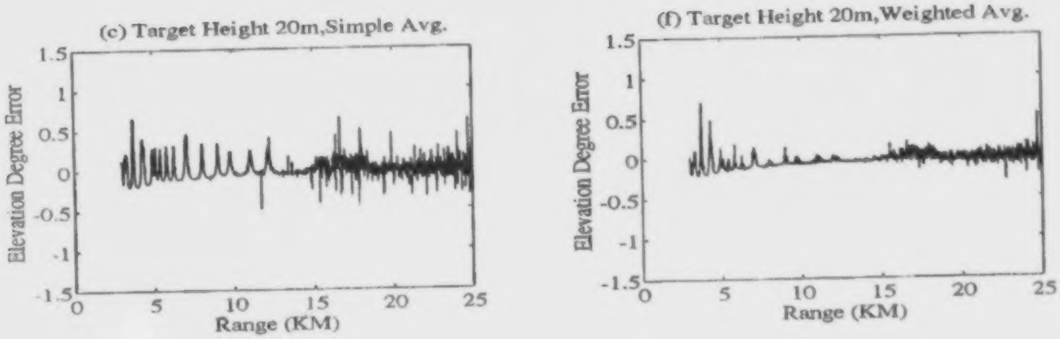

(c) Target Height 20m,Simple Avg.

(f) Target Height 20m,Weighted Avg.

Figure 4.6.2 Amplitude elevation monopulse for 3 target heights using 3 frequencies; a),b), c) used simple averaging of the monopulse errors and d), e), f) used a weighted average.

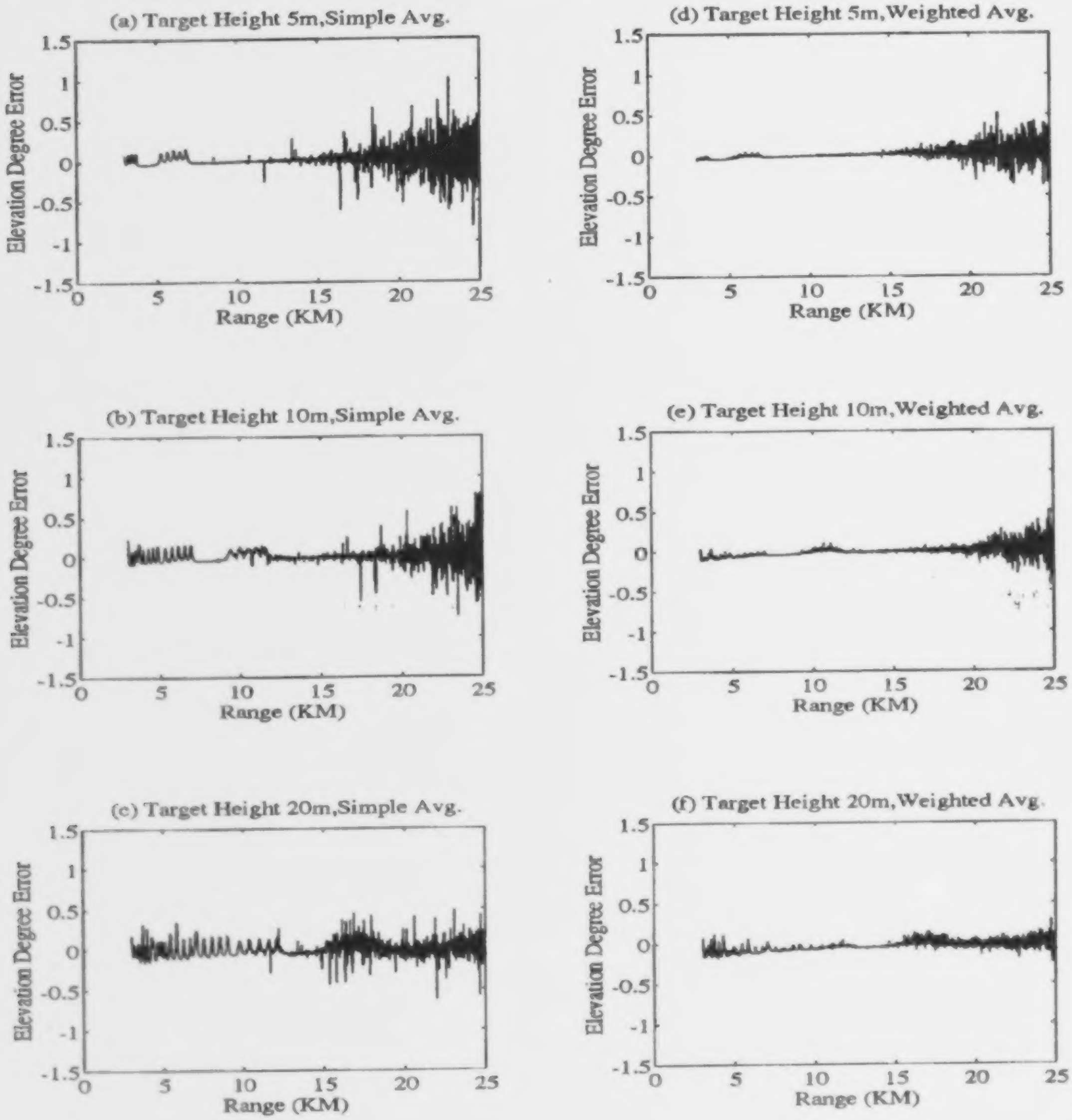

Figure 4.6.3 Amplitude elevation monopulse for 3 target heights using 5 frequencies; a),b), c) used simple averaging of the monopulse errors and d), e), f) used a weighted average.

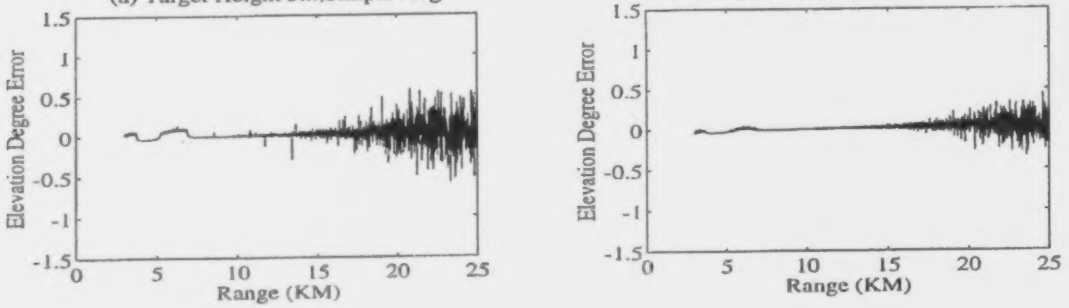
(a) Target Height 5m,Simple Avg.

(d) Target Height 5m,Weighted Avg.

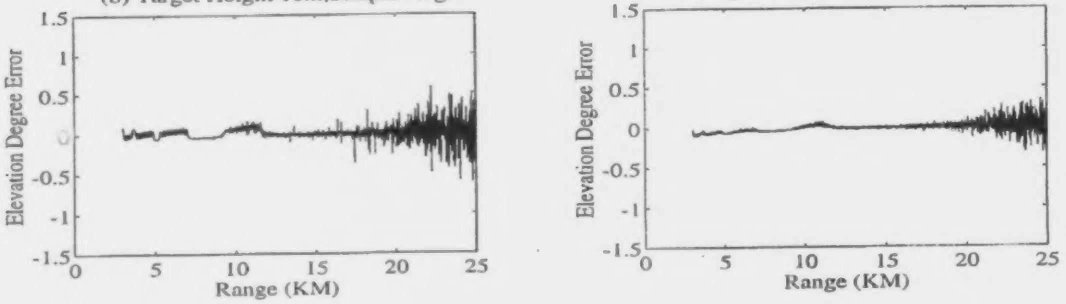
(b) Target Height 10m,Simple Avg.

(e) Target Height 10m,Weighted Avg.

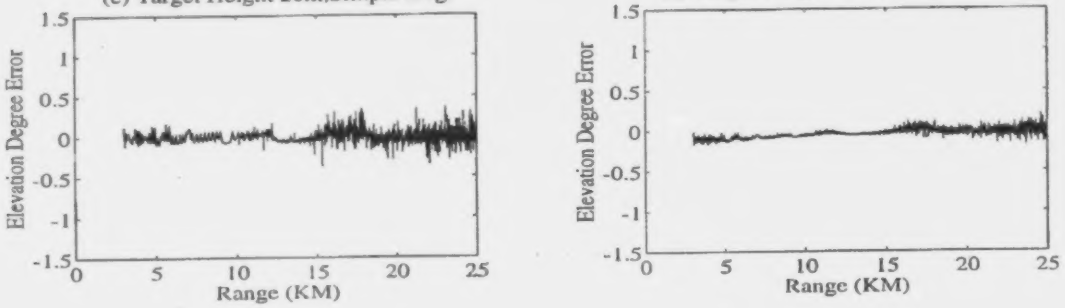
(c) Target Height 20m,Simple Avg.

(f) Target Height 20m,Weighted Avg.

Figure 4.6.4 Amplitude elevation monopulse for 3 target heights using 9 frequencies; a),b), c) used simple averaging of the monopulse errors and d), e), f) used a weighted average.

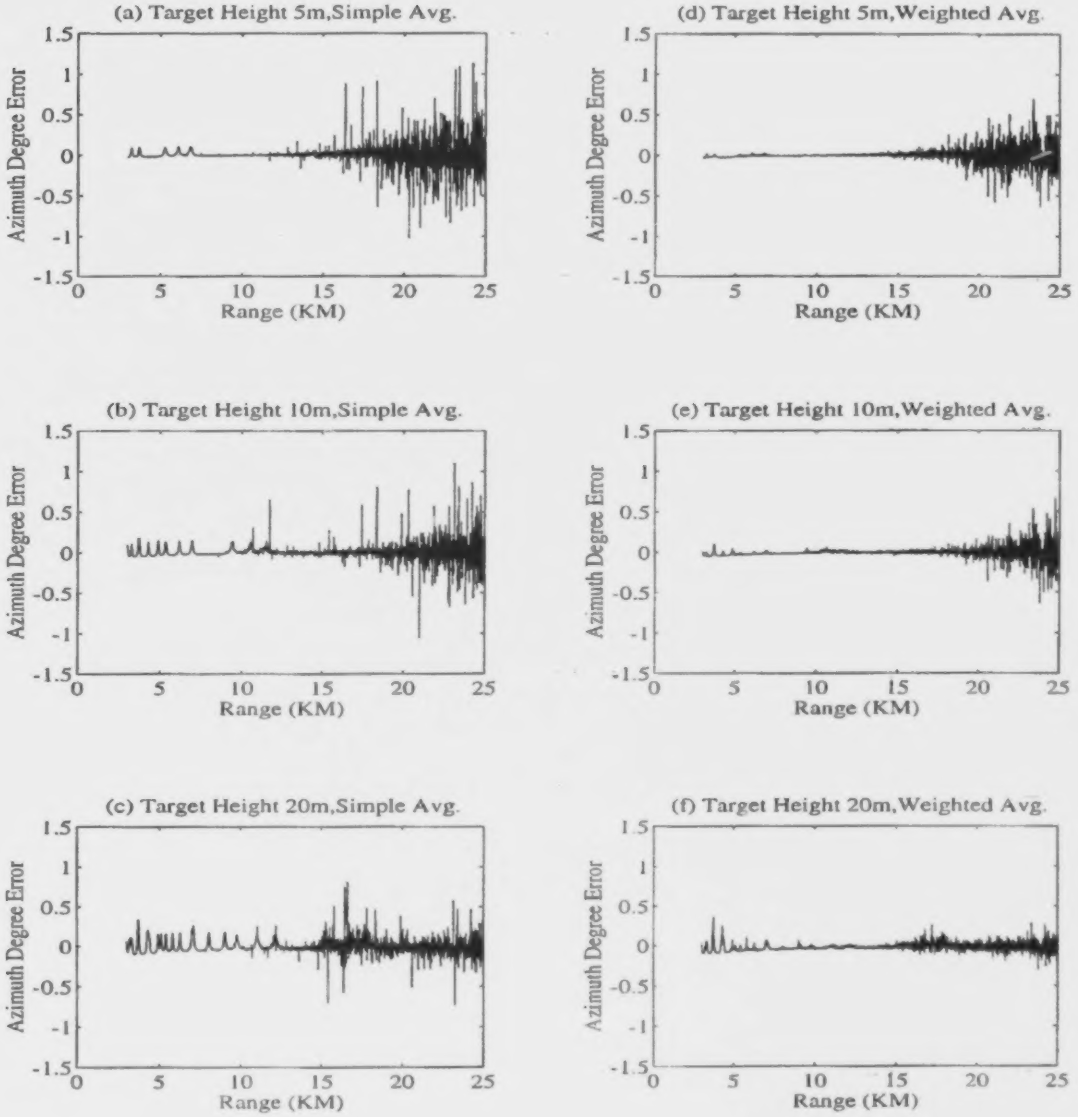

Figure 4.6.5 Amplitude azimuth monopulse for 3 target heights using 3 frequencies; a),b), c) used simple averaging of the monopulse errors and d), e), f) used a weighted average.

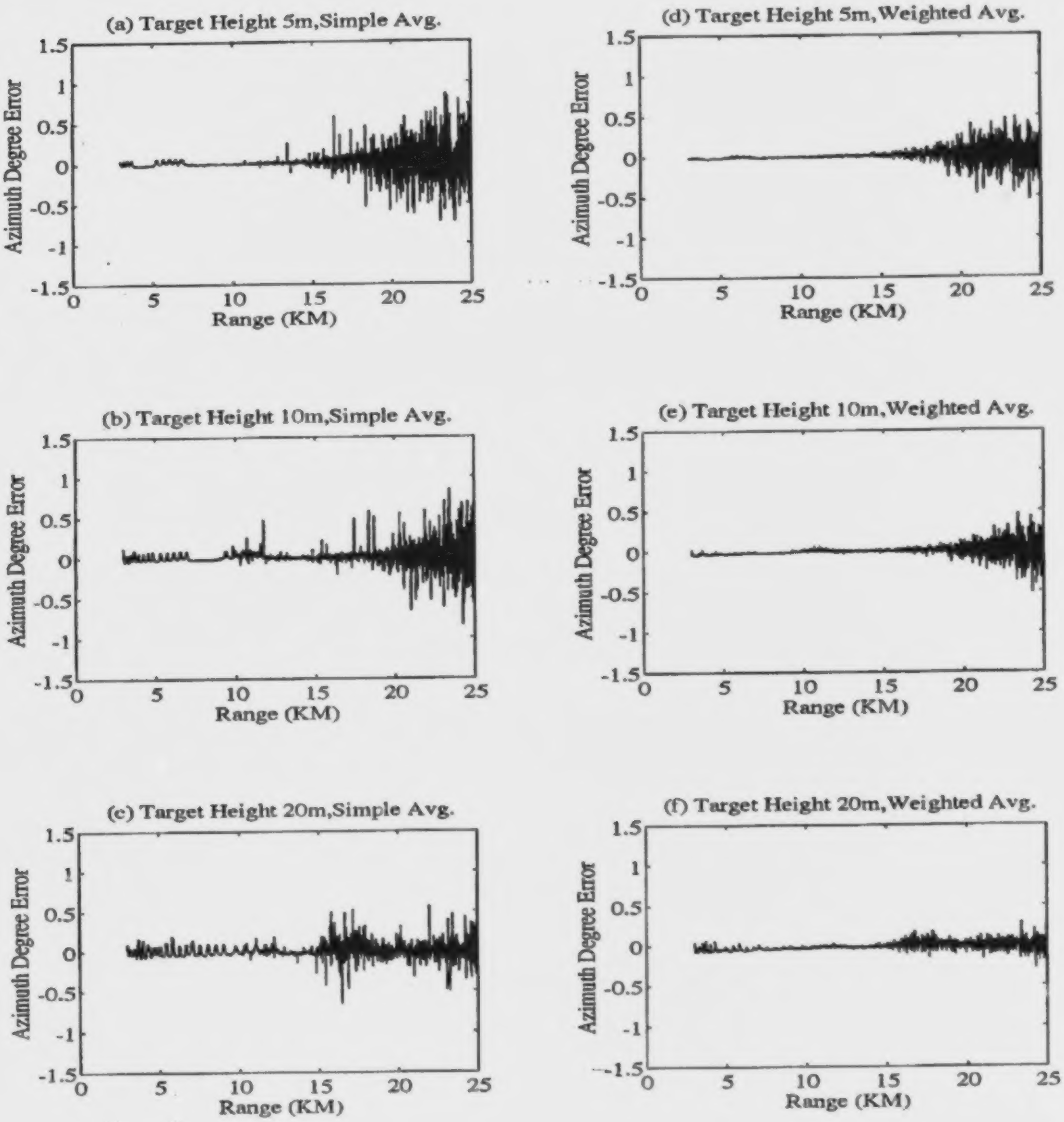

Figure 4.6.6 Amplitude azimuth monopulse for 3 target heights using 5 frequencies; a),b), c) used simple averaging of the monopulse errors and d), e), f) used a weighted average.

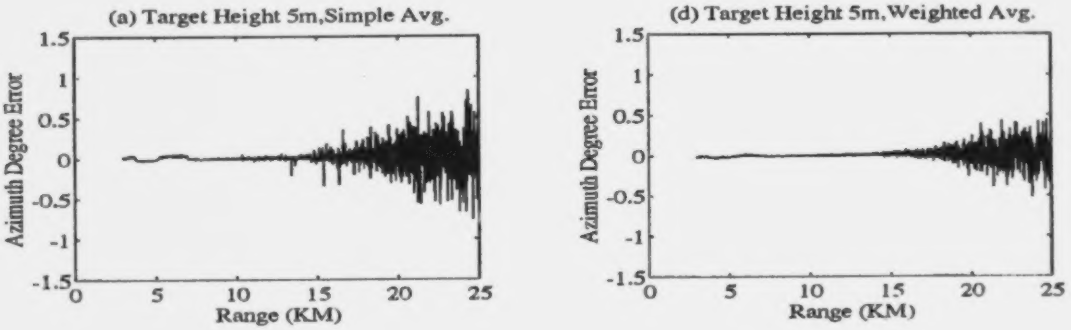
(a) Target Height 5m,Simple Avg.

(d) Target Height 5m,Weighted Avg.

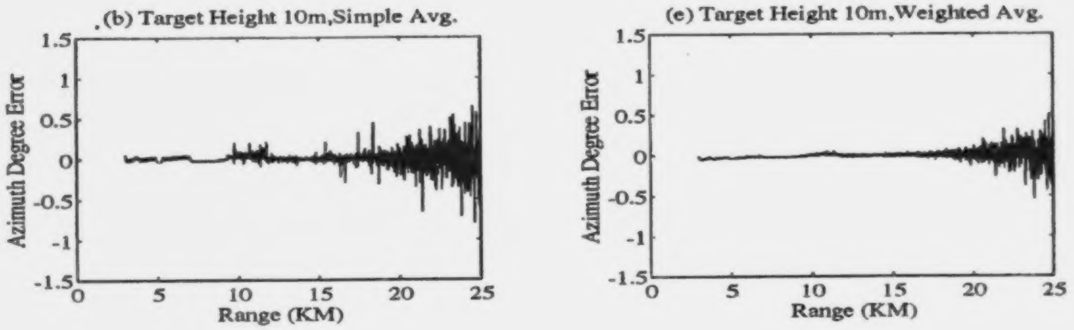
(b) Target Height 10m,Simple Avg.

(e) Target Height 10m,Weighted Avg.

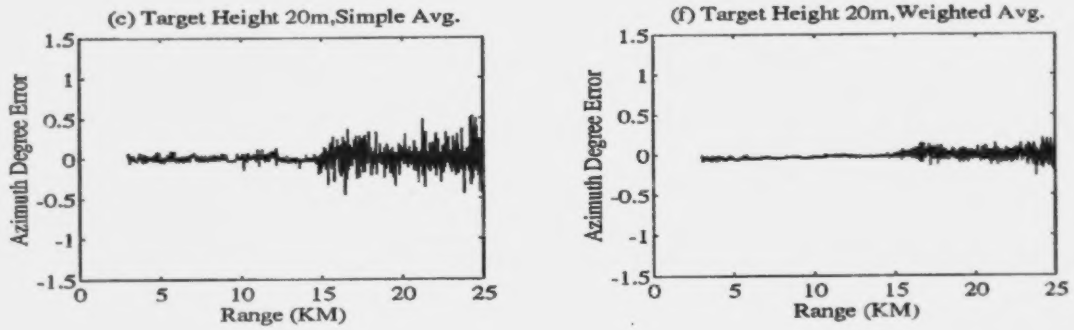
(c) Target Height 20m,Simple Avg.

(f) Target Height 20m,Weighted Avg.

Figure 4.6.7 Amplitude azimuth monopulse for 3 target heights using 9 frequencies; a),b), c) used simple averaging of the monopulse errors and d), e), f) used a weighted average.

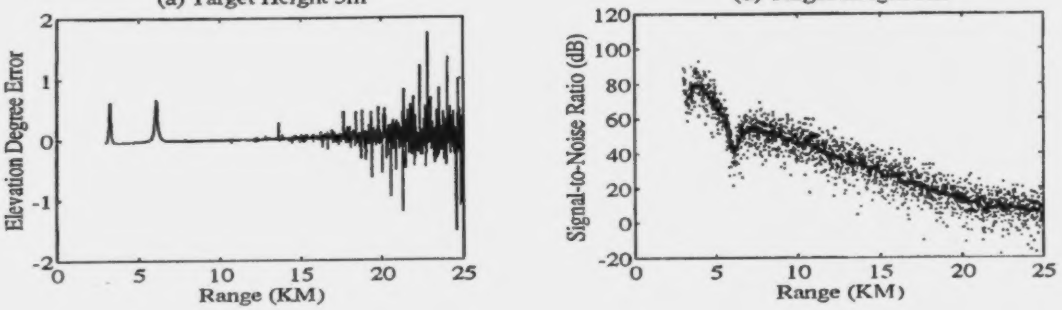
(a) Target Height 5m

(d) Target Height 5m

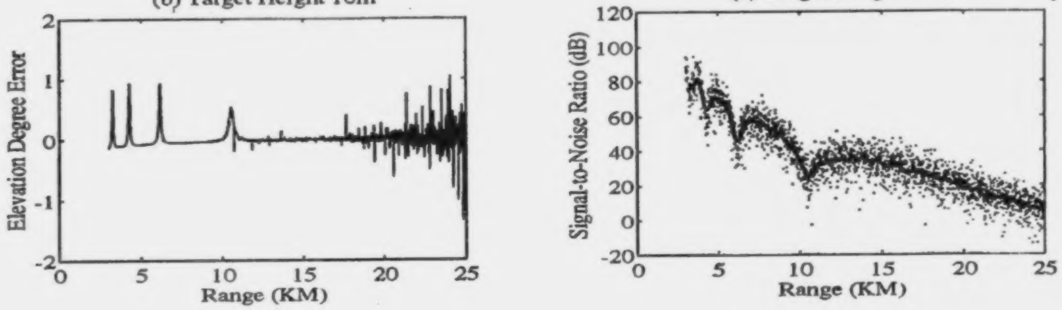
(b) Target Height 10m

(e) Target Height 10m

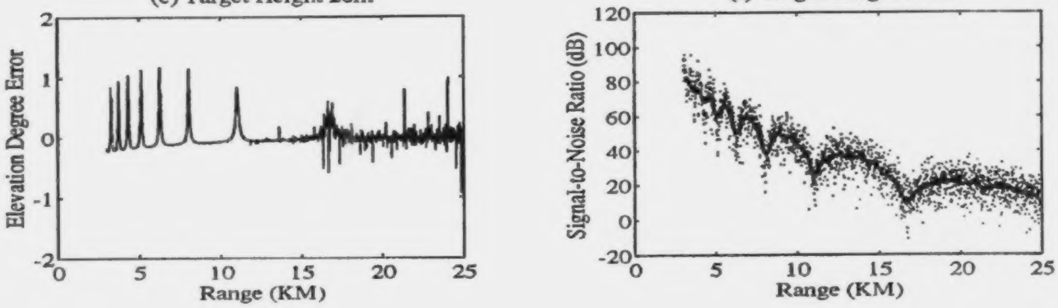
(c) Target Height 20m

(f) Target Height 20m

Figure 4.6.8 Effect of range and input SNR on output SNR and direction estimation for amplitude elevation monopulse at three different target heights, 1freq.

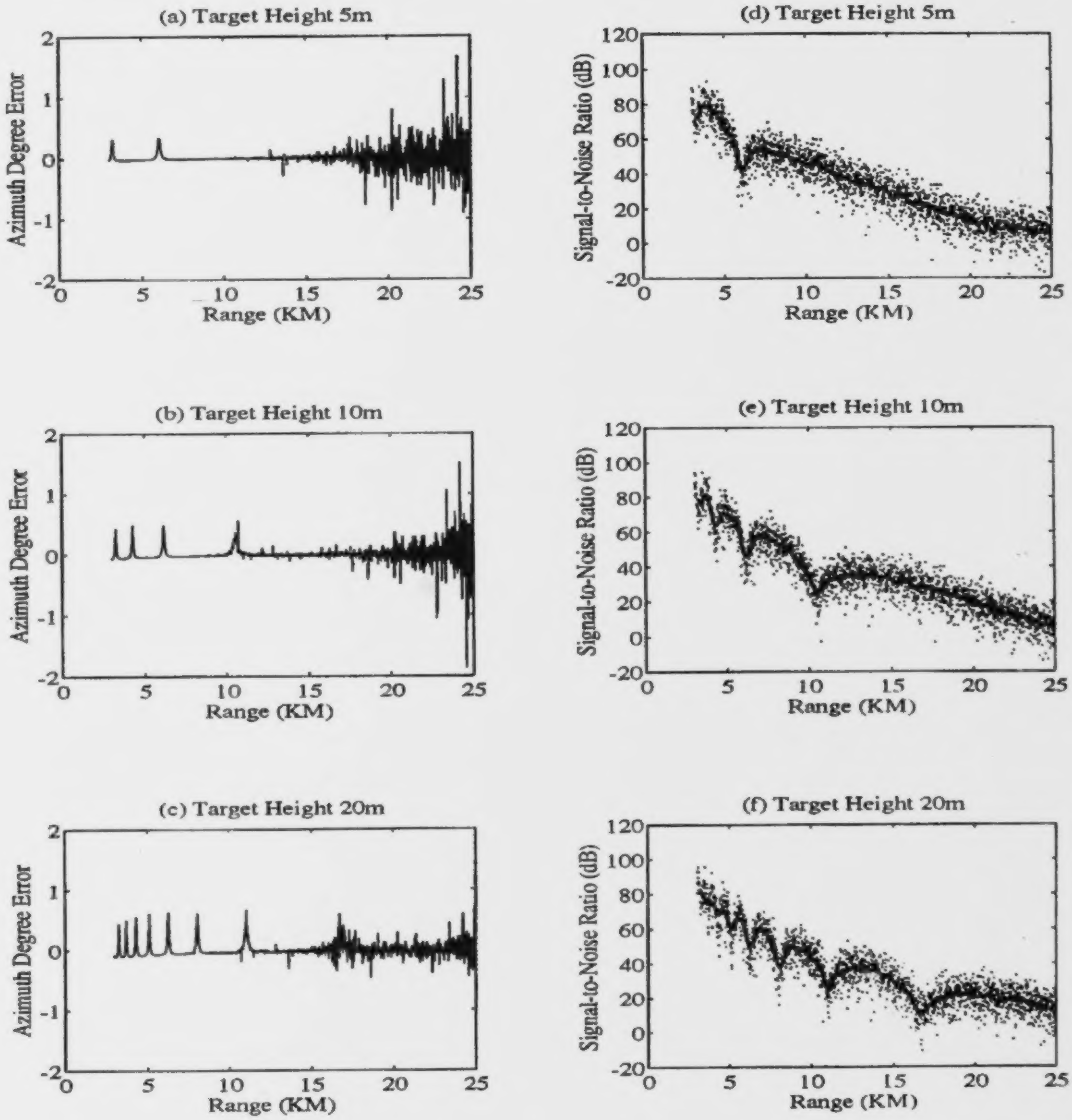

Figure 4.6.9 Effect of range and input SNR on output SNR and direction estimation for amplitude azimuth monopulse at three different target heights, 1 freq.

Figures 4.6.8 and 4.6.9 are typical examples showing the effect range on the output signal to noise ratio, and direction estimation errors for amplitude monopulse using one frequency, at three different target heights for the elevation and azimuth directions respectively. The solid line in the output SNR plots shows the average output SNR at each range.

5.0 Radar Trials Support

Most of the radar trials support consisted of preliminary data evaluation to ensure that the new data acquisition facility for sampling and recording the IF data from the EARS was working correctly as well as the rest of the radar system. A brief chronological summary of the trials support is as follows:

a) June

- new data began to be produced by the upgraded EARS and recorded by the new data acquisition system sampling at the intermediate frequency. The Scientific Authority was assisted with evaluation of the data to determine if any modifications needed to be made to the acquisition system. It was determinedthat the system was in full working order ready for trials to commence.

b) July

- analysis of the preliminary data from the new EARS to evaluate the data quality.

c) August

- analysis and quality evaluation of preliminary data from the EARS.
- half day spent at a meeting at AREA5 to determine the status of the experimental system, propose solutions to any problems and go over the proposed trials plan to be implemented in September 1994.

Appendix H contains a description of each of the experiments performed in the trials during late August and early September of 1994, mostly in table format.

Acknowledgements

AIT would like to acknowledge the following people for their efforts during the period of this contract: the Scientific Authority, Mr E. S. Riseborough, the DREO supervisor of the project, who provided valuable advice and support; Ms M. Toulgoat for her assistance in directing the main-beam cancellation studies; the technical support team at Area 5 who maintained the Radar systems and assisted with the collection of the experimental data.

APPENDIX A
STATEMENT OF WORK

ANNEX A

CONTRACT TITLE: Multi-Function Radar Simulation and ECCM Data Analysis

BACKGROUND

The Defence Research Establishment, Ottawa, (DREO), is carrying out a program of research in support of Active Phased Array Radar (APAR). This is a multi-function radar (MFR), which will be developed by Canada, Germany, and The Netherlands. There are plans to install APAR onto the Canadian Patrol Frigate at mid-life refit in 2005. At present, a research and development emphasis is being placed on Electronic Counter Counter Measures (ECCM) of MFR, including side-lobe and main-beam nulling of jammers. This will be studied by using simulators, and real data collected from an experimental array radar system (EARS) at DREO. This system consists of an eight element vertical array, and an eight element side-lobe canceller. A data base is available from main-beam and side-lobe interference experiments performed in January 1993 at the Experimental Radar Site located on the Ottawa River. The data collected during these trials were used for initial tests on the standard matrix inversion algorithm. A simulator was developed to test the effect of ship motion on monopulse estimation of targets by the APAR. This has to be modified to evaluate the effect of multipath on jammer suppression and to perform a subsequent analysis of both monopulse and revise maximum likelihood estimation.

WORK STATEMENT

The contractor is required to provide a system analyst and a programmer to carry out the following tasks:

1: Main-beam and Side-lobe Canceller Data Analysis

a) Experimental main-beam, and side-lobe beacon interference data was collected in January 1993 at the Ottawa River Site. The experiments used a helicopter, corner reflector, skidoo, and a building as radar targets. The radar and beacon were both operating at 9.6 GHz, with the beacon located either in the main-lobe or the side-lobe of the main antenna. The main antenna consisted of an eight element vertical array. An eight element side-lobe canceller array was positioned beneath the main array in a horizontal position. The radar collected data on the target for one pulse, off target the next, and continued this sequence. Data was also collected while the beacon was off and system noise data was also collected. The data file sizes were in the order of 5 to 15 MBytes.

i) The contractor shall implement on the VAX 3800 and IBM Compatible computers the main-beam and side-lobe jammer cancellation algorithms supplied by the Scientific Authority. The contractor shall use simulated data to compare cancellation performance of these algorithms with standard algorithms such as the sampled matrix inversion technique.

ii) The contractor shall calibrate the experimental array radar data. The contractor shall convert the calibrated experimental data to a format compatible for processing by the implemented main-beam and side-lobe canceller algorithms.

iii) The contractor shall then evaluate the performance of the main-beam and side-lobe canceller algorithms using the formatted data and document the results.

System Analyst: 200 days Senior Programmer: 68 days

b) The Experimental Array Radar System (EARS) used to collect the january 1993 data is now being upgraded to include a new transmitter, data acquisition system and data logger. The system will be ready in early 1994 to collect data. It will collect data at an intermediate frequency of 6 MHz and collect all of the range cells in one scan. The data acquisition system is capable of collecting data at a rate of 20 MHz for each radar pulse on each of the 16 channels available in the main and side-lob canceller arrays and each file will consist of approximately 10 GBytes of data.

i) The contactor shall generate In-phase and Quadrature components from the intermediate frequency data using standard algorithms.

ii) The contractor shall then calibrate, and process the data for input to the main-beam and side-lobe canceller algorithms implemented in a).

iii) The contractor shall then perform a sensitivity analysis on these algorithms using the new EARS data and document the results.

System Analyst: 160 days Senior Programmer: 68 days

2. APAR System Study

a) An APAR simulator was developed to evaluate azimuth and elevation monopulse performance in the presence of multipath and ship motion. This simulator includes a model of the APAR configuration, multipath, beam-steering including electronic stabilization, Taylor and Bayliss aperture weighting, and array positioning due to ships motion. The contractor shall modify the simulator to aid in the evaluation of the effect of multipath on jammer suppression. The modifications to the simulator include:

i) Adding the APAR side-lobe canceller (SLC) array configurations to the simulator. The geometry will be supplied by the scientific authority. After the geometry is input, a beamformer has to be added to the SLC's in order to determine the jammer direction. The beamforming network model shall be supplied by the scientific authority.

ii) Adding signals from up to 4 wide-band noise sources.

iii) Modelling the individual array elements to match the APAR specifications. The scientific authority will supply system specifications, element beam patterns, and frequency response.

iv) Modifying the format of the data output from the simulator to be of the form used by the anti-jamming algorithms developed in Section 1.

The contractor shall then simulate threat scenarios as set out by the scientific authority and evaluate the performance of the anti-jamming algorithms developed in Section 1, and document the results.

System Programmer: 80 days

b) Using the modified simulator of a) the contractor shall evaluate the performance of APAR for azimuth and elevation monopulse estimation, and revised maximum likelihood elevation estimation. These programs will be supplied to perform the evaluation.

System Programmer: 20 days

3. Radar Trial Support.

The contractor shall support radar trials at Area 5 and possibly other locations by aiding in the definition of the experiments, aiding in the data collection, system troubleshooting, and performing on-site data analysis of logged data as required by the Scientific Authority.

System Analyst: 30 days

APPENDIX B
EARS PROJECT PERSONNEL

EARS Project Personnel

DREO Personnel

Ross Turner	Scientific Advisor
Ed Riseborough	Group Leader/Scientific Authority
Denis Lamothe	Technical Support S/H Unit, High Speed Data Aquisition

AIT Project Personnel

Stephen Sung	AIT Manager
Dan Brookes	Technical Leader/ Scientific Analyst
Anna Wilkinson	Senior Programmer

Applied Silicon Personnel

Ross Fines	Director/Contract manager
John Curnow	Contract Manager
Bob Moore	RF radar technician
Dany Longval	Digital Engineer
Mike Cromby	Digital Engineer
Manual Pablo-Dura	Digital technologist
Pierre Menard	Technician

APPENDIX C
TASK SHEETS

Table 1 Labour Breakdown by Task

Task	Systems Analyst(D.B.)	Senior Programmer(A.W.)
1 a) i)	25	10
ii)	25	10
iii)	135	42
b) i)	40	20
ii)	50	20
iii)	57	23
2 a) i)		15
ii)		12
iii)		24
iv)		6
v)		17
b)		17
3	28	
Total (days)	360	216

Table 2 Labour Breakdown by Month

Month ARO	Systems Analyst(D.B.)	Senior Programmer(A.W.)
1	20	12
2	20	12
3	15	9
4	20	12
5	20	12
6	20	12
7	20	12
8	20	12
9	20	12
10	20	12
11	10	6
12	20	12
13	20	12
14	20	12
15	15	9
16	20	12
17	20	12
18	20	12
19	20	12
Total (days)	360	216

APPENDIX D

LIST OF PROGRAMS AND SUBROUTINES

The following is a list of some of the software developed and/or used on the contract, in alphabetical order.

Fortran 77 Software:

BEAMPAT0.FOR
BEAMPAT1.FOR
BEAMPAT2.FOR
CALCDIRECTION.FOR
CREATETJSIG.FOR
DREFCO.FOR
FFTPC.FOR
GENXSLC.PK2
GENXSLCDATA.FOR
HILBT.FOR
MAINMENU.FOR
MATIN.FOR
MOODE1.FOR
MOODE2.FOR
MULTIFRML.FOR
MULTIFRML2.FOR
PLOTIQ.FOR
PLOTSLCSUMFFTPC3.FOR
PMAT.FOR
PROJMAT.FOR
ROTSLC.FOR
RUNGMONOP_A.FOR
RUNGMONOP_B.FOR
SGJ2.FOR
SIMGAUSJAM.FOR
TESTHILBT.FOR
TJDIR.FOR
VMUL.FOR
VMUL2.FOR

Matlab Software:

computequ.m
globalvars.m
jplot.m
loadpar.m
maingmonop_a.m
maingmonop_b.m
mincal.m
mincal2.m
naerravg.m
neerravg.m
noremjam.m
piq00avg.m
piq3avg.m
plotfspec.m
pltresults.m
plot1.m
plot2.m
pmake.m
pdir.m
psnr.m
psnr2.m
radarpar.m
remjam.m
setonparam.m
setgmonop_a.m
setparam.m
snrparam.m
spacfft.m
templot.m
tgmonop.m
taavg.m
taerravg.m
taz.m
teamp.m
teamp1.m
teamp2.m
teavg.m
teerravg.m
tel.m
tperraz.m
tperrel.m
viewpar.m

APPENDIX E
BRIEF DESCRIPTION OF SIDELOBE CANCELLATION ALGORITHM

Sidelobe Cancellation Algorithm

The narrow band version of the sidelobe cancellation algorithm is developed briefly as follows:

Consider the schematic shown in Figure E1 where the signals from the main-beam and sidelobe canceller arrays are combined as shown. The signals from each of the sidelobe canceller receiver elements are combined in the beamformer network to give the beamformed output. For the single jammer case, the maximum of the beamformed output should correspond to the jammer direction. For example, the beamforming network corresponds to either a digital beamformer (ie. a simple N point spatial FFT using 8 inputs from the receiver array and the rest zero filled) or the output from a Rotman lens attachment as in the September 1994 experiments. The residual signal, r(t), obtained by subtracting the weighted beamformed output from the main-beam signal, y(t), is given by:

$$r(t) = y(t) - w \cdot \mathscr{F}_m$$

where

$r(t)$ = residual signal
$y(t)$ = main-beam signal
w = complex weight factor
$\mathscr{F}_m$ = maximum beamformed (spatial FFT) output
t = time

The average residual power P_r is therefore given by:

$$\begin{aligned} P_r &= E[r^* \cdot r] \\ &= E[|y(t)|^2 - (w \cdot \mathscr{F}_m)^* \cdot y(t) - y^*(t) \cdot (w \cdot \mathscr{F}_m) + |(w \cdot \mathscr{F}_m)|^2] \\ &= E[|y(t)|^2] - w^* \cdot E[\mathscr{F}_m^* \cdot y(t)] - w \cdot E[y^*(t) \cdot \mathscr{F}_m)] + |w|^2 \cdot E[|\mathscr{F}_m|^2] \\ &= P_{mb} - w^* \cdot E[\mathscr{F}_m^* y(t)] - w \cdot E[y^*(t) \cdot \mathscr{F}_m)] + |w|^2 \cdot E[|\mathscr{F}_m|^2] \end{aligned}$$

where E[] represents the expectation operator and P_{mb} is the main-beam power.

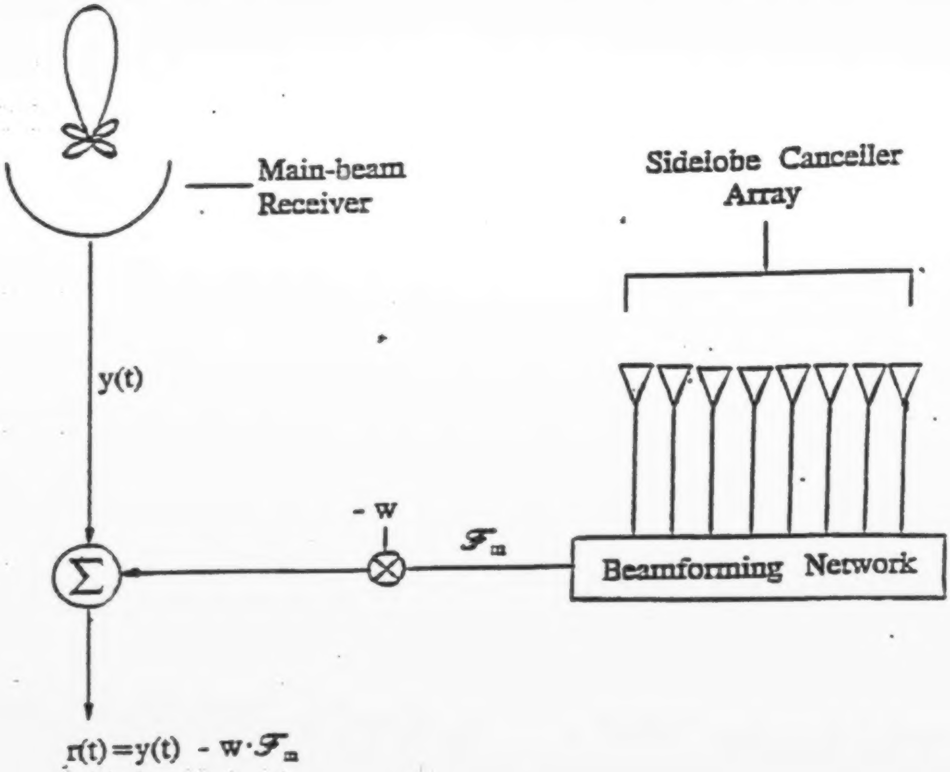
Main-beam
Receiver
Sidelobe Canceller
Array
y(t)
- w
$\mathcal{F}_m$
Beamforming Network
Σ
$r(t) = y(t) - w \cdot \mathcal{F}_m$

Figure E1 Schematic diagram of sidelobe canceller receiver arrangement

To reduce the effect of a jammer signal entering a sidelobe of the main-beam receiver, the residual power in the direction of the jammer must be minimized. This is done by finding the value of w that minimizes P_r , i.e.:

$$\partial P_r / \partial w = - E[y^*(t) \cdot \mathcal{F}_m)] + w^* \cdot E[|\mathcal{F}_m|^2] = 0$$

leads to:

$$w^* = E[y^*(t) \cdot \mathcal{F}_m)]/E[|\mathcal{F}_m|^2]$$

$$w = E[y(t) \cdot \mathcal{F}^*)]/E[|\mathcal{F}_m|^2]$$

The above weights must be estimated when just the jammer signal is present i.e. when the return signal from the main-beam antenna is not coming from the range cell of the target (source) being jammed.

Since the main-beam antenna of the Area 5 Experimental Array Radar System (EARS) consisted of an 8 element vertical array, the instantaneous, total main-beam output signal after jammer cancellation was calculated according to:

$$P_T (t) = \sum_{n=1}^{n=8} (r_n^*(t) \cdot r_n(t))$$

APPENDIX F
AREA 5 TRIALS
JULY-SEPT. 1995

This appendix is a summary of the experiments carried out at the Area 5 test site from July to Sept. 1995.

F1. AREA 5 EARS 'PRE-TRIALS'

Date: Wed. July 27, 1995

Time: 13:30-15:30

This set of EARS pre-trials serves two main purposes. The first is to check the system operation using the two kilohertz pulse repetition frequency and pulse widths shorter than one microsecond. The second purpose is to test the relative returns from the new bargewith one of the three corner reflectors mounted on it.

The new barge was recently made using the dock floats encased with framing lumber. The corners were reinforced with metal corner brackets and nails were also used. A vertical section of four inch PVC pipe was used to support the corner reflector. The barge was anchored in the line of sight to the silo at a range of approximately 1300 meters.

The transmitted pulse widths were changed manually on the RTCU. The keypad was used to change the pulse width of the 10-SIG9 RTCU output. This is the exciter RF output enable. The delay of 10-SIG9 was not changed. The width of the TWT pulse input was not changed.

The raft was used to tow the barge into position. It was moved to a greater range than the barge after each reflector change, so its return did not affect the barge return. It was moved out about 300 meters, or until its return and the barge return were sufficiently separated. The MTU was set to enable data collection over a range of 500 meters to 9500 meters. Each file was recorded for about ten to thirty seconds.

A 3.5 megahertz CW signal was always on the vertical array channel seven IF receiver output. It was derived from the exciter 60 MHz LO signal. This is input six in the data file. The dta file input seven had a constant +0.5 VDC signal. The corner reflector was mounted about nine feet up from the water surface on the PVC pipe.

Tape File Order	PRF (kHz)	Pulse Width (ns)	SLC Atten. (dB)	Vert. Array Atten. (dB)	Target	Notes
1	1	1000	34	28	Trailer	Pointer to White Trailer
2	1	500	34	28	Trailer	
3	1	400	34	28	Trailer	
4	1	300	34	28	Trailer	
5	1	200	34	28	Trailer	
6	2	200	34	28	Trailer	
7	?	?	24	20	Barge	Barge and Raft together at setup
8	1	1000	24	20	Barge	Nothing on Barge
9	1	400	24	20	Barge	Nothing on Barge
10	2	400	24	20	Barge	Small CR+body
11	2	400	30	26	Barge	Middle CR+body
12	2	200	30	26	Barge	Middle CR+body
13	2	200	36	32	Barge	Large CR+body
14	2	400	36	32	Barge	Large CR+body
15	2	1000	36	32	Barge	Large CR+body
16	2	500	36	32	Barge	Body only on barge
17	2	500	24	16	Barge	Body only on barge

Notes:- "Body" refers to Gilles Caron in a sitting position on the barge.
- "CR" means corner reflector.
- Raft range approx. 1300 m

There was a problem in setting the attenuation on file 3, so it may not have been saved. There was also a problem in saving file seven, so it may not have been saved. Therefore, there could be 15, 16, or 17 files on the tape. The raft was always farther away from the barge, except on file seven.

The 60 MHz signal lwvel into the vertical array channel seven was at a consan level throughout. It was set to produce a near full scale ADC level using a VA attenuation of 28 dB. Therefore, when the VA attenuation was set to less than 28 dB the ADC channel 8, 3.5 MHz CW signal was probably saturated. This means a loss of amplitude information but the pahse will be preserved sinc the zero crossings will still be the same.

F2. AUGUST 16 TRIALS:

Two files were recorded on tape. On each file, the Main Bang has been attenuated by 50 dB on channel 5 of the vertical array. The 3.5 MHz CW signal is still on channel 7 of the vertical array. Channel 8 of the vertical array is set to +0.5 VDC. The acquisition range is from 0 to about 3000 metres. On the first file, the vertical array IF attenuation was 4 dB and the SLC attenuation was 0 dB. The normal free-running 60 MHz source is used.

On the second file the vertical array IF attenuation was 4 dB, and on the SLC the IF attenuationwas 42 dB. The external phase locked HP3335 is used fo the 60 MHz. It should be possible to average the vertical array channel 5 (the main bang) over many PRFs to reduce the noise, on both files.

F3. PROPOSED EARS TIMING TESTS, 26 AUG. 1994.

Collect 5 to 10 seconds of data for each of the following scenarios:

1) Replace teh RTCU with the PG2011 programmable pulse generaator. Use the master trigger as the input to the PG2011. Use the power-on setting to emulate the RTCU.

2) Replace the RTCU with the PG2011. Recall teh setup from memory 2 and use the master trigger. This causes the rising edge of the master trigger to start the outputs, rather than the falling edge.

3) Replace the RTCU with the LCIU prototype timing circuit built by Gilles Caron. This will also use the rising edge of the master trigger to start the outputs.

4) Put the RTCU back in the system. Use the HP8112A pulse generator with the 10 MHz clock as the trigger input. Trigger on both the rising and falling edges of the 10 MHz to cause a 20 MHz output. Adjust the levels and triggering to produce a 50% duty cycle TTL clock at the MTU. Remove the TTL timing IC from the MTU board and install a 50 ohm termination resistor. Connect the 8112 output through an RG58 coax to the external MTU clock output.

5) Use the HP8112A to replace the internal MTU clock. Use the PG2011 to replace the RTCU with the memory 2 setup.

6) Use the HP8112A to replace the internal MTU clock. Use the LCIU prototype timing circuit board to replace the RTCU.

Results:

There were two backup tapes used. On the first tape there were six files collected, as follows:

File 1 - seemed ok but there wass some doubt aboutthe data acquisition window signal out of the MTU. It may have been high all the time. Did scenario 1.

File 2 - Scenario 2, but the same problem as file 1

File 3 - Scenario 3, ok.

File 4 - Scenario 1, The PG2011 may have been triggering on both the rising and falling edges of the 10 microsecond PRF. This would be show by the presence of two main bangs in each PRF.

File 5 - Scenario 2, Ok

File 6 - Scenario 1, Ok

On tape 2 there were two files, each with about 20 seconds of data.
File one is Scenario 5, and should be ok. File 2 is scenario 6 and should be ok, but I increased the high level of the TWT gate slightly. I tried to do scenario 4, but the RTCU would only produce a 500 Hz square wave as the TWT gate signal. It has a problem.

F4. AUGUST 23/94, DOPPLER TEST WITH BOAT

Doppler Test with Boat, Aug. 23, 1994

Time (us)	Range (m)	SLC Attenuation (dB)	Vert. Array Attenuation (dB)
27.0	4050	0	0
23.0	3450	2	0
21.0	3150	6	0
18.5	2780	6	4
17.6	2650	8	4
16.5	2480	14	4
15.6	2350	14	8
14.3	2150	14	12
13.4	2020	16	12
12.0	1800	16	16
11.4	1710	20	16
9.9	1490	28	16
9.3	1430	28	24
7.0	1050	28	24

Additional Notes:

- Middle triangular corner reflector held in bow of boat by two people, about 1m off the water surface.
- 64.0 IF (4.0 MHz offset video).
- 0.5 VDC into channel 8 of the vertical array.
- Vertical array channel 5 attenuated by 25 dB for the 'main bang'.
- Vertical array channel 7 had a 4.0 MHz CW reference input.
- Data was collected for about 5 minutes.
- Weather sunny at 21 deg C with light breeze.
- 1 KHz prf, 1us pulse width, internal MTU clock.

F5. AUGUST 31 TRIALS:

Local Coherency Setup Data, Aug. 31, 1994					
Tape File #	Pulse Width (ns)	DC Level on Chan. 7 (V)	Range Window (m)	IF Attenuation (SLC & Vert) (dB)	IF Reference Frequency (MHz)
1	1000	0.3	1500-2000	4.0	63.5
2	500	0.5	"	4.0	63.5
3	400	0.7	"	4.0	63.5
4	300	0.9	"	4.0	63.5
5	200	0.4	"	4.0	63.5
6	200	0.2	"	4.0	64.0
7	300	0.0	"	4.0	64.0
8	400	0.6	"	4.0	64.0
9	400	0.8	"	4.0	64.0

Additional Notes:

- delay from prf trailing edge was 750ns
- 10.00 MHz clock was within 300 Hz
- 2 KHz prf used

August 31, 1994,Tape #2					
Tape File #	**Target**	**Pulse Width**	**SLC Attenuation (dB)**	**Vert. Array Attenuation. (dB)**	**Range Sampling Window (m)**
1	White Trailer	1us	34	30	0-3000
2	White Trailer	1us	34	30	0-3000
3	"	400ns	34	"	0-3000
4	"	400ns	"	"	0-3000
5	Silo	1us	0	0	11500-14000
6	Silo	400ns	0	0	"
7	Silo	300ns	0	0	"

Additional Notes:

- -There was 0.7 Volts DC on channel 7 for all files.
- -A PG2011 pulse generator was used to replace the RTCU and was triggered on the rising edge of the master trigger.
- -A 64.0 MHz IF reference was used.
- -Attenuated the 'main bang' on channel 5 of the vertical array.

F6. SEPT. 1 TRIALS

The following table describes the trials done on September 1, 1995. The stepped staircase input was to check that the data acquisision system actually records each PRF. A circuit triggers on the rising edge of each master trigger. Using a 4 bit counter and a DAC it produces 16 different DC levels. Each successive PRF should have a different DC level which will be different from the DC level on the previous or the following PRF. The 16 different levels were measured on an oscilloscope as (mV): -590, -510, -434,-356,-278,-200,-124,-40, 36,112,118,268,344,420,500,576. The absolute levels read back may be slightly different than those above due to random noise and DC offsets. The step size is about 78 mV. It is important that each PRF has a different DC level on the one specified channel; if not, then the DLCS has a problem.

Sept.1 Trials with Boat and Old Helicopter Beacon

Tape File #	Channel 7 Signal Level (VDC)	Range Sampling Window (m)	Notes
1	0.9	1000-3500	Boat moving in at full throttle Boat range is 20.4us at start
2	0.8	0-2000	Boat moving in at full throttle to start then down to half at 5.6us
3	0.7	1000-2000	Boat fixed at 1600 m range and about 50m offshore from the white trailer
4	0.6	1000-2000	Same as Above
5	0.5	1000-2000	Same as Above but with 400ns pulse width
6	N.A.	1000-2000	Stepped staircase in Vert. Array #8 only
7	N.A.	1000-2000	Stepped staircase in Vert. Array #1 only
8	N.A.	1000-2000	Stepped staircase in SLC #8 only
9	0.4	1000-2000	Stepped staircase in SLC #1 only

Addtitional Notes:

-In files 1 and 2 the mid size triangular corner reflector was used as target
-In file 2 the IF attenuations were increased during the run; the boat range was 11us at the start (to return leading edge).
-In files 3,4,5 the corner reflector was not used, just the return from the broadside of the boat
-full throttleworresponded to about 16 mph or 25 2kph.
-freq. was 933 MHz

F7. SEPT. 7 TRIALS.

EARS Main-beam Nulling Trials Using the Raft and Boat, Sept. 7, 1994

Tape File #	Boat Range (m)	Raft Range (m)	Range Window (m)	SLC Attenuation (dB)	Vert. Array Attenuation (dB)	Jammer State	Notes
1	500	6050	200-7000	12	6	off	
2	500	6050	"	12	6	on	
3	500	6050	"	14	8	on	
4	500	6050	"	14	8	off	
5	750	6050	"	20	12	on	
6	750	6050	"	22	14	on	
7	750	6050	"	22	14	off	
8	750	6050	"	20	12	off	
9	1000	6050	"	18	12	on	
10	1000	6050	"	20	14	on	
11	1000	6050	"	20	14	off	
12	1000	6050	"	18	12	off	
13	900	3000	300-4000	26	16	off	
14	900	3000	"	26	16	on	Jammer not well aimed
15	900	3000	"	26	16	on	Jammer ok now
16	680	3000	"	28	20	on	
17	680	3000	"	28	20	off	Boat off-line, drifting
18	320	3000	"	30	24	on	
19	320	3000	"	30	24	off	
20	320	3000	"	32	26	on	400ns pulse width
21	320	3000	"	32	26	off	400ns pulse width

Additional Notes:

-Conditions: 20deg C, overcast, light breeze, ripples when raft at 6050 m but winds picked up and waves started when raft at 3000 m.
-Distances measured on A-scope form the start of the 'main bang' to the start of the target return (25m precision).
-Start of the 'main bang' was 660 ns after the rising edge of the prf.
-The IF receiver attenuators were set so the jammer and target signal were below the ADC saturation level.
-The PG2011 pulse generator was used in place of the RTCU.
-All channels were connected to the DLCS.
-A 1us pulse width was used in all but the last two files.
-Water level 7

F8. MAIN-BEAM NULLING, SEPT. 8

EARS Main-beam Nulling Trials Using the Raft and Helicopter, Sept. 8, 1994

Tape File #	Heli. Height (ft)	Heli. Range (m)	Range Window (km)	SLC Atten. (dB)	Vert. Array Atten. (dB)	Jammer State	File Length (Sectors)	Notes
1	100	4000	3.5-5.5	20	14	on	2448	
2	100	4000	3.5-5.5	20	14	off	2448	
3	200	4000	3.5-5.5	20	14	on	2800	
4	200	4000	3.5-5.5	20	14	off	2448	
5	300	4000	3.5-5.5	20	14	off	2448	
6	300	4000	3.5-5.5	20	14	on	2448	
7	100	4000	3.5-5.5	18	12	on	2448	
8	100	4000	3.5-5.5	18	12	off	2800	
9	200	4000	3.5-5.5	18	12	off	2800	
10	200	4000	3.5-5.5	18	12	on	688	
11	200	4000	3.5-5.5	18	12	on	3856	
12	300	4000	3.5-5.5	18	12	off	688	system controller problems |
13	300	4000	3.5-5.5	18	12	off	2800	|
14	300	4000	3.5-5.5	18	12	off	3856	|
15	300	4000	3.5-5.5	18	12	off		|
16	300	4000	3.5-5.5	18	12	off	688	|
17	200	4000	4.0-7.0	18	12	on	16528	|
18	200	4000	4.0-7.0	10	6	off		|

Additional Notes:

- -Jammer was on the raft positioned about 5 ft off the water and 1880 m from the receiver.
- -File 17 was a recording of the helicopter flying toward the receiver at 100 knots; the data collection started at 6000m and ended at 3800 m.
- -Approximately 7.6 hrs were needed to backup the almost 1 Gigabyte of data from the aquisition systerm to tape.
- -Height of the corner reflector was 9.14 m.
- -Frequency was 9.17 GHz.
- -Water level 7

F9. SIDELOBE JAMMER TRIALS, SEPT. 9.

Sidelobe Jammer Cancellation Trials, Sept. 9. 1994

Run #	Corner Reflector	Jammer State	Vert. Array Attenuation (dB)	SLC Attenuation (dB)	Range Window (km)	Pulse Width (ns)	Notes
1	small corner relector mounted at 2'	on	4	36	2.0-3.0	1000	
2	"	off	4	36	"	"	
3	"	off	8	40	"	"	
4	"	on	8	40	"	"	
5	"	on	8	40	"	"	
6	"	off	8	40	"	400	
7	"	off	0	32	"	"	
8	"	on	0	32	"	"	
9	"	on	4	36	"	"	
10	"	off	4	36	"	"	
11	"	on	0	32	"	"	
12	"	off	0	32	"	"	
13	dismounted	off	8	40	"	"	
14	"	on	8	40	"	"	
15	"	on	4	36	"	1000	
16	"	off	4	36	"	"	
17	medium sized reflector @ 2'	on	12	36	"	"	
18	"	off	12	36	"	"	
19	"	off	14	38	"	"	
20	"	on	14	38	"	"	

-continued-

Sidelobe Jammer Cancellation Trials, Sept. 9. 1994 (cont'd)

Run #	Corner Reflector	Jammer State	Vert. Array Attenuation (dB)	SLC Attenuation (dB)	Range Window (km)	Pulse Width (ns)	Notes
21	small corner relector mounted at 2'	on	14	38	2.0-3.0	400	
22	"	off	14	38	"	"	
23	"	off	16	38	"	"	not a good file
24	"	off	16	38	"	"	antenna sweep from -8 to 24 degrees
25	"	on	16	38	"	"	"
26		on	30	38	1.0-8.0	1000	"

Additional Notes:

- -Azimuthal angle between jammer and raft was 9.9 deg.(jammer defined 0 deg).
- -Weather conditions: 22 deg. C, calm, cloud cover, very humid (>90%).
- -Water level 6.5.
- -Radar frequency set at 9.17 GHz.
- -At -20 deg. the receiver antenna was aimed at the edge of the tall bay door.
- -Raft located at range of 2480m from receiver and equipped with corner reflector.
- -Boat with jammer positioned at range of 2130m.

F10. SEPT. 12 TRIALS

Trials Sept. 12, 1994

Run #	Corner Reflector	Heli. Range (m)	Heli. Height (m)	Jammer State	SLC Attenuation (dB)	Vert. Array Attenuation (dB)	Range Window (km)	Notes
1	mounted @ 7.5'	2450	100	on	10	6	5.0-7.0	heli. hovering in line with tall bay and silo
2		2450	100	off	"	"	"	
3		2300	200	on	"	"	"	
4		2300	200	off	"	"	"	
5		2300	300	on	"	"	"	
6		2300	300	off	"	"	"	
7	dismount	2300	100	on	"	"	"	
8		2300	100	off	"	"	"	
9		2200	200	on	"	"	"	heli. out of line
10		2350	200	on	"	"	"	
11		2350	200	off	"	"	"	
12		2350	300	on	"	"	"	
13		2350	300	off	"	"	"	
14		1000	50	sweep on	14	14	"	heli. roughly in line with silo
15		1000	50	"	"	"	"	heli. in line with point (3.1 deg)
16		1000	50	"	"	"	"	
17		1000	300	off	"	"	"	
18		7000-3000	300	off	"	"	3.0-7.0	heli. in line with silo and tall bay, moving in direction of tall bay
19		7000-3000	200	off	8	4	"	

Additional Notes:

-Raft anchoredat 5900m range from receiver and equipped with corner reflector.
-Helicopter equipped with jammer.
-Synthesizer frequencies were 63.5 and 60 MHz.
-Weather conditions: 20 deg. C, light NW breeze, slight haze, light cloud.
-Water level 7
-Radar frequency at 9.17 GHz.

F11. SLC TRIALS, SEPT. 13.

Run No.	Corner Refl.	Jammer	Vert. Array Atten. (dB)	SLC Atten.(dB)	Acq. Wind.(km)	Pulse Width (ns)	Notes
1	small @ 2 ft.	on	4	36	2-3	1000	
2	"	off	4	36	2-3	1000	
3	"	off	8	40	2-3	1000	
4	"	on	8	40	2-3	1000	
5	"	on	8	40	2-3	400	
6	"	off	8	40	2-3	400	
7	"	off	0	32	2-3	400	
8	"	on	0	32	2-3	400	
9	dismounted	off	4	36	2-3	400	
10	"	on	4	36	2-3	400	
11	"	on	0	32	2-3	400	
12	"	off	0	32	2-3	400	
13	"	off	8	40	2-3	400	
14	"	on	8	40	2-3	400	
15	"	on	4	36	2-3	1000	
16	"	off	4	36	2-3	1000	
17	medium @ 2 ft.	on	12	36	2-3	1000	
18	"	off	12	36	2-3	1000	
19	"	off	14	38	2-3	1000	
20	"	on	14	38	2-3	1000	
21	"	on	14	38	2-3	400	
22	"	off	14	38	2-3	400	
23	"	off	16	38	2-3	400	this file is garbage
24	"	off	16	28	2-3	400	ant.sweep-8 to 24°
25	"	on	16	38	2-3	400	
26	No Raft, Boat	on	30	38	2-3	1000	

Notes: Raft equipped with corner reflector at 2400 m, Boat at 2130 m.
Raft at 9.9° wrt jammer defined to be at 0°; Weather- 22°C, calm, cloud cover, very humid (>90%)
Water Level - 6.5; Radar Carrier Frequency at 9.17 GHz.

F12. SLC TRIALS, SEPT. 14.

Sidelobe Cancellation Trials, Sept. 14, 1994

Run #	Corner Reflector	Raft Position	Jammer State	Vert. Array Attenuation	SLC Attenuation	Range Window (km)	Pulse Width (ns)	Notes
1	small reflector @ 30"	2050	on	12	42	2.0-3.0	1000	
2	"	2050	off	12	42	"	"	
3	"	2050	off	16	46	"	"	
4	"	2050	on	16	46	"	"	
5	"	2050	on	8	38	"	"	
6	"	2050	off	8	38	"	"	
7	"	2000	off	8	38	"	400	
8	"	2000	on	8	38	"	"	
9	"	2000	on	12	42	"	"	
10	"	2000	off	12	42	"	"	
11	"	2000	off	16	46	"	"	
12	"	2000	on	16	46	"	"	
13	dismounted	1800	off	16	46	1.8-2.8	"	
14	"	"	on	16	46	"	"	
15	"	"	on	12	42	"	"	
16	"	"	off	12	42	"	"	
17	"	"	off	8	38	"	"	
18	"	"	on	8	38	"	"	
19	"	"	on	12	42	"	1000	
20	"	"	off	12	42	"	"	

-continued-

Sidelobe Cancellation Trials, Sept. 14, 1994 (cont'd)

Run #	Corner Reflector	Raft Position	Jammer State	Vert. Array Attenuation	SLC Attenuation	Range Window (km)	Pulse Width (ns)	Notes
21	medium reflector @ 30"	1760	off	22	46	1.6-2.6	1000	
22	"	"	on	22	46	"	"	
23	"	"	on	18	42	"	"	
24	"	"	off	18	42	1.6-2.8	"	boat position changed; just at outside edge of range window
25	"	"	off	18	42	1.6-2.6	400	
26	"	"	on	18	42	"	"	
27	"	"	on	30	42	"	400	stop transmitting, sweep from -20 to 20 deg azim.

Additional Notes:

-Boat at 2400m
-Raft equipped with corner reflector
-Azimuth angle between raft and jammer was 14 deg (jammer in 2nd sidelobe).
-Weather conditions-20 deg C, clear, wind from NW causing some whitecaps.
-Water level 7.
-Frequency was 9.17 GHz.
-The Rotman lens beamforming network was removed for these runs.

Sidelobe Jammer Cancellation Trials, Sept. 9. 1994

Run #	Corner Reflector	Jammer State	Vert. Array Attenuation (dB)	SLC Attenuation (dB)	Range Window (km)	Pulse Width (ns)	Notes
1	small corner relector mounted at 2'	on	4	36	2.0-3.0	1000	
2	"	off	4	36	"	"	
3	"	off	8	40	"	"	
4	"	on	8	40	"	"	
5	"	on	8	40	"	"	
6	"	off	8	40	"	400	
7	"	off	0	32	"	"	
8	"	on	0	32	"	"	
9	"	on	4	36	"	"	
10	"	off	4	36	"	"	
11	"	on	0	32	"	"	
12	"	off	0	32	"	"	
13	dismounted	off	8	40	"	"	
14	"	on	8	40	"	"	
15	"	on	4	36	"	1000	
16	"	off	4	36	"	"	
17	medium sized reflector @ 2'	on	12	36	"	"	
18	"	off	12	36	"	"	
19	"	off	14	38	"	"	
20	"	on	14	38	"	"	

-continued-

Sidelobe Jammer Cancellation Trials, Sept. 9. 1994 (cont'd)

Run #	Corner Reflector	Jammer State	Vert. Array Attenuation (dB)	SLC Attenuation (dB)	Range Window (km)	Pulse Width (ns)	Notes
21	small corner relector mounted at 2'	on	14	38	2.0-3.0	400	
22	"	off	14	38	"	"	
23	"	off	16	38	"	"	not a good file
24	"	off	16	38	"	"	antenna sweep from -8 to 24 degrees
25	"	on	16	38	"	"	"
26		on	30	38	1.0-8.0	1000	"

Additional Notes:

-Azimuthal angle between jammer and raft was 9.9 deg.(jammer defined 0 deg).
-Weather conditions: 22 deg. C, calm, cloud cover, very humid (>90%).
-Water level 6.5.
-Radar frequency set at 9.17 GHz.
-At -20 deg. the receiver antenna was aimed at the edge of the tall bay door.
-Raft located at range of 2480m from receiver and equipped with corner reflector.
-Boat with jammer positioned at range of 2130m.

APPENDIX G
BRIEF DESCRIPTION AND MANUAL FOR GENXSLC

1. GENERAL INFORMATION

Program Name: GENXSLC.FOR

Associated Subroutines:

```
CURVECR1(RNG,WVL,HTANT,TRGHT,H1,H2,CR1,T1,
         D1,EDIAM,ERAD,RESOLN,PI,DIELRL,PI,
         DIELRL,DIELIM,SWH)

PHASEADJ(PHRET,HRETURN,REG,R,HT,HC,HE,
         DE,HE,DE,AOB,TB,ST,WVL,DDD)

NOIS(XNOISE,AVE,STD,ITYPE,ISEED)

SWERL(THETA,SWRII,ISEED)

TAPER(ITPR,W1,W2,W3,W4)

CALCHEIGHTS(HTANT,NE1,HBOTL,HBOTR)

JAMMERSETUP(NJAM,JAMHGT,JAMAOB,JAMRNG,
         JAMJNRDB)

SLCSETUP(RNG,TRGHT,AOB,JAMRNG,JAMHGT,
     JAMAOB,NSLC,SLCRNG,SLCHGT,SLCAOB)

CALCTHEO(PI,CORANTHGT,CORHGT,WVL,DCONE,
         CR1,THEO)

SUMIQ(IDATA,QDATA,TRGIDATA,TRGQDATA,W1,W2,
     W3,W4,ICOL,IDATSUM1,DATSUM1,IDATSUM2,
     QDATSUM2,ISUMCH,QSUMCH,TRGIDATSUM1,
     TRGQDATSUM1,TRGIDATSUM2,
     TRGQDATSUM2,TRGISUMCH,TRGQSUMCH)

STEAR(IDATA,QDATA,PHASE)
```

MAINMENU(IPAR,MAXRNG,MINRNG,NRECS,NSAMPS,
TRGHT,ASTHT,MAXFRE,MINFRE,FRQINC,
HTANT,T1,T2,SWH,RESOLN,DIEL1,DIEL2,
COEF,ACF,AOB,AOB2,ITPR)

GENSLCDATA(LRNG,NSLC,IBS,SLCSTR,SLCRNG,SLCHGT,
SLCAOB,RNG,HTANT,T2,T1,WVL,EDIAM,
ERAD,RESOLN,PI,DIELRL,DIEL2IM,SWH,
ICR1,DCONE,IJAM,NJAM,JAMRNG,JAMHGT,
JAMHGT,JAMAOB,STDPW,ISEED,JXXNN,
ITARG,SLCISUM2,SLCQSUM2)

CALCDIRECTION(PI,HTANT,HEIGHT,RNG,COEF,THEATAB)

Input Files:

ELTAYWTS.DAT (Taylor weights for elevation monopulse)

ELBAYWTS.DAT (Bayliss weights for elevation monopulse)

TAYLORWT.DAT (Taylor weights for azimuth monopulse)

BAYLISWT.DAT (Bayliss weights for azimuth monopulse)

To Compile and Link: f77 genxslc.for

To Run the Software:

type: a.out or mv a.out genxslc
then type: genxslc

Output Files:

FILENAME.DAT (non-jammed data for I and Q differences)

FILENAME.OFT (off-target data for I and Q differences)

FILENAME.ONT (on-target data for I and Q differences)

FILENAME.OFS (off-target data for I and Q sums)

FILENAME.ONS (on-target data for I and Q sums)

FILENAME.SNR (signal-to-noise ratios)

FILENAME.TDI (direction of target)
FILENAME.JDI (direction of jammer)

2 MAIN MENU

```
*********************DATA GENERATION*********************
--------------------------------------------------------
0 >  TERMINATE SESSION
1 >  LOAD OLD SET-UP FILE
2 >  [MAX,MIN]RANGE,NRECS,NSAMPS:
3 >  TARGET HEIGHT AND ARRAY STEERING HEIGHT:
4 >  [MAX,MIN,INC]FREQUENCY:
5 >  HEIGHT OF CENTER OF ARRAY:
6 >  SIDE TILT ANGLE AND TILT BACK ANGLE:
7 >  WAVE HEIGHT AND RESOLN (REFLECTION):
8 >  COMPLEX DIELECTRIC CONSTANT:
9 >  EARTHS RADIUS COEF. AND ARRAY CONFIG. FILE:
10 >  TARGET AOB AND ARRAY STEERING AOB:
11 >  TAPER OPTION (0=OFF,1=ON):
12 >  SAVE CURRENT SETUP
13 >  CREATE SYNTHETIC DATA
************************************************************'
```

To select a menu item input the corresponding number. All items will return to the main menu.

2.0 TERMINATE SESSION

The program will exit at this point.

2.1 LOAD OLD SET-UP FILE

Prompt: INPUT OLD SET-UP FILE NAME
Response: a previously set-up file name
Format: A40

If the file does not exist the program will exit displaying a system error message.

2.2 [MAX,MIN]RANGE,NRECS,NSAMPS

Prompt:	ENTER MAXIMUM,MINIMUM,NRECS,NUMBER OF SAMPLES/RANGE
Response:	maximum range value to start simulation at minimum range value to finish simulation at number of records between the two range values number of samples to collect at each range
Format:	2F10.3,2I5

2.3 TARGET HEIGHT AND ARRAY STEERING HEIGHT

Prompt:	ENTER TARGET HEIGHT AND ARRAY STEERING HEIGHT
Response:	height of target in meters height to be used for array steering in meters
Format:	2F10.3

2.4 [MAX,MIN,INC]FREQUENCY

Prompt:	ENTER MAXIMUM,MINIMUM AND FREQUENCY INCREMENT
Response:	maximum frequency to start simulation at minimum frequency to finish simulation at increment between the two frequency values
Format:	3F10.3

2.5 HEIGHT OF CENTER OF ARRAY

Prompt:	ENTER HEIGHT OF CENTER OF ARRAY
Response:	array center height in meters
Format:	F10.3

2.6 SIDE TILT ANGLE AND TILT BACK ANGLE

Prompt:	ENTER SIDE TILT ANGLE AND TILT BACK ANGLE
Response:	side tilt angle in degrees tilt back angle in degrees
Format:	2F10.3

2.7 WAVE HEIGHT AND RESOLN (REFLECTION)

Prompt:	ENTER WAVE HEIGHT AND RESOLN (REFLECTION)
Response:	significant wave height resolution
Format:	2F10.3

2.8 COMPLEX DIELECTRIC CONSTANT

Prompt:	ENTER THE COMPLEX DIELECTRIC CONSTANT: DIEL1,DIEL2
Response:	complex dielectric constants
Format:	2F10.3

2.9 EARTHS RADIUS COEF. AND ARRAY CONFIG. FILE

Prompt:	ENTER THE EARTH RADIUS COEFFICIENT AND 1 FOR NEW ARRAY FILE
Response:	earth's radius coefficient (1.33 for curved earth geometry) 1 to create a new array configuration file (a file containing locations of all array elements)
Format:	2F10.3

2.10 TARGET AOB AND ARRAY STEERING AOB

Prompt:	ENTER TARGET AOB AND ARRAY STEERING AOB
Response:	angle off boresight for target angle off boresight for array steering
Format:	2F10.3

2.11 TAPER OPTION (0=OFF,1=ON)

Prompt:	ENTER 0 FOR TAPER OPTION OFF, 1 FOR TAPER OPTION ON
Response:	0 or 1
Format:	I1

2.12 SAVE CURRENT SETUP

Prompt:	INPUT NEW SET-UP FILE NAME
Response:	a set-up file name
Format:	A40

If the file already exists the program will exit displaying a system error message.

2.13 CREATE SYNTHETIC DATA

Prompt:	SIGNAL/NOISE RATIO (IN DB) AND 1 TO RESET RANDOM NUMBER SEED
Response:	snr value to use in noise subroutine 1 to reset the random number generator
Format:	F10.3,I1

Set-up complete. Proceed with simulation using the scenario displayed in the main menu and the responses to the additional prompts after 'CREATE SYNTHETIC DATA' is chosen from the main menu.

UNCLASSIFIED

SECURITY CLASSIFICATION OF FORM
(highest classification of Title, Abstract, Keywords)

DOCUMENT CONTROL DATA

(Security classification of title, body of abstract and indexing annotation must be entered when the overall document is classified)

1. ORIGINATOR (the name and address of the organization preparing the document. Organizations for whom the document was prepared, e.g. Establishment sponsoring a contractor's report, or tasking agency, are entered in section 8.)

AIT Corporation
9 Auriga Drive
Nepean, Ontario, K2E-7T9

2. SECURITY CLASSIFICATION (overall security classification of the document including special warning terms if applicable)

Unclassified

3. TITLE (the complete document title as indicated on the title page. Its classification should be indicated by the appropriate abbreviation (S,C or U) in parentheses after the title.)

Final Report - Multi-Function Radar Simulation and ECCM Data Analysis.

4. AUTHORS (Last name, first name, middle initial)

Brookes, E. Daniel
Wilkinson, Anna

5. DATE OF PUBLICATION (month and year of publication of document)

June 1995

6a. NO. OF PAGES (total containing information. Include Annexes, Appendices, etc.)

172

6b. NO. OF REFS (total cited ir document)

None

7. DESCRIPTIVE NOTES (the category of the document, e.g. technical report, technical note or memorandum. If appropriate, enter the type c report, e.g. interim, progress, summary, annual, or final. Give the inclusive dates when a specific reporting period is covered.)

Final Contract Report

8. SPONSORING ACTIVITY (the name of the department project office or laboratory sponsoring the research and development. Include the address.)

DND - Defense Research Establishment Ottawa
Surface Radar Section
Shirley's Bay, Ottawa

9a. PROJECT OR GRANT NO. (if appropriate, the applicable research and development project or grant number under which the document was written. Please specify whether project or grant)

041LC

9b. CONTRACT NO. (if appropriate, the applicable number under which the document was written)

05SV.W7714-3-9700

10a. ORIGINATOR'S DOCUMENT NUMBER (the official document number by which the document is identified by the originating activity. This number must be unique to this document.)

DT-00892

10b. OTHER DOCUMENT NOS. (Any other numbers which may be assigned this document either by the originator or by the sponsor.

DREO CONTRACTOR REPORT 98-626

11. DOCUMENT AVAILABILITY (any limitations on further dissemination of the document, other than those imposed by security classificatio

(X) Unlimited distribution
( ) Distribution limited to defence departments and defence contractors; further distribution only as approved
( ) Distribution limited to defence departments and Canadian defence contractors; further distribution only as approved
( ) Distribution limited to government departments and agencies; further distribution only as approved
( ) Distribution limited to defence departments; further distribution only as approved
( ) Other (please specify):

12. DOCUMENT ANNOUNCEMENT (any limitation to the bibliographic announcement of this document. This will normally correspond to the Document Availability (11). However, where further distribution (beyond the audience specified in 11) is possible, a wider announcement audience may be selected.)

UNLIMITED

UNCLASSIFIED

SECURITY CLASSIFICATION OF FORM

13. ABSTRACT (a brief and factual summary of the document. It may also appear elsewhere in the body of the document itself. It is highly desirable that the abstract of classified documents be unclassified. Each paragraph of the abstract shall begin with an indication of the security classification of the information in the paragraph (unless the document itself is unclassified) represented as (S), (C), or (U). It is not necessary to include here abstracts in both official languages unless the text is bilingual.)

This document summarizes the work done by Advanced Information Technologies Corporation (AIT) in fulfilment of DND contract 05SV.W7714-3-9700 from November 1993 to June 1995. Part of the work involved the calibration, processing and analysis of data from the Experimental Array Radar System (EARS) at Defence Research Establishment Ottawa (DREO) to validate main-beam and side-lobe jammer suppression algorithms developed by their scientists. The algorithms were developed into software by AIT and evaluated first with simulated, then with real data. Another major task was the ongoing development and implementation of a phased array radar (based on a proposed array configuration) simulation program to carry out a Multi-Function Radar (MFR) system study. Work was also carried out in support of experimental radar trials with EARS to assist in the data collection and in planning some of the trials.

14. KEYWORDS, DESCRIPTORS or IDENTIFIERS (technically meaningful terms or short phrases that characterize a document and could be helpful in cataloguing the document. They should be selected so that no security classification is required. Identifiers, such as equipment model designation, trade name, military project code name, geographic location may also be included. If possible keywords should be selected from a published thesauri, e.g. Thesaurus of Engineering and Scientific Terms (TEST) and that thesaurus-identified. If it is not possible to select indexing terms which are unclassified, the classification of each should be indicated as with the title.)

Beamforming network
EARS
ECCM
Eigen Decomposition
IF sampling
Hilbert transform
jammer suppression
main-beam jammer
monopulse radar
Multi-function radar
multipath
radar jamming
RML (Refined Maximum Likelihood)
Rotman lens
side-lobe jammer
SEWE (Subspace Evaluation Without Eigenvectors)
SMI (Sampled Matrix Inversion)